Molecular Characterization of Tomato Mutants and Natural Variants Compromised in Ethylene Biosynthesis

Thesis submitted for the award of the degree of

DOCTOR OF PHILOSOPHY

by

KAPIL SHARMA

Supervisor

Prof. R. P. Sharma

Repository of Tomato Genomics Resources

Department of Plant Sciences

School of Life Sciences

University of Hyderabad

2016

Repository of Tomato Genomics Resources
Department of Plant Sciences
School of Life Sciences
University of Hyderabad

DECLARATION

I, Kapil Sharma, hereby declare that the work described in this thesis entitled "**Molecular Characterization of Tomato Mutants and Natural Variants Compromised in Ethylene Biosynthesis**" submitted by me under the supervision of **Professor R. P. Sharma**, Department of Plant Sciences, is an original research work. I also declare that it has not been submitted previously in part or in full to this University or any other University or Institution for the award of any degree or diploma. A report on plagiarism statistics from the University Librarian is enclosed.

Date
Place: Hyderabad

Kapil Sharma
Enrol. No. 09LPPH06

Prof. R. P. Sharma
Supervisor

Repository of Tomato Genomics Resources
Department of Plant Sciences
School of Life Sciences
University of Hyderabad

CERTIFICATE

This is to certify that the thesis entitled **"Molecular Characterization of Tomato Mutants and Natural Variants Compromised in Ethylene Biosynthesis"** is based on the results of the work done by **Mr. Kapil Sharma** for the degree of **Doctor of Philosophy** under my supervision. This work presented in this thesis is original and has not been submitted for any degree or diploma of any other University. A report on plagiarism statistics from the University Librarian is enclosed.

Head
Dept. of Plant Sciences

Dean
School of Life Sciences

Prof. R. P. Sharma
Supervisor

Dedicated to
My adorable Parents
& Family

ACKNOWLEDGEMENTS

It is the time to put down my feelings in words of thanks to many people who helped me throughout my PhD journey. I owe my gratitude to all those people who have made possible to write this thesis but also helped in shaping up my carrier towards the next scientific endeavor.

First, my deepest gratitude to my supervisor Prof R. P. Sharma. I have been very fortunate to have a mentor like you who gave me the freedom to explore on my own and encouragement to experiments and think in the better scientific perspective. His enthusiasm, immense knowledge, constructive criticism and patience have helped me overcome many disastrous situations and finally finish this dissertation. I hope that one day I would become as good advisor and good writer like you Sir.

My co-supervisor Dr. Y. Sreelakshmi, who is always there to listen and give important guidance throughout this journey. My heartfelt thanks to you Ma'am for your encouragement, insightful comments, and constant inspiration.

I also would like to thanks Prof. A. R. Reddy, my doctoral committee member for his guidance and timely suggestion throughout my research work.

My sincere thanks to Prof. Reddana (Dean, School of Life Sciences), Prof. A. S. Raghavendra, Prof. Aparna Dutta Gupta, Prof M. Ramnadham (Former Dean, School of Life Sciences); Prof. Ch.V Ramana (Head, Dept. of Plant Sciences), and Prof. A. R. Reddy, Prof. A. R. Podille, (Former Head, Dept. of Plant Sciences) for providing me the opportunity to utilize the facilities of the Department and School.

I take this opportunity to thank Dr. Suraj for helping me in generation of primary polyclonal antibodies against ACS2 specific peptide in Rabbit used in my research work.

I am highly grateful to Dr. Soni and Dr. Chaitanya for teaching the basis of TILLING experiments, Dr. Vajir and Prateek while carrying out the Metabolite and Carotenoids analysis, Dr. Reddaiah and Dr. Suresh, for their help in commencement and setup of new experiment in physiological experiments, fruit ripening experiments, field work and many more, which had greatly eased my effort to execute the work.

I am also thankful to all my past and present lab member of RTGR for enduring me throughout my stay in the lab. I would like to mention Dr. Sulabha, Dr. Rahul, Dr. Vijee, Dr. Mickey, Dr. Sherin, Dr. Alka, Rakesh, Rachana, Sapana, Himabindu, Kamal, Pallawi, Hyma, Anusha, Aparna, Anjana, Kalyani, Jayram, Swati, Gyatri, and Sumona for helping me in oneway or the otherway to gain better insight into my work.

I extend my thanks to field assistant (Narshimha, Zamir, Yaddagiri) and lab accountant Venkat Reddy and Anil for maintenance of plants and clearance of bills.

Many friends outside the lab have helped me to stay sane during my difficult time. List are long but I would like to mention Anirudh, Naveen, Ahan, Abhay, Shyam, Soorat, Satpal, Dilip, Pawan, Sachidanand, Bhanu, Sumit, Deepankar. Their support and care helped me overcome many setbacks and stay focused on my PhD work. I greatly value their friendship and I sincerely appreciate their belief in me.

Finally and the most importantly, none of this would have been possible without the love and patience of my family. I am grateful to my parents who provide a carefree environment, so that I can always concentrate on my studies. My heartfelt thanks must go to all my family member; my father, mother, my brother, and bhabhi their moral support, encouragement and cooperation has allowed me to achieve this level. My special thanks to my wife Supriya in my life. She has been the pillar of strength during all the tough times of my study.

Finally, the financial support provided by the University of Hyderabad and UGC New Delhi, in the form of fellowship; DBT for the travel support to attend international conferences and workshop are gratefully acknowledged.

Last but not the least, I am highly grateful to God for his blessings and strength which has helped me to successfully achieve this goal.

Kapil Sharma

2016

TABLE OF CONTENTS

3.4.2 Purification of PCR products

3.5 Sequencing and bioinformatics analysis

3.5.1 Project Aligned Related Sequences and Evaluate SNPs (PARSESNP)

3.5.2 PSSM

3.5.3 SIFT

3.5.4 Phylogenetic analysis

3.6 In silico characterization of Tomato ACS2-1 protein

3.7 Morphological and Physiological characterization of mutants

3.7.1 Seed germination profiling

3.7.2 Ethylene emission from seedlings of WT and mutants

3.7.3 Seedlings phenotype

3.7.4 Demonstration of triple response in etiolated seedlings

3.7.5 Comparisons between plant texture, leaf morphology and flower phenotype

3.7.6 Off-vine leaf senescence study

3.7.7 Estimation of the ethylene emission from leaves of wild type and mutants

3.7.8 Chronology of fruit development between wild type and mutant fruits

3.7.9 On-vine fruit senescence study

3.7.10 Comparisons of fruit morphology

3.7.11 Fruit firmness

3.7.12 Estimation of ethylene emission from fruits of WT and mutants

3.7.13 Genetic analysis

3.8 Biochemical characterization of mutants

3.8.1 Estimation of chlorophyll from leaves of control and mutant plants

3.8.2 Estimation of Sugar content and pH

3.8.3 In-vitro ACC extraction and determination

3.8.4 In-vitro ACS enzyme activity determination

- 3.8.4.1 Extraction and purification
- 3.8.4.2 Reaction of ACS enzyme with substrate

3.8.5 In-vitro ACO enzyme activity determination

- 3.8.5.1 Extraction
- 3.8.5.2 Reaction of purified enzyme with substrate and reading

3.8.6 Production of polyclonal antibodies specific to ACS2 protein

- 3.8.6.1 Peptide synthesis
- 3.8.6.2 Raising polyclonal antibodies in rabbit

LIST OF ABBREVATIONS

1-MCP	1-Methylcyclopropene
Ab	Antibody
ABA	Abscisic acid
ACC	1-Aminocyclopropane-1-carboxylic acid
ACS	ACC synthase
ARF	Auxin response factor
Aux/IAA	Auxin/Indole-3-Acetic Acid
AuxREs	Auxin response elements
AV	Arka-Vikas
bp	base pair
BR	Brassinosteroid
cDNA	Complementary DNA
CDPK	Calcium-dependent protein kinase
CK	Cytokinin
CTR	Constitutive triple response
cv	Cultivar
DNA	Deoxyribonucleic acid
dNTP	Deoxyribonucleotide triphosphate
DPA	Days post anthesis
EBF	EIN3 binding F-box protein
EIL	EIN3-like
EIN	Ethylene insensitive
EMS	Ethyl Methyl Sulfonate
ERF	Ethylene response factor
ERS	Ethylene response sensor
EtBr	Ethidium bromide
ETO	Ethylene overproducer
ETR	Ethylene receptor
FW	Fresh weight
GA	Gibberrilic acid or Gibberellin
GC	Gas chromatography
hr	Hour

IAA	Indole-3-Acetic acid
JA	Jasmonic acid
Kb	Kilo base
MeJA	Methyl Jasmonate
min	Minute
mRNA	Messanger RNA
Nr	*Never-ripe*
PCR	Polymerase chain reaction
PLP	Pyrodoxal-5'-phosphate
RNA	Ribonucleic acid
RNAi	RNA interference
SAM	S-Adenosine methionine
Sl	*Solanum lycopersicum*
TSS	Total soluble solids
UPLC	Ultra-High performance liquid chromatography
v/v	volume/volume
WT	Wild type
w/v	weight/volume

CHAPTER 1

INTRODUCTION

Tomato is one of the model crop species which has been studied extensively for the various plant developmental processes, particularly for mechanisms regulating fruit ripening. Among the five "classical" naturally occurring plant hormones, ethylene (Kende and Zeevaart, 1997) regulates a multitude of plant processes, ranging from seed germination to organ senescence. The commercial value of tomato is derived from fruit, therefore the role of ethylene as an inducer of fruit ripening is of particular economic importance (Abeles, 1992). Moreover, ethylene is also induced in response to biotic and abiotic stress, such as pathogen attack, wounding, water-logging, and drought (Yang and Hoffman, 1984).

Ripening is a complex, genetically programmed process that initiates drastic changes in color, texture and aroma of fruit. Based on ripening pattern fruits are classified as climacteric and non-climacteric. The **climacteric** fruits characteristically show a major peak in respiration and a concomitant burst of ethylene in tomato, apple, melon and banana. The **non-climacteric** fruits do not show any dramatic change in respiration and ethylene production remains at a very low level. In climacteric fruits, ethylene is a key player and affects the transcription and translation of many ripening-related genes (Gray et al. 1994; Deikman 1997; Giovannoni 2001).

Due to its role in the regulation of flower senescence and fruit ripening, the control of ethylene production and perception has been used as a major tool to prevent fruit/flower spoilage and prolong marketability. Tomato being a climacteric fruit, its ripening is influenced by the ethylene. Several transgenic approaches have been directed to reduce ethylene/perception and biosynthesis to delay the fruit ripening in tomato. In tomato, ethylene is perceived six ethylene receptors which initiate downstream ethylene signaling pathway. Ethylene synthesis involves a two-step pathway where S-adenosyl-L-methionine is converted to ethylene via 1-aminocyclopropane-1-carboxylic acid (ACC). The enzymes catalyzing the two reactions of this pathway are ACC synthase (ACS) and ACC oxidase (ACO). ACS, a crucial enzyme of ethylene biosynthetic pathway, belongs to a multigene family, showing similarity to pyridoxal-5'-phosphate (PLP)-dependent aminotransferases. Out of the nine *ACS* genes identified in tomato, *ACS2* and *ACS4* are responsible for the autocatalytic production of ethylene during the climacteric phase of tomato fruit ripening.

At present there are no reported spontaneous mutants in tomato that are defective in ethylene biosynthesis pathway. A mutant defective in ethylene biosynthesis can be a good substitute for delayed ripening in tomato rather than the transgenic plants

with delayed fruit ripening. Since *ACS2* plays a key role in regulating tomato fruit ripening, isolation and characterization of tomato *ACS2* mutants would be of a great value.

However to isolate a mutant defective in a specific genes require special efforts. Several approaches such as classical breeding, induction of mutations and selection of desired phenotype can be used for producing plants with delayed ripening trait. However the standard approach involving forward genetics is too difficult to apply for mutant isolation, as it involves field based screening of fruits with delayed ripening. Though a large field based study involving selection of mutant lines do yield several mutants, it is not suitable for isolation for a gene specific mutant. At the same time it is a valuable approach for isolation of trait-based mutant lines.

During past fifteen years alternate tools have become available that allows isolation of a mutant in a desired gene. TILLING (Targeting Induced Local Lesions in Genomes) is the most popular strategy for isolating mutations located in a specific region of the genome (McCallum et al., 2000). It is a PCR-based strategy that allows identification of an allelic series of induced point mutations in a selected gene(s) of interest. It has been used for high-throughput isolation of mutants in Arabidopsis as well as several plant and animal species (Arabidopsis, maize, wheat, barley, *Drosophila* and zebra fish) [McCallum et al., 2000; Till et al., 2006]. To use this technique, first genome wide mutations are induced by chemical mutagenesis (i.e. ethyl methane sulphonate, EMS). The mutagenized lines are screened for gene specific mutants using TILLING. The isolated mutants are then characterized in details for functional analysis of the mutant gene.

Importantly, the TILLING allows us to identify mutations that usually escape identification with forward genetics approach particularly when a mutant does not have a phenotype. The TILLING also allows the identification of mutants with gain/loss of function of the gene, and one can examine its subsequent effect on plant development and fruit ripening. One of the advantages of TILLING and EcoTILLING approaches is that the isolated mutants after backcrossing can be commercially released as TILLING is a **non-transgenic approach** and does not require regulatory approvals. Moreover, the detailed characterization of mutants also help to elucidate structure-function relationship of the gene.

Considering the importance of the *ACS2* gene in regulating fruit ripening, it was chosen for isolation of gene specific mutants by TILLING. A large EMS (ethyl methane

sulphonate) mutagenized population of an Indian table variety of tomato, namely, Arka Vikas and a processing variety of tomato M82 from Israel was used for isolating *ACS2* mutants. In addition a large collection of different tomato cultivars was screened for natural polymorphism in *ACS2* gene using EcoTILLING.

In view of above advantages in present study, TILLING and EcoTILLING, the reverse genetics strategies were used to isolate mutations in *ACS2* gene of tomato. Further, to understand the natural diversity of the *ACS2* gene, its sequences was examined in five wild relatives of tomato. The major objectives of this study were:

1. Identification and characterization of *ACS2* alleles by TILLING
2. Identification and characterization of natural variants in *ACS2* gene by EcoTILLING
3. Nucleotide diversity analysis of *ACS2* gene in five wild relatives of tomato

CHAPTER 2

REVIEW OF LITERATURE

2.1 Tomato

Tomato is one of important member of the Solanaceae family. The Solanaceae family contains vast diverse group of plants having different characters viz., tuber-bearing potato (*Solanum tuberosum* L.), fruit-bearing vegetables such as tomato (*Solanum lycopersicum* L.), pepper (*Capsicum annum* L.) and eggplant (*Solanum melongen*a L.), ornamental plants such as petunia (*Petunia hybrida hort.*) and tobacco (*Nicotiana tabacum* L.), herbs such as jimson weed (*Datura stramonium* L.), plants with edible leaves (e.g. *Solanum aethiopicum* L., *Solanum macrocarpon* L.). Tomato is believed to be native to South America, most probably the mountain regions in Peru. Tomato made its way from Central America/Mexico to European countries after discovery of new world (Peralta et al., 2006). Tomato belongs to the genus Solanum, subfamily Solanoidaeae and tribe solaneae (Taylor, 1986). Modern taxonomists recently changed the scientific name of tomato from *Lycopersicum esculentum* to *Solanum lycopersicum* (Spooner et al., 1993). The tomato has a considerable small size of the diploid genome (n=12, 950 Mb) and approximately 34,000 genes (Tomato Genome Consortium 2012). The raw sequence data from the genome sequencing projects has also been made available by the 150 tomato genome project consortium. Open access availability of information related to genetic markers, an extensive collection of monogenic mutant lines, and several genetic and epigenetic databases make an it perfect model system for genetic, genomic and molecular study. This section describes the attributes that have made tomato a model plant system for studying different aspects of fruit development and ripening and comparative genomics amongst several members of Solanaceae.

Tomato is a rich source of antioxidants such as lycopene, β-carotene, vitamins A, C, K, minerals and fibers (poor man's Apple, Table 2.1). Of the 14 carotenoids found in human serum, tomato and tomato products contribute to nine carotenoids, including α-carotene, β-carotene, lycopene, lutein, and β-cryptoxanthin in the human diet (Giovannucci, 2002). Carotenoids obtained from tomato are known to neutralize free radicals and overcome the risk of DNA damage by ultraviolet rays, chronic diseases like prostate cancer and cardiovascular diseases and age-related muscular disintegration (Giovannucci, 2002; Stahl et al., 2006; Kavanaugh et al., 2007).

2.1.1 Tomato production

Tomato (*Solanum lycopersicum*) is one of the most popular vegetable crops grown worldwide for its fruit. According to the UN Food and Agriculture Organization (FAO), it ranks second, after the potato, in terms of consumption and is grown in 144 countries

(FAOSTAT Database, 2004). The worldwide production of tomatoes in the year 2013 was about 163 million tons. India observed ~48.3% increase in tomato production from the year 2010 to 2013. In 2010, the total output of tomato was 12.4 million tons that risen to 18.2 million tons (FAOSTAT Database, 2014).

2.2 Ethylene

2.2.1 Effect of ethylene on various plant developmental process and fruit ripening in crop plants

Among the hormones that govern plant development, gaseous alkene ethylene is the simplest in the structure (Abel et al., 1995). This 2-carbon olefin is a potent elicitor of morphological changes during all stages of the plant life cycle **(Fig. 2.1)**. At germination, ethylene causes the hypocotyl to swell and broaden, girdling it as it penetrates through the soil (Goeschl et al., 1966). As the plant matures, ethylene influences sex determination and promotes fruit ripening (Abeles et al., 1992). Ethylene plays a role in senescing flowers and leaves (Bleecker et al., 1997). Ethylene also protects plants from the barrages of nature, strengthening trunks of wind-battered trees, assisting flooded plants to survive submergence, and avoiding pathogenic attack (Dolan et al., 1997; Shibaoka et al., 1994). Under stressful conditions such as heat and drought, the up-regulated levels of ethylene, inhibit root growth and development, and, also reduce shoot/leaf expansion (Sharp, 2002; Pierik et al., 2006). Ethylene is best known for its involvement in stress-induced leaf senescence and abscission (Abeles et al., 1992). There is also evidence that stress induced ethylene may directly reduce photosynthesis (Rajal and Peltonen-Sainio, 2001). Stress triggered ethylene production, for example under heat, flooding, air pollution, soil compaction, and drought, can also induce more direct yield detriments, notably reduced grain-filling rates and/or increased embryo and grain abortion (Hays et al., 2007; Wilkinson and Davies, 2010).

There is also growing evidence that environmentally-induced increases in plant ethylene generation can be growth-promotive under some circumstances or in some genotypes, such as during shade avoidance and plant competition, and when overcoming submergence stress (Sharp, 2002; Pierik et al., 2006). A role for ethylene in stomatal control is also gaining support. It has been shown experimentally to close stomata (Desikan et al., 2006), and instances of stomatal closure via environmentally-induced ethylene accumulation have now been recorded (Vysotskaya et al., 2011). The detrimental effects of ethylene on crop performance and yield are not necessarily confined to a stressful environment, as they may also be linked to genotypic variability in productivity

Table 2.1. Nutrients present in tomato fruit

Nutritional value per 100 g	
Energy	74 kJ (18 kcal)
Carbohydrates	3.9 g
Sugars	2.6 g
Dietary fiber	1.2 g
Fat	0.2 g
Protein	0.9 g
Water	94.5 g
Vitamin A equiv.	42 µg (5%)
lutein and zeaxanthin	123 µg
Vitamin C	14 mg (17%)
Vitamin E	0.54 mg (4%)
Potassium	237 mg (5%)

(Source: USDA Nutrient Database)

Table 2.2. List of countries by tomato production in 2013 mostly based on FAOSTAT FAO accessed in August 2014.

Rank	Country/Region	Tomato production (tons)
1	People's Republic of China	50,552,200
2	India	18,227,000
3	United States	12,574,550
4	Turkey	11,820,000
5	Egypt	8,533,803
6	Iran	6,174,182
7	Italy	4,932,463
8	Brazil	4,187,646
9	Spain	3,683,600
10	Mexico	3,282,583

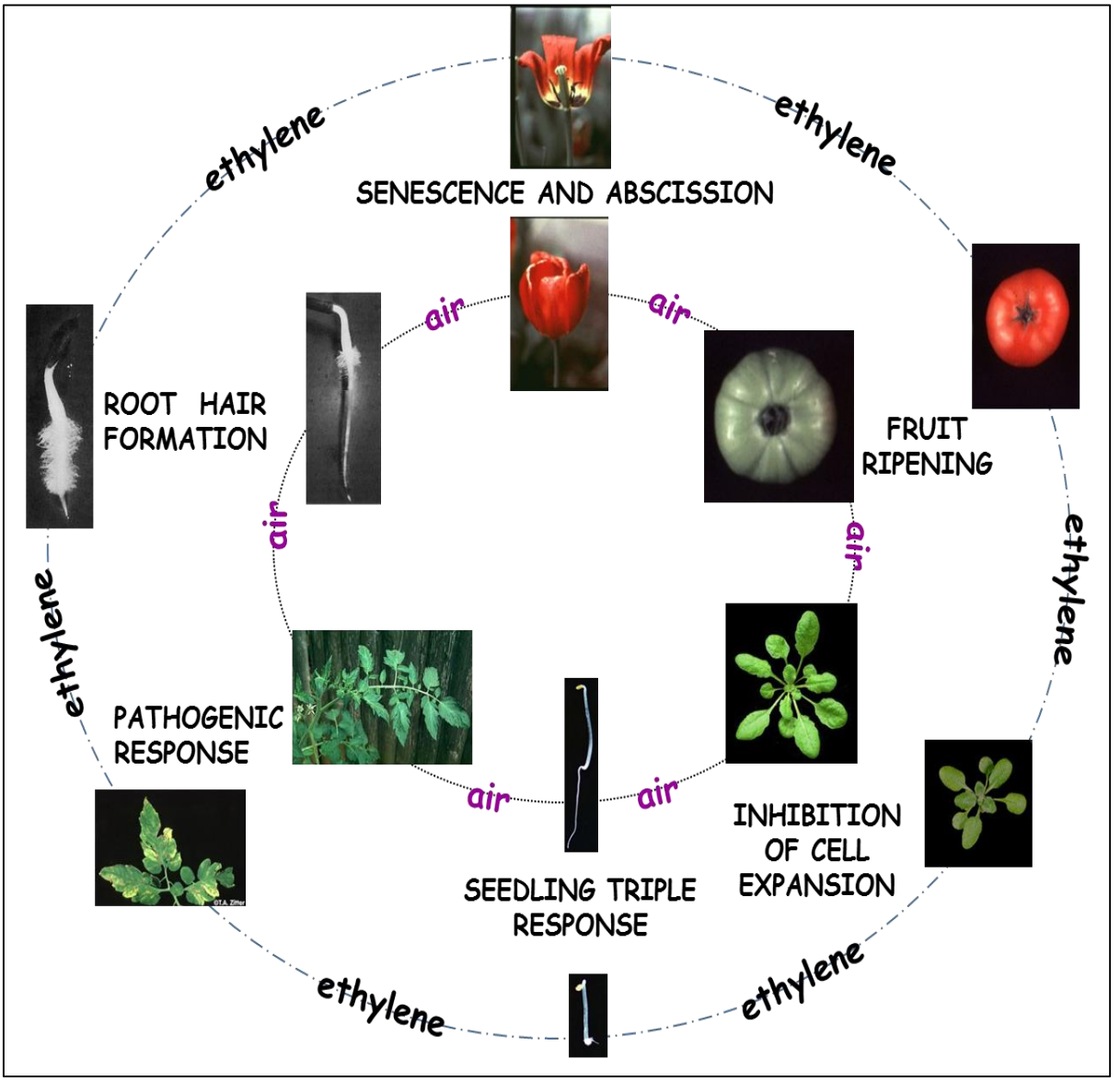

Figure 2.1. Effects of ethylene on different aspects of plant development (Johnson et al., 1998).

through plant architecture. The slow filling rates in a percentage of the grains lower down on a rice spikelet or wheat ear, called inferior grains, have been linked with high rates of ethylene evolution (Yang et al., 2000; Zhao et al., 2007; Zhang et al., 2009).

The commercial implications of ethylene, particularly in fruit ripening, have made this a well-studied hormone. In recent years remarkable progress in genetic, biochemical, and molecular analyzes of ethylene signaling have confirmed earlier physiological studies. An emerging theme from recent studies is that the phytohormone (ethylene) acts as a potentiator or enhancer in many fundamental processes of plant development but is not required for survival.

In the model organism *Arabidopsis thaliana* (as well as many other plants especially in tomato), exposure to high concentration of ethylene induces a trio of morphological changes in dark-grown (etiolated) seedlings, (i) exaggerated curvature of the apical hook, (ii) radial swelling of the hypocotyl, and (iii) inhibited elongation of the hypocotyl and root, called the triple response (Ecker, 1995, Neljubov, 1901). These highly reproducible phenotypes have been used as a powerful tool to isolate mutants that fail to display the triple response to external ethylene (*e*thylene-*in*sensitive or *ein* mutants), or mutants that constitutively show the triple response, even in the absence of ethylene (Bleecker et al., 1988; Guzman et al., 1990). This second class can be further subdivided based on sensitivity to ethylene synthesis inhibitors. Constitutive response mutants whose phenotypes are suppressed by ethylene synthesis inhibitors produce 10-100 fold more ethylene than wild-type seedlings and are called *eth*ylene *o*verproducer (*eto*) mutants. Mutants that display the triple response in the absence of ethylene or ethylene synthesis inhibitors are termed *c*onstitutive *t*riple *r*esponse (*ctr*) mutants (Guzman et al., 1990; Kieber et al., 1993).

2.2.2 Establishment of ethylene as a phytohormone

Ethylene is the simplest of the olefin gasses and was the first known gaseous biological signaling molecule. It is synthesized by plants during certain stages of development and in response to abiotic and biotic stresses. Ethylene affects many aspects of plant growth, development as well as responses to environmental cues. Research leading to the discovery of ethylene as a plant hormone started in the 1800s with scientists examining the effects of the illuminating gas on plants. In 1901, Dimitry Neljubov determined that ethylene be the active component of illuminating gas that affects plants and thus launched this important field of research. It is accepted that in 1934 Richard Gane provided the conclusive evidence that plants biosynthesize ethylene.

This early research showed that ethylene is both biosynthesized and sensed by plants. From the 1930s to the 1960s, there was little research on ethylene as a hormone because many researchers did not believe that ethylene was indeed a plant hormone. Moreover the detection of ethylene emitted from plant was difficult. However, in the late 1950s, the application of gas chromatography led to an increased interest in ethylene research. From the 1960s through the early 1980s, the biochemical pathway for ethylene biosynthesis in plants was elucidated, and membrane-bound ethylene-binding sites were discovered and characterized. The use of *Arabidopsis thaliana* as a model plant system and the widespread use of molecular biological techniques starting in the 1980s correlate with a second and larger increase in ethylene research. In recent years, detailed models for the regulation of ethylene biosynthesis and ethylene signal transduction have emerged. Chuanli et al., (2015) suggested that the genes involved in the ethylene biosynthesis and signaling are conserved throughout the plants starting from the ancestral green algae (charophytes).

2.2.3 ACC (Ethylene precursor) discovery

In 1934, conclusive evidence that ethylene is a natural product from plants was presented by the English scientist (Gane, 1934). It took another 30 years before the primary steps of the ethylene biosynthesis pathway were elucidated **(Fig. 2.2)**. Lieberman and Mapson (1964) first reported that ethylene could be produced from the amino acid methionine, taking advantage of the high rates of ethylene production from apples for their experimental work **(Fig. 2.2)**. Thirteen years later, Adams and Yang (1977) made substantial progress in understanding the biosynthesis pathway of ethylene, when they discovered that S-adenosyl-L-methionine (SAM) was an intermediate between methionine and ethylene. Yang and co-workers also showed that 5'-methylthioadenosine (MTA) was formed as a byproduct from SAM and that MTA could be recycled back to methionine (Murr and Yang, 1975). The elaborated details of the different reaction steps of the methionine cycle in plants, now often referred to as the Yang cycle, was mainly inspired by the biochemical similarities between the plant pathway and the methionine salvage cycle which was already known for prokaryotes, yeast, and mammalians. A comprehensive overview of the methionine and SAM metabolism in plants is provided by Sauter et al. (2013). The major discovery that made the methionine cycle in plants unique from all other organisms was the characterization of 1-aminocyclopropane-1-carboxylic acid (ACC) as the intermediate between SAM and ethylene (Adams and Yang, 1979). Adams and Yang (1979) were able to identify ACC as the precursor of ethylene by feeding experiments on apple tissue, using radiolabeled methionine. Upon incubation of

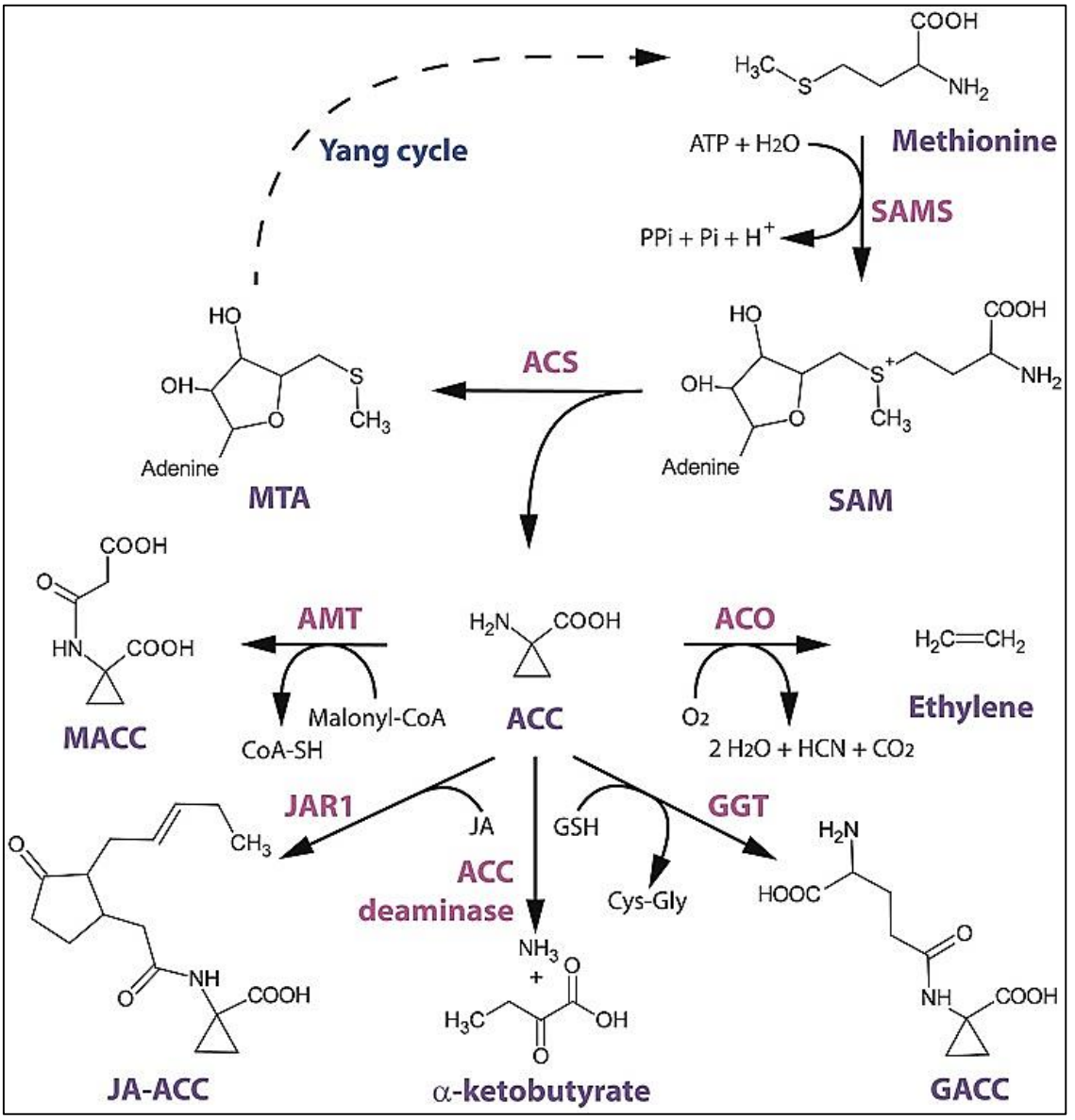

Figure 2.2. Schematic representation of ethylene biosynthesis and ACC conjugation. The amino acid methionine is converted to S-adenosyl-L-methionine (SAM) by SAM-synthetase (SAMS) from ATP. The general precursor SAM is then converted to ACC by ACC-synthase (ACS). The formation of ACC also involves the cleavage of 5-methylthioadenosine (MTA), which is recycled back to methionine by the Yang cycle (dotted line indicates multiple enzymatic steps). ACC is then converted to ethylene by ACC-oxidase (ACO) in the presence of oxygen. ACC can also be converted to its major conjugate 1-malonyl-ACC (MACC) by the yet uncharacterized ACC-N-malonyl transferase (AMT) in presence of malonyl-Coenzyme-A. A second derivate of ACC is γ-glutamyl-ACC (GACC) which is formed by γ-glutamyl-transpeptidase (GGT) involving glutathione (GSH) conversion to Cys-Gly. Another novel derivate of ACC is jasmonyl-ACC (JA-ACC), which is formed by jasmonic acid resistance 1 (JAR1). ACC can also be metabolized by the bacterial (and plant) ACC deaminase into ammonium and α-ketobutyrate (Van de Poel et al., 2014).

Apple disks under anaerobic condition, they observed a shift from ethylene production in air, toward an unknown compound that was retained in the tissue when treated with nitrogen. Evidently, oxygen is obligatory required for oxidation of ACC to ethylene.

By using a pH-dependent ion mobility assay, Yang characterized this unknown component as an amino acid. Subsequently, the component was identified as ACC, using co-migration of synthetic ACC in paper chromatography and paper electrophoresis assay (Adams and Yang, 1979). They further showed that the conversion of radioactively labeled methionine toward ethylene decreased when unlabeled ACC was supplemented. At the same time the conversion of labeled ACC to ethylene was almost not affected when unlabeled methionine was supplemented, suggesting that externally supplied ACC is in fact used to produce ethylene. Additional evidence for ACC being the intermediate precursor between SAM and ethylene was obtained by treating apple tissue with [S]-trans-2-amino-4 (2'-aminoethoxy) trans-3-butenoic acid, also known as AVG (2-amino-ethoxy-vinylglycine), a pyridoxal-5'-phosphate (PLP or vitamin B6) dependent enzyme inhibitor, which was later known to inhibit the enzymatic conversion of SAM toward ACC. The identification of ACC as the precursor of ethylene was a major breakthrough in the understanding of the ethylene biosynthesis pathway in plants, and was part of the foundation for many new discoveries in the field of ethylene biology.

2.2.4 Ethylene biosynthesis

The biosynthetic pathway of ethylene in flowering plants was defined over 30 years ago (Yang and Hoffman, 1984) and includes mainly two committed enzymatic steps. The first, conversion of S-adenosyl methionine (SAM) to 1-aminocyclopropane-1-carboxylate (ACC) and methylthioadenosine (MTA), by the enzyme ACC synthase (ACS) (in an elimination reaction), that requires a pyridoxal phosphate (PLP) as a cofactor. In the second step, ACC is converted to ethylene, CO_2 and hydrogen cyanide by ACC oxidase (ACO). The toxicity of cyanide production is neutralized at the cellular level by the detoxifying enzyme β-cyanoalanine synthase (Yip and Yang, 1988). Recent evidence indicated that the iron center in the ACO active site is also protected from cyanide poisoning. In the presence of oxygen, bicarbonate ion and ascorbate cofactors, ACO breaks the ACC ring and releases the unstable cyanoformate ion, sequestering cyanide until the reaction products have diffused away (Murphy et al., 2014). ACC synthesis is rate limiting for ethylene production during vegetative growth, although ACO activity may be limiting under some conditions (e.g. in fruit and flowers; Yang and Hoffman, 1984).

Biosynthesis of ethylene frequently involves spatial or temporal separation of the two committed reaction steps. A recent study characterized the distribution of ethylene metabolic enzymes and intermediate metabolites in ripening tomato fruits and found the locular gel and central tissues to be sites where intermediates including free and conjugated ACC accumulate, while ACC synthesis is concentrated in central tissues and peak ethylene production to be observed in the fruit's outer (pericarp) layer (Van de Poel et al., 2014). These data suggest that intermediates may be stored in tissue that has limited biosynthetic capacity. Recent work indicates that some cells actively export ACC (Pesquet and Tuominen, 2011), and that at least one amino acid transporter, the LYSINE HISTIDINE TRANSPORTER1 (LHT1) of Arabidopsis (Shin et al., 2014) promotes uptake of extracellular ACC. Additionally, the importance of long-range transport of ACC for optimal ethylene synthesis in specific tissues has been characterized in a number of contexts, particularly flooding and hypoxia (Bradford and Yang, 1980; Van de Poel and Van Der Straeten, 2014).

In Arabidopsis, as well as in other plant species *ACS* and *ACO* genes are encoded by a multigene family. In tomato, to date nine genes encoding the *ACS* (*ACS1A, ACS1B, ACS2-8*) are described (Gapper et al., 2013). The newly released tomato genome sequence reported the presence of another three putative *ACS* genes (Tomato Genome Consortium, 2012). The transcriptional analysis indicates that *ACS1A*, *ACS2*, *ACS4*, *ACS6* are differentially expressed during the ripening process of fruits (Barry et al., 2000; Van de Poel et al., 2012; Gapper et al., 2013). The *ACS6* is primarily involved in system 1 ethylene synthesis and responsible for the basal level of ethylene production in the mature green fruit. The *ACS1A* along with pre-climacteric ethylene synthesis also regulates the ethylene synthesis during the transition from system 1 to system 2. The *ACS4* expression occurs at the onset of ripening and it together with *ACS2* maintains the system II autocatalytic ethylene production. The increased production of ethylene during the ripening causes negative feedback inhibition of system I gene *ACS1A* **(Fig. 2.3)**. Oeller et al. (1991) demonstrated that the suppression of *ACS2* in antisense transgenic plants leads to inhibition of ripening and ethylene production.

Similar to *ACS*, in tomato *ACO* is also encoded by a multigene family consisting of five (*ACO1-5*) genes (Gapper et al., 2013). Analysis of tomato genome sequence indicated that it has another three putative *ACO* genes (Tomato Genome Consortium, 2012). The *ACO1*, *ACO3,* and *ACO4* are differentially expressed during the fruit

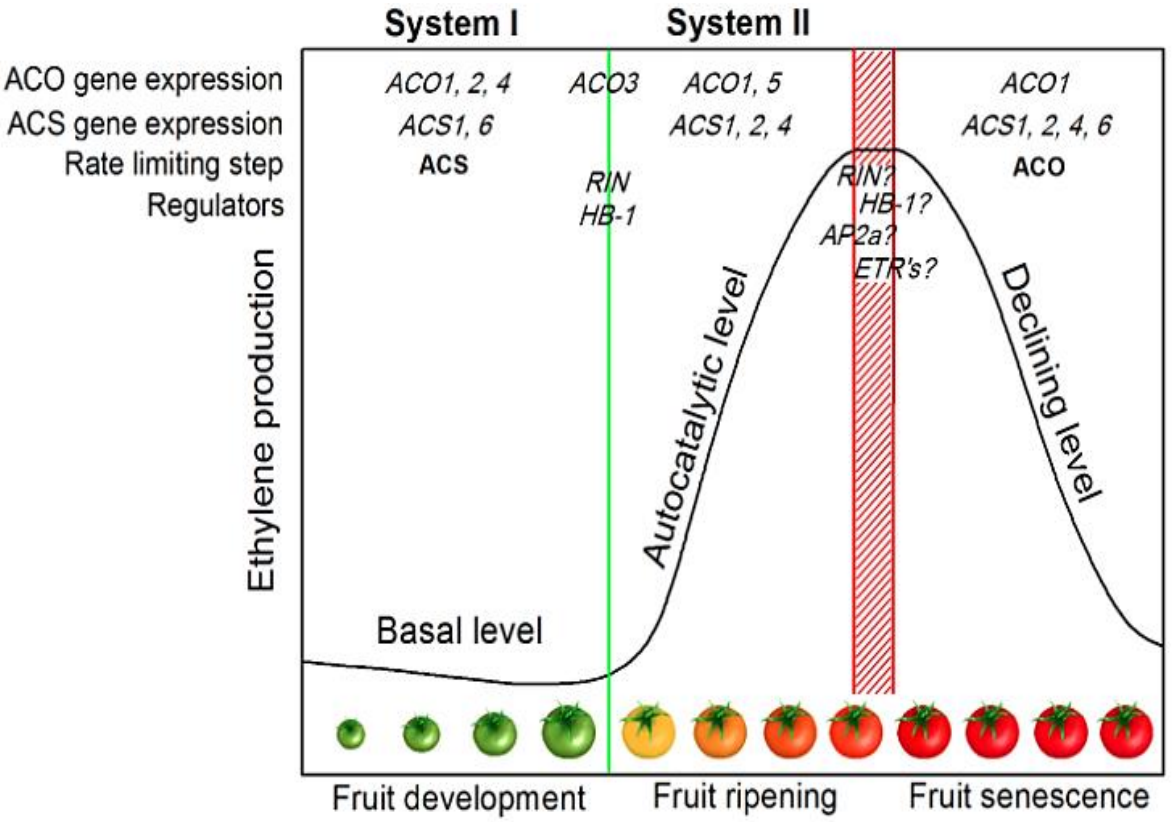

Figure 2.3. Regulation of ethylene biosynthesis during tomato fruit development, ripening and senescence (Van de Poel et al., 2012). The genes contributing to ethylene biosynthesis during system I and II phase, and also during fruit senescence are listed along with regulatory transcription factors.

ripening (Nakatsuka et al., 1998; Van de Poel et al., 2012). The *ACO1* and *ACO4* expressed in all phases (pre-climacteric, climacteric and even in transition phase) of fruit development and their transcript levels increase with the climacteric rise of ethylene **(Fig. 2.3)**. The *ACO3* is expresses at the low level in mature green fruit. Though it gets induced at the onset of ripening, its increase is not sustained during the climacteric phase of ethylene emission. The antisense suppression of *ACO1* prevents the normal ripening with reduced production of ethylene and thus provides an effective mean of regulating the fruit ripening process (Hamilton et al., 1990).

2.2.4.1 ACC synthase (ACS)

On the basis of C-terminal sequences, three types of ACS proteins are recognized. Type I ACS proteins contain in their C-terminal domain one putative calcium-dependent protein kinase (CDPK) phosphorylation target site and three mitogen-activated protein kinase (MAPK) phosphorylation sites (Yoon and Kieber, 2013). Type II ACS proteins only contain the MAPK phosphorylation sites, while type III ACS do not contain any phosphorylation sites (Yoon and Kieber, 2013). These post-translational phosphorylation sites play an important role in the stability of the ACS protein (Chae and Kieber, 2005). Both in Arabidopsis (Chae et al., 2003; Kim et al., 2003; Liu and Zhang, 2004; Wang et al., 2004; Yoshida et al., 2005, 2006; Joo et al., 2008; Christians et al., 2009; Lyzenga et al., 2012) and in tomato (Tatsuki and Mori, 2001; Kamiyoshihara et al., 2010) it was shown that differential phosphorylation of certain ACS members directed the protein for proteasomal degradation. Protein stability of certain ACS members is further regulated by the protein phosphatase 2A (PP2A; Skottke et al., 2011) and PP2C (Ludwikow et al., 2014), demonstrating a complex balance between phosphorylation and dephosphorylation to secure protein activity and stability.

2.2.4.2 ACC oxidase (ACO)

The second ethylene biosynthesis protein is ACC-oxidase (ACO), which converts ACC to ethylene in the presence of oxygen. It took a long time before ACO activity could be demonstrated *in vitro*. The key step (aspect) in isolating ACO was the addition of ascorbic acid (vitamin C) to the extraction media, as was first reported by Ververidis and John (1991) who isolated ACO from melon tissue and quantified in vitro ACO activity. The exact role of ascorbic acid for protein stability/activity remained uncertain till recently (Rocklin et al., 2004). It is new reported, that ascorbic acid participates in the ring opening of ACC, by providing a single-electron to the active site (Murphy et al., 2014). This catalytic reaction releases ethylene and a cyanoformate ion $[NCCO_2]^-$, which

is subsequently decomposed into CO_2 and CN^- (Murphy et al., 2014). The reactive cyanide (CN^-) is subsequently detoxified by β-cyanoalanine synthase to produce β-cyanoalanine (Miller and Conn, 1980). ACO belongs to the superfamily of dioxygenases that require iron (Fe^{2+}) as cofactor and bicarbonate as an activator (Dong et al., 1992; Zhang et al., 2004). The subcellular localization of ACO remains undefined, as some studies localized ACO in the cytosol (Reinhardt et al., 1994; Chung et al., 2002; Hudgins et al., 2006), while other localized ACO at the plasma membrane (Rombaldi et al., 1994; Ramassamy et al., 1998). Although the ACO protein sequence does not contain any predicted transmembrane domains, it is still possible that the protein associates with the plasma membrane via indirect/direct interactions. Expression of different members of the tomato ACO family in *Escherichia coli* showed that each isoform had a specific in vitro enzyme activity (Bidonde et al., 1998).

2.2.5 ACC acts as a metabolic signaling molecule

1-Aminocyclopropane-1-carboxylic acid holds a key position in many physiological processes as it is the direct precursor in the biosynthesis of ethylene. A balanced supply and consumption of ACC is essential to achieve the necessary production level of ethylene within a given spatial and temporal context. The pool of ACC is regulated by a complex interaction of production, consumption, modification, and transport. Interestingly, recent findings suggested an even more important role for ACC, as a signaling molecule independent from ethylene (Yoon and Kieber, 2013). The most information came from examination of Arabidopsis and its mutants.

Xu et al. (2008) investigated the role of ACC as a signaling molecule in relation with FEI1 and FEI2, which are leucine-rich repeat receptor-like kinases. The *fei1 fei2* mutant exhibits a severe defect in anisotropic root growth due to reduced cellulose microfiber content in the cell wall at the root tip. The *fei1 fei2* phenotype was reversed by the application of ethylene biosynthesis inhibitors, but not by ethylene signaling inhibitors. The application of ethylene biosynthesis inhibitors aminooxyacetic acid (AOA) or α-aminoisobutyric acid (AIB) reversed the phenotype of the *fei1 fei2* mutant. Among these two, AOA inhibits of PLP-dependent enzymes, and affects the activity of ACS, resulting in a reduced ethylene production. AIB, on the other hand, is a structural analog of ACC and acts as a competitive inhibitor of ACC for ACO enzyme, preventing ethylene production. In contrast, ethylene signaling inhibitors such as 1-methylcyclopropene (1-MCP) and silver ions, did not affect the *fei1 fei2* phenotype. Similarly, genetic analysis showed that the *fei1 fei2* mutant crossed with *etr1-3* (a mutation

in the ethylene receptor causing severe ethylene insensitivity), or *ein2-50* (a central regulator of ethylene signaling causing ethylene insensitivity) reversed the phenotype. Taken together, this study showed that the typical *fei1 fei2* phenotype was not affected by ethylene signaling, but could be reversed by accumulation of ACC by ethylene biosynthesis inhibitors. This suggested that the signal reversing the *fei1 fei2* phenotype originated independent from ethylene signaling, involved ACS and is possibly ACC itself (Xu et al., 2008).

Tsang et al. (2011) examined ACC signaling with respect to cell elongation and cell wall composition of roots. Specific ethylene biosynthesis inhibitors [AVG, AOA, and 2-anilino-7-(4-methoxy phenyl)-7, 8-dihydro-5(6H)-quinazolinone (7303)] could reverse the inhibition of root cell expansion which was induced by an isoxaben treatment (a cellulose biosynthesis inhibitor causing cell wall stress). Similarly, as observed by Xu et al. (2008), ethylene signaling inhibitor (silver ions) could not reverse the isoxaben-induced reduction in root cell elongation. Also, the *ein3 eil1* ethylene insensitive mutant responded to ACC and isoxaben, providing genetic evidence for an ACC signaling mechanism independent of ethylene signaling. They also showed that the application of ACC without isoxaben, inhibited root cell elongation and was partially ethylene-dependent and partially ethylene-independent. Altogether, their results demonstrated that monitoring of cell wall integrity requires an ACC sensing/signaling mechanism, which can lead to a reduction of root cell elongation when disrupted. Also, Tsang et al. (2011) showed that this inhibition of root cell elongation required auxin and reactive oxygen species (ROS) signaling, downstream of ACC signaling.

Tsuchisaka et al. (2009) made an octuple *acs* mutant to study the interplay between different *ACS* isoforms. The octuple line was created by the introduction of two amiRNA lines (*ACS8* and *ACS11*) into the hexuple mutant *acs2, 4, 5,6,7,9* creating an octuple mutant line with complete or severe inhibition of ACS function. The lines that showed a very strong silencing of *ACS8* and *ACS11* displayed embryo lethality. This suggests that ethylene biosynthesis (or ACC biosynthesis) is essential for Arabidopsis seed viability, while this is not the case for the single (*ctr1* and *ein2*) and double (*ctr1 ein2*) ethylene signaling mutants (Kieber et al., 1993; Roman et al., 1995; Alonso et al., 1999). This phenotypic discrepancy between ethylene biosynthesis and signaling once more suggests that ACC can acts as a signaling molecule itself, independent from ethylene, at least during embryo development and Arabidopsis viability.

Taken together these reports suggest a role for ACC as a signaling molecule to regulate plant development and growth, independent from ethylene. The exact molecular mechanism by which ACC signaling operates, and whether or not there is an ACC receptor and downstream signaling components, remains to be investigated. Future biochemical studies with specific ethylene biosynthesis and signaling inhibitors, in combination with genetics to create higher order ethylene biosynthesis/signaling mutants (like *etr1ers1etr2ein4ers2ctr1ein2* or multiple *aco* knock-outs), could shed light on the role of ACC as a signaling molecule. It also still needs to be elucidated whether this unique title of "signaling molecule" is to be awarded to ACC, or rather to one if it's (unknown) downstream derivatives.

2.2.6 Ethylene signaling cascade

In higher plants, ethylene response pathway consists of ethylene receptors (CTR, EIN2, EIL/EIN3, and EER), and downstream genes. Major breakthroughs in understanding of the ethylene signaling pathway in 1980s and 1990s came with the emergence of Arabidopsis as a model system for plants. The use of Arabidopsis allowed for the genetic dissection of numerous signaling pathways, developmental processes, and metabolic pathways (Somerville and Koornneef 2002; Koornneef and Meinke 2010). Bleecker et al. (1988), isolated Arabidopsis ethylene response (*etr*) mutants by genetic screening. The screen was based on the triple response of etiolated pea seedlings that Neljubow had observed 100 years earlier. Bleecker's screen yielded a dominant ethylene-insensitive mutant, *etr1-1*, and the first ethylene response mutant in Arabidopsis (Bleecker et al., 1988).

Subsequent to isolation of *etr* mutant in the early 1990s, Chang together with Bleecker used chromosome walking to identify the *ETR1* gene (Chang et al., 1993). *ETR1* was among the first genes to be isolated by map-based cloning in Arabidopsis and the first plant hormone receptor gene to be cloned in any plant. The *ETR1* sequence showed similarity to the two-component family of histidine kinase receptors widely found in prokaryotes (Chang et al., 1993); *ETR1* was the first two-component homolog identified in a higher eukaryote (Koshland, 1993). Because of the similarity to this prokaryotic receptor family, it was speculated that *ETR1* might encode an ethylene receptor. Subsequently, Eric Schaller demonstrated that the ETR1 protein is a homo-dimer capable of binding ethylene and that binding was disrupted by the *etr1-1* mutation (Schaller and Bleecker 1995; Schaller et al., 1995). This was a breakthrough, as ethylene

binding by ETR1 was directly linked to ethylene responses through the *etr1* mutant phenotype.

Soon after the isolation of the *etr1-1* mutant, Ecker's laboratory isolated many additional mutants that helped to elucidate the ethylene signaling pathway. They screened two different kinds of mutants based on the triple response assay: ethylene-insensitive (*ein*) mutants that lack the triple response phenotype and constitutive triple response (*ctr*) mutants that display the triple response even in the absence of ethylene treatment (Guzman and Ecker 1990; Kieber et al., 1993; Roman et al., 1995). In addition to new dominant alleles of *etr1* (*ein1*), they isolated mutants of *ein2*, *ein3*, *ein4*, *ein5*, *ein6*, *ein7*, and *ctr1* (all recessive).

On the basis of genetic epistatic relationships, these mutants were placed in ethylene response pathway that suggested the relative order of action of each of above components (Roman et al., 1995; Kieber et al., 1993). The recessive *ein* mutants acted at or down-stream of *ctr1*, which acted at or down-stream of the dominant mutants **(Fig. 2.4A)**. Many molecular details have since been added to this framework (Merchante et al., 2013; Shakeel et al., 2013) **(Fig. 2.4B, C)**, based on cloning of the corresponding genes followed by functional studies ranging from genetic analyses of mutants to cellular and biochemical analyses of the encoded proteins.

2.2.6.1 Ethylene Receptors

Soon after the cloning of *ETR1*, it was discovered that ETR1 belongs to a family of homologous ethylene receptors in plants. Arabidopsis has five members **(Fig. 2.4A)**, whereas tomato has seven (Klee 2004). The most closely related *ETR1* homolog, *ETHYLENE RESPONSE SENSOR* (*ERS1*), was discovered by Hua et al. (1995) by screening an Arabidopsis DNA library for clones that hybridized with an *ETR1* probe. In the absence of a mutant phenotype for *ERS1*, a mutation analogous to the dominant mutation of *etr1-4* was introduced into an *ERS1* transgene, creating a dominant mutant version of *ERS1* that conferred ethylene insensitivity similar to that of *ETR1*. It was confirmed a decade later that *ERS1* and the other Arabidopsis ethylene receptors (ETR2, EIN4, and ERS2) bind ethylene (O'Malley et al., 2005).

The *ETR2* ethylene receptor gene was discovered serendipitously in a chromosome walk to clone an unrelated gene by Sakai et al. (1998). Upon realizing the sequence similarity between an unidentified gene within the walk and the *ETR1* gene, Sakai et al. (1998) undertook experiments that revealed that the gene corresponded to an unpublished, dominant ethylene-insensitive mutant, *etr2-1*, which had been isolated by

Bleecker. Using *ETR2* as a probe, Hua et al. (1998) isolated the *EIN4* and *ERS2* ethylene receptor genes via hybridization screening of an Arabidopsis DNA library. *EIN4* corresponded to the dominant ethylene-insensitive *ein4-1* mutant isolated by Roman et al. (1995). For *ERS2*, a dominant ethylene-insensitive phenotype was obtained using *ERS2* transgenes carrying dominant mutations analogous to that of *etr2-1* and *ein4-1* (Hua et al., 1998).

Identification of the ethylene receptors was followed by more than a decade of intense characterization. Ethylene receptors have a hydrophobic N-terminal domain comprising the ethylene-binding domain (Schaller and Bleecker 1995; Rodriguez et al., 1999; O'Malley et al., 2005; Hall et al., 1999), followed by a cytosolic GAF domain, which plays a role in protein–protein interactions between the receptors (Xie et al., 2006; Grefen et al., 2008; Gao et al., 2008). Following, the GAF domain is a histidine kinase domain, and in some of the ethylene receptors, a C-terminal receiver domain. (Receptors named ERS lack a receiver domain.) The ethylene receptors are disulfide-linked homodimers that exist in clusters (Schaller et al., 1995; Hall et al., 2000; Takahashi et al., 2002; Gao et al., 2008; Chen et al., 2010) localized at the ER membrane (Chen et al., 2002) and the Golgi apparatus membrane (Dong et al., 2008). It is thought that one ethylene molecule is bound per receptor dimer (Schaller et al., 1995; Rodriguez et al., 1999).

The Arabidopsis ethylene receptors are further classified into two sub-families. Subfamily I receptors (ETR1 and ERS1) are predicted to contain three N-terminal transmembrane domains and histidine autokinase activity (ERS1 also has serine/threonine kinase activity) (Gamble et al., 1998; Moussatche and Klee, 2004; Chen et al., 2009). Subfamily II receptors (ETR2, ERS2, and EIN4) are predicted to have four N-terminal transmembrane domains and a less conserved histidine kinase domain that displays serine/threonine kinase activity (Gamble et al., 1998; Moussatche and Klee 2004; Chen et al., 2009). There is debate regarding the extent to which the kinase domain plays a role in ethylene signaling (Gamble et al., 2002; Wang et al., 2003; Hall and Bleecker 2003; Qu and Schaller 2004; Hall et al., 2012). Auto-phosphorylation of the receiver domain is believed to play a minor role in ethylene response (Wang et al., 2003) but the receiver domain appears to play a role in recovery following exposure to ethylene (Binder et al., 2004b; Kim et al., 2011). The exact signaling mechanism of the receptors is still unknown.

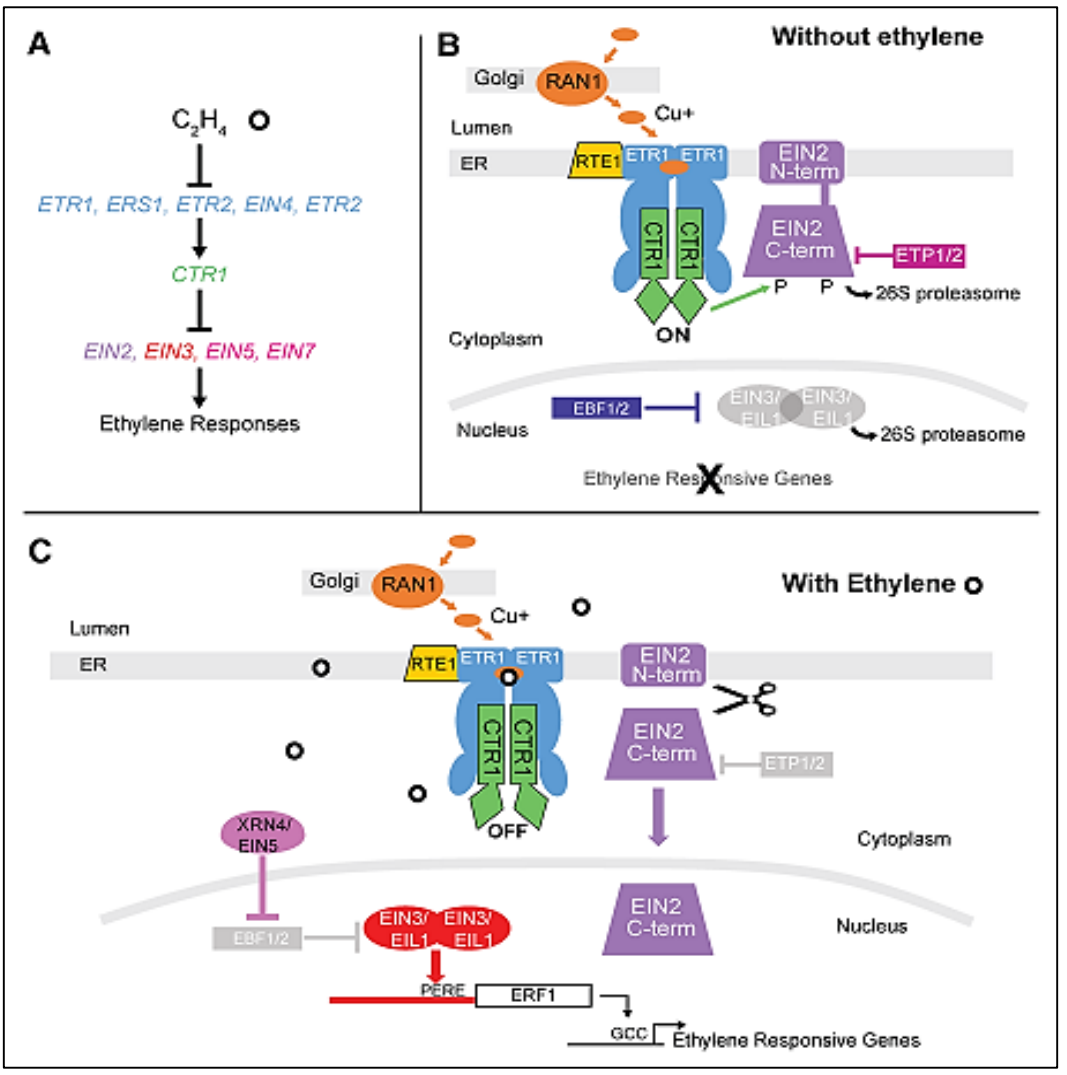

Figure 2.4. Illustration of the ethylene signal transduction pathway in Arabidopsis. **(A)** Ethylene signaling pathway based on mutants and their genetic epistatic relationships. **(B)** The current view of the ethylene signaling without ethylene and **(C)** with ethylene. Ethylene (white circle) is perceived by a family of five receptors represented here by the ETR1 dimer. Copper (orange oval), transported by RAN1, serves as a cofactor for ethylene binding and is required for proper biogenesis of the receptors. Interaction of RTE1 with ETR1 (but not the other ethylene receptors) is believed to promote the signaling conformation of ETR1. In **B**, in the absence of ethylene binding, ETR1 activates the associated CTR1 protein kinase, which phosphorylates the C-terminus (C-term) of EIN2, potentially leading EIN2 to be targeted for degradation by two F-box proteins (ETP1 and ETP2) via the 26S proteasome. Consequently, two F-box proteins, EBF1 and EBF2 (EBF1/2), target the key transcription factors EIN3 and EIL1 for degradation by the 26S proteasome preventing downstream ethylene signaling from occurring. In **C**, when ethylene is bound, the receptors no longer activate CTR1, allowing the unphosphorylated EIN2 C-term to be cleaved (by an unknown protease) and translocated into the nucleus where it plays a role in activating downstream responses. The EBF1/2 F-box proteins are somehow repressed, involving the general exoribonuclease XRN4 (also called EIN5/EIN7), and thus the EIN3/EIL1 proteins are now stabilized. EIN3/EIL1 homodimers bind to the PERE element of target genes, such as ERF1, activating their expression. Also, the expressed ERF1 transcription factor binds to the GCC-box in the promoters of additional ethylene-responsive genes leading to ethylene responses (Bakshi et al., 2015).

Although the mechanisms of ethylene receptor signaling are not entirely understood, genetic analyzes have revealed that the ethylene receptors are negative regulators of ethylene signaling. This conclusion is based on the isolation of recessive loss-of-function mutations in the ethylene receptor genes in Arabidopsis by Hua and Meyerowitz (1998) and later by Qu et al. (2007). These studies showed that the receptors have some functional redundancy, which explains why no recessive mutations and only dominant gain-of-function mutations were obtained from genetic screens. Hua and Meyerowitz (1998) created a quadruple mutant of four of the receptor genes, and found that the mutant confers constitutive ethylene responses. Therefore, by deduction, functional ethylene receptors must repress ethylene responses (in the absence of ethylene binding) whereas ethylene binding inactivates the receptors resulting in ethylene responses. This is known as the inverse agonist model (Hall et al., 1999).

Soon after demonstrating that ETR1 binds ethylene, the Rodriguez et al. (1999) demonstrated that the binding requires a copper cofactor, confirming an earlier prediction that a transition metal is likely needed for ethylene binding. About the same time, RESPONSIVE-TO-ANTAGONIST1 (RAN1), a copper-transporting P-type ATPase homologous to the human Menkes/Wilson proteins, was shown to be required for the biogenesis of the ethylene receptors (Hirayama et al., 1999; Woeste and Kieber 2000; Binder et al., 2010) **(Fig. 2.4B, C)**. The first *ran1* mutants were isolated in a genetic screen originally aimed at identifying ethylene receptor mutants that respond to a competitive inhibitor of ethylene (before *ETR1* was found to encode the ethylene receptor). The screen instead yielded mutants that alter the ethylene receptor indirectly as a result of reduced availability of copper ions. The strongest *ran1* mutant allele confers constitutive ethylene responses, which are thought to arise from the receptors being improperly folded and non-functional without the copper cofactor (Woeste and Kieber 2000).

Another ethylene receptor modifier, REVERSION-TO-ETHYLENE-SENSITIVITY1 (RTE1), was identified in a genetic screen for suppression of ethylene insensitivity of an *etr1* mutant (Resnick et al., 2006) **(Fig. 2.4B, C)**. Though its biochemical function is unknown, RTE1 appears to specifically target the ETR1 receptor (Resnick et al., 2006; Zhou et al., 2007; Rivarola et al., 2009; Dong et al., 2010) and may play a role in ETR1 folding, keeping ETR1 functionally active (Resnick et al., 2008). *RTE1* is homologous to tomato *Green-ripe*, found through a dominant ethylene-insensitive mutant in which Green-ripe is overexpressed (Barry and Giovannoni 2006).

In tomato, ethylene receptor family is expanded to seven members comprising of ETR1, ETR2, ETR3 (NR), ETR4, ETR5, ETR6, and ETR7 (Solyc05g055070) and all these have similar binding affinities to ethylene (Tieman and Klee, 1999; Adams-Phillips et al., 2004a; O'Malley et al., 2005, Tomato Genome Consortium, 2012). Similar to Arabidopsis, tomato ethylene receptor family is divided into two subfamilies. In tomato, ETR1, ETR2 and ETR3 (NR) represent subfamily 1, while ETR4, ETR5, and ETR6 receptors lacking His–kinase domain and having an additional transmembrane domain represent subfamily 2. Unlike Arabidopsis, in tomato only ETR3 (NR) lacks receiver domain.

2.2.6.2 The role of CTR1 Protein Kinase in the Ethylene Receptor Complex

The *CTR1* gene encoding a serine/threonine protein kinase was the first gene reported in the ethylene signaling pathway (Kieber et al., 1993). The *CTR1* was cloned by using a T-DNA insertion tag combined with genetic mapping of *ctr1*. The constitutive triple response phenotype of *ctr1* mutants indicated that *CTR1* is a negative regulator of ethylene responses (that is, CTR1 kinase activity represses ethylene responses). The epistasis analysis indicated that *CTR1* acts at or down-stream of the ethylene receptors (Roman et al., 1995) **(Fig. 2.4A)**. Currently it is known that N-terminal regulatory domain of CTR1 physically associates with the ethylene receptors (Clark et al., 1998; Cancel and Larsen, 2002; Gao et al., 2003), and that this interaction is required for CTR1 kinase activity (Huang et al., 2003). Nonetheless, how the receptors activate CTR1 is still not understood, however ETR1 histidine kinase activity does not seem to be involved (Gao et al., 2003).

Till recently, the substrate of CTR1 phosphorylation was not identified. The CTR1 sequence is closely similar to that of the Raf family of protein kinases, which are MAPKKKs (Kieber et al., 1993). Therefore, CTR1, is often referred as a "Raf-like kinase," presumably act in a canonical MAPK pathway. Though candidate MAPKKs/MAPKs have been proposed (Ouaked et al., 2003; Yoo et al., 2008; Novikova et al., 2000); so far no CTR1-containing MAPK pathway has been conclusively identified. The discovery that CTR1 phosphorylates EIN2 (described below) suggests that the primary ethylene signaling pathway does not require an MAPKK substrate for CTR1.

In contrast to Arabidopsis where a single *CTR* gene is present, in tomato four *CTR*s (*CTR1*, *CTR2*, *CTR3* and *CTR4*) genes have been identified (Adams-Phillips et al., 2004a, 2004b). Genetic complementation analysis of Arabidopsis *ctr1* mutation suggested that the tomato *CTR1*, *CTR2*, and *CTR3* are functionally redundant and play a role in

ethylene response. The *CTR2* is more similar to Arabidopsis *EDR1* (*Enhanced Disease Resistance 1*) which plays role in disease resistance, stress responses, and ethylene-induced leaf senescence (Adams-Phillips et al., 2004a, 2004b; Tang et al., 2005). The expression analysis of *CTRs* genes indicated that these genes are differentially expressed in different tissue and also in response to ethylene (Adams-Phillips et al., 2004b). Among them, *CTR1* is highly expressed and is induced during ripening and on exposure to ethylene (Adams-Phillips et al., 2004a). The silencing of *CTR1* using VIGS in tomato induced constitutive ethylene responses including epinasty and upregulation of ethylene-induced genes (Liu et al., 2002; Fu et al., 2005).

2.2.6.3 The EIN2 Protein Bridges the ER Membrane and the Nucleus

The *EIN2* gene, which was the last of the central ethylene pathway genes to be identified, was cloned by map–based cloning by Alonso et al. (1999). The biochemical function(s) of EIN2 have remained elusive. The N-terminus of EIN2 consists of twelve predicted transmembrane domains that show sequence similarity to Nramp metal ion transporters (Alonso et al., 1999), but it is unclear whether EIN2 is capable of transporting metals. The EIN2 C-terminal portion consists of a plant-specific domain that activates downstream ethylene responses by an unknown mechanism (Alonso et al., 1999).

The epistatic relationship between *ein2* and *ctr1* indicated that *EIN2* acts at or downstream of *CTR1* (Roman et al., 1995) **(Fig. 2.4A)**, and till now, the ethylene signaling pathway has been depicted with EIN2 being controlled by a putative CTR1-containing MAPK pathway (Gray, 2004). Additionally, EIN2 was predicted to localize to the nuclear membrane so that it would be able to signal to the transcription factor EIN3, the next known downstream component of the pathway. Consequently, models of the ethylene signaling pathway often showed EIN2 situated at the nuclear membrane (Gray, 2004). In 2009, a decade after the *EIN2* gene was cloned, and that EIN2 was localized to the ER membrane by Bisson et al. (2009). Given this finding, there was now a physical gap that needed to be bridged between the ER membrane-localized EIN2 and EIN3 in the nucleus.

Chen et al. (2011) provided a critical breakthrough in understanding how EIN2 is regulated by the proteomic study of ethylene-treated and untreated Arabidopsis seedlings using mass spectrometry. A goal of the study was to identify missing pathway components that could not be obtained through genetic screens or other means, but it instead offered hints that the EIN2 C-terminal domain might be differentially

phosphorylated in response to ethylene (Chen et al., 2011). In the ethylene-treated samples, no phosphorylation of EIN2 was detected, but in the untreated samples, phosphorylation of conserved residues of EIN2 was detected. Given that CTR1 was known to be an active protein kinase in the absence of ethylene, CTR1 was a logical candidate for directly phosphorylating EIN2. Ju et al. (2012) showed that CTR1 can interact with and directly phosphorylate EIN2 **(Fig. 2.4B, C)**. They additionally showed that preventing phosphorylation on a particular serine residue results in constitutive ethylene responses. A similar result was shown for a different EIN2 serine residue by Qiao et al., (2012). This indicated that the lack of phosphorylation of EIN2 activates EIN2 signaling, whereas phosphorylation serves to keep EIN2 inactive.

Another breakthrough was the discovery by three different groups that in the presence of ethylene, the C-terminus of EIN2 is proteolytically cleaved and moves into the nucleus (Qiao et al., 2012; Wen et al., 2012; Ju et al., 2012) **(Fig. 2.4B, C)**. The cleavage appears to be controlled by phosphorylation of EIN2 by CTR1, because preventing phosphorylation with alanine substitutions results in constitutive cleavage and nuclear translocation of the C-terminus of EIN2, concomitant with constitutive ethylene responses (Qiao et al., 2012; Wen et al., 2012; Ju et al., 2012). This cleavage and translocation provide a mechanism by which the ethylene signal is transmitted from the site of perception at the ER membrane into the nucleus, filling an important gap in the pathway. The phosphorylation of EIN2 by CTR1, together with cleavage of EIN2 and translocation of the EIN2 C-terminal domain into the nucleus, represented significant advances in understanding the ethylene signaling pathway shown in **Figure 2.4**.

Additional progress came from protein–protein interaction studies. Screening for proteins interacting with the C-terminus of EIN2, Qiao et al., (2009) discovered two F-box proteins, ETP1 and ETP2 (EIN2-TARGETING PROTEIN 1/2), targeting EIN2 for degradation in the absence of ethylene. The C-terminal domain of EIN2 was also found to physically interact with the kinase domain of all five Arabidopsis ethylene receptors (Bisson and Groth, 2010). The ER-localized ethylene receptor complex, therefore, contains both CTR1 and EIN2. The biological relevance of the EIN2-receptor association is unknown, in addition to understanding the function of the cleaved EIN2 C-terminus in the nucleus and its connection to the regulation of EIN3.

Wang et al. (2007) demonstrated that *EIN2* gene is differentially expressed in leaf and at different developmental stages of fruits. In fruits, the *EIN2* gene expresses at

mature green (MG) and breaker stage (BR), and then rapidly declines during subsequent ripening suggesting that the expression of *EIN2* gene is independent of ethylene.

2.2.6.4 The EIN3 Transcription Factor and its Regulation

The next known downstream component in the ethylene pathway is ETHYLENE-INSENSITIVE3 (EIN3), a plant-specific transcription factor and a positive regulator of ethylene responses. Chao et al. (1997) cloned *EIN3* by plasmid rescue based on a T-DNA insertion mutant. Genetic epistasis had placed *EIN3* (as well as *EIN2* and *EIN5*) at or downstream of *CTR1* (Roman et al., 1995), and further analyses placed *EIN3* downstream of *EIN2* and *EIN5* (Guo and Ecker 2003). Using *EIN3* as a hybridization probe, Chao et al. (1997) isolated the homolog EIN3-LIKE (EIL1), which is partially redundant with EIN3 (An et al., 2010; Binder et al., 2007).

Guo and Ecker, (2003) found that EIN3 protein levels are highly responsive to ethylene; EIN3 starts accumulating within 15 minutes of ethylene treatment and is turned over within 30 minutes after removal of ethylene treatment. The key regulatory mechanism underlying this response was discovered simultaneously by three groups (Guo and Ecker, 2003; Potuschak et al., 2003; Gagne et al., 2004). Using protein–protein interaction screens, EIN3-BINDING F-BOX PROTEIN1 and 2 (EBF1/2) were found to interact with and target EIN3 for degradation by the 26S proteasome. This post-translational regulation of EIN3 and the similar regulation of EIL1 (An et al., 2010) were the major findings that explained how ethylene responses could be so rapid. Regulation of protein turnover is now known to be a common feature in many phytohormones signaling pathways (McSteen and Zhao, 2008).

Regulation of EIN3 and EIL1 is more complex and there are regulators whose functions are yet to be understood. For example, *EIN5*, encodes a 5′ to 3′ exoribonuclease known as *EXORIBONUCLEASE4* (*XRN4*) (also allelic with *ein7*) (Potuschak et al., 2006; Olmedo et al., 2006). EIN5 appears to regulate *EBF1/2* expression indirectly, consequently affecting EIN3 protein levels (Potuschak et al., 2006; Olmedo et al., 2006). However, the mechanism for this regulation is not yet understood.

In tomato four members of *EILs* (*EIL1*, *EIL2*, *EIL3*, and *EIL4*) gene are reported (Tieman et al., 2001; Yokotani et al., 2003). The *EIL1*, *2* and *3* are functionally redundant and capable of complementing to *ein3-1* mutant of Arabidopsis (Tieman et al., 2001). These genes express independently of ethylene, and their levels do not increase during ripening or even after exogenous application of ethylene. The *EIL4* shows fruit-specific expression and is abundantly present in fruits. The antisense suppression of

EIL1-3 exhibited ethylene insensitive phenotype (Tieman et al., 2001; Yokotani et al., 2003; Chen et al., 2004). The over-expression of *LeEIL1*::*GFP* in the *Nr* mutant restored the ripening and induced the expression of a subset of the ripening-related gene (Chen et al., 2004).

2.2.6.5 Downstream of *EIN3* transcription factor/*ERF* (*Ethylene Response Factor*)

Currently it is believed that there is a largely linear changes take place in primary signaling events for ethylene, although, non-linear models that invoke feedback are now being explored. Downstream of EIN3 and EIL1, a second level of transcriptional regulation was uncovered resulting in a complex web of transcriptional regulation to modulate diverse responses to ethylene. For instance, in the tobacco EREBPs was discovered that EIN3 and EIL1 are responsible for activating Arabidopsis EREBP genes. In particular, the Arabidopsis ETHYLENE RESPONSE FACTOR1 (ERF1) is a GCC-box-binding transcription factor that was found by Solano et al. (1998) on the basis of homology to tobacco EREBP1, which had been purified by Ohme-Takagi and Shinshi (1995). Solano et al. (1998) found that dimerized EIN3 binds directly to a conserved ethylene response element in the promoter region of *ERF1* (PERE element), activating expression of the *ERF1* gene. In turn, the ERF1 protein binds to the GCC-box in the promoters of secondary target genes, such as chitinase and PDF1.2. This finding is linked ethylene perception and the entire signaling pathway to a transcriptional cascade that controls downstream responses to ethylene **(Fig. 2.4C)**.

In Arabidopsis, 145 *ERF* genes are reported which are involved in a broad range of developmental process (Gutterson and Reuber, 2004). In tomato 85 *ERF* genes present, in which 57 genes are differentially expressed during the different stages of fruit development (Sharma et al., 2010). To date several *ERF* genes (*ERF1-4*, *3b*, *Pti4*, *ERF6*, *AP2a*) have been described and their role in fruit development and ripening are investigated at molecular level (Tournier et al., 2003; Pirrello et al., 2006; Chen et al., 2008; Chung et al. 2010; Lee et al., 2012). The expression of *ERF2, 3b,* and *Pti4* genes are induced during fruit ripening. The accumulation of *ERF3b* transcript is induced before the onset of ripening and after that its level decreases. The transcripts of *ERF2* and *Pti4* genes are almost absent in ripening impaired *rin*, *nor* and *Nr* mutants, whereas *ERF3b* transcript level is stimulated in ethylene under-producing fruits of *ACC oxidase* anti-sense line and *Nr* mutant. The overexpression of *ERF2* exhibited enhanced ethylene response with exaggerated hook formation in seedlings while its suppression caused no visible

phenotype (Pirrello et al., 2006). Two other ERF *AP2a* and *ERF6* are characterized in tomato serving as negative regulators of ethylene and carotenoids biosynthesis in fruits (Chung et al., 2010; Lee et al., 2012).

2.3 Fruit ripening

Fruit ripening is a complex metabolic process regulated by the interaction of phytohormones, transcriptional regulators and various biological (pathogen, wound) and environmental factors (temperature, light). During ripening fruit undergoes several ripening-associated changes such as color, flavor, texture, aroma and susceptibility to the pathogens. Recent advances in molecular genetics and introduction of high throughput technologies like transcriptomics, proteomics and metabolomics have further expanded the information regarding the molecular events associated with fruit development and ripening.

2.3.1 Tomato: A model for climacteric fruit ripening

The **climacteric** is a stage of fruit ripening associated with increased ethylene production and a rise in cellular respiration (Alexander and Grierson, 2002; Seymour et al., 2013) **(Fig. 2.5)**. Apples, bananas, melons, apricots, tomatoes come under climacteric fruit category **(Fig. 2.6)**. Citrus, grapes, strawberries are non-climacteric (they ripen without ethylene and respiration bursts). The non-climacteric fruits like melons, apricots, grapes, and strawberries though have several active ethylene receptors but do not respond to ethylene for stimulating ripening. Climacteric is the final physiological process that indicates the end of fruit maturation and the starting of fruit ripening process. Its defining point is the sudden rise in respiration of the fruit and normally takes place without any external influences. After completion of the climacteric phase, respiration rates (noted by carbon dioxide production) return to or below the point before the event. The climacteric event also leads to other changes in the fruit including pigments alteration and sugar accumulation. For those fruits raised as food, the climacteric event marks the peak of edible ripeness, with fruits having the best taste and texture for consumption. After the event, fruits are more susceptible to fungal infections (invasion) and begin to degrade with cell death.

2.3.2 Physiological changes during fruit ripening

Anatomically, fruits are swollen ovaries that may also contain associated flower parts. Their development follows fertilization and occurs simultaneously with seed maturation. Initially, fruits enlarge through cell division and then by increasing cell

volume. Finally the embryo matures and the seed accumulates storage products, acquires desiccation tolerance, and loses water and the fruit fully ripens.

2.3.3 Biochemical changes during fruit ripening

2.3.3.1 Carotenoids accumulation

The change of color from green to red is a crucial indicator of tomato ripening. This change is associated with the degradation of chlorophylls and the shift of the carotenoid composition from leaf-like xanthophylls (mainly lutein and neoxanthin) to carotenes (mainly phytoene, lycopene and β-carotene) as described by Fraser et al. (1994). Time-lapse imaging showed that in the fruit tissues, the degradation of chlorophylls is slow, while the accumulation of red carotenoids is rapid (Egea et al., 2011). The carotenoid biosynthetic pathway in tomato is well described (Hirschberg, 2001; Giuliano, 2014) and is detailed in **Figure 2.7**. The first committed step is the condensation of two molecules of geranylgeranyl diphosphate (GGPP) to form the colorless carotene 15-cis-phytoene, a reaction catalyzed by phytoene synthases (PSY); 15-cis-phytoene is then desaturated and isomerized to all-trans-lycopene through the action of two desaturases and two isomerases: phytoene desaturase (PDS), ζ-carotene desaturase (ZDS), pro-lycopene isomerase (CRTISO) and ζ-carotene isomerase (ZISO). The formation of δ-carotene and γ-carotene from lycopene are catalyzed by lycopene ε-cyclase (ε-LCY) and β-cyclases (β-LCY and CYC-β), and then the orange α-carotene and β-carotene are synthesized by β-cyclases.

Finally, these carotenes are transformed into lutein and zeaxanthin by heme and non-heme β-carotene hydroxylases (CYP97 and CRTR-b). Zeaxanthin is converted to violaxanthin by the action of zeaxanthin epoxidase (ZEP) and further to neoxanthin by the action of the NXD and ABA4 proteins. These two xanthophylls are cleaved by 9-cis-epoxycarotenoid dioxygenase (NCED), a key enzyme in the biosynthesis of ABA (Ji et al., 2014).

The carotenoid biosynthesis pathway could be divided into two parts, upstream of lycopene and down-stream of lycopene **(Fig. 2.7)**. In the upstream part, the key rate-limiting steps are catalyzed by PSY1, PDS, ZDS, ZISO and CRTISO (Fraser et al., 1994; Giuliano et al., 1993; Fantini et al., 2013). The expression of *Psy1*, *Ziso*, and *Crtiso* is directly regulated by the ripening inhibitor (RIN) protein, which is a member of the MADS-box family of transcription factors (Martel et al., 2011; Fujisawa et al., 2013). In the downstream part, lycopene cyclases (ε-LCY, β-LCY/CYC-β) are also key enzymes,

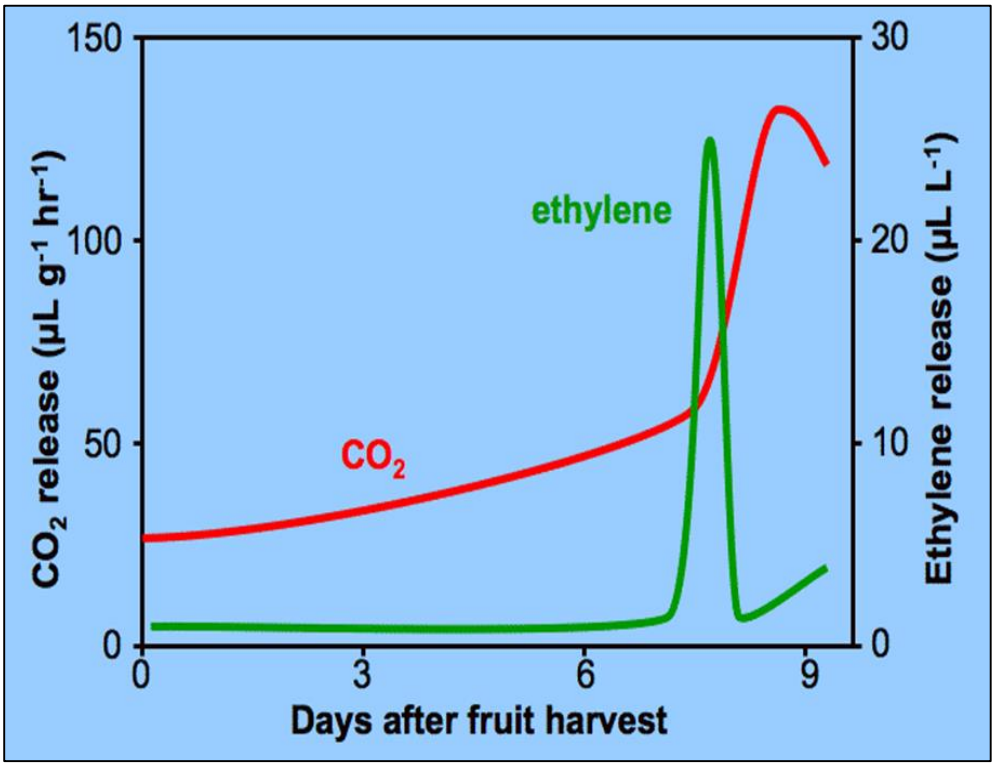

Figure 2.5. Graphical representation of climacteric fruit ripening. The fruit ripening involves a spike in respiration correlating with a burst of ethylene synthesis.

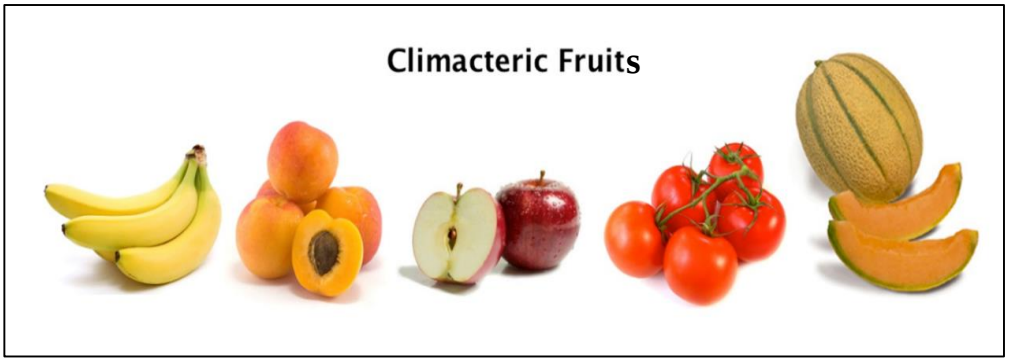

Figure 2.6. Examples of climacteric fruits.

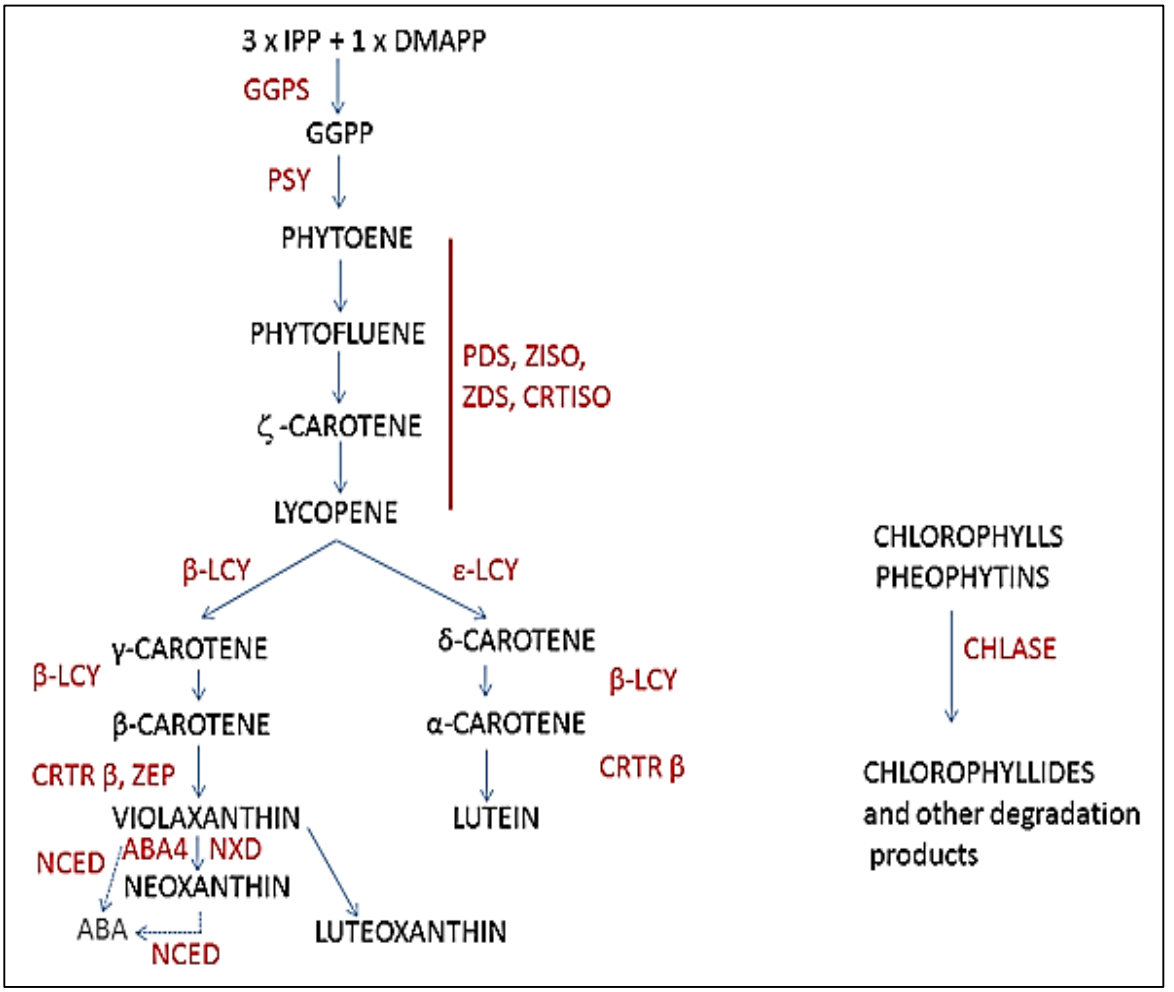

Figure 2.7. Carotenoid biosynthetic pathway (Giuliano, 2014). Names of intermediate compounds are in black and names of enzymes are in red. IPP = isopentenyl diphosphate, GGPS = GGPP synthase, GGPP = geranyl-geranyl pyrophosphate, PSY = phytoene synthase, PDS = phytoene desaturase, ZISO = zeta-carotene isomerase, ZDS = zeta-carotene desaturase, CRTISO = carotenoid isomerase, ε-LCY = lycopene ε-cyclase, β-LCY = lycopene β-cyclase, CRTR-β = β-carotene hydroxylase, ZEP = zeaxanthin epoxydase, NXD = neoxanthin synthase, CHL = chlorophyllases, ABA = abscisic acid (Su et al., 2015).

catalyzing the transformation of lycopene to δ-and β-carotene (Ronen et al., 1999; Ronen et al., 2000; Rosati et al., 2000; Ma et al., 2011).

2.3.3.2 Cell wall modification and softening

Firmness and juiciness are the most important textural components in the case of fleshy fruits (Toivonen and Brummell, 2008). Both features are largely determined by the characteristics of parenchyma cells (shape and size, cell wall thickness and strength, cell turgor) and the extent and strength of adhesion areas between adjacent cells (Harker et al., 1997). During ripening, parenchyma cell walls are extensively modified, altering their mechanical properties, and cell adhesion is significantly reduced as a result of middle lamella dissolution. Cell wall and middle lamella modifications leading to fruit softening arise from the action of cell wall modifying enzymes (e.g. polygalacturonase, pectin methylesterase, pectate lyase, β-galactosidase, cellulase), generally encoded by ripening-related genes (Brummell and Harpster, 2001; Goulao and Oliveira, 2008; Mercado et al., 2011). Other cell wall proteins, with no hydrolytic enzymatic activity, such as expansins, also have a role in softening (Brummell et al., 1999). In general, the cell wall disassembly process responsible for softening involves the depolymerization of matrix glycans, the solubilization and depolymerization of pectins and the loss of neutral sugars from pectin side chains (Brummell, 2006; Goulao and Oliveira, 2008). The extension of these changes varies considerably among different species (Mercado et al., 2011). Recently, it has been suggested that the structural integrity of the xyloglucan network maintained by xyloglucosyltransferase/endo-hydrolase (XTH) could be significant during fruit softening. This activity is higher during fruit expansion and then declines or remains constant during ripening (Goulao et al., 2007; Mercado et al., 2011). Miedes and Lorences (2009) suggested that XTH genes could be involved in the maintenance of cell wall structure rather than cell wall disassembly, and therefore the decrease in *XTH* gene expression and activity could contribute to softening. Supporting this hypothesis, overexpression of the *XTH1* gene in tomato reduced fruit softening (Miedes et al., 2010). On the other hand, although less studied than cell wall disassembly, cellular turgor also plays a role in fruit softening (Harker et al., 1997). A loss of turgor pressure is observed during fruit ripening due to the regulated accumulation of apoplastic solutes (Wada et al., 2009). Transpirational water loss through the cuticle could also be involved, especially in fruits with thick and well developed cuticles, such as tomato (Saladie´ et al., 2007; Lara et al., 2014). Cell turgor may also be influenced by cell wall modifications taking place during fruit softening (Thomas et al., 2008), and it is, therefore, difficult to separate

active turgor changes from effects due to passive water loss and modification of cell wall mechanical properties.

Pectin is the most abundant polymer in the middle lamella, and it regulates intercellular adhesion (Willats et al., 2001), but primary fruit cell walls are also rich in polyuronides, accounting for up to 60% of cell wall mass in many fruits (Redgwell et al., 1997a). Probably, pectins are the cell wall components that change most during fruit softening, but their role in fruit firmness and softening is considered controversial. This could be due to the results obtained with tomato fruit, which has been used extensively as a model to study fruit ripening. Ripening of this fruit is characterized by large increases in polygalacturonase mRNA levels and protein and enzymatic activities, which correlate with the rate of softening (Brummell and Harpster, 2001). However, the down-regulation of a polygalacturonase gene to reach a residual gene expression of 1% when compared with wild-type fruits did not reduce softening, although transgenic overripe fruits showed an improved storage life (Smith et al., 1990; Kramer et al., 1992; Brummell and Labavitich, 1997). Moreover, although depolymerization of solubilized pectins was suppressed in transgenic tomatoes, the solubility of pectins remained at wild-type levels (Smith et al., 1990). These early findings led to the hypothesis that polygalacturonase-mediated pectin disassembly is neither necessary nor sufficient to induce fruit softening, especially at early stages of the process (Hadfield and Bennett, 1998). This hypothesis was later supported by studies performed in the tomato mutant *rin*, showing altered ripening behavior (Giovannoni et al., 1989). However, the more recent evidence in different species suggests a significant role of pectin modifications in fruit softening. Thus, the downregulation of a pectate lyase or polygalacturonase gene in strawberry significantly reduced fruit softening (Jiménez-Bermúdez et al., 2002; Quesada et al., 2009). Similarly, silencing of the *PG1* gene in apple, crisp fruit with textural features completely different from strawberry, also diminished softening (Atkinson et al., 2012).

2.3.3.3 Folate biosynthesis

Folates represent all forms of vitamin B found in biological systems while folic acid is the synthetic form found in dietary supplements and fortified foods (Tamura et al., 2006). Iniesta et al. (2009) investigated the level of 5-methyltetrahydrofolate in commercial raw tomato cultivar harvested in Murcia (Spain). They found the maximum level in Ronaldo cultivar, equal to 31.5 μg/100 g FW. In particular, folates have a role in various one-carbon transfer reactions, including purine and pyrimidine biosynthesis, amino acid metabolism, methylation of nucleic acids, proteins, and lipids (Lucock, 2000).

For these reasons, folates are essential for fetal growth (Wagner, 1995). The recommended daily allowance (RDA) of folates is 400 μg for adults and 600 μg for pregnant women (National Institutes of Health, Office of Dietary Supplements: http://ods.od.nih.gov/factsheets/Folate-HealthProfessional/). Green leafy vegetables, beans, and certain fruits are rich sources of folates, as are fermented products. However, most staple crops, although rich in starch content, contain a low folate level while populations are consuming monotonous diets, mainly consisting of these staple crops, often suffer from a suboptimal folate intake.

Folates are a group of water-soluble B vitamins (B9), derived from tetrahydrofolate (THF), the most reduced folate form. THF contains three building blocks-the pteridine, p-aminobenzoate (p-ABA), and glutamate moieties-which are produced separately and subsequently joined **(Fig. 2.8)**. Folates can differ in the length of the glutamate tail (ranging from one to approximately eight γ-linked $_{L}$-glutamates and the one-carbon (C1) attached to the molecule (a methyl-, formyl-, methylene-, methenyl-, or formimino-unit) **(inset Fig. 2.8)**. Each of them has a specific role in C1 metabolism (Ravanel et al., 2011). THF and derivatives thereof can only be synthesized de novo by plants and micro-organisms. Thus, humans are entirely dependent on their diet to obtain the necessary amount of folates needed for a broad range of physiological and molecular processes.

2.3.3.4 Alteration in sugar and pH

Two important quality attributes of processing tomatoes are pH and titratable acidity (TA). In tomato fruits, ripening is also associated with increased sugar levels represented as °Brix value of fruits. In all tomato cultivars examined, pH increased as the fruit ripened from the green to pink to the red stage and continued to rise as the red ripe fruit remained on the vine. TA was at its maximum at the beginning of the ripening process then decreased as the fruit reached the ripe stage and continued to decline with over-maturity. Soluble solids have been shown to increase during ripening then remain constant with over-maturity (Gautier et al., 2008).

2.3.4 Molecular regulation of tomato fruit ripening

2.3.4.1 Transcriptional regulation

The availability of mutants has been critical to elucidating gene function in plants, and tomato has one of the best collections of characterized fruit ripening-related mutants (maintained and accessible through the Tomato Genetics Resource Center at the University of Davis (http://tgrc.ucdavis.edu/). Several single locus mutations, resulting in

ripening inhibition phenotypes have facilitated understanding of transcriptional control upstream of the required ethylene response for fruit ripening in tomato. Most notable are three ripening mutants, *ripening-inhibitor* (*rin*), *non-ripening* (*nor*) and *colourless non-ripening* (*Cnr*), which show severely inhibited ripening, do not produce elevated endogenous ethylene, or ripen in response to exogenous ethylene, and produce fruit that remain firm and green for extended periods (Tigchelaar et al., 1978; Manning et al., 2006). Molecular characterization of *RIN–MADS* provided the first evidence for transcriptional control of fruit ripening. *RIN* encodes an MADS-box transcription factor protein of the SEPALATTA clade (Hileman et al., 2006). *Cnr* is a rare epigenetic mutation, resulting from heritable hypermethylation in the promoter of the *Cnr* locus SQUAMOSA binding protein (SBP/SPL) causing greatly reduced transcription (Manning et al., 2006). The expression of *CNR* is reduced in the *rin* mutant indicating that it may act downstream of RIN-MADS and CNR is also required for RIN binding to target promoters (Martel et al., 2011). In addition to these genes, several other transcription factor have also been identified like *TAGL1*, *HB1*, *TDR4/MBP7* (*FUL1/FUL2*), *AP2a* and *ERF6* regulating different processes of fruit ripening (Seymour et al., 2013). The orthologs and homologs of these genes in Arabidopsis regulate the several developmental processes of plants including siliques development and seed dispersal.

2.3.4.2 Post-transcriptional regulation

The production of ethylene throughout the plant is low (basal level). The level of ethylene increases in response to both developmental cues and environmental signals (De Paepe and Van Der Straeten 2005; Chae and Kieber 2005). For example, the increased emission of ethylene in many fruits during ripening (climacteric ripening); however, other events and cues also stimulate ethylene biosynthesis including many biotic and abiotic stressors. Because of this, ethylene is often called the "stress" hormone. Under some conditions, ACC oxidase is a site of regulation. However, the major site for the regulation of ethylene biosynthesis occurs at ACC synthase. A major focus of research has been to determine the mechanism(s) for the regulation of ACC synthase.

eto1 was the first ethylene biosynthesis mutant in Arabidopsis identified by screening displayed constitutive ethylene response phenotype (Guzmán and Ecker 1990). Subsequent studies showed that *eto1*, along with two other mutants with similar traits, *eto2*, and *eto3*, have higher ACC synthase activities (Woeste et al., 1999; Vogel et al., 1998). Subsequently, several laboratories showed a correlation between ACC synthase

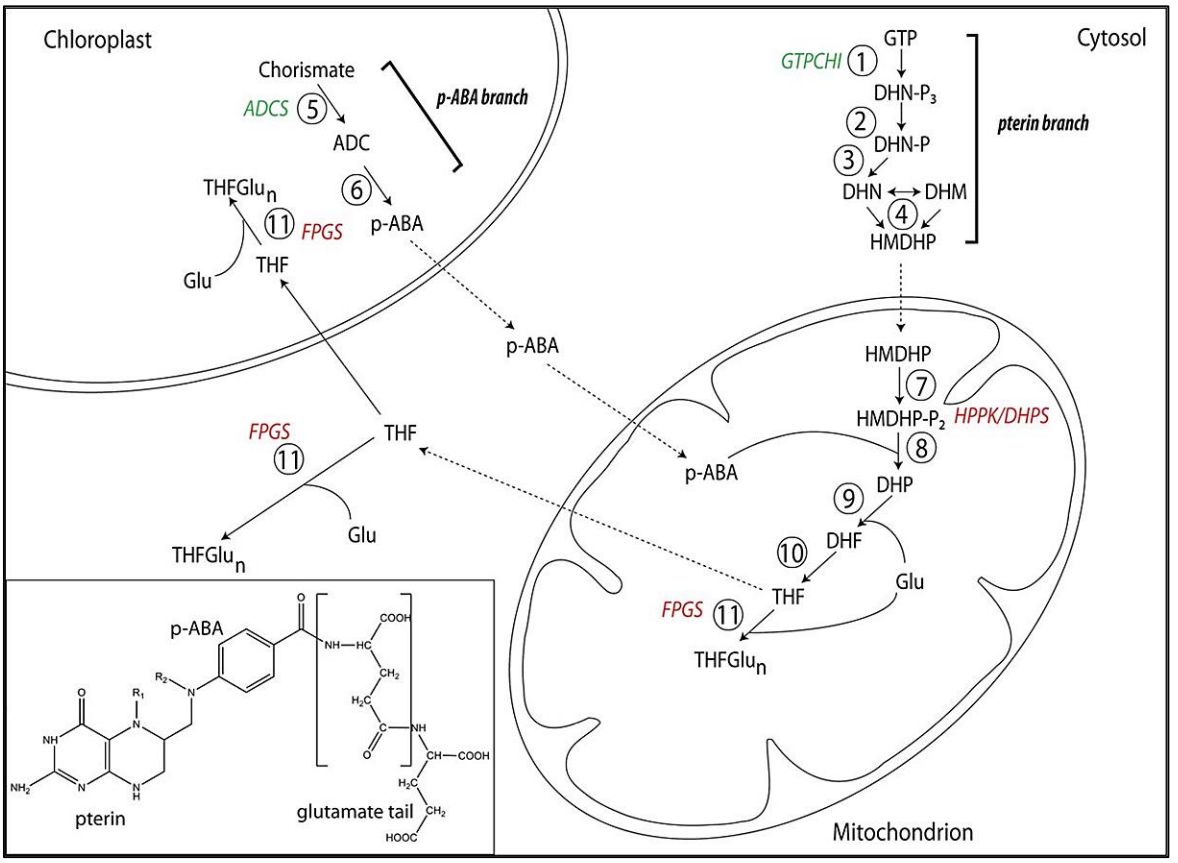

Figure 2.8. The folate biosynthesis pathway in plants, characterized by its compartmentalization in the plastids, the cytosol, and the mitochondria and folate structure (inset). Dashed lines indicate hypothetical transport steps. Compound abbreviations: ADC: aminodeoxychorismate; DHF, dihydrofolate; DHM, dihydromonapterin; DHN, dihydroneopterin; DHP, dihydropteroate; Glu, glutamate; HMDHP, hydroxymethyldihydropterin; THF, tetrahydrofolate. Enzymes: 1, GTP cyclohydrolase I; 2, dihydroneopterin triphosphate pyrophosphatase; 3, non-specific phosphatase; 4, dihydroneopterin aldolase; 5, aminodeoxychorismate synthase; 6, aminodeoxychorismate lyase; 7, hydroxymethyldihydropterin pyrophosphokinase; 8, dihydropteroate synthase; 9, dihydrofolate synthetase; 10, dihydrofolate reductase; 11, folylpolyglutamate synthetase (Blancquaert et al., 2014).

protein levels and ethylene levels (Chae et al., 2003; Joo et al., 2008; Christians et al., 2009). Above studies established a central role for ACC synthase as a principle regulator of ethylene biosynthesis. ACS enzymes are classified in three types. Type 1 ACC synthases contain target motifs for mitogen-activated protein kinases (MAPKs) and calcium-dependent protein kinases (CDPKs), whereas type 2 ACC synthases only contain target motifs for CDPKs and type 3 enzymes carry neither motif (Liu and Zhang 2004; Kamiyoshihara et al., 2010). Stress-activated MAPKs cause increased phosphorylation of specific ACC synthase isoforms resulting in protein stabilization and increased ethylene production (Han et al., 2010; Joo et al., 2008; Liu and Zhang 2004; Sebastià et al., 2004). Not surprisingly, dephosphorylation also has a significant role in ACS protein turnover (Skottke et al., 2011). Research from several laboratories has now linked the phosphorylation state of specific ACC synthase isoforms to protein stability. In some cases, the phosphorylation state was shown to be regulated by environmental signals and involves ubiquitin-dependent proteolysis (Skottke et al., 2011; Christians et al., 2009; Tan and Xue 2014; Chae et al., 2003; Wang et al., 2004; Yoon and Kieber 2013; Liu and Zhang 2004; Han et al., 2010; Lyzenga et al., 2012; Prasad et al., 2010; Prasad and Stone 2010). Although more research is needed to understand fully how ethylene levels are regulated, these studies provide important mechanistic insights into how environmental signals and developmental cues affect ethylene biosynthesis.

A network of regulatory inputs has been superimposed on the ACS subclades to provide very finely modulated control of ethylene synthesis. Although the type 1, 2 and 3 designations accurately represent ACS subclades, several recently elucidated regulatory factors target ACSs of different kinds, suggesting the rapid evolution of regulatory mechanisms. For instance, the putative target site for destabilizing phosphorylation by CK1.8 (T463) is present in type 2 isozymes ACS5 and ACS9 and several type 1 isozymes, but absent from type 3 isozymes ACS4 and ACS8. Similarly, interaction with 14-3-3 proteins stabilizes at least one isozyme of each type (ACS2, ACS5, and ACS7; Yoon and Kieber, 2013a, 2013b). An abundant family of small dimeric proteins that typically bind phosphoserine, 14-3-3 proteins interact with a broad array of 'client' phosphoproteins; the effects of 14-3-3 binding are variable (Denison et al., 2011). The mechanism for 14-3-3 stabilization of ACS2 and ACS7 is not known. In the case of ACS5, 14-3-3 interaction antagonizes ETO/EOL-mediated turnover both by stabilizing the ACS protein and by destabilizing ETO/EOL proteins. Interaction of 14-3-3 with ACS is not dependent on the TOE (Target of ETO1) sequence of ACS5 (Yoon and Kieber, 2013a). Because the

14-3-3 binding is phosphorylation-dependent, the discovery of 14-3-3-mediated stabilization suggests that these isozymes may undergo stabilizing phosphorylation in the catalytic domain, the only domain that is common to all three types.

2.3.4.3 Regulation at other phytohormones level

After successful flower pollination and ovule fertilization, the fruit and seed initiation, a stage that is commonly referred to as fruit set, and subsequent development of both fruit and seeds occur concomitantly according to a precise, genetically controlled process mediated by phytohormones (Gillaspy et al., 1993). Recent reviews have highlighted the role of several plant hormones and their interplay in the control of fruit development (Ruan et al., 2012; Kumar et al., 2014). The genes, whose functional characterization in tomato revealed an involvement in the growth period of fruit development are described below. Auxin and GA appear to be the predominant hormones required for fruit initiation in response to fertilization, since exogenous applications of both hormones lead to fruit initiation and parthenocarpic development (de Jong et al., 2009). A role for cytokinin, ethylene, and ABA in fruit formation has been demonstrated but is less well documented thus far (Kumar et al., 2014).

Current evidence supports that combined action of three hormones, auxin, gibberellins (GAs), and cytokinin plays a significant role in the regulation of fruit set. Individually, any of these hormones can only initiate the fruit development to a certain extent; however, their combined application has been found to induce normal fruit growth even in the absence of fertilization in both dry and fleshy fruits (Nitsch, 1952; Crane, 1964; Gillaspy et al., 1993; Mariotti et al., 2011). Importantly, auxin, GA, and cytokinin levels increase at fruit set, and the requirement of their higher levels of fruit set has been already validated by their exogenous treatment, which causes parthenocarpic fruit formation in tomato. Evidence suggests that auxin and GAs also act in a similar way during fruit set in dry fruits. A fertilization-triggered auxin signal is involved in the promotion of GA biosynthesis in the ovule, which in turn activates GA signaling in ovules and valves and coordinates silique growth in Arabidopsis (Dorcey et al., 2009). Additionally, it has been observed that interaction between auxin and GA signaling pathways is essential for the promotion of fruit set in fleshy fruits (Vivian-Smith and Koltunow, 1999; Srivastava and Handa, 2005; de Jong et al., 2009; Carrera et al., 2012; Ruan et al., 2012).

Recently, Kang et al. (2013) demonstrated that a number of auxin biosynthesis genes encoding proteins such as YUCCA5, YUCCA11, and tryptophan aminotransferase

related1, and GA biosynthesis genes encoding enzymes such as GA 20-oxidase3, and GA 3-oxidase3, 4, 5, and 6 had achene-preferential expression and were largely absent in the receptacle of strawberry. Evidence suggests that auxin promotes fruit set and growth, at least partly, by controlling the GA levels **(Fig. 2.9)** (Serrani et al., 2008; Dorcey et al., 2009). Earlier studies at the molecular level had established a role for an Auxin Response Factor (ARF7) in mediating the crosstalk between auxin and GA. Silencing of this gene caused formation of parthenocarpic fruits with morphological characteristics that seem to be the result of both increased auxin and GA responses, suggesting that ARF7 also acts as a modifier of the GA response during early stages of fruit development (de Jong et al., 2009; de Jong et al., 2011). Consistent with this observation, a point mutation in a gene encoding DELLA protein was found to be responsible for the constitutive GA responses in *procera* (*pro*) mutant plants (Carrera et al., 2012). Transcriptome analysis suggested that parthenocarpic capacity of *pro* is mainly associated with changes in the mRNA levels of genes involved in GA and auxin pathways, including *ARF7* (Carrera et al., 2012). Further, GA-mediated responses are under the tight regulation of growth-repressing DELLA proteins. According to the "relief of restraint" model, any activation of GA signaling requires degradation of DELLA proteins (Harberd, 2003). The involvement of GA-mediated signaling during fruit set has been further substantiated as any reduction in DELLA activity has been found to promote the parthenocarpic fruit growth in both dry and fleshy fruits (Marti et al., 2007; Dorcey et al., 2009). However, a DELLA-independent pathway also participates during fruit growth in Arabidopsis, suggesting additional opportunities for fine-tuning of fruit growth (Fuentes et al., 2012). GA has also been implicated in fruit patterning. GA synthesis is a direct and necessary target of basic helix-loop-helix (bHLH) INDEHISCENT (IND) protein. Another bHLH protein, ALCATRAZ (ALC), which is also required for fruit opening, interacts with DELLA repressors. It has been proposed that interaction between DELLA and bHLH proteins be a versatile regulatory module and is needed for tissue patterning in Arabidopsis (Arnaud et al., 2010).

ARFs and Aux/IAA proteins also govern the fate of fruit initiation events. Silencing of ARF7, a negative regulator of fruit set, in tomato transgenic lines also results in up-regulation of the *GH3* gene. GH3 genes encode IAA-amido synthetases that convert free auxin to its conjugated form and maintains auxin homeostasis inside a cell. The up-regulation of *GH3* further indicates that its induction may compensate for excessive auxin in *ARF7*-silenced plants. Further, differences in cell size between *ARF7*-

silenced lines and the wild type at six days post-anthesis, with significant cell size increase in the mesocarp and endocarp layers, suggests that down-regulation of *ARF7* inhibits cell division and promotes cell expansion (de Jong et al., 2009; de Jong et al., 2011). Nevertheless, *ARF7* is not the only gene encoding proteins involved in such interaction, as additional auxin regulators such as ARF8, IAA9, PIN4 (PIN-FORMED), and TIR1 (Transport inhibitor response1) have also been implicated in auxin and GA-induced parthenocarpic fruits (Goetz et al., 2007; Wang et al., 2009; Ren et al., 2011; Mounet et al., 2012).

As both ARF8 and IAA9 are implicated in parthenocarpic fruit formation in tomato and Arabidopsis and belong to the same signaling cascade, it has been suggested that these proteins may form a transcriptional repressor complex that is destabilized by the aberrant forms of ARF8 to allow transcription of auxin-responsive genes (Goetz et al., 2007). None of these studies mentions if any GA-induced response was observed in the transgenic plants; however down-regulation of *ARF7* in *TIR1* over-expressing transgenic tomato plants further supports the involvement of more auxin-related genes in crosstalk between auxin and GA during fruit set.

Besides auxin and GA, cytokinin is also known to induce fruit set in several fruit crops (Matsuo et al., 2012). The endogenous level of cytokinin is directly correlated with the fruit growth, especially in stimulation of cell division. Its external application causes parthenocarpic fruit formation (Gillaspy et al., 1993; Srivastava and Handa, 2005; Mariotti et al., 2011; Matsuo et al., 2012). It was found that cytokinin-treated tomato seedlings mimic the *diogeotropica* (*dgt*) mutant phenotype such as reduced shoot growth, reduced apical dominance, and exhibit auxin inhibited responses (Coenen et al., 2003). In Arabidopsis, cytokinin has been implicated in the development of the medial region of the gynoecia and formation of valve margins during early fruit development (Marsch-Martinez et al., 2012). Collectively, these results suggest that cytokinin could act via inhibiting auxin responses, at least partially, during fruit set and growth. However, very little information is available on the underlying mechanisms of its action during fruit set.

Ethylene and brassinosteroids (BR) are also believed to play important roles in fruit set (Fu et al., 2008; Serrani et al., 2008; Wang et al., 2009). Ovule lifespan is an important factor in determining the ability to set fruits. GA-induced fruit set is negatively affected by ovule senescence. Recent evidence in Arabidopsis suggests that ethylene is involved in both the control of the ovule lifespan and the determination of the pistil/fruit fate. The proposed model suggests that ethylene may modulate the onset of

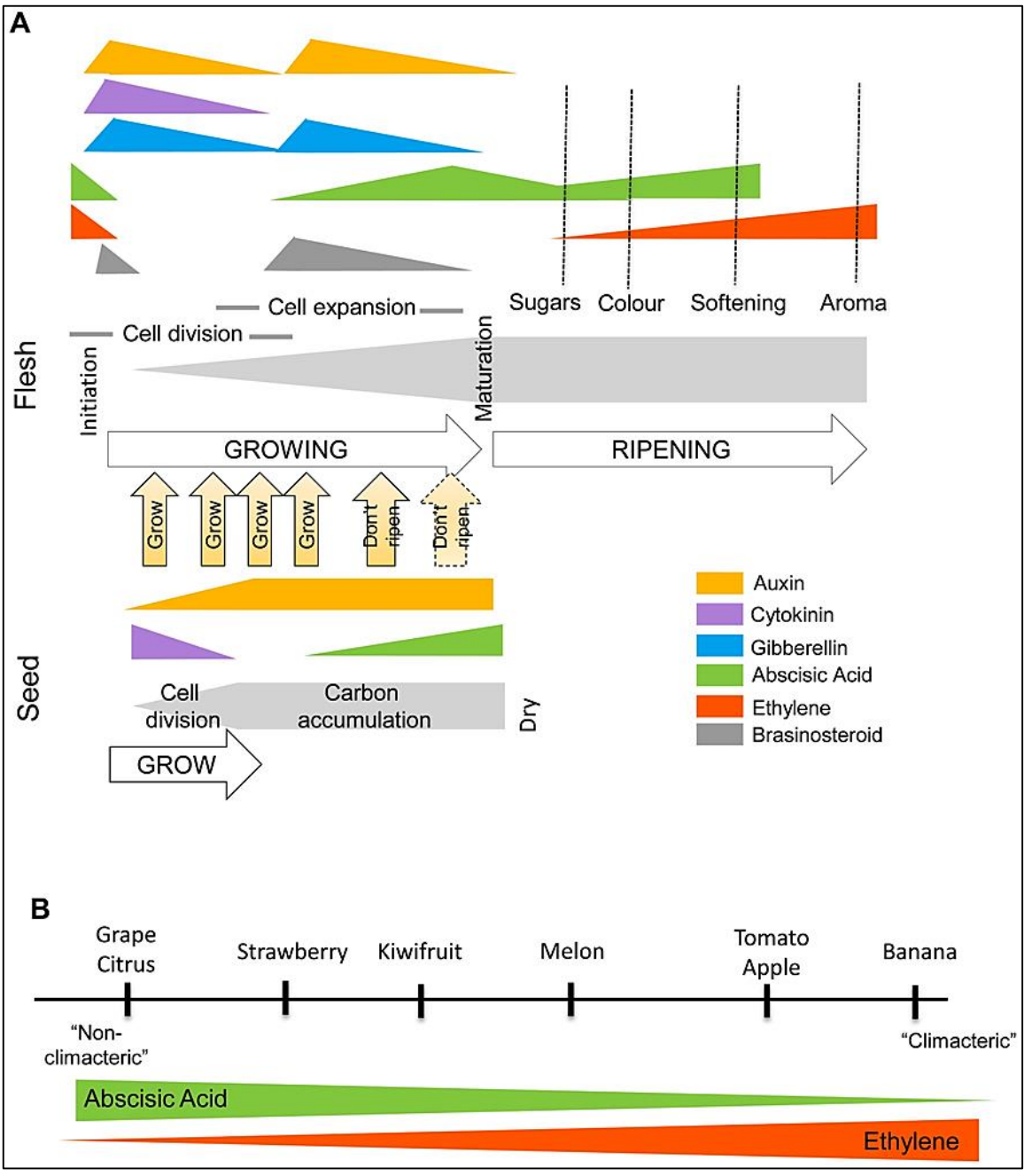

Figure 2.9. Changes in the hormonal levels during fruit development and ripening. **(A)** Differential hormone concentrations occur in the seed and the surrounding tissue with the developing seed influencing its environment. The increased levels of auxin, cytokinin, gibberellin, and brassinosteroid at fruit set, and an involvement of auxin, gibberellin, and brassinosteroid at fruit growth. For fruit maturation, there is an inhibition of auxin transport from the seed and increase in ABA. This triggers the ripening/senescence program that leads to an increase in ABA and/or ethylene biosynthesis and response in the surrounding tissue. **(B)** The spectrum of ripening dependencies to ABA and ethylene. All fruit appear to respond to ABA and ethylene. In historically considered "climacteric fruit," ABA indirectly regulates ripening through ethylene. In "non-climacteric" fruit, the ABA has a more dominant role but the fruit still have ethylene-dependant ripening characters (McAtee et al., 2013).

ovule senescence and, consequently, the window of GA fruit set responsiveness by altering GA perception and signaling. Though an actual mechanism remains unidentified, it is suggested that the ethylene produced in ovules would directly prevent the GA response, for example, by stabilizing the DELLAs via CTR1 (Carbonell-Bejerano et al., 2011). Evidence indicates there is a transient increase in ethylene production in tomato pistils after pollination, which eventually decreases after fertilization. The ethylene-associated changes are also reflected in the mRNA levels of several ethylene-related genes such as *1-aminocyclopropane-1-carboxylate* (*ACC*) *synthase2* and *ACC oxidase1* (*ACO1*), *Ethylene-insensitive3-related* (*EIL3*). Many genes encoding ethylene response factors (ERFs) also show a marked shift in their expression during flower to fruit transition (Vriezen et al., 2008; Pascual et al., 2009). In cucumber, exogenous application of BR induces parthenocarpic fruit formation, by inducing cell division, whereas its inhibitor abolishes the natural parthenocarpic capacity in a parthenocarpic cucumber. However, this effect seems to be limited to a few fruit crops only as no such effect of BR application could be repeated in tomato (Marti et al., 2007).

Additionally, the plant hormones/growth regulators abscisic acid (ABA) and polyamines (PAs) are implicated in fruit development, but knowledge of their precise role and mode of action remains sketchy (Gillaspy et al., 1993; Nitsch et al., 2009). ABA levels show a decrease at fruit set and this decline is associated with the down-regulation of ABA biosynthesis genes encoding enzymes such as 9-cis-epoxycarotenoid dioxygenase 1 (NCED1) and neoxanthin synthase (NSY) and up-regulation of ABA degradation gene encoding protein; namely, ABA-8'-hydroxylase CYP707A, after pollination (Vriezen et al., 2008). ABA has also been found to abolish GA-induced changes during fruit set in pea (García-Martínez and Carbonell, 1980).

In tomato and peach fruits, the maximum ABA content precedes the climacteric ethylene production. It has been shown that ABA promotes ripening by promoting ethylene biosynthesis through up-regulation of ethylene biosynthesis genes (Sun et al., 2012a). In addition, GA has been found to delay fruit ripening in many other fruits such as tomatoes, peach mango, sapota etc. (Dostal and Leopold, 1967; Martínez-Romero et al., 2000; Singh et al., 2007; Sudha et al., 2007). Besides these hormones, the endogenous level of methyl jasmonate (MJ) has been found to increase with the progression of ripening in apple, mangoes, pears and tomatoes (Fan et al., 1998). Cytokinin and BRs are known to induce ethylene production by increasing ACS protein stability; however, no such evidence is available, which suggests that these two hormones regulate expression

of ACS genes or stabilize their proteins in fleshy fruits (Abel et al., 1995; Yamagami et al., 2003).

2.3.4.4 Light-mediated regulation

Light plays a significant role in plant growth and development. It is associated with various fundamental processes of plants such as germination, photomorphogenesis, photosynthesis, photoperiodism, photorespiration, phototropism, and circadian rhythms. Plants accomplish these phenomenon using a light signaling machinery consisting of (1) photoreceptor genes, (2) gene encoding early signaling intermediates, (3) *COP* (*CONSTITUTIVE PHOTOMORPHOGENIC*)/*DET* (*DE-ETIOLATED*)/*FUS* (*FUSCA*) genes, (4) genes encoding downstream effectors (Quail et al., 2002; Jiao et al., 2007). In Arabidopsis and other plants, the roles of light signaling genes have been investigated in details during plant growth and development. In tomato, studies with photomorphogenic mutants and transgenic plants have provided information regarding the role of light signaling gene in ripening and nutritional quality of fruits (Azari et al., 2010b).

Light appears to have a dual effect on tomato fruits, it contributes to $1/7^{th}$ energy needs of developing fruits via carbon fixation in photosynthesis (Hetherington et al., 1998), and it also assists in the development of chlorophyll and chloroplast (Waters and Langdale, 2009; Powell et al., 2012). The overexpression of *Golden 2-like* (*GLK*) transcription factor that determines chlorophyll distribution in developing tomato fruits enhanced fruit photosynthesis as well as carbohydrate and carotenoid contents in ripe fruits (Powell et al., 2012). Photosynthesis is also essential for properly timed development of seeds (Lytovchenko et al., 2011). Several studies have indicated that in addition to contributing to fruit photosynthesis, light also modulates fruit ripening, particularly the accumulation of pigments. Developing fruits exposed to direct sunlight accumulate more carotenoids than the shaded fruits (McCollum, 1954). In recent years, use of photomorphogenic mutants has greatly aided the identification of signaling partners regulating light mediated specific developmental responses. In tomato naturally occurring high pigment mutants such as *hp1* and *hp2* show exaggerated light responsiveness, higher anthocyanin levels during vegetative development and higher carotenoid levels in ripe fruits (Azari et al., 2010b; Kilambi et al., 2013). A recent study on tomato photomorphogenic mutants has revealed that phytochromes act as a regulatory switch during the fruit development (Gupta et al., 2014). Cryptochromes were

also predicted to influence fruit ripening, as showed by overexpressing *CRY2* gene in tomato.

2.3.5 Metabolic regulation of tomato fruit development and ripening

Tomato is an extremely interesting system to study maturation and ripening processes because of the dramatic metabolic changes that occur during development. Metabolic events throughout the development period of tomato have been addressed in detail (Boggio et al., 2000; Chen et al., 2001). Tomato fruit at different developmental stages can be distinguished on the basis of their metabolic complement (Carrari and Fernie, 2006). GC-MS has been used to characterize tomato pericarp composition in transgenic plants (Roessner-Tunali et al., 2003), to assess metabolic diversity of tomato species (Schauer et al., 2005) and to measure metabolic changes associated with tomato fruit development (Carrari and Fernie, 2006) **(Fig. 2.10)**.

The modification of carbon metabolism and photo-assimilate partitioning by the manipulation of key enzymatic activities, such as those involved in primary carbon metabolism and photo-synthesis, was expected to have an impact on fruit growth. To investigate this, the Arabidopsis Hexokinase 1 (*AtHXK1*) gene was constitutively overexpressed in tomato plants (Menu et al., 2004). Overexpressing lines exhibited marked phenotypic and biochemical changes in developing fruits, such as reduced fruit size and a decrease in cell expansion. The carbon supply required to support these processes was lower throughout development, most probably due to decreased photosynthesis. Consequently, any sucrose provided to these fruits would be used to fuel cell metabolism at the expense of starch storage. Fruit displayed reduced respiratory rates, which were accompanied by lower ATP levels and ATP/ADP ratios in fruit extracts, indicating profound metabolic perturbations.

The role of sucrose synthase (SuSy) in tomato fruit development has been studied by silencing a fruit-specific isoform (D'Aoust et al., 1999). The inhibition of SuSy activity affected fruit set and very early fruit development related to the reduced unloading capacity for sucrose. The QTL *Lin5* has been identified as a major QTL controlling fruit weight and sugar content (Fridman et al., 2000), and the associated gene was found to code for a cell wall-bound invertase (Fridman et al., 2004). When *Lin5* was RNAi silenced, fruit yield was greatly reduced, as well as fruit size, seed size, and seed number (Zanor et al., 2009). In these transgenic plants, metabolic changes were largely confined to sugar metabolism, since sucrose content increased while glucose and fructose contents decreased, as observed at the red ripe stage. The changes in expression of

primary metabolites like organic acids, sugars, amino acids, etc. during tomato fruit development and ripening are categorized as follows:

2.3.5.1 Changes in the level of organic acids content

Organic acids are important components in tomatoes that strongly influence fruit taste and overall quality. Citric acid is the major fruit acid, followed by malic acid and several less abundant acids such as ascorbic acid, dehydroascorbic acid, Citra malic, shikimic, fumaric, isocitric, succinic, lactic, maleic, saccharic, gluconic, gulonic, and tartaric acids (Oms-Oliu et al., 2011). The citric acid cycle involves the biosynthesis of fumaric, isocitric and succinic acids, many of which serve as precursors for the biosynthesis of amino acids. Shikimic acid, which is only detected and is highly abundant in very young fruit, is also a precursor for the biosynthesis of tryptophan, phenylalanine and tyrosine (Carrari and Fernie, 2006). Compounds such as Citra malic and saccharic acids do not appear at the beginning of development, whereas fumaric and lactic acids are not detected during postharvest storage. Citric acid content increases with maturation up to a maximum during the postharvest stage, whereas malic acid concentration decreases during maturation and ripening (Oms-Oliu et al., 2011). As fruit reaches maturity and begins to ripen, increased catabolic activity of malic enzyme, which decarboxylates L-malic acid to pyruvate, and the continued activity of malate dehydrogenase and citrate synthase result in a decline in L-malic acid levels and the preferential accumulation of citric acid. Comprehensive phenotyping of an aconitase mutant (Aco1) of *Solanum pennellii* (Carrari et al., 2003), as well as *Solanum lycopersicum* plants in which the mitochondrial malate dehydrogenase (mMDH) was repressed via antisense and RNA interference techniques (Nunes-Nesi et al., 2005), uncovered large changes in both leaf metabolism and plant performance, such as a decreased flux through the TCA cycle and enhanced photosynthetic activity (Carrari and Fernie, 2006). It has been demonstrated that citric and malic acid metabolism is under ethylene regulation; the metabolization of malic and citric acid is enhanced in transgenic antisense LeACS2 lines, with suppressed ethylene biosynthesis, when exposed to ethylene (Gao et al., 2007). Fumaric acid, a precursor of malic acid in the citric acid cycle, declines during maturation and disappears during postharvest, whereas ascorbic acid, dehydroascorbic acid, isocitric acid and succinic acid contents seem to increase during ripening but decrease again during postharvest storage down to pre-ripening concentrations (Oms-Oliu et al., 2011). This might suggest that these metabolites are upregulated only during climacteric ripening. Although the general structure of the TCA pathway in plants is well known, its

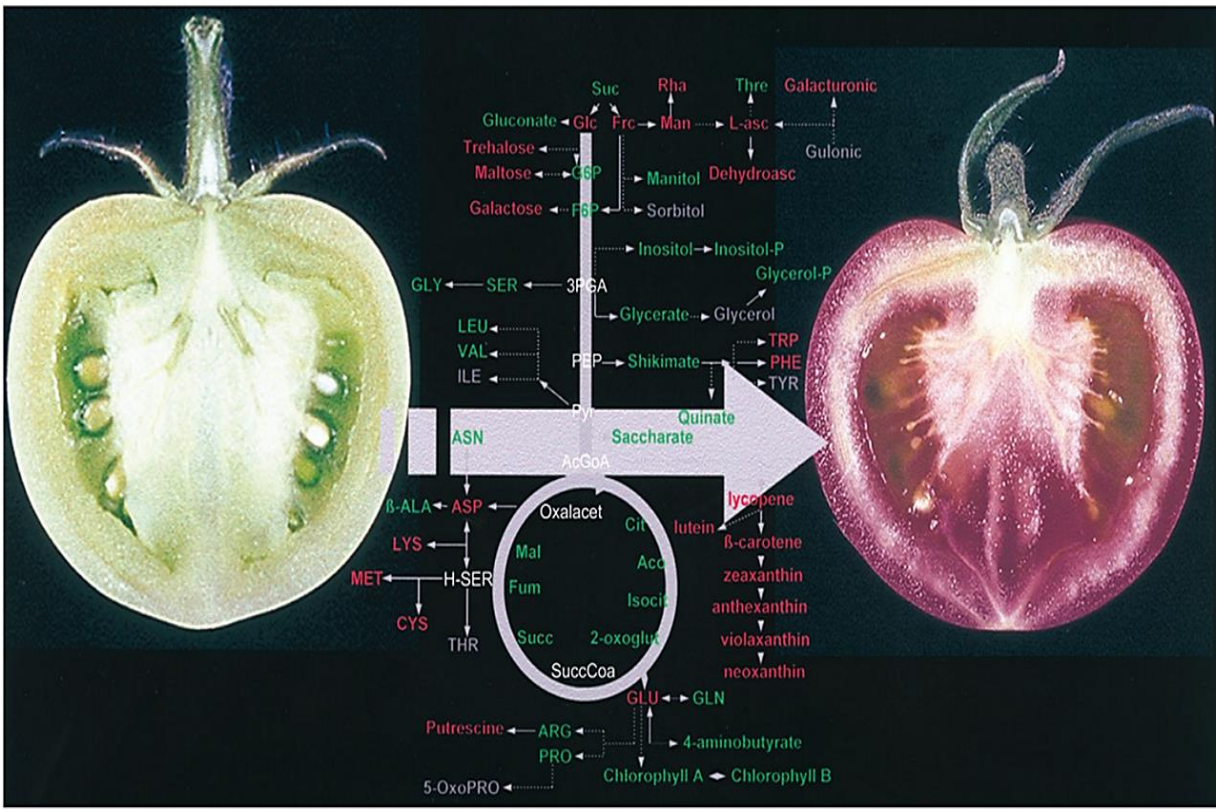

Figure 2.10. Changes in metabolites accumulation during tomato fruit ripening. The green colored metabolites name corresponding to green fruit tissue and red colored names related to red fruit tissue respectively. Picture taken from Carrari and Fernie, 2005.

regulation is still poorly understood (Fernie et al., 2004). The glycolysis and TCA cycle are the predominant carbon fluxes in the fruit during ripening. An increased respiration during ripening, typical for climacteric fruit, would justify the increased content of some TCA cycle intermediates such as isocitric and succinic acid.

Tartaric acid also accumulates during ripening and continues to increase during storage (Oms-Oliu et al., 2011). The decrease in ascorbic acid at late maturity stages could be related to the synthesis of L-tartaric acid. Compounds such as gluconic and 2-keto-L-gulonic acid, which are believed to be intermediates of tartaric acid biosynthesis via ascorbic acid (DeBolt et al., 2006), accumulate during postharvest storage. Thus, the accumulation of gluconic acid, 2-keto-L-gulonic acid, and tartaric acid could result from the degradation of ascorbic acid. This is in line with low concentrations of ascorbic acid in postharvest tomato samples (Oms-Oliu et al., 2011).

2.3.5.2 Alteration in sugar and sugar alcohols expression

The major sugar and sugar alcohols in tomato fruit are glucose, fructose, sucrose, galactose and inositol, whereas maltose, raffinose, glucose-6-phosphate, mannitol and sorbitol are only present in minor concentrations (Oms-Oliu et al., 2011). As ripening commences, plastid-stored starch is converted to sugars such as d-glucose and d-fructose, which accumulate to levels above those required for respiration (Tucker, 1993). Both glucose and fructose occur in equal quantities in fruit during ripening (Oms-Oliu et al., 2011), which is generally attributed to invertase activity responsible for breaking down sucrose (Richardson et al., 1990). As a result, ripe tomatoes have increased levels of fructose, glucose whereas sucrose levels decrease progressively during maturation and ripening of fruit.

Sugar phosphates are important intermediates of the metabolic pathways of central metabolism, but their concentration is usually limited due to their high turnover rate. Oms-Oliu et al. (2011) suggested that the concentration of glucose-6-phosphate mainly diminished towards the postharvest stages. The catabolism of sugar and sugar phosphates through the glycolytic pathway and TCA cycle may increase in parallel to climacteric respiration changes contributing to the observed changes. In red fruit, which contain little starch, respiration is responsible for predominant carbon fluxes in the fruit (Rontein et al., 2002).

Galactose, galacturonic acid, and mannose have been identified as primary cell wall components associated with ripening-related softening. Their levels increase throughout maturation and ripening in parallel to the decreasing firmness (Oms-Oliu et

al., 2011), indicating a breakdown of the cell wall complex (Oms-Oliu et al., 2011). Tomato fruit development is marked by significant changes in cell wall components associated with polysaccharide-degrading enzymes changing activity during climacteric development (Carrari et al., 2006). Polygalacturonase has been the most studied amongst these enzymes. This enzyme breaks down pectins to galacturonic acid, and its activity increases dramatically during tomato ripening. Strong suppression of β-galactosidase activity early during ripening was also correlated with reduced softening and reduced losses of galactose (Brummell and Harpster, 2001).

Levels of galactinol, myo-inositol and raffinose were higher during the first stages of development than during fruit maturation and ripening (Oms-Oliu et al., 2011). Myo-inositol is an important precursor in the biosynthesis of many cell wall polysaccharides. The raffinose family oligosaccharides (RFOs) is also a group of carbohydrates hypothesized to play a role in plant development. Galactinol synthase catalyzes the first committed step in the biosynthesis of RFOs acting on UDP-galactose and myo-inositol to form galactinol. RFOs are then synthesized by donation of galactose from galactinol to sucrose catalyzed by raffinose synthase (Zhao et al., 2004). Although a ripening-related decline in galactinol and myo-inositol can be observed (Oms-Oliu et al., 2011), the expected increase in raffinose is not happening.

2.3.5.3 Amino acids expression profiling

Oms-Oliu et al. (2011) demonstrated that concentrations of amino acids vary with different stages of maturity and ripening. Significant increases in glutamic and aspartic acid, methionine, phenylalanine and threonine are visible, whereas, at the same time, a reduction in levels of GABA, β-alanine, glycine and valine is shown throughout maturation and ripening. Other amino acids, such as asparagine, glutamine, leucine, isoleucine and serine increase at the breaker stages and decrease at subsequent postharvest stages. Besides fatty acids, free amino acids provide an important source of precursors for various aroma volatiles in tomato fruit, such as 2-phenylethanol, 2-isobutylthiazole, and phenylacetaldehyde (Buttery and Ling, 1993).

Also in other fruit, such as banana, the composition and concentration of amino acids during ripening, together with the activity of the enzyme systems required for their conversion to esters, are the major determinants of quantity and quality of the resulting aroma profile (Wyllie and Fellman, 2000). According to these authors, compounds such as 3-methylbutyl and 2-methylpropyl esters that characterize the banana volatile profile are mainly linked to the increasing availability of free leucine, alanine and valine during

the banana climacteric (Wyllie and Fellman, 2000). Oms-Oliu et al. (2011) suggest, samples with high levels of isoleucine, leucine and phenylalanine were those showing high ethylene production rates. Such increased free amino acid contents can favor the production of 3-methylbutanal and 3-methylbutanol, derived from leucine, and 2-methylbutanal and 2-methylbutanol, derived from isoleucine (Mathieu et al., 2009).

Amongst the free amino acids, GABA, glutamic acid, glutamine and aspartate show the highest relative content in tomato fruit throughout maturation and ripening (Oms-Oliu et al., 2011). Similar results were reported by others (Boggio et al., 2000; Pratta et al., 2004). In developing fruit, most of the total amino acid content found in the pericarp belongs to the glutamic acid family (Valle et al., 1998). GABA is the predominant N-form at the earlier stages of the tomato fruit ripening, showing a decrease from the breaker to the postharvest stages (Oms-Oliu et al., 2011). Glutamine, detectable in mature green fruit, decreases substantially through maturation and ripening (Oms-Oliu et al., 2011). Glutamine is known to be an important nitrogen transport compound in plants (Joy, 1988), so this pattern presumably reflects the changes in the need for this element as growth processes are progressively taken over by ripening-related processes (Wang et al., 1996). On the other hand, glutamic acid represents the most abundant free amino acid during ripening and postharvest. Its content is very low in small green, immature and mature green fruit, but its levels progressively increase with fruit ripening (Oms-Oliu et al., 2011). Similar results have been reported by Boggio et al. (2000) and Le Gall et al. (2003). Amongst all tested amino acids, glutamic acid contents showed the largest changes while ripening with an almost 40-fold increase (Oms-Oliu et al., 2011). Shelf-life of tomato fruit has been inversely correlated with the amount of glutamic acid synthesized during ripening (Pratta et al., 2004).

Finally, an increase in methionine is observed at the onset of ripening (Oms-Oliu et al., 2011). This can be understood given methionine is an important ethylene precursor (Adams and Yang, 1977). However, methionine levels continue to increase during postharvest storage when ethylene production drops again (Oms-Oliu et al., 2011).

2.4 Mutagenesis

Mutation is the genetic change in a living organism that provides the basis for species evolution and plays a significant role for improving the traits of crop species for production of new cultivars in crop species. These genetic variations arise spontaneously with a low frequency of 10^{-4}-10^{-11} per base/base pair per replication (Drake et al., 1998) hence it is impractical to rely on spontaneous mutation for accelerated plant breeding.

Muller (1927) demonstrated the use of X-ray for inducing mutations in fruit flies and since then Stadler (1929) showed the mutational effect of X-ray on barley and ultraviolet (UV) radiation on maize (Stadler and Sprague, 1936). Thus, variability in the crop plant can be induced by subjecting the crop plants with either physical or chemical mutagens. A large number of induced mutants have been a major resource for plant breeding and plant science research. The mutant variety database has approximately 3200 induced mutants at FAO/IAEA (http://mvgs.iaea.org/Search.aspx) and TGRC (http://tgrc.ucdavis.edu) that have become an established resource for genomics studies and crop improvement. Ethyl methane sulfonate (EMS), nitroso guanidine, nitrosourea N-ethyl-N-nitrosourea (ENU) are extensively used chemical mutagens that generate point mutations (McCallum et al., 2000a) that results in G/C to A/T transitions (Taylor et al., 2003) thereby causing amino acid substitutions affecting protein structure and function. X-ray, gamma rays, electrons and fast neutrons are physical mutagens that introduce deletions, inversions, insertions and even translocations of different sizes of fragments (Shikazono, 2005). Mutations in a mutagenized population can be analyzed by various methods using either forward genetics or reverse genetic approach.

2.4.1 Chemical mutagenesis: Ethyl methane sulphonate (EMS)

Chemical mutagens cause single base pair changes by alkylation of nucleotides. An appropriate dosage of mutagen is a mandate for induced mutagenesis to maintain a balance between survival and fertility whereas low dosage cause lower frequency of mutations leading to the screening of a large population to score for mutations. Chemical compounds that are widely used in plant breeding experiments are ethyl methane sulphonate (EMS), 1-methyl-1-nitrosourea (MNU) and 1-ethyl-1-nitrosourea (ENU). However, EMS is the most popular chemical mutagen in plants (Van Harten, 1998; Menda et al., 2004; Watanabe et al., 2007; Minoia et al., 2010; Saito et al., 2011) that selectively alkylates guanine bases and transfers to other molecules at a position of higher electron density (Heslot, 1977). It induces mainly point mutations at random locations in the genome of the species and with the majority of GC to AT base pair transitions (Till et al., 2007). However, small deletions (Schreck, 2002; Alcantara et al., 1996). Kreig (1963) also observed a low frequency of GC to CG or AT to GC transition. A broad range of alleles could be obtained within a relatively small population on EMS mutagenesis (Emmanuel and Levy, 2002).

2.4.2 Physical mutagenesis

Though physical mutagenesis has proved to be an effective mutagen, particularly for producing large DNA fragment deletions, the application of neutrons in induced mutagenesis has been limited to screening of few knockout mutants (Naito et al., 2005) when complex rearrangement of genes is a required. Physical mutagens include non-ionizing radiations such as UV or ionizing radiations such as X-rays, gamma rays, alpha and beta rays, fast and slow neutrons.

2.4.2.1 X-rays and γ-rays rays

Among the physical mutagens, X-ray and gamma rays are the most commonly used mutagens in mutation breeding. Pioneer work on mutagenic effects of X-rays on fruit flies were carried out by Muller, (1927). Induced mutations were first generated in plants using X-rays by Städler (1928) for mutagenesis on crop plants after he observed a strong mutator phenotype in barley seedlings and sterility in maize tassels. Exposure of plants to the γ-radiation causes damage such as double-strand breaks and also produces a range of damage to DNA due to the production of free radicals. A range of mutants in Arabidopsis (Redei and Koncz, 1992), rice (Cheema and Atta, 2003; Sato et al., 2006), and tomato (Menda et al., 2004). Negi et al. (2010) isolated a short root mutant in tomato from a 250 Gy γ-irradiated M_2 population in Ailsa Craig cultivar.

2.4.2.2 Fast neutron and accelerated ions

Fast neutrons induce relatively small segment deletions or translocations. These are uncharged particles of high kinetic energy generated in nuclear reactors. However, X-rays and gamma-rays are preferred because of their ease of use and safety in the application, good penetration, high reproducibility, high translocation frequency and fewer disposal (radioactive) problems. International Rice Research Institute, IRRI has large collection of rice deletion mutants (Leung et al., 2001) and NIAS (National Institute of Agrobiological Sciences, Japan) has developed deletion population using ion beam as a mutagen (Annual Report, 2010). A site named "Genes That Make Tomatoes" (http://Zamir.sgn.cornell.edu/mutants/) list mutants isolated using fast neutron irradiation of tomato. Also in rice, fast neutron mutagenesis has been used to produce about 8000 M_4 lines in an indica variety IR64 (Wu et al., 2005). Several Arabidopsis mutants (Hase et al., 2000; Kitamura et al., 2004) were identified using accelerated carbon ions.

2.4.3 Forward and Reverse genetic approach

Forward genetics approach is suitable for gene identification with a detectable mutant phenotype. However, the approach suffers from drawbacks as a mutation in one

member of the gene family does not necessary lead to a mutant phenotype due to functional redundancy. Some mutations may require specific conditions to give rise to a detectable mutant phenotype. Screening mutants using forward genetics seems to be laborious as it requires a large population for screening. Despite these limitations, forward genetics plays a significant role in identifying functions of those genes that control visible morphological traits that are easily phenotyped. However, scoring the genes relating to the mutant phenotype remains a challenge though map based cloning and the advent of whole genome sequencing has paved a way further to locate the exact position of the scorable phenotype.

Reverse genetics aims to discover a mutation in a target gene of interest to gain insight into its function. The advent of whole genome sequencing in many species has enabled a reverse genetic approach to successfully annotate unknown gene function. Several reverse genetic approaches were employed to mutate the gene sequence to study its function. A large collection of induced mutagenized population has to be developed and screened to increase the probability to score mutation in the gene of interest. Alternatively, directed approaches could be used where the function of the target gene is specifically altered. Thus, the availability of complete genome sequences combined with reverse genetics can allow every gene to be characterized. Several approaches have been developed for reverse genetics such as TILLING, RNAi, transposon mutagenesis, Nuclease-mediated gene modifications etc. Among these approaches, TILLING is the most widely adopted approach for identifying mutations in randomly mutagenized populations.

2.4.3.1 TILLING

TILLING (Targeting Induced Local Lesions in Genomes) is a sensitive screening method for directed identification of a mutation in a particular gene. This technique has proven to be a valuable methodology for finding induced mutations as well as naturally existing polymorphisms. The genomic region to be assessed for mutation is amplified by PCR along with wild type genomic DNA, the heteroduplex present in the DNA is detected by mismatch cleavage by CEL 1 nuclease. The cleavage of PCR product indicates the presence of single nucleotide or small insertion/deletion mutation. As TILLING requires a highly concrete and discrete PCR product for CEL I digestion, a successful PCR is one of the most important steps for optimal TILLING reaction to identify mutations. Samples are analyzed by polyacrylamide gel electrophoresis (PAGE) or on a capillary sequencer.

With the availability of Next Generation sequencing technologies (Tsai et al., 2013), the landscape has changed significantly allowing for a sequencing revolution. Such low-cost sequencing has made re-sequencing of gene fragments of interest in thousands of mutagenized lines. Several laboratories have integrated TILLING projects with NextGen sequencing technology platforms, e.g. Seq-TILLING. A major advantage to large-scale Seq-TILLING is that DNA samples can be analyzed in much deeper pools than with the CEL I based approach compared to the 8-fold pooling in traditional TILLING. Globally several groups have setup TILLING for different plants such as Arabidopsis (Till et al., 2003), maize (Till et al., 2004), lotus (Perry et al., 2003), pea (Triques et al., 2007), sorghum (Xin et al., 2008), barley (Caldwell et al., 2004), wheat (Slade and Kanuf, 2005), tomato (Minoia et al., 2010), beetroot (Kornienko, 2013) Drosophila (Winkler et al., 2005), Caenorhabditis (Gilchrist et al., 2006), zebrafish (Wienholds et al., 2003) and rat (Smits et al., 2004). Several mutant lines with desirable phenotypes have been identified and have been released for the cultivation. One advantage of TILLING is that the mutant lines can be directly released for cultivation as these are not classified as genetically modified organisms (GMO).

Development of a densely mutagenized population determines the frequency of a mutation in a species. However, others factors such as the choice and the dose of mutagen, G/C content of the genome and tolerance of each genotype to mutagenesis plays an equally important role in accessing the frequency of a mutation. A major advantage of TILLING is that it generates an allelic series of mutants that provides a better understanding of gene function (Till et al., 2003).

2.4.3.2 EcoTILLING

EcoTILLING is a variant technique of TILLING that is widely applied to collections of natural variants for discovering polymorphisms in a particular we are interested in. Various cultivars of a species are rich of genetic information and is exploited to understand many aspects of plant development. The method also finds its application to finding homo and heterozygosity of the polymorphism within a gene fragment and assists in estimating phylogenetic diversity and selection pressures are acting on a gene fragment. EcoTILLING approach was initialized on *Arabidopsis thaliana* (Comai et al., 2004) and then extended to several other species such as tomato (Rigola et al., 2009), Musa sp. (Till et al., 2010), *Vigna radiata* (Barkley et al., 2008) and in Cucumis sp. (Nieto et al., 2007).

2.4.3.3 HRM based TILLING

Traditional TILLING suffers from the drawbacks associated with several labor and time-consuming process of PCR, endonuclease digestions, gel electrophoresis runs and visual analysis. However, HRM is a non-enzymatic mutation screening technique that reveals sequence variants due to distinct patterns in DNA melting curve shape (Zhou et al., 2004; Gady et al., 2009). It has been used recently in many ways as a novel approach to study genetic variation in many species with applications ranging from qualitative SNP detection to the semi-quantitative analysis of methylation. PCR is performed using gene specific primers by heating to 95°C when the two strands of DNA separate or "melt" apart and the process is monitored in real-time using a fluorescent dye that intercalates to double-stranded DNA and fluoresce brightly but do not to bind and fluoresce at a low basal level in the absence of double stranded DNA. The HRM plots the data as a graph known as a melt curve, showing the level of fluorescence vs. the temperature. HRM tool has been employed in a number of plant systems for either detecting mutation e.g. Tomato (Gady et al., 2012) or for the detection of nucleotide diversity in different cultivars of rice (Zhu et al., 2013). The method is mainly optimized to detect misincorporation in small amplicon (<450 bp) and is best suited for target genes with multiple small exons separated by large introns (Parry et al., 2009).

2.4.3.4 Exome sequencing

The part of the genome formed by removal of introns through the splicing mechanism is called as the exome. Exons are usually flanked by untranslated regions (UTRs) that are excluded in exome studies. Thus, exome sequencing selectively sequences the coding regions of the genome. Hence, it has emerged as a cheaper and effective alternative to whole genome sequencing to find out the variation in the coding region of genomes that is responsible for a mutation and/or phenotype. Henry et al. (2014) used multiplexed global exome capture and next generation sequencing to identify ~18,000 induced mutations from 72 independent M_2 rice individuals.

2.4.3.5 Gene targeting strategies

Gene targeting methods aims to mutagenize a gene of interest to reveal its function without mutagenesis of the entire genome. These methods are powerful tools for studying basic and applied biology. Presently the technique has been extensively used for crop improvement and gained popularity and to suppress the expression of several targeted genes in the plant system.

Short interfering RNA and microRNA are widely used gene silencing strategy that initiates with the introduction of dsRNA into the nucleus by a homology-based

detection of the target mRNA. The expression of dsRNAs can be restricted to a particular tissue at a defined growth stages using a tissue specific promoter to control the extent and timing of gene silencing.

Zinc Finger Nucleases are chimeric proteins composed of a synthetic zinc finger-based DNA-binding domain and a DNA cleavage domain that is specifically designed to cleave long stretch of double-stranded DNA sequence to obtain zinc finger arrays with different sequence specificity. (Durai et al., 2005, Camenisch et al., 2008). Using this technique plant genes were edited in various genomes e.g. Maize (Shukla et al., 2009), tobacco (Townsend et al., 2009) *Arabidopsis thaliana* (Zhang et al., 2010), tomato (Moon et al., 2010).

TALENs are composed of an engineered array of DNA Binding Domains (DBD) fused to a non-specific FokI nuclease domain. TALENs can be customized by assembling them according to the desired target sequence to be edited. TALENs overcomes over ZFNs as the latter recognize only a limited number of target sites in the genome while the former can easily be designed to target any recognition site provided only that there is a thymine (T) before the first nucleotide of the target site. TALENs have been widely used in plants species such as tobacco (Zhang et al., 2013), rice (Li et al., 2012), Brachypodium (Shan et al., 2013), barley (Wendt et al., 2013), and Arabidopsis (Christian et al., 2013).

Both ZFNs and TALENs suffer from drawbacks due to complicated design and laborious assembly of specific DNA-binding proteins for each target gene. Clustered Regularly Interspaced Short Palindromic Repeats (CRISPR/Cas) system generates double Strands Breaks (DBS) and specificity is provided by a 20-bp sequence corresponding to the sequence that has to be edited (Jinek et al., 2012). CRISPR system has been applied in Arabidopsis (Feng et al., 2013; Li et al., 2013; Mao et al., 2013) tobacco (Li et al., 2013; Nekrasov et al., 2013), and the crop plants rice (Feng et al., 2013; Jiang et al., 2013; Mao et al., 2013; Miao et al., 2013; Shan et al., 2013), wheat (Shan et al., 2013b) and sorghum (Jiang et al., 2013).

2.5 Wild relatives of Tomato

Solanaceae or Nightshade family is diverse, comprising of approximately ten thousand species. The domesticated tomato (*Solanum lycopersicum*) and its wild relatives belong to the *Lycopersicon* clade of this family. Members of this clade have originated from South America near the Andean region. The microhabitats and extreme ecological conditions contribute to the diversity of wild species. This broad variation is reflected in

various aspects i.e. morphological, physiological, sexual and molecular features of tomato wild relatives (Peralta and Spooner, 2006). The wild relative species can be discriminated based on their fruit color. Most of them have green colored fruits, with the exception of two species-*S. galapagense* (yellow and orange fruits) and *S. pimpinellifolium*, the only wild species with red colored fruits. *S. lycopersicum var cerasiforme* fruit is larger than *S. pimpinellifolium* and is commonly referred to as cherry tomato. This has been considered as the direct ancestor of domesticated tomato (Rick and Chetelat, 1995). The modern cultivated tomato is cosmopolitan and is grown under various environmental conditions all over the globe.

Wild relatives harbor high genetic diversity and are a primary source of genetic variation. Wild relatives of many crops have been extensively used in breeding programs to improve the agronomic traits. Several studies on tomato wild relatives identified many useful traits, such as tolerance to drought and salinity in *S. pennellii* (Dehan et al., 1978; Shalata et al., 1998), accumulation of health-promoting phytochemicals in *S. habrochates* and resistance to multiple pathogens exhibited by *S. cheesmannii*, *S. lycopersicoides*, *S. neorickii* and *S. chilense* (Robert, 2001; Rick et al., 1994). Previously breeding studies were carried on mapping populations that are based on interspecific crosses between a cultivar and related wild species from the *Lycopersicon* group. Though this approach permitted the identification of QTL for a trait of interest, it is time-consuming and laborious. With the emergence of new molecular techniques and bioinformatics tools, and the availability of genome sequences, genotyping by sequencing is possible (Hohenlohe et al., 2011; Elshire et al., 2011). Increasing community-wide resources and germplasm banks have added value in understanding the genetic diversity of wild species. Tomato JBrowse, a recent resource developed by Wageningen University, Netherlands provides huge data on the SNPs of more than 150 tomato species that can be used for better understanding of natural diversity (Aflitos et al., 2014).

CHAPTER 3

MATERIALS AND METHODS

3.1 TILLING (Targeting Induced Local Lesions In Genomes)

3.1.1 Plant material and mutagenesis

An Indian cultivar of *Solanum lycopersicum*, Arka Vikas (Sel 22) was used as the core genetic resource for the development of the mutagenized population. It is a pure line selection from an American variety *Tip-Top* developed by Indian Institute of Horticulture Research (IIHR), Bangalore, India. Plants of this variety are semi-determinate having dark green foliage with medium to large, oblate fruits with the light green shoulder. It is cultivated as a Kharif/Rabi crop, tolerant to heat and moisture stress and matures in 140 days with an average produce of 35-40 tons per hectare (http://www.iihr.res.in/).

Seeds of the Indian cultivar, Arka Vikas, (10-15 g) were imbibed in double distilled water in germination boxes for one day. Thereafter the seeds were submerged in 500 ml of ethyl methane sulphonate [(EMS) Sigma Aldrich] solution of 60 mM (0.75%, w/v) and 120 mM (1.5%, w/v), and incubated in darkness with gentle shaking at 25±2°C for 24 hr as described by Koornneef et al. (1990) and Menda et al. (2004). The treated seeds, tied together in a muslin cloth, were extensively washed under running tap water for 8 hr and then dried on blotting sheets. Treated seeds were sown in nursery beds (2 m x 1 m) containing red loam sandy soil. To ensure uniform spread of the seeds in nursery beds during sowing, the seeds were first mixed with dry sand and sprinkled over the bed and covered with a thin layer (~1 cm) of red loamy soil and vermiculite mixture. These beds were then covered with black polyethene sheets till germination and watered daily using a sprinkler. A batch of 100 seeds was used as a control and processed through the same procedure as mentioned above without any EMS treatment. (**Note:** EMS is an excellent mutagen and consequently highly carcinogenic and also volatile. All necessary safety precautions should be taken when conducting a mutagenesis experiment. The experiment should be carried out in a fully functional and inspected chemical fume hood with double gloves, safety glasses and dressed in full safety gear, including lab coat and inform all lab members regarding the experiment).

3.1.2 Growth conditions

Seeds from all the tomato genotypes mentioned were surface sterilized with 4% (w/v) sodium hypochlorite for 10 min to soften the seed coat and then washed in running tap water till the traces of hypochlorite were removed. Thereafter, the seeds were spread on wet blotting paper placed in petri plates and incubated in darkness for germination. The emergence of radicle was scored as the first sign of germination. The

germinated seeds were then transferred to coconut peat mixture (Sri Balaji Agroservices, Madanapalle, Andhra Pradesh, India) placed in a plastic germination box (9.5 cm length, 9.5 cm breadth, 5 cm height). The boxes were kept under continuous white light (100 μmol $m^{-2}s^{-1}$) in growth room for the establishment of seedlings. Unless specified all the plants were grown in an open field at the University of Hyderabad under drip irrigation.

3.1.3 Development of mutant populations

Three weeks old M_1 seedlings were transplanted in the open field at a spacing of 1.3 m x 40 cm. These were cultivated by standard agronomic practices for tomato and irrigated by drip irrigation facility. The plants were grown to maturity, and M_2 seeds were harvested from each of the plants separately. The populations were advanced to M_3 generation in the next round of cultivation. For this, few seeds of each M_2 line were surface sterilized with 4% sodium hypochlorite solution and germinated in Soilrite under glasshouse conditions. Four plantlets, with an average height of 10 cm, from each line (namely, A, B, C and D) were transplanted in the open field and grown to maturity. All the M_2 and M_3 seeds of both the populations (60 and 120 mM EMS-treated) were properly labeled, cataloged and stored in -20°C freezers. Similarly, the M_2 seeds (3,000 lines) of M82 cultivar procured from Dani Zamir, Israel were germinated, and four plantlets of each line were advanced to M_3 generation as described above **(Fig. 3.1)**. **Table 3.1** describes in detail the dosage of EMS and size of populations developed in our study.

3.1.4 Setup of molecular screening platform in tomato

3.1.4.1 DNA extraction and pooling

Individual lines from the above-mentioned populations were germinated in 96 deep well plates and ten days old cotyledons were used for DNA isolation. Unlike the conventional protocol followed for TILLING in other species where DNA is first isolated, equalized and then pooled; eight folds tissue pooling in two-dimensional fashion was done prior to DNA isolation (NEATTILL) as described in Sreelakshmi et.al. (2010). In the present study, we used an in-house standardized DNA extraction protocol (Sreelakshmi et al., 2010) from tomato cotyledons/leaves. Briefly, the harvested tissue (100 mg) was mechanically disrupted using three steel balls in a Mini-Bead Beater for 2 min in the presence of 750 μL preheated (65°C) extraction buffer (0.1 M Tris-HCl, pH 7.5; 0.05 M EDTA, pH 8.0; 1.25% (w/v) SDS) containing 0.2 M β-mercaptoethanol and 20 mg of insoluble polyvinylpolypyrrolidone (PVPP). The samples were then incubated with 4 μL of RNase (10 mg/mL stock) for 30 min at 37°C in a water bath. This was

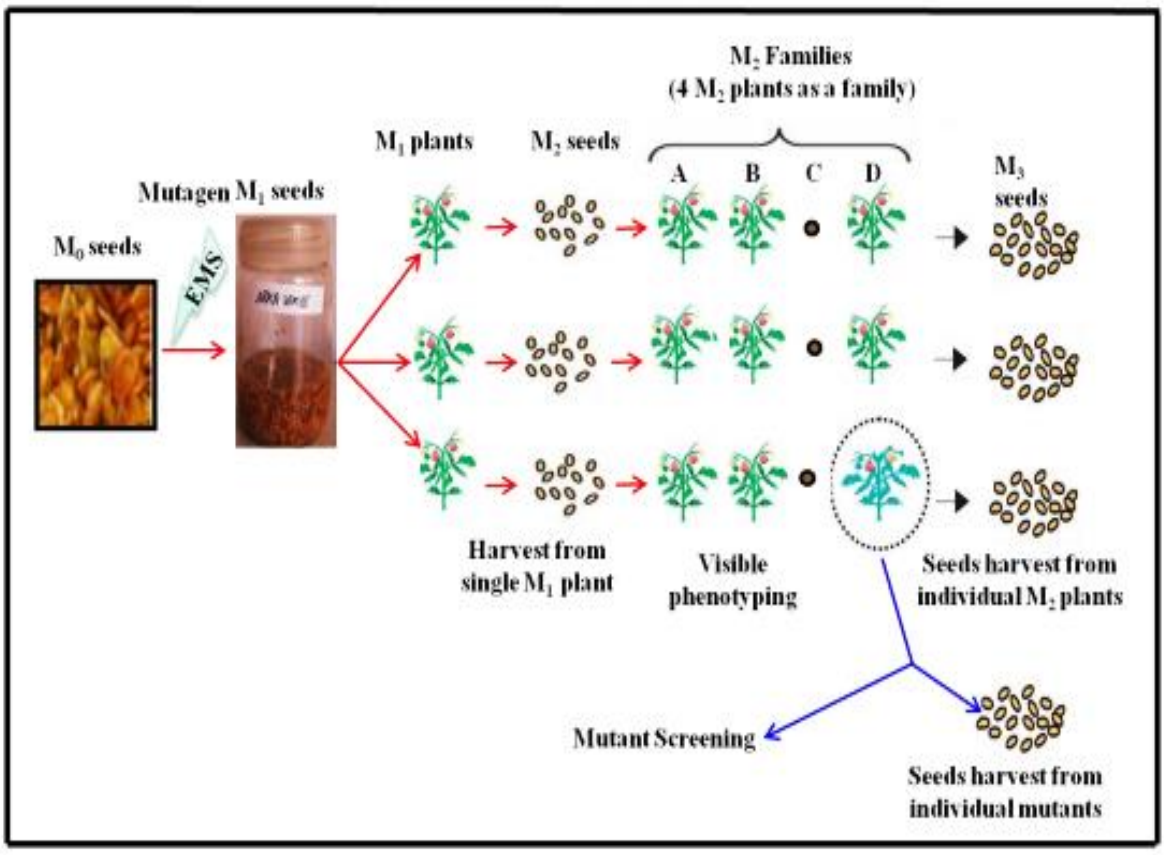

Figure 3.1. Pictorial representation showing how EMS mutagenized tomato population was raised. Tomato seeds (M_0) were treated with EMS and the M_1 plants were grown in the open field and allowed to self-pollination to produce M_2 seeds. M_2 seeds were collected from each individual M_1 plant to generate M_2 family. Four plants (named as A, B, C and D) from each M_2 line were grown. Each M_2 plant was also visually phenotyped for morphological alterations throughout the plant life cycle to identify mutants. M_3 seeds were collected from each M_2 individual plants.

Table 3.1 EMS-mutagenized TILLING population used in this study. Four populations were used for TILLING. The number of M_2 and M_3 lines screened for mutations using TILLING is indicated in the table.

S. No.	Population	Tomato cultivar	EMS concentration	Population size
1	I	Arka Vikas M_2	60 mM	2304
2	II	Arka Vikas M_2	120 mM	3000
3	III	M82 M_2 *	60 mM	3000
4	IV	M82 M_3	60 mM	3072

*This population was originally obtained from Dani Zamir, Hebrew University, Israel. The raising of this population is described in Menda et al., (2014). The population IV consisted of M3 seeds harvested from population III.

followed by the addition of 400 µL of 6.0 M ammonium acetate in order to precipitate the proteins. Thereafter, the samples were incubated at 4°C for 15 min followed by centrifugation at 3124 *g* for 30 min (for 96 well plates) in Sorvall RC evolution centrifuge or at 18,894 *g* (for individual microfuge tubes). The clear supernatant was transferred to a new microfuge tube plates, and an equal volume of chilled iso-propanol was added. The samples were incubated for 2 hr at -20°C. Samples were then centrifuged at 4°C for 30 min followed by 70% (v/v) ethanol wash. To remove the traces of salts from samples, one more round of ethanol wash was given. The DNA samples were air dried, and the pellet was dissolved in 200 µL TE buffer supplemented with RNase (3.3 µg/mL) and kept for overnight dissolution. The yield and quality of the isolated DNA was estimated by electrophoretic separation on agarose gels as well as using Nanodrop spectrophotometer. A working stock of 1 ng/µL DNA was prepared and 5 µL from it were aliquoted into 96 well PCR plates, dried, sealed with aluminium sealing films and stored at -20°C until further use.

For pooling of cotyledons for DNA isolation, two sterile plates were set up, one for column pooling and second for row pooling. Since harvesting of the cotyledon was done in column wise fashion, a simplified procedure was adopted to ensure the correct pooling of cotyledons. The right cotyledon from all eight seedlings (arranged in a column in 8 × 8 grid plate) was excised and harvested to make a single column pool, and placed in well 1A of 'column' plate whereas left cotyledon from each seedling was placed in wells of column 1A to 1H of the 'row' plate. The next harvest of right cotyledons generated 8-pooled well 1B of 'column' plate and left cotyledons were again placed in wells of column 1A to H of the 'row' plate, increasing number of cotyledons to two. The entire process of pooling batches of eight seedlings from 8 × 8 grids was repeated for 3rd - 8th columns of the 8 × 8 grid. At the end of total harvest of 8 × 8 grids, 8 cotyledons from grid were pooled in column fashion and 8 cotyledons were pooled in row fashion. Using 12 plates of seedlings we obtained two plates of cotyledons arrayed in row and column fashion. The pooled plates bearing cotyledons were sealed with rubber sealing mats and stored at -80°C freezer until DNA isolation. On completion of pooling of all the mutant lines in the population, we again harvested the seedlings as in the previous case and subjected it to second round of pooling to generate backup plates (Sreelakshmi et al., 2010).

3.1.4.2 Candidate gene

The ethylene biosynthesis gene *ACC* synthase isoform *ACS2* (*1-aminocyclopropane-1-carboxylate synthase 2*) was used as a candidate gene for the mutation detection in tomato M_2 mutant population. The ORF of tomato *ACS2* has 2522 bp and consists of 4 exons and three introns (Solyc01g095080.2.1; http://solgenomics.net/feature/17805455/details) **(Fig. 3.2)**. The cDNA has 1458 bp encoding a deduced protein of 486 amino acids. The ACS2 protein had a predicted MW 55 kDa and a pI of 5.53.

3.1.4.3 Selection of targets in gene of interest for mutation

The CODDLE (Codons Optimized to Discover Deleterious Lesions; (http://www.proweb.org/coddle) program was used to screen the regions of the genes that had the highest probability of being affected by EMS. For CODDLE analysis, gene sequence was fed in the Codons Optimized Detection of Deleterious Lesions (CODDLE) input utility page (http://www.proweb.org/input/). CODDLE generates a gene model (intron/exon position) and a protein conservation model by searching the Blocks Database (Henikoff et al., 2000). Once a gene model and a protein conservation model are assembled, CODDLE (http://www.proweb.org/coddle/) presents candidate regions that are most likely to be susceptible to deleterious mutations after EMS treatment (McCallum et al., 2000b). CODDLE reports the expected missense and nonsense changes arising due to the mutagenic effect. Amplicons of ~950-1500 bp were selected from these regions, and specific primers were designed using Primer 3 software (http://frodo.wi.mit.edu/primer3/) **(Fig. 3.2)**.

3.1.4.4 Primer design and Nested PCR strategy

All the primers were designed using Primer version 3.0 software. For all sets of primer, the Tm was kept between a range of 50-60°C, the length between 20-25 bases, and GC content near to 40-45%. Using primer version 3.0 software, two different major sets (including two subsets each) of primers were designed covering entire ORF and also -866 bp of 5' upstream region considered as a promoter region. The exon 4 of *ACS2* gene was comparatively longer (997 bp) than the rest three exons (e.g. exon1 (171 bp), exon 2 (129 bp), and exon 3 (161 bp). The subset 1 of the primer set I (-866 bp to 29 bp) covers 5' upstream sequences and 29 bp of the first exon. The subset 2 of the primer set I start from -196 bp 5' upstream and end at 648 bp in third intron covering the first exon, first intron, second exon, second intron and third exon respectively. The subset 1 of the primer set II swept the region from 1252 to 2202 bp, covering a small portion of 3rd intron and half of the 4th exon. The subset 2 of the set II primers covers the region from

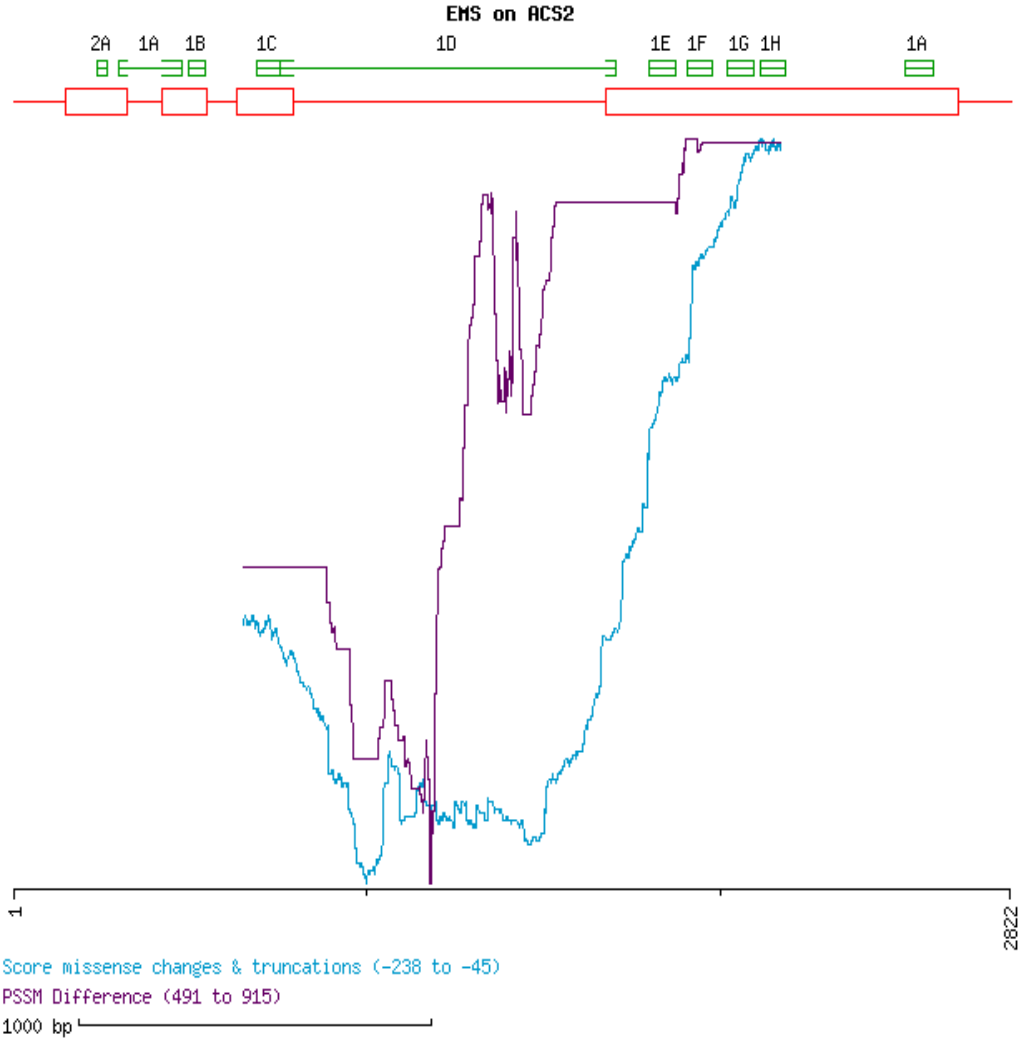

Figure 3.2. Output of the CODDLE program using *ACS2* gene sequence. The *ACS2* gene is represented by orange open boxes (exons) connected by black lines in between (introns). The green colored boxes represent the protein conservation models. The probability curve traced in blue below the gene model represents those regions of the gene where G: C to A: T transitions are most likely to result in deleterious effects on the encoded protein.

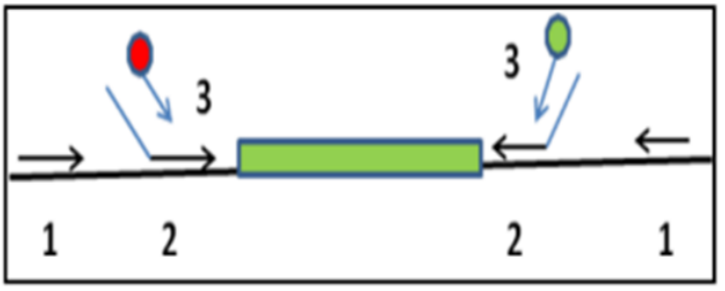

Figure 3.3. Nested PCR strategy using universal M13 tailed primers. Targets were amplified with sequence specific primers 1F and 1R (black arrows). The large product was taken as a template and a nested PCR with an internal gene specific primers 2F and 2R (black part of the arrow) containing universal M13 primers (blue part of the arrow) in combination with IR-dye labeled universal M13 primers (blue arrows with dye) was performed. The red and green circles indicate the position of the IRD700 and IRD800 labelling respectively.

2015 to 2942 bp, including remaining half portion of the 4th exon as well as a small portion of 3' noncoding (420 bp) sequences. 100 µM solution of each primer was prepared in TE buffer and aliquots were stored at -80°C to avoid repeated freeze–thaw cycles.

To improve the sensitivity and specificity of PCR for robust mutant detection, we adopted nested PCR strategy **(Fig. 3.3)** with labeled M13 universal primers. In nested PCR, two separate amplifications are used. The first uses a set of primers that yields a large product, which was then used as a template for the second amplification. The second set of primers anneals to sequences within the initial product producing a second smaller product. Based on nested strategy, we designed primers for screening the promoter and four exons of *ACS2* gene **(Table 3.2)**. An advantage of nested PCR is the consistency of reactions with all samples so that any fraction of the pooled DNA which bears the mutation can be amplified and visualized. Moreover, the use of M13 universal primers is cost effective.

3.1.4.5 PCR based Screening for mutations

The DNA from M_2 lines was used for screening mutations in the gene of interest. We used PCR-based mutation screening that involves three steps – firstly, amplification of the fragment of interest followed by heteroduplex formation and mismatch cleavage by CELI enzyme and finally, detection on denaturing polyacrylamide gels. PCR was performed in Tetrad Machine (Bio-Rad) in 96-well microtitre plates. In the first step of the nested PCR approach, the PCR reaction consisted of 5 ng DNA, 1X PCR buffer, 2.5 mM dNTPs, external forward and reverse primers {3 pmoles each, (IDT)} and 0.18 µL Taq DNA polymerase (in-house isolated) in a total volume of 20 µL. The cycling conditions were: 94°C for 4 min; 35 cycles of 94°C for 20 sec, T_m-4°C for 45 sec, 72°C for 2 min; 72°C for 10 min; and 12°C forever. The PCR product was diluted 2-5 folds depending on the yield, and 1 µL was used as the template for second step PCR. This reaction consisted of 1X PCR buffer, 2.5 mM dNTPs, primer cocktail {1pmole in the ratio of 1.2:0.7:1.5:0.5 (700 IR dye labelled forward : unlabelled forward : 800 IR dye labelled reverse : unlabelled reverse)} and 0.18 µL of Taq DNA polymerase. The cycling conditions were 94°C for 4 min; 94°C for 20 sec, 60°C for 45 sec with a touchdown of -2°C/cycle for 5 cycles, 72°C for 1.5 min; 25 cycles of 94°C for 20 sec, 52°C for 45 sec, 72°C for 1.5 min; and final extension at 72°C for 10 min. This was followed by heteroduplex formation: 98°C for 10 min, 80°C for 20 sec, 80°C for 7 sec with a touchdown of 0.3°C/sec for 70 cycles; and 12°C forever.

3.1.4.6 Mismatch-specific cleavage reaction and precipitation of PCR products

Once the fragment of interest was amplified, the labeled products were digested with single strand mismatch-specific enzyme, CEL I. The mutated nucleotides form a loop during heteroduplex formation and become the targets of digestion for CEL I enzyme. The digestion was carried out in a total volume of 45 µL containing 20 µL of labelled PCR product, 1X CEL I digestion buffer (10 mM HEPES buffer pH 7.0, 10 mM KCl, 10 mM $MgCl_2$, 0.002% (v/v) Triton X-100 and 10 µg/mL BSA) and CEL I enzyme at 1:300 dilution (1 µL/300 µL CELI digestion buffer). The mixture was incubated at 45°C for 15 min and then the reaction was stopped by adding 10 µL stop solution (2.5 M NaCl, 75 mM EDTA, pH 8.0 and 0.5 mg/mL blue dextran). The DNA was precipitated by the addition of 125 µL of cold absolute ethanol and incubated at -80°C for 15-30 min. This was followed by centrifugation at 4500 rpm for 30 min in a SH-3000 plate rotor in Sorvall Centrifuge. The pellet was washed with 70% (v/v) ethanol, dried in a dry bath at 80°C and then resuspended in 8 µL of formamide loading buffer (37% (v/v) de-ionized formamide, 1 mM EDTA and 0.02% (w/v) bromophenol blue). The PCR products were denatured by heating the plates/tubes to 94°C for 2 min and then placed on ice.

3.1.4.7 Detection of mutation using Li-COR

The labelled precipitated and denatured samples were then analysed on Li-COR DNA analyser 4300 (Li-COR Inc., Nebraska, USA) which include two major steps– acrylamide gel preparation, sample loading and gel running as described by Sreelakshmi et.al. (2010).

In TILLING protocol, denaturing acrylamide gels were used for separation of CELI digested PCR products. Prior to the casting of a gel, the glass plates were cleaned and assembled with spacers and rails following the protocol provided with the Li-COR DNA analyzer. 20 mL of gel matrix is sufficient to cast a 15x15x2 mm sized 6.5% gel. For the preparation of gel matrix, 4 mL of 20% acrylamide gel matrix, 8.8 g of Urea, 2 mL of 10X TBE (Tris Boric acid EDTA) buffer were mixed by gentle stirring. If necessary, the magnetic stirrer was heated up to 35°C for proper dissolution of urea. The final volume was made up with Milli-Q water. To this mixture, 15 µL of TEMED and 150 µL of 10% (w/v) APS (ammonium persulfate) was added, and the matrix was mixed with the help of glass rod. Quickly the mix was poured carefully between the glass plates, avoiding air bubbles. Later, the shark tooth comb was inserted, and the pressure plate was applied upon inserted comb place. The comb was inserted in such a way that the flat end of the comb creates a shallow trough after solidification. The excess acrylamide was

Table 3.2 List of primer sequences designed for TILLING/EcoTILLING *ACS2* gene using nested PCR strategy.

Gene	Primer		Start – end position	Length	Tm (^{0}C)	GC (%)	Sequence	Amplicon Size (bp)
	M13 F			18	52	50	TGTAAAACGACGGCCAGT	-
	M13 R			19	52	42	AGGAAACAGCTATGACCAT	-
ACS2 (Solyc01g095080.2)	SET I	F1	-866	20	55	40	CTCGATGACCTTTAAAATCG	895
		R1	29	20	55	45	GAGTTGGTCTTTGCAATCTC	
		F2	-196	22	57	41	TCCCTCACATTCCTTAATTCTC	844
		R2	648	22	60	45	TTACGCTGGGTAGTATGGTGAA	
	SET II	F1	1252	24	51	38	GACCATTGCTTATCGAGGTAAAAT	975
		R1	2202	23	51	39	CGAAAGTCGATTCCCTTAAAAGT	
		F2	2015	21	53	52	TTAGCGGCAATGCTATCGGAC	945
		R2	2942	26	51	42	CACAAACACCATAATCTCTCCATCTC	
ACS4 (cDNA) (Solyc05g050010.2.1)	SET III	F1	0	27	74	54	GGATCCATGGATTTGGAGACGAGTGAG	1643
		R1	1428	29	65	35	CTCGAGTTAAGCTAATAACATTTTCATCG	

poured onto the comb. The gel was allowed to set for 90 min before starting the run. After complete polymerization, the gel cast was thoroughly washed on both the front and back sides of the casting plate, the casting comb was removed, and remaining acrylamide was washed off from the well. Before placing the plates in the Li-COR DNA analyzer, the plates were cleaned with Kimwipes, to ascertain that the laser detection region of plate is clean and also the comb was re-inserted such that small wells are formed between two shark teeth.

The plate assembly was inserted into Li-COR DNA analyzer, and the wells were cleaned before beginning the pre-electrophoresis run. The upper and lower tank buffer was filled with 1X TBE buffer. The pre-run of the gel was started for 15 min, ensuring that the lasers focus properly. About 0.5 µL of the sample was loaded per well on acrylamide gel (6.5%, w/v) and the electrophoresis was carried out for 4 h at 1,500 V, 40 W and 40 mA at 50°C in Li-COR 4300 DNA analyzer. The two TIFF images obtained for 700 and 800 channels of Li-COR analyzer were analyzed in Adobe Photoshop software **(Adobe Systems Inc.)**, and the gel was visually assessed for mutations. The mutations were confirmed on complementary plates (row and column) and the plant ID in the DNA pools was identified. Few of the seeds from the identified original seed packet were germinated, and the plants were grown to maturity. DNA was isolated from juvenile leaves and was again subjected to the mutation screening protocol as described above to identify the homozygous/heterozygous lines. The genomic DNA isolated from specific line harbouring the mutation was PCR amplified and sequenced by Big Dye Terminator chemistry on ABI sequencer (Applied Biosystems, Foster City, California, USA) to identify the specific base change.

3.2 EcoTILLING

EcoTILLING protocol involves steps that are almost similar to TILLING procedure with few exceptions. The genomic DNA isolated from the collection of tomato natural accessions was used as a template. For EcoTILLING, a collection of 391 *S. lycopersicum* accessions (Appendix I) obtained from NBPGR (National Bureau of Plant Genetic resources (http://www.nbpgr.ernet.in/), IIVR (Indian Institute of Vegetable Research, Varanasi, India (http://www.iivr.org.in/) Bejo Sheetal, Jalna, India and TGRC (Tomato Genetic Resource Center, University of California, Davis (http://tgrc.ucdavis.edu/) were used. In order to facilitate heteroduplex formation, reference cultivar (AV) genomic DNA was used. The details of primers used for PCR amplification of *ACS2* gene were listed in **Table 3.2** and. Nested PCR was set up in 20

µL volume. The reaction mixture consisted of 5 ng of genomic DNA as template, 1X PCR buffer, 2.5 mM dNTPs, 0.18 µL of in-house purified Taq polymerase, 1 picomoles each of labeled and unlabelled primers in a ratio of 1.2:0.7:1.5:0.5 (F_L:F_{UL}:R_L:R_{UL}). The PCR conditions were 94°C-4 min, 5 cycles of 94°C-20sec, 60°C-45 sec with a decrement of 2°C per cycle, 72°C-1 min 30 sec, 30 cycles of 94°C-20 sec, 52°C-45 sec, 72°C-1 min 30 sec followed by 72°C-10 min and held at 4°C. The amplification was followed by further denaturation and SNP detection as described for TILLING **(section 3.1)**.

3.3 Amplification of the *ACS2* gene from tomato wild relatives

To assess the natural distribution and diversity of single nucleotide polymorphisms existing in *ACS2* gene, the target gene was amplified from the five wild relatives of tomato considered in the study. The wild tomato TGRC accessions *S. pimpinellifolium* (LA1589), *S. galapagense* (LA0483), *S. chilense* (LA1969), *S. pennellii* (LA0716) and *S. neorickii* (LA2133) were obtained from Tomato Genomics Resource Centre (University of California, Davis). Genomic DNA isolated from the young leaves of these plants was used as a template. The primers and PCR conditions designed and optimized for TILLING and EcoTILLING protocols were used for amplifying the target genes. For SNP analysis, the amplified products were purified and directly sent for sequencing.

3.4 Silica based purification of PCR products

The target sequences amplified from tomato wild relatives and also the PCR products of confirmed mutations were sequenced to determine the exact position and nature of the nucleotide base changes. Before sequencing, the amplified PCR products were purified by silica-based purification. Silica purification is a simple and time-saving protocol as described in Boyle and Lew (1995). The protocol involves two major steps- preparation of silica suspension and purification of PCR products.

3.4.1 Preparation of Silica suspension

5.0 g of Silica (Sigma, S-5631) was suspended in 50 mL of autoclaved milli-Q water and allowed to settle down for 2 h. The supernatant containing the fine particulate was discarded, and this step was repeated once followed by centrifugation at 2000 *g* for 2 min. The supernatant was discarded, and the slurry was stored at 4°C. Usually, one mg of the silica suspension (= 10 µL) binds to 3-4.5 µg of DNA.

3.4.2 Purification of PCR products

The PCR product was mixed with two volumes of 6 M NaI in a microfuge tube and incubated for 5-10 min. For agarose gel excised DNA fragments, the agarose is melted at 55°C in 6 M NaI with occasional mixing. To this mixture, 10 µL (~1 mg of

silica suspension) of silica suspension was added and incubated at room temperature for 5 min with intermittent mixing or gentle vortex. The contents of the microfuge tube were then centrifuged for 1 min at 18,894 *g*. The supernatant was discarded, and the pellet was resuspended in 500 µL wash solution (50 mM NaCl, 10 mM Tris-HCl pH 7.5, 2.5 mM EDTA and 50% (v/v) ethanol). The suspension was gently mixed and then centrifuged for 1 min. The wash step was repeated once again followed by a pulse spin to remove the residual liquid. The pellet was then air dried for 10 min, and an appropriate volume of milli-Q water or TE was added to dislodge the pellet. The contents were allowed to stand for 5 min at room temperature and then centrifuged at 18,894 *g* for 1 min. The supernatant containing the DNA of interest was then transferred to a fresh microfuge tube, and thus, the samples were purified.

3.5 Sequencing and bioinformatics analysis

Silica-purified amplicons were outsourced to Macrogen Inc. (Korea) for sequencing on both the strands. The raw sequencing data was analyzed by CHROMAS (http://www.technelysium.com.au) v2.4. Sequences were assembled and compared, and inspections of differences or similarities were analyzed using the Multialin Interface page (Corpet et al., 1988). In heterozygous mutations the chromatograms showed two peaks at the same position whereas the sequences from homozygous lines were aligned by Multialin online server to the wild-type reference sequence (Arka Vikas/M82) to ascertain the specific nucleotide change. The protein sequences were aligned using PRALINE (Bawono and Heringa, 2014) software (http://www.ibi.vu.nl/programs/pralinewww/). Other softwares used for further analysis of the nucleotide sequence were:

3.5.1 Project Aligned Related Sequences and Evaluate SNPs (PARSESNP)

The PARSESNP (http://blocks.fhcrc.org/proweb/parsesnp/) is a web-based tool useful for the analysis of polymorphisms in target genes in TILLING and EcoTILLING protocols. It determines the position of the altered nucleotide base from the reference sequence (genomic or cDNA) and the effect of the polymorphism on nature of the amino acid changed (if any). If a homology model was provided, PARSESNP also determines the severity of the mutation or polymorphisms based on PSSM and SIFT scores. The graphical output of PARSESNP depicted the SNPs detected along the gene sequences.

3.5.2 PSSM

The change in the Position-Specific scoring matrix (PSSM; based on protein homology model) predicted the severity of missense mutations. A large change in PSSM score (>10) indicated a mutation that was likely to have a deleterious effect on protein function.

3.5.3 SIFT

Bioinformatics program SIFT (Sorting Intolerant from Tolerant, www.sift.dna.org) predicted the impact of missense mutations on protein function. For missense/nonsynonymous polymorphisms, the deleterious effect of the mutation was estimated by assigning SIFT value using version 4.0.5 of SIFT (Ng and Henikoff, 2003; Sim et al., 2012). The prediction is based on database sequence homology and physical properties of amino acids. The probability of SIFT score less than 0.05 was predicted to be damaging to the function of the encoded protein, those greater than or equal to 0.05 were predicted to be tolerated.

3.5.4 Phylogenetic analysis

We used FigTree v1.3.1 software for analyzing the phylogenetic relationship of protein sequences. The sequences were aligned using ClustalX v2.1 software. Phylogenetic relationships were performed using neighbor-joining method. Neighbor-joining is a bottom-up clustering method which uses distance measures to correct for multiple hits at the same sites and chooses a topology showing the smallest value of the sum of all branches as an estimate of a correct tree. This method computes the length of the branches of the tree and in each stage; two nearest nodes of the tree are chosen and defined as neighbors. This process is carried out until all the nodes are paired together. The bootstrap values are denoted by the branch that is a measure of the evolutionary changes existing within the genotypes.

3.6 In silico characterization of tomato ACS2-1 protein

Homology modeling of ACS2 proteins of WT and *acs2-1* mutant was performed using ITASSER software (Zhang et al., 2008; Roy et al., 2010), using the templates of ACS protein from tomato (PDB ID; 1iayA, 1iaxA; Huai et al., 2001). The 3-D models were drawn with the software PyMol (http://www.pymol.org).

3.7 Morphological and Physiological characterization of mutants

3.7.1 Seed germination profiling

To monitor seed germination, seeds were surface sterilized using 4% (v/v) sodium hypochlorite. After washing, seeds were placed in plastic petri plates containing premoistened filter paper and sealed with para film. Three different sets of petri plates

(each set contains three such petri plates), for WT, *acs2-1* and *acs2-2* mutant seeds respectively, were kept in dark. Seed germination was monitored visually at a fixed interval of time. The emergence of radicles from the seeds is the first sign of seed germination. In each set, 10-12 seedlings were used.

3.7.2 Ethylene emission from seedlings of WT and mutants

To monitor the ethylene emission, germinated seedlings (6-8 for each set) were transferred to a glass vial containing 0.8% (w/v) agar. The vial was sealed by serum cap and incubated in darkness for 24 hr. Thereafter from the head space one mL volume containing ethylene was withdrawn from vial using an injection syringe and injected into a gas Chromatogram (model GC-17A, Shimadzu, Kyoto, Japan) fitted with a flame ionization detector and an activated "Porapack T" column. The amount of ethylene released was calculated by comparing the peak area with the area obtained by using 1 mL of pure ethylene gas as standard. The time course of ethylene evolution was determined by GC at regular interval for 10 days from germination.

3.7.3 Seedlings phenotype

Seedlings phenotype was monitored by measuring the length of the roots and counting lateral roots of WT and mutants. Germinated seeds (after emergence of radicle) of WT and mutants were grown on 0.8% (w/v) agar in three different sets of air-tight petri plates and kept in vertical orientation under continuous white light (100 μmole m^{-2} s^{-1}) for five days. Each such set contained three biological replicates. In each replicate, 10-12 seedlings were used.

3.7.4 Demonstration of triple response in etiolated seedlings

To elicit triple response, germinated seedlings (15-18 in each set) of WT and mutants were grown in an air-tight seed germination plastic box containing 0.8% (w/v) agar, in the dark, for five days. A known volume of ethylene was injected in each container only once. After five days, seedling's phenotype was observed for the triple response compared to the control seedlings. Hypocotyls and roots length were also measured for above seedlings.

3.7.5 Comparisons between plant texture, leaf morphology and flower phenotype

The plants were grown in greenhouse under natural photoperiod (12-14 h day, 10–12 h night) at 28±1°C during day and ambient temperature (14-18°C) in night. The difference in plant texture between WT and mutants was visually recorded. To monitor deference in leaf morphology, leaves were harvested and photographed from the 7^{th} node of the wild-type and mutant plants (45 days old). To observe flower morphology and the

pattern of the flower in flower inflorescence, flower from second and third truss were examined.

3.7.6 Off-vine leaf senescence study

Three different biological replicates in two set were used. Each set of leaf (containing three replicates) were placed in petri plates on wet germination paper in light and dark condition respectively. The leaves were harvested from seventh node of 45 days old wild type (M82) and *acs2-1, acs2-2* mutant plants grown in greenhouse. The petri plates were kept under continuous white light (100 μmole m^{-2} s^{-1}) and in darkness respectively to record senescence in mutant and wild type leaves.

3.7.7 Estimation of the ethylene emission from leaves of wild type and mutants

The plants were grown in greenhouse condition under natural photoperiod (12–14 h day, 10–12 h night) at 28±1°C during day and ambient temperature (14-18°C) in night. Fresh leaves were harvested from the 7^{th} node of 45 days old wild-type and mutant plants. Leaves were kept on premoistened filter paper in an air-tight petri plates and incubated for 3-4 hr at the room. Thereafter, from head space one mL volume containing ethylene was withdrawn from petri plates using an injection syringe. The head space gas was injected into a gas Chromatogram (model GC-17A, Shimadzu, Kyoto, Japan) fitted with a flame ionization detector and an activated "Porapack T" column. The amount of ethylene released was calculated by comparing the peak area of sample with the area obtained by using 1 mL of pure ethylene gas as standard.

3.7.8 Chronology of fruit development between wild type and mutant fruits

The fruit development was monitored on vine from post-anthesis (days post-anthesis - DPA) at different stages of ripening: mature green (MG), breaker (BR), Turning (TUR), Pink (P), red ripe (RR). The transition between different stages of ripening was visually monitored by the changes in fruit color. To precisely determine the age of fruits, flowers were tagged at anthesis and this time point was considered as zero DPA. Few other features of flowers and fruits were also monitored like no. of flower per truss, total no. of flowers per plant at a particular time point, total no. of fruit set per truss and no. of locules per fruit, of mutants compared to WT.

3.7.9 On-vine fruit senescence study

Fruit senescence study of wild-type (M82) and mutants (*acs2-1, acs2-2*) tomato fruit was carried out on-vine. For on-vine fruit senescence study, second fruit truss of wild type and mutants was selected. The transition between different stages of ripening was visually monitored by the changes in fruit color. To precisely determine the age of

fruits, flowers were tagged at anthesis and this time point was considered as zero DPA (Days Post Anthesis). The plants were grown in greenhouse under natural photoperiod (12-14 h day, 10-12 h night) at 28±1°C during day and ambient temperature (14-18°C) in night. The fruits were photographed from mature green stage onwards.

3.7.10 Comparisons of fruit morphology

WT and mutant (*acs2-1, acs2-2*) fruits at different maturity stages were harvested from the second truss of the vine. The transition between different stages of ripening was visually monitored by the changes in fruit color.

3.7.11 Fruit firmness

The firmness of fruits was measured using Durofel DFT 100 (Agro-Technologie, Tarascon, France). Firmness value was recorded by measuring each fruit at equatorial plane two times. Three-four fruits of each wild-type (M82) and mutants (*acs2-1, acs2-2*) were used for measurements.

3.7.12 Estimation of ethylene emission from fruits of WT and mutants

The fruits of wild type and mutant lines at different maturity stages (MG: mature green, TUR: turning and RR: red ripe) were harvested from second truss of the vine. The fruits were placed in an air-tight plastic container for 3-4 hr at room temperature. Thereafter incubation the head space one mL volume containing ethylene was withdrawn from the container using an injection syringe. The head space gas was injected into a gas Chromatogram (model GC-17A, Shimadzu, Kyoto, Japan) fitted with a flame ionization detector and an activated "Porapack T" column. The amount of ethylene released was calculated by comparing the sample peak area with the area obtained by using 1 mL of pure ethylene gas as standard. The plants were grown as in section 3.7.9 greenhouse condition. Five biological replicates were taken at each maturity stage.

3.7.13 Genetic analysis

The crossing was carried out on young unopened floral buds. 4±1 day's old unopened floral buds of WT were carefully emasculated by removing anther cone with the help of needle and forceps. The emasculated flower was covered with a thin cotton patch to prevent cross pollination. After 24 h when stigma becomes receptive, the pollens from mutant plants (male parent) collected from newly opened flowers were applied to stigmas of WT (female parent). The pollinated flowers were again covered with the cotton patch. The crossed flowers were labeled, and seeds from each crossed fruit were separately collected. Ten F_1 plants were grown from each plant, and seeds from individual fruits were collected separately for analyzing the F_2 segregation. For

segregation analysis, 140 F_2 plants were grown in the pots and the fruit senescence phenotype on-vine was scored.

3.8 Biochemical characterization of mutants

3.8.1 Estimation of chlorophyll from leaves of control and mutant plants

Chlorophyll content was measured from the leaves of mutant and WT plants using the modified protocol of Kousar et al., (2007). Briefly, a known amount of fresh leaf tissue (100-200 mg) was submerged in 2 mL of 80% (v/v) acetone, and after stirring stored in darkness. After centrifugation at 13,225 *g* at 4°C, supernatants were collected, and absorbance was recorded at 663 nm, and 645 nm in Uvikon spectrophotometer. The amount of *Chl A* and *chl B* were calculated using the formula of Arnon (1949). The chlorophylls a and b and total chlorophyll were calculated by the following formulae.

$$\text{Chla } (\mu g/mL) = (12.7 \text{ X } A_{663} - 2.79 \text{ X } A_{645})$$

$$\text{Chlb } (\mu g/mL) = (22.9 \text{ X } A_{645} - 4.68 \text{ X } A_{663})$$

$$\text{Total Chl } (\mu g/mL) = (20.2 \text{ X } A_{645} + 8.02 \text{ X } A_{663})$$

Where; A is the absorbance at 663 nm and 645 nm.

3.8.2 Estimation of Sugar content and pH

Sugar content of fruits was measured using a pocket refractometer (ATAGO, Tokyo, Japan). Entire pericarp tissue of the fruit was homogenized using mortar and pestle and 300 µL homogenate was layered on the optical lens of the refractometer. The sugar content was recorded as °Brix. One unit of °Brix is approximately 1% (w/v) soluble solids as measured by refractometer (Tieman et al., 1992). For every fruit sample ($n \geq 5$), two parallel measurements were carried out. The pH values of red tomato sap were also measured using the pH meter.

3.8.3 In-vitro ACC extraction and determination

To correlate with ethylene level 1-aminocyclopropane-1-carboxylic acid (ACC) level (a direct precursor of ethylene) were estimated at mature green, turning and red ripe stages of WT (M82) and mutant tomato fruits. For the estimation of ACC in fruit tissue, usage of pure standard is a prerequisite for comparisons and calculations. To prepare standard ACC solutions, ACC was procured from Sigma-Aldrich, St. Louis, MO, a US based company. A known concentration of ACC standard was oxidized to ethylene by mixing with cold mixture of 4% (w/v) NaOCl and saturated NaOH (2:1, v/v). The mixture was vortexed and incubated on ice for 4 minutes. After incubation, the tube was again stirred on a vortex and a 1 mL headspace gas sample was withdrawn by a hypodermic syringe for ethylene estimation using Gas Chromatography. 1-

Aminocyclopropane-1-Carboxylic Acid (ACC) was extracted from the fruit tissue of tomato by homogenization in presence of 5% (w/v) sulphosalicylic acid. The extracted ACC in the aqueous phase was used to determine the ACC concentration (Bulens et al., 2011; Yang et al., 1984). The 200 µL of 10 mM mercuric chloride was added to the aqueous extract in a glass test tube (15×125 mm) and the tube was sealed and incubated on ice. Cold mixture of 4% (w/v) NaOCl and saturated NaOH (2:1, v/v) was injected into the test tube. The mixture was stirred and incubated on ice for 4 minutes, thereafter the tube was agitated on a vortex and a 1 mL headspace gas sample was withdrawn by a hypodermic syringe for ethylene determination using Gas Chromatography. The amount of free, bound in the form of Malonyl-ACC (MACC) and total amount of ACC was calculated in mature green, turning and red ripe stages of the WT (M82) and mutant fruits. For calculation of total ACC, acid hydrolysis of extract was performed by adding 50 µL of 6 M hydrochloric acid into the extract. After vortexing, the extract was kept in a water bath for 3 hr at 99°C. After hydrolysis, the extract was kept at room temperature for cooling. After cooling the extract, 50 µL of 6M NaOH was added in the extract for neutralization. After neutralization, the extract was centrifuged, and the yellow supernatant was obtained which was further used for ethylene emission monitored by GC as mentioned. The ACC and MACC amounts were calculated based on the amount of ethylene gas released from the sample and spiked sample using the following formulae:

$$ACC = \frac{n_{sample} . V_{extract}}{V_{reading} . Eff . w}$$

$$Eff = \frac{n_{spike} - n_{sample}}{n_{blank}}$$

$$MACC = ACC_{tot} - ACC_{free}$$

Where, ***n***sample- number of moles ethylene formed, ***V***extract- total volume of liquid in the sample after extraction, ***V***reading- amount of extract used for the reading, ***Eff***- reaction efficiency of ACC turnover, ***w***- weight of the used sample, Total ACC- hydrolyzed ACC concentration.

3.8.4 ACS enzyme activity determination

Since, ACC is the end product of the reaction catalyzed by 1-Aminocyclopropane-1-carboxylate synthase (ACS), Therefore, ACS enzyme activity (In-

vitro) in WT and mutant fruits was determined at different maturity stages of fruits (Bulens et al. 2011). The ACS enzyme activity was determined using following protocol:

3.8.4.1 Extraction and purification

To determine ACS activity, the fruit tissue was extracted in extraction buffer containing tricine (200 mM, pH 8.5), pyridoxal-5-phosphate (PLP, 2 mM) and DTT (10 mM). Before extraction of ACS, 15 mg PVP was added to 2 mL precooled Eppendorf tube. To the tube then 1 g frozen crushed fruit tissue was added followed by addition of 1 mL of extraction buffer. The sample was vortexed until a homogenous mixture was obtained at centrifuged at 21,000 *g* for 30 minutes at 4°C temperature. A 1.25 mL aliquot of supernatant was collected and desalted on Sephadex G25 (4 mL pre-swollen bead volume) column for removing interfering metabolites. The eluted sample fraction was collected in the precooled tube.

3.8.4.2 Reaction of ACS enzyme with substrate

The reaction mixture consisted of 750 µL purified enzyme in a tube containing 75 µL tricine reaction buffer (200 mM, pH 8.0) and 75 µL of 1.2 mM S-Adenosine Methionine (SAM) chloride (substrate). After vortexing, the mixture was incubated in a thermomixer for 2 hr at 25°C with gentle shaking. After 2 h incubation reaction was stopped by adding 100 µL of 100 mM mercuric chloride. It was followed by addition of cold mixture of 4% (w/v) NaOCl and saturated NaOH (2:1, v/v) respectively, was injected into the test tube containing 475 µL reacted extract and 425 µL of distilled water. The mixture was stirred and incubated on ice for 4 minutes, after incubation the tube was again agitated on a vortex and a 1 mL headspace gas sample was withdrawn by a hypodermic syringe for ethylene determination using Gas Chromatography. ACS activity was calculated using following formulae:

$$ACS_{activity} = \frac{n_{sample}.V_{extract}.D_{column}.D_{reaction}}{Eff.V_{reading}.w.t}$$

$$\text{with } D_{column} = 1.4 \text{ and } D_{reaction} = 1.33$$

Where, ***n***sample- no. of moles of ethylene formed in the sample, ***V***reading- the amount of extract used in the reading, ***V***extract- the volume of the liquid in the sample after extraction (considering the water content of the tissue), ***D***column- the dilution factor due to sample clean up on the column, ***D***reaction- the dilution factor due to the reaction step, ***w*** (g FW)- the weight of the used sample and ***t*** (h)- the incubation time.

3.8.5 In-vitro ACO enzyme activity determination

To ascertain whether the increasing amount of ACC and increased ACS activity would interfere with ACO activity, ACO activity was also estimated In-vitro. Following steps are involved in determining ACO activity:

3.8.5.1 Extraction

To 500 mg of frozen crushed fruit tissue in a precooled 2 mL Eppendorf tube containing 50 mg PVPP, 1 mL extraction buffer containing Tris 100 mM pH 8.0, 10% glycerol (v/v) and 30 mM sodium ascorbate was added. The sample after vortexing and incubation in a thermomixer for 10 min. at 4°C with gentle shaking was centrifuged for 30 minutes at 22,000 *g* at 4°C. After centrifugation, the supernatant containing extracted ACO enzyme was collected and subjected to enzyme activity estimation.

3.8.5.2 Reaction of purified enzyme with substrate and reading

200 µL purified enzyme extract was transferred to a glass vial containing 1.8 mL of reaction buffer containing 10% glycerol (v/v), 5 mM sodium ascorbate, 20 mM sodium bicarbonate, 0.02 mM iron sulphate, 1 mM ACC (substrate) and 1 mM DTT. After sealing the glass vial it was vortexed for 5 Sec and the sample was incubated in a water bath for 15 minutes at 30°C with gentle shaking. After incubation mixture was vortexed for 5 Sec to release all ethylene. A 1 mL headspace gas sample was withdrawn by a hypodermic syringe for ethylene determination using Gas Chromatography. Following formulae were used for the calculation of ACO activity:

$$ACO_{activity} = \frac{n_{sample} . V_{extract}}{V_{reading} . w . t}$$

Where, ***n***sample- amount of the ethylene formed, ***V***extract (mL)- the volume of the liquid in the sample after extraction, ***V***reading (mL)- the amount of extract used in the reading, ***w*** (g FW)- the weight of the sample and ***t*** (h)- the incubation time.

3.8.6 Production of polyclonal antibodies specific to ACS2 protein

Antibodies (also known as immunoglobulins) are gamma globulin proteins that are found in blood or other bodily fluids of vertebrates and are used by the immune system to identify and neutralize foreign objects. The Ig monomer is a "Y"-shaped molecule that consists of four polypeptide chains; two identical heavy chains and two identical light chains connected by disulfide bonds (Woof and Burton, 2004). The amino acid sequence in the tips of the "Y" varies greatly among different antibodies and is composed of 110-130 amino acids; which give the antibody its specificity for binding antigen. While many species are used for polyclonal antibody production (chicken, goats,

horses, mice, sheep etc.), the rabbit is most commonly used for reasons of historical antecedents, cost benefits and ease of handling. Young rabbits (2.5-3 kg; 10-16 weeks) should be used. At this age, the maternal antibodies have decreased to undetectable levels while the immune system is approaching adult levels. Older rabbits are not useful for antibody production as immune system peaks at puberty. Female rabbits are preferred for their docility and higher immune response (Halliday et al., 2004).

To check the expression level of ACS2 protein in fruit tissues of WT and mutants at different maturity stages, primary antibodies specific to ACS2 protein are required. Following steps were followed to generate primary polyclonal antibodies:

3.8.6.1 Peptide synthesis

ACS2 protein sequence was sent to PEPTIDE 2.0, a U.S.A. based company for the prediction of the antigenic peptide. The company predicted three probable antigenic peptides within the provided ACS2 protein. Out of three peptides, the one with the amino acid sequence "EHGENSPYFDGWKAYDSD", situated towards the N-terminal region of the protein was selected for peptide synthesis by PEPTIDE 2.0 Company. The peptide was conjugated to KLH (keyhole limpet hemocyanin), a carrier protein at the N-terminal region of protein by a sulphydryl group of cysteine residue, to attain the threshold size of antigen to cause the adequate immunogenicity. The purity of peptide (4 mg) obtained in lyophilized powder form, from company was 95% (HPLC and MS grade).

3.8.6.2 Raising polyclonal antibodies in rabbit

The polyclonal antibody was raised in rabbit, following all standard animal ethics and maintaining the rabbit in a hygienic condition. For raising antibody against one of the peptide, a male white rabbit of 1.5-2 kg weight was purchased from the local suppliers and raised in animal house of University of Hyderabad one week prior to injection for acclimatization. Before injecting with antigen, 1 mL of blood was withdrawn from the central ear artery of rabbit as pre-immune serum. The steps involved in the immunization protocol are described below:

3.8.6.2.1 Priming immunization

500 µg of the lyophilized peptide was diluted to 1 mL with 1X PBS (Phosphate Buffer Saline) and mixed with 1 mL of complete Freund's adjuvant (CFA). The peptide and adjuvant were mixed till an emulsified solution was obtained using an 18 G (gauge) needle with 2 mL syringe. The emulsified solution was intramuscularly injected into the rabbit.

3.8.6.2.2 First booster injection

After 3 weeks, the rabbit was bled to check its response to the priming immunization by Dot blot assay. The rabbit was given first booster immunization dose (same composition as the priming immunization but with incomplete Freund's adjuvant (IFA). Further booster immunization (three more) injections were given at 3-week intervals till the final collection of immune serum.

The optimal number of booster immunizations to be given before final collection was determined by accessing the antibody titer value. During booster immunization all the bleeds were collected from the central ear artery with a 19 G (gauge) needle. The final bleed was drawn from the heart (40-50 mL). The blood was allowed to clot and retract at 37°C overnight. The clotted blood was then refrigerated for 24 hr and the serum was clarified by centrifugation at 2500 rpm for 20 min. Straw colored serum was decanted and mixed with 0.001% sodium azide and after aliquoting was stored at -20°C.

3.8.6.3 DOT blot to check antibody titer value

A known amount of peptide solution (2-4 µg) was spotted on nitrocellulose membrane, after air drying for 5 minutes time, blot was kept in blocking buffer containing 1% (w/v) BSA or 4% (w/v) nonfat (skimmed), dry milk powder in TBST (20 mM Tris-HCl, pH 8.0. 150 mM NaCl, 0.1% Tween-20 (v/v) (Tris-buffered saline + Tween-20, TBST)) buffer. After overnight incubation, the membrane was washed 4-5 times with TBST buffer. After washing, the membrane was incubated with different dilutions of primary ACS2 antibody (1/250 - 1/50,000 dilution range) for one hour. Thereafter washes were repeated with TBST buffer 3-4 times to remove unbound primary antibodies. The rinsed membrane was incubated with the secondary anti-rabbit IgG antibody (procured from Sigma-Aldrich, USA) developed in Goat, coupled with alkaline phosphatase (1/80,000 dilution), for one hour. After incubation, the membrane was washed again to remove unbound secondary antibodies. After washing Ag-Ab complex on membrane was visualized by incubating it in a chromogenic mixture, prepared by adding 33 µL BCIP (5-bromo-4-chloro-indolyl phosphate (50 mg/mL dissolved in 100% Dimethyl formamide)) and 66 µL NBT (nitro blue tetrazolium salt (50 mg/mL dissolved in 70% Dimethyl formamide)) to 10 mL of ALP (alkaline phosphatase buffer; 100 mM Tris-HCl pH 9.5, 100 mM NaCl, 5 mM $MgCl_2$). The reaction area turned purple, and when the intensity of the color developed to the desired level, the reaction was stopped by rinsing the membrane in distilled water for a few minutes.

3.8.7 Purification of antibody fractions (IgG and IgM) from serum

To purify different immunoglobulins (Igs) from the ACS2 serum, Di Ethyl Amino Ethane (DEAE) Sepharose CL-6B beads (a product of GE Healthcare Pvt. Ltd. India), a weak anion exchanger, were used. The beads were packed in the 2 mL column volume in a plastic desalting column and were washed with 20 mL milli-Q water. After washing, the column was equilibrated with 10 column volume of 50 mM Tris-HCl pH 8.0. After equilibration the bead matrix, 1 mL of the serum was loaded on bead matrix. Finally the IgG fractions were eluted by 200 mM Tris-HCl pH 8.0 and IgM fractions by 50 mM Tris-HCl pH 8.0 respectively. For each immunoglobulin, 10 fractions of 1 mL each were collected and the absorbance of each fraction was measured at 280 nm to quantify the concentration of immunoglobulins fractions.

3.8.8 Immunoprecipitation of ACS2 protein

For immunoprecipitation different dilutions (diluted in 100 µL of 1X PBS pH 7.4) of purified IgG antibodies (1/25, 1/300 and 1/800) were mixed in one mL of desalted, crude, red fruit protein extract for 1 hr at 37°C with gentle shaking. After incubation samples were mixed with 30 µL of preswollen (in 1X PBS pH 7.4) protein-A Sepharose (Sigma-Aldrich) beads and incubation was continued at 4°C for 1 hr with constant shaking. Thereafter mixture was centrifuged for five minutes at 12,000 *g* at 4°C. The supernatants were analyzed for the reduction in ACS2 activity, and immunoprecipitated pellets were used for western blot analysis.

3.8.9 Western blotting of tomato ACS2 protein

3.8.9.1 Protein extraction, desalting, immunoprecipitation, and estimation

The crude enzyme was extracted in buffer containing tricine (200 mM, pH 8.5), 2 mM pyridoxal-5-phosphate (PLP) and 10 mM DTT (Dithiothreitol). For extraction of ACS, 50 mg PVP was added to 2 mL precooled Eppendorf tube followed by addition of 1 g frozen fruit tissue homogenate and 3 mL of extraction buffer. The mixture was vortexed until a homogenous mixture was obtained, centrifuged at 21,000*g* for 30 minutes at 4°C then 1.25 mL of supernatant was collected and loaded on Sephadex G25 (4 mL pre-swollen bead volume) desalting column for sample clean up. The eluted sample fractions were collected in the precooled tubes. The ACS2 protein-Ab complex was immunoprecipitated by protein-A Sepharose as mentioned. Protein estimation was carried out using Bradford's microassay (Bradford, 1976).

3.8.9.2 SDS-PAGE gel electrophoresis

The immunoprecipitated ACS2 protein isolated from the crude extract of red tomato fruits was separated by sodium dodecyl sulfate gel electrophoresis (SDS-PAGE)

follows Laemmli (1970) protocol. One millimeter (mm) thick separating gel of 12% (w/v) was polymerized in 1.5 M Tris-HCl pH8.8, containing 0.1% (w/v) SDS, 0.1% (w/v) APS and 0.01% (v/v) TEMED. 5% (w/v) stacking gel was made in 1 M Tris-HCl (pH 6.8) containing 0.1% (w/v) SDS, 0.1% (w/v) APS and 0.01% (v/v) TEMED. The glass gel slabs were prepared in an AE-6530 mPAGE electrophoresis unit (ATTO, Japan) according to the manufacturer's instructions. Samples were prepared in 2X sample buffer containing 1 M Tris-HCl (pH 6.8), 4% (w/v) SDS, 20% (v/v) glycerol, 0.1% (w/v) bromophenol blue and 10% (v/v) β-mercaptoethanol. The samples were boiled for 5 minutes for uniform coating of the detergent. After cooling to room temperature, the samples were loaded and electrophoresed at room temperature at 100 V constant power for approximately 90 minutes. The gel running buffer was made of 250 mM Tris, 200 mM glycine and 0.1% (w/v) SDS.

3.8.9.3 Electroblotting of SDS-PAGE gel

Proteins were electroblotted onto PVDF (Immobilon-P, No P-2938; Sigma) membrane using semi-dry blotting method. The PVDF membrane was cut to the size of the resolving gel and wetted with methanol for 2 min, washed with distilled water and then soaked in transfer buffer (25 mM Tris base, 192 mM glycine, 20% (v/v) methanol). Whatman No. 3 chromatographic paper was cut to the size of the gel and soaked in transfer buffer. After electrophoresis, the stacking gel was excised, and the bottom of the left-hand corner of the resolving gel was marked with a cut. The gel was first washed with distilled water, followed equilibration for 5-10 minutes in transfer buffer. Semi-dry blotting was carried out in a BIO-RED's Trans-Blot® SD Semi-Dry Electrophoretic Transfer Cell apparatus. Both anode and cathode plates were washed with distilled water. On the anode plate, three sheets of Whatman papers were layered carefully so that no air bubbles were trapped between the sheets. The PVDF membrane was layered over the sheets, and a small cut was made at the bottom left-hand corner of the membrane to coincide with that of the gel. The gel was carefully layered on top of the membrane on which three more sheets of Whatman papers were layered. Finally, on the top cathode plate was placed. The blotting unit and the whole sandwich consisting of the plates, papers and gel were tightened using in build clamps in the lid of the Trans-Blot unit. The blotting was done at a constant current of 0.8 mA/sq.cm area of the gel for 1.5 h.

3.8.9.4 Immunoblotting of ACS2 protein

Immunoblotting was carried out following the procedure of Towbin et al., (1979) at room temperature. After electroblotting, the non-specific binding sites on the

membrane were blocked by incubating the membrane in 10-15 mL of blocking buffer containing 1% BSA (w/v) or 4% (w/v) nonfat (skimmed), dry milk powder in 20 mM Tris–HCl, pH 8.0. 150 mM NaCl, 0.1% Tween-20 (v/v) (Tris-buffered saline + Tween-20, TBST). After overnight incubation, the membrane was washed 3-4 times with TBST buffer. After washing, the membrane was incubated in primary ACS2 antibody (1/1500 dilution) for one hour. Thereafter washes were repeated with TBST buffer 3-4 times to remove unbound primary antibodies. The rinsed membrane was incubated with the secondary anti-rabbit IgG goat antibody (procured from Sigma-Aldrich, USA), coupled with alkaline phosphatase (1/80,000 dilution), for one hour. After incubation, membrane was washed again to remove unbound secondary antibodies.

After washing, the Ag-Ab complex on membrane was visualized by incubating it in a chromogenic mixture, prepared by adding 33 µL BCIP (5-bromo-4-chloro-indolyl phosphate (50 mg/mL dissolved in 100% Dimethyl formamide)) and 66 µL NBT (nitro blue tetrazolium salt (50 mg/mL dissolved in 70% Dimethyl formamide)) to 10 ml of ALP (alkaline phosphatase buffer; 100 mM Tris-HCl pH 9.5, 100 mM NaCl, 5 mM $MgCl_2$). The reaction area turned purple, and when the intensity of the color developed to the desired level, the reaction was stopped by rinsing the membrane in distilled water for a few minutes.

3.8.10 Phytohormones profiling in leaf and fruit tissue of WT and mutants

3.8.10.1 Plant material and sampling

Phytohormones were extracted from leaves and fruits sample of tomato plants grown in greenhouse condition under natural photoperiod (as described in section 3.7.9) between the months of October to February. Young fully expanded fresh green leaves from 7th node of 45 days old plant were collected, frozen in liquid nitrogen and stored at -80°C further analysis. Similarly, fruits were collected at mature green (MG), turning (TUR) and red ripe (RR) stages respectively, frozen in liquid nitrogen and stored at -80°C until further analysis.

3.8.10.2 Standard chemicals

Unlabeled zeatin, indole-3-acetic acid (IAA), indole-3-butyric acid (IBA), gibberellic acid (GA3), abscisic acid (ABA), jasmonic acid (JA), epibrassinolide (BR), methyl jasmonate (MeJA), and salicylic acid (SA), were purchased from Sigma-Aldrich (Steinheim, Germany).

3.8.10.3 Sample preparation

Frozen leaf material (about 125 mg fresh weight) was homogenized in liquid nitrogen with mortar pestle, and homogenate was transferred to 2 mL Eppendorf tube. After mixing with 500 µL of pre-chilled extraction solvent (methanol: isopropanol, 2:1 (v/v) with 0.1% of HCl) homogenate was extracted in thermomixer (4°C) for 30 min at 500 rpm. Thereafter 1 mL of dichloromethane (DCM) was added to the tubes and mixing was continued at 4°C for another 30 min. The mixture was then centrifuged at 13,000 *g* for 5 min at 4°C and 900 µL of the lower phase was transferred to a fresh Eppendorf tube, and was dried completely using a Speed Vac (Thermo Scientific). The dried sample was resuspended in 70 µL of precooled 100% methanol and centrifuged at 13,000 *g* for 5 min and the supernatant was analyzed by UPLC/ESI-MS. Hormones were determined in 5 independent samples for each mutant and WT plants. The hormones were quantified using standard curves with the eight unlabeled hormones (SA, ABA, JA, MeJA, IAA, IBA, Zeatin and GA3) **(Fig. 3.4)**.

3.8.10.4 UPLC/ESI-qMS/MS analysis

The UPLC system consisted of an Acquity UPLC™ System (Waters, Milford, MA USA) quaternary pump equipped with an autosampler. For the analysis of the extracts, a Hyperseal GOLD C_{18} (Thermo Scientific) column (2.1 × 75 mm, 2.7 µm) was used. Gradient elution was performed using 0.1% formic acid (solvent A) and acetonitrile with 0.1% formic acid (solvent B) at a constant flow rate of 0.4 ml min^{-1}. The injection volume was 7.5 µL, run time was 9 min and column temperature was set at 20ºC. All seven hormone were analyzed using gradient method as follow (t (min), % A): (0, 95), (1, 95), (6, 20), (7, 95), (8, 95). For ABA, JA and SA detection, MS experiments were performed on an Exactive™ Plus Orbitrap mass spectrometer (Thermo Fisher 188 Scientific, USA) in all ion fragmentation (AIF) mode (range of m/z 50-450) equipped with positive heated electrospray ionization (ESI) in negative ion mode. However Zeatin, IAA, IBA and MeJA were analyzed using Turbo Ionspray source in positive ion mode. For both methods capillary temperature was 350°C, sheath gas flow (N_2) 35 (arbitrary units), AUX gas flow rate (N_2) 10 (arbitrary units), collision gas (N_2) 4 (arbitrary units) and the capillary voltage was 4.5 kV under ultra-high vacuum $4e^{-10}$ mbar. For mass accuracy, external calibration of the instrument was done by direct infusion of calibration solutions in both positive and negative ion modes. The positive mode calibration solution comprise of caffeine, Met-Arg-Phe-Ala acetate salt (MRFA), n-butyl amine and Ultramark™ 1621, whereas negative mode consists of sodium dodecyl sulfate, sodium taurocholate and UltramarkTM 1621.

3.8.11 Carotenoids and Xanthophylls profiling from the fruit and leaf tissue of WT and mutants

3.8.11.1 Sample preparation and extraction

Carotenoids were extracted following the procedure of Gupta et al. (2015). The Freeze-dried material of tomato fruit and leaf (150 ± 10 mg) was homogenized into a powder with a mortar and pestle or hand-held homogenizer (IKA A11) and transferred to Eppendorf tube. Further extractions were carried out in micro-centrifuge tubes (2 mL) and were carried out on the ice and extracts were shielded from strong light. For extraction, 1000 µL of chloroform and 500 µL of dichloromethane were added to the tube. The suspension was mixed in a thermomixer at 1000 rpm for 20 min at 4°C. Thereafter NaCl saturated water was added (500 µL) and was mixed by inversion. A clear phase separation was achieved by centrifugation at 5000 *g* for 10 min at 4°C. The underlying hypophase was removed with a pipette and the aqueous phase was re-extracted with chloroform (500 µL) and dichloromethane (250 µL). The pooled chloroform and dichloromethane extracts were dried by centrifugal evaporation. Dried residues were resuspended in 1 mL of methanol: tert-methyl butyl ether (MeOH: MTBE) (25:75) for red ripe and leaf samples and 200 µL for mature green and breaker samples. For validation of the method, apo-carotenal was used as an internal calibration verification standard with a percent recovery calculated by using the apo-carotenal standard curve.

3.8.11.2 Standards and solvents

The carotenoid standards violaxanthin, neoxanthin, antheraxanthin, lutein, zeaxanthin, phytoene, β-cryptoxanthin, phytofluene, α-carotene, β-carotene, ζ-carotene, δ-carotene, γ-carotene, neurosporene and lycopene were purchased from CaroteNature GmbH (Lupsingen, Switzerland). Internal standard Apo-carotenal was purchased from Sigma Chemical Co. (Poole, Dorset, UK). Carotenes and xanthophylls were initially dissolved in hexane/2% dichloromethane and ethanol respectively, and then diluted in MeOH: MTBE (25:75). Six serial dilutions were made for each and standard dilution concentrations were determined spectrophotometrically using their respective molar extinction coefficients. Immediately afterward, 20 µL of each standard was injected to detect corresponding retention time and spectra for each standard as criteria for proper peak identification. Calibration curves and linear regression equations were generated for each external standard and internal standard. Methanol, tert-methyl butyl ether,

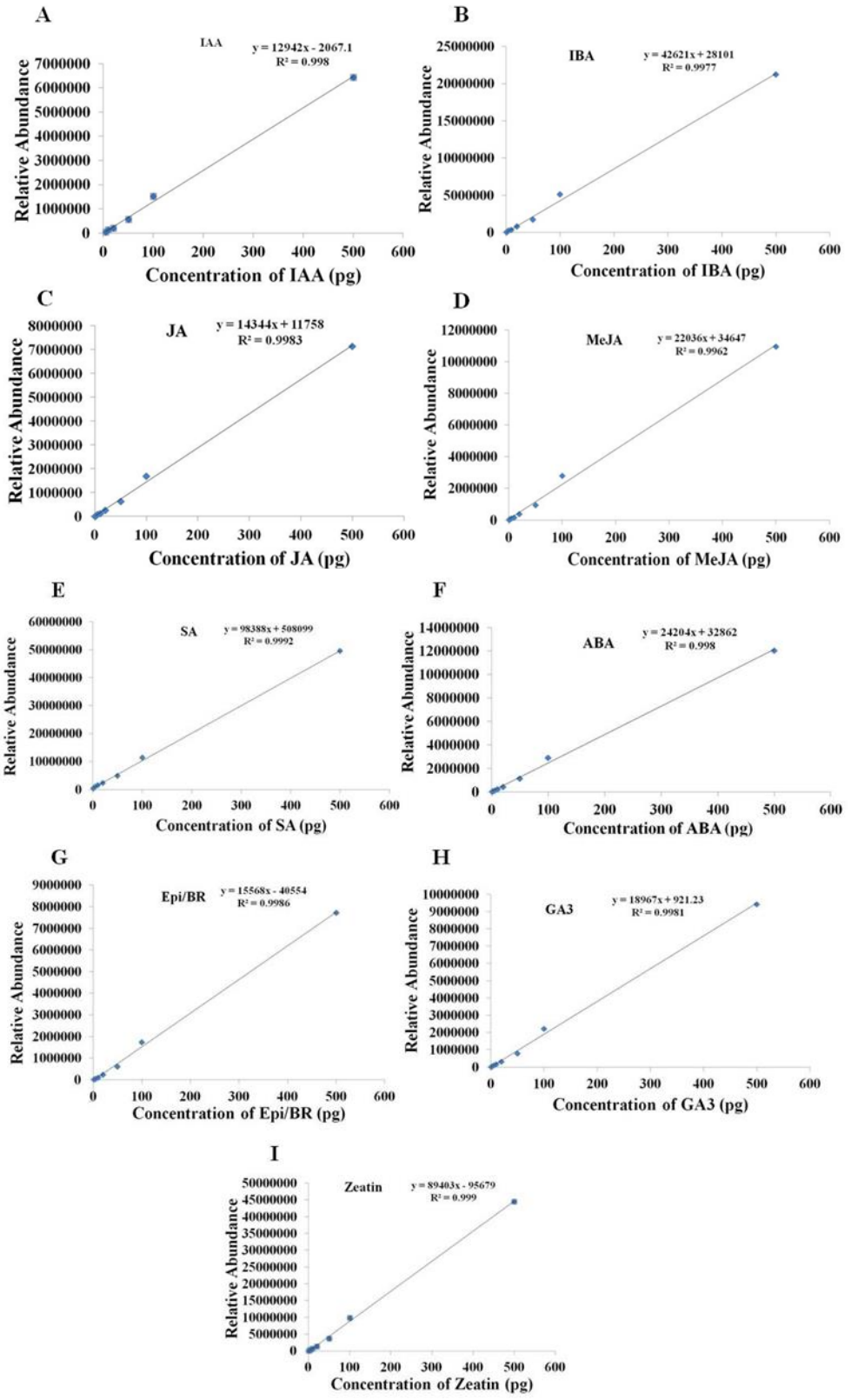

Figure 3.4. The calibration curves of different hormones. **A**- IAA, **B**- IBA, **C**- JA, **D**- MeJA, **E**- SA, **F**- ABA, **G**-Epi/BR, **H**- GA3 and **I-** Zeatin, plotted against different concentration range.

chloroform, and dichloromethane were purchased from Sigma Chemical Co. (Poole, Dorset, UK). All the solvents used were of HPLC grade.

3.8.11.3 Isoprenoid separation and detection by U-HPLC-PDA

Chromatographic separation was carried out on Thermo ACCELA ultra-high performance liquid chromatography (U-HPLC) unit with a photodiode array (PDA) detector. Data were collected and analyzed using the Xcalibur software supplied. Throughout chromatography, the spectrum was monitored continuously from 250 to 700 nm. Column temperature was maintained at 20°C. A reverse-phase C30, 3 µm column (250 x 4.6 mm) coupled to a 20 x 4.6 mm C30 guard (YMC Inc., Wilmington, NC, USA) with mobile phases consisting of 5% aqueous methanol (A), 2% aqueous methanol (B) and tert-methyl butyl ether (C) was used. The gradient elution used with this column was 70% A, 30% C at 0 min, followed by linear gradient to 60% A, 40% C at 2.00 min, a step to 60% B, 40% C at 2.01 min followed by a linear gradient to 100% C by 12 min and return back to initial conditions by 13.00 min. A conditioning phase (7.00 min) was then used to return the column to the initial concentrations of A and C. The flow rate of 1.00 mL was used throughout the chromatographic conditions.

3.8.12 Folate estimation using LC-MS

3.8.12.1 Plant material

Red fruit of WT (M82) and TILLING mutants (*acs2-1, acs2-2*), and population of natural accessions of Tomato (*Solanum lycopersicum* L.) from TGRC (Tomato Genetics Resource Center at University of California, Davis) (tgrc.ucdavis.edu/), IIVR (Indian Institute of Vegetable Research, Varanasi, U. P., India) (www.iivr.org.in/), IIHR (Indian Institute of Horticultural Research, Bengaluru, India (http://www.iihr.res.in/), NBPGR (National Bureau of Plant Genetic Resources, New Delhi, India) (www.nbpgr.ernet.in/) and Bejo Sheetal (Bejo Sheetal Seeds Pvt. Ltd. Jalna, India) (http://www.bejosheetalseeds.com/) were taken for the folate estimation. *Solanum lycopersicum cv.* Arka Vikas (originally obtained from Indian Institute of Horticulture Research, Bangalore) was used as the reference variety.

The first and second flowers from first and second truss (preferably 1st truss) of the plants were tagged and fruits at mature green and red ripe stages were harvested from at least three (3-5) different plant of each accession. The fruits were homogenized in liquid nitrogen using homogenizer (IKA, A11 basic, Germany) and the powder was stored at -80°C till further use.

3.8.12.2 Chemicals and folate standards

5-Methyltetrahydrofolate (5-CH_3-THF), tetrahydrofolate (THF), 5-methenyltetrahydrofolate (5,10-CH^+THF), 5-formyltetrahydrofolate (5-CHO-THF) and 5, 10-methylenetetrahydrofolate (5,10-CH_2THF) were purchased from Schirck's Laboratory (Jona, Switzerland). Folic acid (FA) and methotrexate (MTX) were obtained from Sigma-Aldrich Co. (St. Louis, USA). LC-MS grade acetonitrile was purchased from Sigma-Aldrich Co. (St. Louis, USA). Milli-Q water (18.2 Ω at 25°C) was obtained from a purified water system (Millipore, Bradford, USA). Ascorbic acid and 2-mercaptoethanol (MCE) were purchased from Sigma-Aldrich Co. (St. Louis, USA). Formic acid (HCOOH) of LC-MS grade were obtained from Fisher Scientific (Loughborough, UK). Potassium dihydrogen phosphate, dipotassium hydrogen phosphate, and activated charcoal were obtained from HiMedia (Mumbai, India).

3.8.12.3 Standard stock preparation

Stock solutions of folate standards (1 mg/mL) were prepared in 50 mM potassium phosphate solution, pH 4.5 containing 1% (w/v) of ascorbic acid and 0.5% (v/v) of 2-mercaptoethanol except FA and MTX, which were dissolved in neutral or basic pH potassium phosphate buffer. The standard stock solutions were freshly diluted in the extraction buffer to prepare working solutions. The remaining stock solutions were flushed with nitrogen gas, and small aliquots were stored at -80°C. MTX was used as an internal standard for the quantification of folate in LC-MS.

3.8.12.4 Enzyme preparation for folate extraction

Protease (from *Streptomyces griseus*, RM6186), α-amylase (from *Bacillus sp.*, A6814) were purchased from HiMedia (Mumbai, India) and Sigma-Aldrich Co. (St. Louis, USA) respectively. Protease (2 mg/mL) and α-amylase (20 mg/mL) were dissolved in Milli-Q water, and aliquots were stored at -20°C. Rat plasma was obtained from National Institute of Nutrition (NIN), Hyderabad, India. To remove endogenous folate from rat plasma and α-amylase, 100 mL of rat plasma and α-amylase were mixed with 5 g of activated charcoal. This mixture was incubated on ice for 1 h with intermittent stirring followed by centrifugation at 5,000 *g* (Sorvall Lynx 6000, Thermo Scientific, USA) for 10 min at room temperature. The supernatant was filtered through a 0.22 µm filter, divided into 1 mL aliquots, and stored at -20°C. Protease was used without pre-treatment and was stored in -20°C.

3.8.12.5 Sample extraction procedure for LC-MS

Total folate was extracted following the procedures of Tyagi et al. (2015). 100 mg powdered tissue was homogenized in 650 µL of extraction buffer (50 mM potassium phosphate, 1% (w/v) ascorbic acid, 0.5% (v/v) β-mercaptoethanol, 1 mM calcium chloride, pH 4.5, flushed with nitrogen) in a 2 mL Eppendorf tube. Extraction was carried out by placing the tube in a boiling water bath for 10 minutes, and then rapidly cooling on ice followed by incubation with 10 µL of α-amylase for 10 minutes at room temperature. Subsequently, 2.5 µL of the protease was added to it and kept for 1 h at 37°C in an orbital shaker (Scigenics Biotech), followed by boiling for 5 minutes, and cooling on ice. For deconjugation of folate poly glutamate to mono glutamates, 100 µL of rat plasma was added to each sample tube and incubated on an orbital shaker at 37°C for 2 h. followed by boiling for 5 minutes and cooling on ice. The sample was centrifuged for 30 minutes (14,000 *g*, 4°C), and the supernatant was filtered through the 0.22 µm filter (MDI Advanced Micro-devices). Then, resulting extract was ultra-filtered at 12,000*g* for 12 minutes using 10 kDa molecular weight cut-off membrane filter (Pall Corporation, USA) for sample cleanup prior to LC-MS analysis. Immediately, the resulting extract was transferred to autosampler vial, and 7.5 µL was directly injected on the column.

3.8.12.6 Liquid chromatography condition and mass spectrometry settings

For LC-MS, all the parameters used were essentially followed according to Tyagi et al. (2015). The chromatographic separation of folate derivatives were done on a reversed phase Luna C18 column (5 µm particle size, 250 mm × 4.60 mm ID) (Phenomenex, USA) using Waters Acquity™ UPLC system (Milford, USA) running in HPLC mode, coupled to a binary pump, an autosampler, and controlled by Xcalibur 3.0 software (Thermo Fisher Scientific, San Jose, USA). For mass spectrometry, Exactive™ Plus Orbitrap mass spectrometer (Thermo Fisher Scientific, USA) was operated in alternating full scan and all ion fragmentation (AIF) mode equipped with positively heated electrospray ionization (ESI).

3.8.12.7 Folate quantification

The external standard was used for folate quantification. Sensitivity was confirmed by evaluating the limit of detection (LOD; calculated as: 3.3σ/S, where σ is the standard deviation and S is the slope of calibration curve) and limit of quantification (LOQ; calculated as: 10σ/S). Least-square regression analysis was used for data fitting. After confirmation of individual peak identity on the basis of m/z and their

fragmentation products, quantification was done according to the response of the mass detector to the folate standard. The linearity of each folate standard was evaluated by plotting the peak area at different concentrations and sample concentrations were calculated from the simple linear equation $y=mx+c$. Endogenous residual folate of rat plasma was corrected by running blank samples and subtracting the concentration from the sample extracts. The sum of all the folate vitamers was expressed as microgram per 100 gram of fresh weight.

3.8.13 Primary Metabolite Profiling

3.8.13.1 Plant material

Tomato fruit and leaf tissue (Solanum lycopersicum cv M82) of WT and mutants were harvested at different growth and maturity stages like mature green (MG), turning (TUR), red ripe (RR) and senescence (S). Five tomato fruits were taken at each stage from five plants while five different, matured and fully expanded leaves from 7th node from basal region of 45 days old plant, were taken into consideration to perform the primary metabolite analyses by GC-MS.

3.8.13.2 Extraction and derivatization

Metabolite analysis by GC-MS was carried out by a method modified from Roessner et al. (2000). Tomatoes were cut, and the fleshy, edible, pericarp tissue was frozen in liquid nitrogen and crushed to a powder with a homogenizer (IKA, A 11 basic analytical mill, Germany). Samples were stored at -80°C until further analysis. For each individual sample, frozen tomato tissue (100±10 mg) was extracted with 1400 µL of 100% MeOH solution containing 60 µL ribitol (0.2 mg ribitol/mL water) as an internal standard. The mixture was extracted for 15 minutes at 70°C and mixed vigorously with 1400 µL of water. The mixture was transferred in GL-14 Schott Duran glass vial and kept for centrifugation for 15 minutes at 4°C, 2200*g*. After centrifugation, the upper methanol/water phase (150 µL) was taken and dried for four hours under vacuum.

The residue was re-dissolved in 80 µL of 20 mg/mL methoxyamine hydrochloride in pyridine and derivatized at 37°C for 90 minutes followed by a 30 minutes treatment with 80 µL MSTFA (N-methyl-N-(trimethylsilyl)trifluoroacetamine) and 20 µL of FAME (fatty acid methyl ester) mix at 37°C. Sample volumes of 1 µL were then injected into the GC-MS column **(Fig. 3.5)**.

3.8.13.3 GC-MS analysis

3.8.13.3.1 Instrumentation

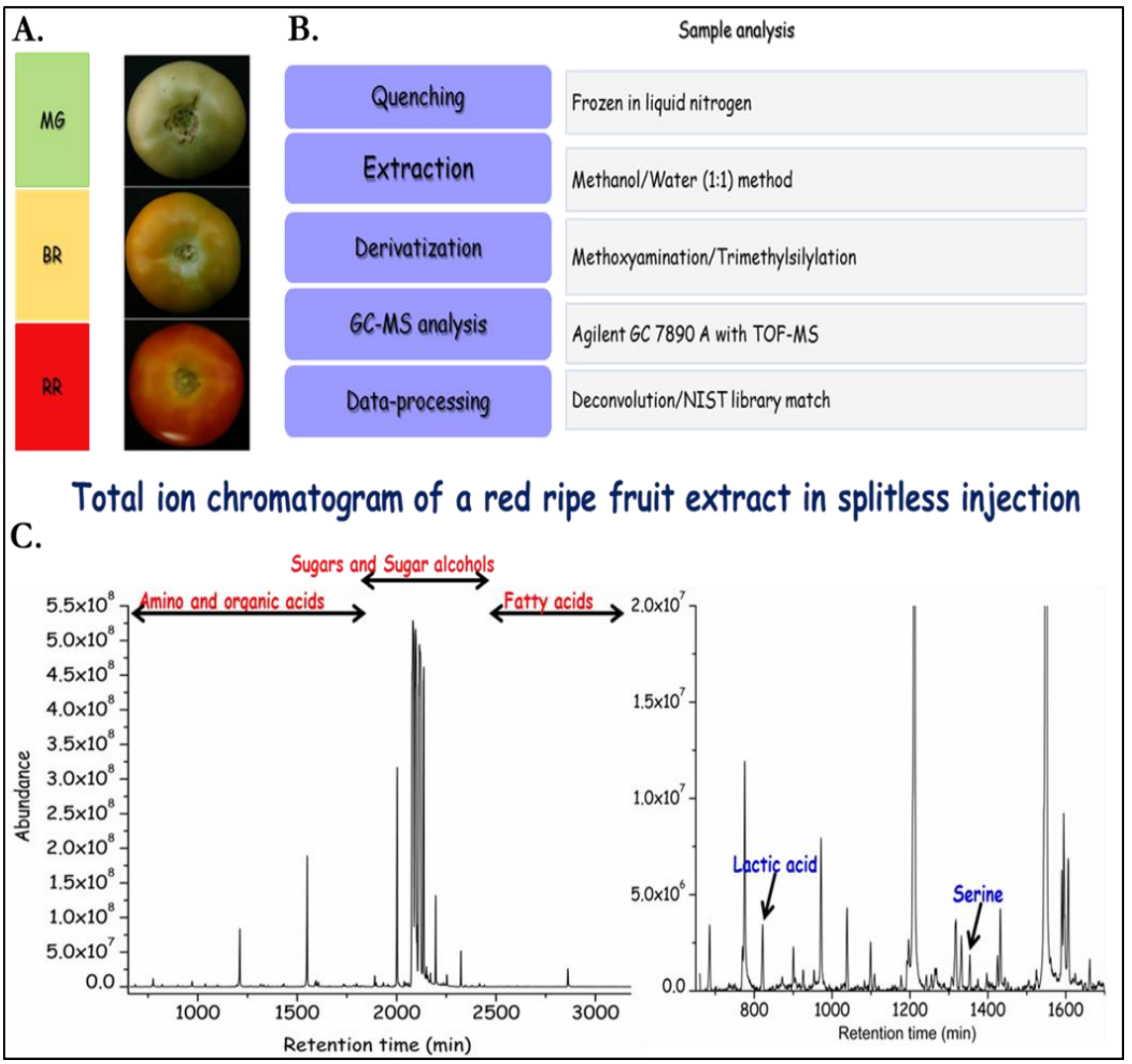

Figure 3.5. Extraction, analysis and identification of primary metabolites using GC-MS. (**A**) Fruit samples used for analysis. (**B**) Steps involved in fruit sample extraction, derivatization, analysis and data processing. (**C**) The total ion chromatogram (TIC) indicating the separation of metabolites according to their retention time (RT).

The GC-MS system used comprised a GC 7890A (Agilent Technologies, Palo Alto, CA, USA) and a MS Pegasus 4D with Time of Flight detector (LECO Corporation, 3000 Lakeview Avenue, MI 49085, USA). The GC-MS system consisted of inbuilt ChromaTOF® software (v4.51.6.0) for raw data processing provided by LECO. Gas chromatography was performed on a 30 m RXi - 5 m column with 0.25 mm inner diameter and 0.25 µm film thickness (LECO, Restek, USA). The injection and interface temperatures were set at 250°C. Helium was used as the carrier gas at a flow rate of 1.5 mL min^{-1}.

3.8.13.3.2 Metabolite analysis

The analysis was performed using the following temperature program; 5 minutes at 70°C followed by a ramp of 5°C/minute up to 280°C, which was sustained for 5 minutes. Mass spectra were recorded at two scans s^{-1} with an m/z 50-600 scanning range. For less concentrated compounds, the MS detector was switched off within the range of overloaded peaks. The temperature of the ion source was adjusted to 200°C. Transfer line temperature was set at 250°C.

The metabolite identification was carried out with the NIST (National Institute of Standards and Technology) GC/MS Metabolomics library software (NIST/EPA/NIH Mass Spectral Library 14, Department of Commerce, USA).

For comparative purposes, within each chromatogram the peak areas of the compounds were normalized by the sample fresh weight and by the peak area of the internal ribitol standard, resulting in relative response ratios for all compounds.

3.8.13.4 Statistical analysis for primary metabolites

Statistical analysis was done using MetaboAnalyst 3.0, a web-based suite for high-throughput metabolomic data analysis. MetaboAnalyst 2.0 has four kinds of data analysis modules: binary/multiple-group data analysis, two-factor/time-series data analysis, metabolite set enrichment analysis and metabolic pathway analysis. Pearson's correlation was set as a default setting. PCA and partial least squares discriminant analysis (PLS–DA) were both available in the MetaboAnalyst 2.0. (Xia et al., 2012).

3.8.14 Treatment of 1-MCP on fruits (on-vine)

The dose of 1-MCP (1-Methylcyclo propene, an inhibitor of ethylene action) for delaying ripening of tomato fruits was standardized by serial dilutions. Experimental setup included treatment of 1-MCP (200 mg/5 mL water) at MG stage in a tightly sealed, zip polybag using cello tape **(Fig. 3.6)**. On-vine condition, 1-MCP treatment was given to the fruits of second truss of the WT and also mutant plants (Five biological replicates

were used for the experiment). After treatment by 1-MCP, the fruits were visually observed for delayed in ripening (on-vine). Fruits were harvested after attaining at turning and red stages as well as mature green fruits after treatment. Primary metabolite extraction was carried out as described earlier, from fruit tissue of MG, TUR and RR stages of 1-MCP treated fruits, for GC-MS analysis to monitor the difference in expression of primary metabolites compared to untreated tomato fruit tissue.

3.8.15 Statistical analysis

All results are expressed as mean value±SE of three or more replicates based on fresh weight (FW). A t-test was used for determining the significant difference between the mean values of the reference cultivar and the respective accessions. The differences were considered to be significant for $p \leq 0.05$. Histogram (group error bars) analysis of data was performed using Sigma Plot v11.0 software.

Figure 3.6. Experimental setup for the on-vine treatment of 1-MCP to the fruits. Photograph shows an on-vine attached tomato green fruit enclosed by a airtight polybag containing 1-MCP solution at the bottom.

CHAPTER 4

IDENTIFICATION AND CHARACTERIZATION OF *ACS2* (*ACS2-1, ACS2-2*) ALLELES BY TILLING

4.1 Introduction

Ripening, or fruit maturation, is the physiological process giving rise to fully developed mature fruit. During ripening, important biochemical reactions occur. Many of these are beneficial to the fruit, such as the acquisition of color, accumulation of sugars and volatile compounds. While few changes are detrimental to long storage, such as loosening of the cell wall, which leads to loss of fruit firmness and reduction of shelf-life. In tomato fruits the onset of ripening is preceded by the climacteric increase of respiration and the biosynthesis of ethylene (Lelievre et al., 1997) from S-adenosylmethionine (Yang, 1985). The S-adenosylmethionine is converted by ACC synthase (ACS) to 1-amino-cyclopropane-1-carboxylic acid (ACC), which is subsequently converted to ethylene by ACC oxidase (ACO). The control of ripening is executed at several points: ethylene synthesis, ethylene perception, ethylene signaling pathway etc. Several tomato germplasms with altered ripening have been identified (Moore et al., 2002). Among these: *ripening-inhibitor* (*rin*), *never-ripe* (*Nr*), *non-ripening* (*nor*), *high-pigment 2* (*hp-2*) and *colorless non-ripening* (*Cnr*) have been identified as spontaneous mutants. The *Nr* mutant is an ethylene receptor mutant that results in non-ripening, ethylene insensitive fruit (Wilkinson et al., 1995).

On the other hand, there are no reports of spontaneous mutants in tomato that are defective in ethylene biosynthesis pathway. Such mutants are valuable for non-transgenic regulation of fruit ripening. In this context isolation of *ACS2* mutants would be of great value. However to select such gene-specific mutants special tools are required. We adopted TILLING; a reverse genetic strategy to isolate *ACS2* mutants from EMS-mutagenized populations of tomato.

4.2 Results

4.2.1 Development of TILLING platform

EMS-mutagenized populations (I, II, III, and IV) were used for TILLING (**Table 3.1**, Chapter 3). The size of each population varied due to the percentage of lethality observed. Population I and II consist of 2304 M_2 and 3000 M_2 individuals respectively in Arka Vikas cultivar background. Population III and IV consist of 3000 M_2 and 3072 M_3 respectively in M82 background. These four populations formed the core genetic resource for isolation of mutants using TILLING. Use of in-house expressed and purified Taq polymerase and CELI enzyme aided in reducing the overall cost of TILLING. Further, eight-fold tissue pooling and two-dimensional strategy of arraying samples increased the efficiency of high throughput screening by reducing the number of reactions to be performed per primer pair. The upper limit of CODDLE based primer design was 1500 bp, which defined the PCR product length to be chosen for screening. The nested PCR primers were designed to amplify a fragment within the gene, of 800 bp-1200 bp length. The amplicon length within the above range was considered as optimum due to the consistency of PCR amplification. Overall, an efficient TILLING protocol was standardized for mutations screening in *ACS2* gene.

4.2.2 Tomato *ACS2* is a member of multigene family

The ethylene biosynthesis gene *ACC synthase* isoform *ACS2* (*1-aminocyclopropane-1-carboxylate synthase 2*) was screened for mutation. It is a member of multigene family containing nine members. However *ACS2*, and *ACS4* genes predominantly express during ripening. The ORF of tomato *ACS2* has 2522 bp and consists of 4 exons and three introns (Solyc01g095080.2.1; http://solgenomics.net/feature/17805455/details) **(Fig. 4.1 and 4.3)**.

4.2.3 Selection of targets in gene of interest for mutation

The CODDLE (Codons Optimized to Discover Deleterious Lesions; (http://www.proweb.org/coddle) program was used to identify the regions of the *ACS2* gene that had the highest probability of being affected by EMS. CODDLE predicted the fourth exon of *ACS2* to be susceptible for mutations which may result in loss of function phenotype **(Fig. 4.1)**.

4.2.4 Identification and confirmation of mutations in *ACS2* gene

EMS treated populations (60 mM M82-M_2, M_3, AV-M_3 and 120 mM AV-M_2) were screened by PCR amplification, CEL I digestion, denaturation followed by electrophoresis in Li-COR DNA analyzer. Usage of primers with IR labelled fluorescent

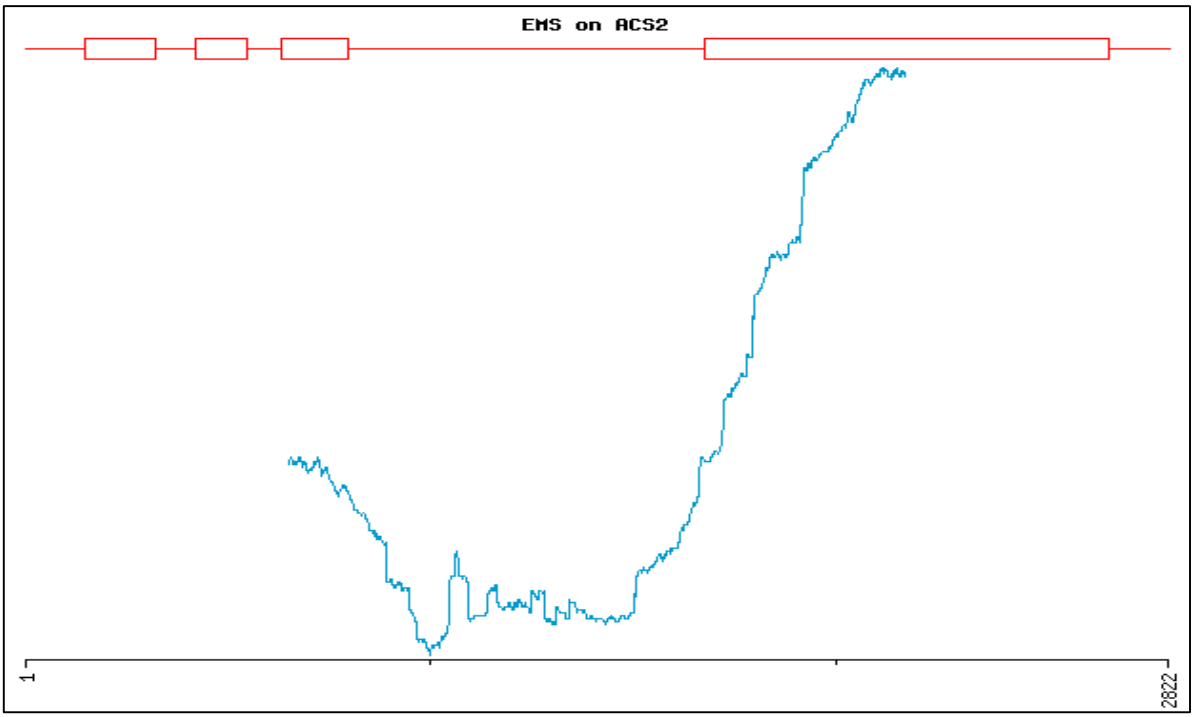

Figure 4.1. *Slacs2* gene structure and prediction of the susceptible region for mutations in *acs2* gene by using CODDLE software. The red outlined boxes corresponds to exons whereas lines joining two boxes represents the introns.

dyes at 5′ end permitted the visualization of mutations in *ACS2* gene **(Fig. 4.2)**. The above screening resulted in the identification of seven mutant alleles of *ACS2* gene **(Table 4.1)**. Out of seven mutant alleles **(Table 4.2)**, two alleles in line no. $M82M_3$-112 and $M82M_3$-162 (*acs2-1* and *acs2-2* respectively) were characterized in detail. Due to biological damage the remaining lines could not be carry forwarded for subsequent generations.

The $M82M_3$-112-3 (*acs2-1*) mutant line was selected on basis of presence of four mutations that were visualized in the Li-COR DNA analyzer. However the sequencing of full length *ACS2* gene from *acs2-1* mutant including promoter region, revealed that the *acs2-1* mutant also possessed an additional mutation in exon II. Consequently, a total of two exonic and three intronic mutations were present in *acs2-1* mutant **(Fig. 4.3, 4.4, 4.7, 4.10A, and Table 4.3)**. On the other hand, *acs2-2* mutant had a total three mutations, two in promoter region while remaining one in the third intron **(Fig. 4.3, 4.5, 4.8, and 4.10C)**. After identification of mutations from the pooled plant DNA, the individual lines containing mutations were identified and reconfirmed by sequencing. These mutant lines were stabilized by self-pollinating up till sixth generation (M_6). After that *acs2-1* mutant was crossed with wild type parent plant (M82) to remove other background mutations.

4.2.5 Mutations lie in the α-helix of ACS2-1 protein surface

The likely effect of the mutations in *acs2-1* and *acs2-2* mutants was examined on the protein structure and function. The nucleotide changes at positions A398 to G and T2119 to A in exon 2 and four respectively, lead to the amino acid changes lysine 100 to arginine and valine 352 to glutamic acid respectively in the ACS2-1 protein **(Fig. 4.6A-B and 4.9A)**. By these changes, SIFT scores resulted in 0.12 and 0.85 units respectively, and PSSM differences were 7.6 and -9.7 respectively **(Table 4.3)**. The 3-D models drawn with the software PyMOL (http://wwwpymol.org) indicated that the amino acid changes are localized in α-helix near protein surface and these amino acids do not take part in the formation of active site interface **(Fig. 4.10B)**. In *acs2-2* mutant, two mutations were located in the promoter region at -292 (T to A), -569 (T to A), and one mutation was at 1595 (T to C) in the intron three **(Fig. 4.3, 4.5, and 4.8)**. All the three mutations are not the part of the coding region; therefore, it would have no effect on structure and function of the ACS2-2 protein **(Fig. 4.6C, 4.9B, and 4.10C)**.

It is predicted that for a loss of function mutation or for mutation intolerance the SIFT score should be less than 0.05 unit, and PSSM difference should be more than 10

units (Beckstette et al., 2006; Huang et al., 2010; Sim et al., 2012). However in *acs2-1* mutant, the PSSM difference and SIFT score values appear to contribute to a gain of function mutation (See later sections). *In-vivo* ACS protein is exists in homodimeric as well as heterodimeric form (Yamagami et al. 2003; Tsuchisaka and Theologis, 2004). Amino acid changes in α-helix of ACS2 protein may interfere with protein folding because valine (V), a neutral non-polar amino acid at position 352 in amino acid chain is converted to glutamic acid (E), an acidic polar amino acid. In addition lysine (K), a basic polar amino acid is changed to arginine (R), a basic polar amino acid. The change in polarity and the functional group present in amino acids can alter the bonding pattern with different amino acids, molecules, etc. As a result, alteration in the folding pattern of ACS2-1 protein, might lead to an overall gain of function by stability in ACS2-1 protein. (See later sections for details)

On the other hand, *acs2-2* mutant exhibits two promoter as well as one intronic mutations respectively. Out of three mutations, two promoter mutations appear to be important for loss of function of *acs2-2* gene. Altered promoter sequence due to the mutations, may modify the affinity of regulatory transcription factor to the promoter region resulting in changes in *acs2-2* gene expression as well as protein expression. This can lead to change ethylene emission from the *acs2-2* mutant plants (See later sections for details)

4.2.6 *acs2-1* mutant shows faster seed germination than wild-type

It is known that ethylene influences seed germination by regulating seed dormancy (Corbineau et al., 2013). Examination of seed germination of *ACS2* mutants and wild type showed that *acs2-1* mutant seeds germinated approximately one day earlier than the wild type (WT). On the other hand, *acs2-2* mutant seeds exhibited a slower germination compared to the WT **(Fig. 4.11)**.

4.2.7 *acs2-1* mutant seedlings exhibits elevated ethylene emission

To ascertain, whether mutation in *acs2-1*, and *acs2-2* gene in turn affected ethylene emission from seedlings, ethylene emission was monitored from germinating seeds for a period of 10 days from sowing. **Figure 4.12** shows that ethylene emission from *acs2-1* seedlings peaked on third day after sowing. At peak emission it had nearly three times higher ethylene emission than the WT seedlings. On the other hand, *acs2-2* seedlings emitted less ethylene than the wild type. In either case though growth proceeds up to 10 days ethylene emission was higher in *acs2-2* seedlings, whereas it was lower in *acs2-1* seedlings compared to wild type.

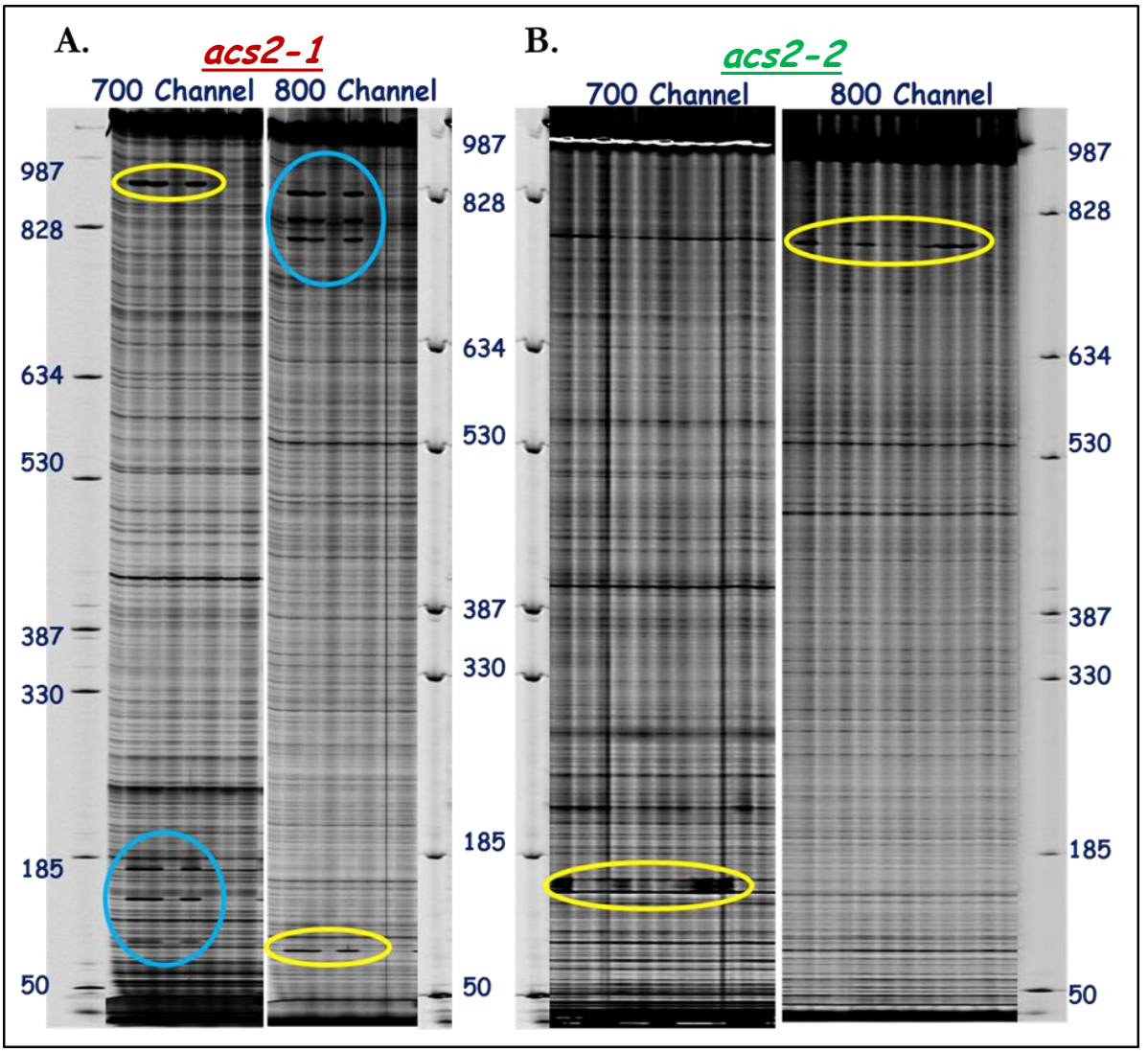

Figure 4.2. Identification and confirmation of mutations on Li-COR gel. **(A)** Mutations in M82M$_3$-112 (*acs2-1*) allele, **(B)** Mutation in M82M$_3$-162 (a*cs2-2*) allele. (**A**) Approximately one Kb *acs2* gene specific PCR product was amplified using subset I of set II primers **(Table 3.2)** followed by digestion with single strand mismatch-specific endonuclease, CEL I and electrophoresis in polyacrylamide gel in Li-COR 4300 DNA Analyzer. The cut fragments observed in 700 channel for *acs2-1* mutant were approximately of 90 bp, 140 bp, 170 bp, and 930 bp size respectively, whereas in complementary 800 channel bands were of 70 bp, 830 bp, 860 bp, and 910 bp size respectively. The blue and yellow colored circles denotes the position of mutations in the *acs2* gene. **(B)** Likewise, the cut fragments in 700 and 800 channels for *acs2-2* mutant were approximately of 150 bp and 850 bp size respectively. Blue and yellow circles indicate the complementary mutations in 700 and 800 channels respectively.

Table 4.1 Size of TILLING population screened and some mutant lines identified and confirmed for mutation.

Population screened	Population size	Identified	Confirmed
60 mM AV-M3	2304	4	1
120 mM AV-M2	3000	0	0
60 mM M82-M2	3000	1	0
60 mM M82-M3	3072	2	2

Table 4.2 Mutant lines identified and confirmed for mutation.

Mutants identified	Position of mutations
M82-M3-112	A398G, C1343T, A1383G, G1410A, T2119A
M82-M3-162A	-569(T-A), -292(T-A), T1595C
M82-M2-539A	Not sequenced
AV-M3-391C30	A1589T, T1593G, A2127G
AV-M3-390-D18	Not sequenced
AV-M3-1453-C34	C1343T, A1383G, G1410A, A1589T, G1577T, T2119A
AV-M3-402-C24	Not sequenced

Table 4.3 Effect of mutations at amino acids, PSSM and SIFT scores for the *acs2-1* allele.

Nucleotide changes	Change in amino acids	PSSM difference	SIFT score
A398G	K100R	7.6	0.12
T2119A	V352E	- 9.7	0.85

WT Genomic sequence 2930

>Solyc01g095080.2 | SL2.40ch01:78214067..78216996 reverse

TTCCTTAATTCTCTTACACCATAACACAACTACAACAAACACATAATACTTTTAATACAATTAGTTATTTATTAGAAGTATTTAAA
GTAAAGCACTTGTGAGTTGTGTACATTTTATTAATCTTCATCTTCTTAATTCTCTTCAGTTTTTAATTTCTTCACTTCTAAACTCATT
TAGTAAAAAAAAAATGGGATTTGAGATTGCAAAGACCAACTCAATCTTATCAAAATTGGCTACTAATGAAGAGCATGGCGAAAA
CTCGCCATATTTTGATGGGTGGAAAGCATACGATAGTGATCCTTTCCACCCTCTAAAAAACCCCAACGGAGTTATCCAAATGGGT
CTTGCTGAAAATCAGGTAATTAATTATCCTTTATTTATATATTTTGCAGTTTGACCAAACAGACTATTATAATTTTTTTCTGAAACC
TCGATGGTGTTAAATTTCTTTTGTAGCTTTGTTTAGACTTGATAGAAGATTGGATTAAGAGAAACCCAAAAGGTTCAATTTGTTC
TGAAGGAATCAAATCATTCAAGGCCATTGCCAACTTTCAAGATTATCATGGCTTGCCTGAATTCAGAAAAGTACATATCGTACTA
TAGTCAGTTAAATTATATTGATAGTATAAAAATTCGTTAATATATTTAACTAACGAGTTTATTTAATCAGGCGATTGCGAAATTT
ATGGAGAAAACAAGAGGAGGAAGAGTTAGATTTGATCCAGAAAGAGTTGTTATGGCTGGTGGTGCCACTGGAGCTAATGAGA
CAATTATATTTTGTTTGGCTGATCCTGGCGATGCATTTTTAGTACCTTCACCATACTACCCAGCGTAAGTATATTTAATTATATAT
GTGTAAAAAAAATTAAAATCATCAAATCATTTTTTTTATTTGTATTACCAAATAAATTGTCTAATTTTCAAGATTGTAACACATTC
ATCAAAGTACCTAATAATATAAACGATTCAGTATATTAACGATGTATATAATTTAATTCCTTTGGCGGATTTGTCTTTTTATGTTG
GGCCATCAGAAGAACATTCTGGTGTATTAATTAATTAATTAATTAATAATAGATGTGTTGTCATTCTTTTTTAAGACAGCGAGAG
TTTAATTAGTCTTAATTACTGGATTATCACGCAAGCTCTTTCTTGAATTTTATTATTCTTATATTAAACACATGATAGCATAATATC
TTTCTTTTGTGGAATCCAGCTTGTTCGTGAAGCTTTGTATTCACACTTATAAAACAACAAAAAATAAAATCTGGTGGTAATTGAT
TAAAGAGAGAAATATAAAAAAATAATAGTCAAATAGACTAATAAGGAAAGAAATAAAAAATACACAAAATACTAAAAAAAA
AGAATTAAGGTATAGTGGTCTATTATTGAGAACTTTTTTGAAGAATTGAACCCCACTTTAATTTCTTGCTTGACCCGTGACCATTG
CTTATCGAGGTAAAATAAAATTTCAAACATTGACTATGACTTGTTAGAGAGTAATTACCACAAGTCAAAATTTTGTTACTCTGTC
TCGTTATTTCATTAGGATCGATAAGATAACATCTAACATATATATCTTTTTTATTAGTACTTGTTTATTTTTAGTAAAAGCACGTTA
TACATTTTACAATAGTCAATTGTTGCATATATTAGTATATATATTTTGCTAAGTCCTAACTAACAATATTTTTGGCAATTGACTAA
TGCAGATTTAACAGAGATTTAAGATGGAGAACTGGAGTACAACTTATTCCAATTCACTGTGAGAGCTCCAATAATTTCAAAATT
ACTTCAAAAGCAGTAAAAGAAGCATATGAAAATGCACAAAAATCAAACATCAAAGTAAAAGGTTTGATTTTGACCAATCCATC
AAATCCATTGGGCACCACTTTGGACAAAGACACACTGAAAAGTGTCTTGAGTTTCACCAACCAACACAACATCCACCTTGTTTGT
GACGAAATCTACGCAGCCACTGTCTTTGACACGCCTCAATTCGTCAGTATAGCTGAAATCCTCGATGAACAGGAAATGACTTACT
GCAACAAAGATTTAGTTCACATCGTCTACAGTCTTTCAAAAGACATGGGGTTACCAGGATTTAGAGTCGGAATCATATATTCTTT
TAACGACGATGTCGTTAATTGTGCTAGAAAAATGTCGAGTTTCGGTTTAGTATCTACACAAACGCAATATTTTTTAGCGGCAATG
CTATCGGACGAAAAATTCGTCGATAATTTTCTAAGAGAAAGCGCGATGAGGTTAGGTAAAAGGCACAAACATTTTACTAATGG
ACTTGAAGTAGTGGGAATTAAATGCTTGAAAAATAATGCGGGGCTTTTTTGTTGGATGGATTTGCGTCCACTTTTAAGGGAATC
GACTTTCGATAGCGAAATGTCGTTATGGAGAGTTATTATAAACGATGTTAAGCTTAACGTCTCGCCTGGATCTTCGTTTGAATGT
CAAGAGCCAGGGTGGTTCCGAGTTTGTTTTGCAAATATGGATGATGGAACGGTTGATATTGCGCTCGCGAGGATTCGGAGGTT
CGTAGGTGTTGAGAAAAGTGGAGATAAATCGAGTTCGATGGAAAAGAAGCAACAATGGAAGAAGAATAATTTGAGACTTAGT
TTTTCGAAAAGAATGTATGATGAAAGTGTTTTGTCACCACTTTCGTCACCTATTCCTCCCTCACCATTAGTTCGTTAAGACTTAATT
AAAAGGGAAGAATTTAATTTATGTTTTTTTATATTTTGAAAAAAATTTGTAAGAATAAGATTATAATAGGAAAAGAAAATAAGT
ATGTAGGATGAGGAGTATTTTCAGAAATAGTTGTTAGCGTATGTATTGACAACTGGTCTATGTACTTAGACATCATAATTTGTCT
TAGCTAATTAATGAATGCAAAAGTGAAGTTATGTTATGACTCTT

Figure 4.3. WT genomic sequence of *ACS2* gene. The genomic sequence was retrieved from SGN. The green and pink colored regions indicates the 5' and 3' UTR regions of the gene respectively whereas the blue colored regions corresponds to the four exons of the gene.

acs2-1 Genomic sequence 2930

>Solyc01g095080.2 | SL2.40ch01:78214067..78216996 reverse

TTCCTTAATTCTCTTACACCATAACACAACTACAACAAACACATAATACTTTTAATACAATTAGTTATTTATTAGAAGTATTTAAA
GTAAAGCACTTGTGAGTTGTGTACATTTTATTAATCTTCATCTTCTTAATTCTCTTCAGTTTTTAATTTCTTCACTTCTAAACTCATT
TAGTAAAAAAAAATGGGATTTGAGATTGCAAAGACCAACTCAATCTTATCAAAATTGGCTACTAATGAAGAGCATGGCGAAAA
CTCGCCATATTTTGATGGGTGGAAAGCATACGATAGTGATCCTTTCCACCCTCTAAAAAACCCCAACGGAGTTATCCAAATGGGT
CTTGCTGAAAATCAGGTAATTAATTATCCTTTATTTATATATTTTGCAGTTTGACCAAACAGACTATTATAATTTTTTTCTGAAACC
TCGATGGTGTTAAATTTCTTTTGTAGCTTTGTTTAGACTTGATAGAAGATTGGATTAAGAGAAACCCAAAAGGTTCAATTTGTTC
TGAAGGAATCAAATCATTCAAGGCCATTGCCAACTTTCAAGATTATCATGGCTTGCCTGAATTCAGAAAGGTACATATCGTACT
ATAGTCAGTTAAATTATATTGATAGTATAAAAATTCGTTAATATATTTAACTAACGAGTTTATTTAATCAGGCGATTGCGAAATT
TATGGAGAAAACAAGAGGAGGAAGAGTTAGATTTGATCCAGAAAGAGTTGTTATGGCTGGTGGTGCCACTGGAGCTAATGAG
ACAATTATATTTTGTTTGGCTGATCCTGGCGATGCATTTTTAGTACCTTCACCATACTACCCAGCGTAAGTATATTTAATTATATAT
GTGTAAAAAAAATTAAAATCATCAAATCATTTTTTTTATTTGTATTACCAAATAAATTGTCTAATTTTCAAGATTGTAACACATTC
ATCAAAGTACCTAATAATATAAACGATTCAGTATATTAACGATGTATATAATTTAATTCCTTTGGCGGATTTGTCTTTTTATGTTG
GGCCATCAGAAGAACATTCTGGTGTATTAATTAATTAATTAATTAATAATAGATGTGTTGTCATTCTTTTTTAAGACAGCGAGAG
TTTAATTAGTCTTAATTACTGGATTATCACGCAAGCTCTTTCTTGAATTTTATTATTCTTATATTAAACACATGATAGCATAATATC
TTTCTTTTGTGGAATCCAGCTTGTTCGTGAAGCTTTGTATTCACACTTATAAAACAACAAAAAATAAAATCTGGTGGTAATTGAT
TAAAGAGAGAAATATAAAAAAATAATAGTCAAATAGACTAATAAGGAAAGAAATAAAAAATACACAAAATACTAAAAAAAA
AGAATTAAGGTATAGTGGTCTATTATTGAGAACTTTTTTGAAGAATTGAACCCCACTTTAATTTCTTGCTTGACCCGTGACCATTG
CTTATCGAGGTAAAATAAAATTTCAAACATTGACTATGACTTGTTAGAGAGTAATTACCACAAGTCAAAATTTTGTTACTTGTC
TCGTTATTTCATTAGGATCGATAAGATAACATCTAGCATATATATCTTTTTTATTAGTACTTATTTATTTTTAGTAAAAGCACGTTA
TACATTTTACAATAGTCAATTGTTGCATATATTAGTATATATATTTTGCTAAGTCCTAACTAACAATATTTTTGGCAATTGACTAA
TGCAGATTTAACAGAGATTTAAGATGGAGAACTGGAGTACAACTTATTCCAATTCACTGTGAGAGCTCCAATAATTTCAAAATT
ACTTCAAAAGCAGTAAAAGAAGCATATGAAAATGCACAAAAATCAAACATCAAAGTAAAAGGTTTGATTTTGACCAATCCATC
AAATCCATTGGGCACCACTTTGGACAAAGACACACTGAAAAGTGTCTTGAGTTTCACCAACCAACACAACATCCACCTTGTTTGT
GACGAAATCTACGCAGCCACTGTCTTTGACACGCCTCAATTCGTCAGTATAGCTGAAATCCTCGATGAACAGGAAATGACTTACT
GCAACAAAGATTTAGTTCACATCGTCTACAGTCTTTCAAAAGACATGGGGTTACCAGGATTTAGAGTCGGAATCATATATTCTTT
TAACGACGATGTCGTTAATTGTGCTAGAAAAATGTCGAGTTTCGGTTTAGTATCTACACAAACGCAATATTTTTTAGCGGCAATG
CTATCGGACGAAAAATTCGTCGATAATTTTCTAAGAGAAAGCGCGATGAGGTTAGGTAAAAGGCACAAACATTTTACTAATGG
ACTTGAAGAAGTGGGAATTAAATGCTTGAAAAATAATGCGGGGCTTTTTTGTTGGATGGATTTGCGTCCACTTTTAAGGGAATC
GACTTTCGATAGCGAAATGTCGTTATGGAGAGTTATTATAAACGATGTTAAGCTTAACGTCTCGCCTGGATCTTCGTTTGAATGT
CAAGAGCCAGGGTGGTTCCGAGTTTGTTTTGCAAATATGGATGATGGAACGGTTGATATTGCGCTCGCGAGGATTCGGAGGTT
CGTAGGTGTTGAGAAAAGTGGAGATAAATCGAGTTCGATGGAAAAGAAGCAACAATGGAAGAAGAATAATTTGAGACTTAGT
TTTTCGAAAAGAATGTATGATGAAAGTGTTTTGTCACCACTTTCGTCACCTATTCCTCCCTCACCATTAGTTCGTTAAGACTTAATT
AAAAGGGAAGAATTTAATTTATGTTTTTTTATATTTTGAAAAAAATTTGTAAGAATAAGATTATAATAGGAAAAGAAAATAAGT
ATGTAGGATGAGGAGTATTTTCAGAAATAGTTGTTAGCGTATGTATTGACAACTGGTCTATGTACTTAGACATCATAATTTGTCT
TAGCTAATTAATGAATGCAAAAGTGAAGTTATGTTATGACTCTT

Figure 4.4. *acs2-1* genomic sequence of *ACS2* gene. The genomic sequence was retrieved from SGN. The green and pink colored regions indicates the 5' and 3' UTR regions of the gene respectively whereas the blue colored regions corresponds to the four exons of the gene. The red colored arrow heads indicating the change in nucleotide bases compared to WT after *acs2-1* sequencing.

acs2-2 Genomic sequence 2930

>Solyc01g095080.2 | SL2.40ch01:78214067..78216996 reverse

TTTTTGTGTTGGGGAGGGGCGGATTTTGGGTTGGATAAGAAAAAAATTTAAAGATAAAATAGAATTTTGGAAAATATTTTTCT
TAATTTTTGAAGGAAAATCATTTTTCTTAAATTTGAGAAAAATGAATTATTCTTAAAAAAAATTTCCAAAAACATTTAAGCTACC
AAATATGAAAAAATAAAAAATATTTTTTTTCCTACCAAATGCACCCTAAATTAGTCAAATATCCAACATTTAAAAGAGCTATGAA
AAAAAAAAAGAAGTAAGAATCGTAGATCTTCTTTTAATGCGTACTTTTATTTTCCAAGATTTGAACAAAAAAATAGACTTTTCTA
TTTTTATTTTCTGATGTAATTCTTATATACGTTAGTCGACATGTTCTCATTACATACTTCAGTCTTTCCCCTTATATATATCCCTCAC
ATTCCTTAATTCTCTTACACCATAACACAACTACAACAAACACATAATACTTTTAATACAATTAGTTATTTATTAGAAGTATTTAA
AGTAAAGCACTTGTGAGTTGTGTACATTTTATTAATCTTCATCTTCTTAATTCTCTTCAGTTTTTAATTTCTTCACTTCTAAACTCAT
TTAGTAAAAAAAAAATGGGATTTGAGATTGCAAAGACCAACTCAATCTTATCAAAATTGGCTACTAATGAAGAGCATGGCGAAA
ACTCGCCATATTTTGATGGGTGGAAAGCATACGATAGTGATCCTTTCCACCCTCTAAAAAACCCCAACGGAGTTATCCAAATGG
GTCTTGCTGAAAATCAGGTAATTAATTATCCTTTATTTATATATTTTGCAGTTTGACCAAACAGACTATTATAATTTTTTTCTGAAA
CCTCGATGGTGTTAAATTTCTTTTGTAGCTTTGTTTAGACTTGATAGAAGATTGGATTAAGAGAAACCCAAAAGGTTCAATTTGT
TCTGAAGGAATCAAATCATTCAAGGCCATTGCCAACTTTCAAGATTATCATGGCTTGCCTGAATTCAGAAAAGTACATATCGTAC
TATAGTCAGTTAAATTATATTGATAGTATAAAAATTCGTTAATATATTTAACTAACGAGTTTATTTAATCAGGCGATTGCGAAAT
TTATGGAGAAAACAAGAGGAGGAAGAGTTAGATTTGATCCAGAAAGAGTTGTTATGGCTGGTGGTGCCACTGGAGCTAATGA
GACAATTATATTTTGTTTGGCTGATCCTGGCGATGCATTTTTAGTACCTTCACCATACTACCCAGCGTAAGTATATTTAATTATAT
ATGTGTAAAAAAAATTAAAATCATCAAATCATTTTTTTTATTTGTATTACCAAATAAATTGTCTAATTTTCAAGATTGTAACACAT
TCATCAAAGTACCTAATAATATAAACGATTCAGTATATTAACGATGTATATAATTTAATTCCTTTGGCGGATTTGTCTTTTTATGT
TGGGCCATCAGAAGAACATTCTGGTGTATTAATTAATTAATTAATTAATAATAGATGTGTTGTCATTCTTTTTTAAGACAGCGAG
AGTTTAATTAGTCTTAATTACTGGATTATCACGCAAGCTCTTTCTTGAATTTTATTATTCTTATATTAAACACATGATAGCATAATA
TCTTTCTTTTGTGGAATCCAGCTTGTTCGTGAAGCTTTGTATTCACACTTATAAAACAACAAAAAATAAAATCTGGTGGTAATTG
ATTAAAGAGAGAAATATAAAAAAATAATAGTCAAATAGACTAATAAGGAAAGAAATAAAAAATACACAAAATACTAAAAAA
AAAGAATTAAGGTATAGTGGTCTATTATTGAGAACTTTTTTGAAGAATTGAACCCCACTTTAATTTCTTGCTTGACCCGTGACCA
TTGCTTATCGAGGTAAAATAAAATTTCAAACATTGACTATGACTTGTTAGAGAGTAATTACCACAAGTCAAAATTTTGTTACTCT
GTCTCGTTATTTCATTAGGATCGATAAGATAACATCTAACATATATATCTTTTTTATTAGTACTCGTTTATTTTTAGTAAAAGCAC
GTTATACATTTTACAATAGTCAATTGTTGCATATATTAGTATATATATTTTGCTAAGTCCTAACTAACAATATTTTTGGCAATTGA
CTAATGCAGATTTAACAGAGATTTAAGATGGAGAACTGGAGTACAACTTATTCCAATTCACTGTGAGAGCTCCAATAATTTCAA
AATTACTTCAAAAGCAGTAAAAGAAGCATATGAAAATGCACAAAAATCAAACATCAAAGTAAAAGGTTTGATTTTGACCAATC
CATCAAATCCATTGGGCACCACTTTGGACAAAGACACACTGAAAAGTGTCTTGAGTTTCACCAACCAACACAACATCCACCTTGT
TTGTGACGAAATCTACGCAGCCACTGTCTTTGACACGCCTCAATTCGTCAGTATAGCTGAAATCCTCGATGAACAGGAAATGACT
TACTGCAACAAAGATTTAGTTCACATCGTCTACAGTCTTTCAAAAGACATGGGGTTACCAGGATTTAGAGTCGGAATCATATATT
CTTTTAACGACGATGTCGTTAATTGTGCTAGAAAAATGTCGAGTTTCGGTTTAGTATCTACACAAACGCAATATTTTTTAGCGGC
AATGCTATCGGACGAAAAATTCGTCGATAATTTTCTAAGAGAAAGCGCGATGAGGTTAGGTAAAAGGCACAAACATTTTACTA
ATGGACTTGAAGTAGTGGGAATTAAATGCTTGAAAAATAATGCGGGGCTTTTTTGTTGGATGGATTTGCGTCCACTTTTAAGGG
AATCGACTTTCGATAGCGAAATGTCGTTATGGAGAGTTATTATAAACGATGTTAAGCTTAACGTCTCGCCTGGATCTTCGTTTGA
ATGTCAAGAGCCAGGGTGGTTCCGAGTTTGTTTTGCAAATATGGATGATGGAACGGTTGATATTGCGCTCGCGAGGATTCGGA
GGTTCGTAGGTGTTGAGAAAAGTGGAGATAAATCGAGTTCGATGGAAAAGAAGCAACAATGGAAGAAGAATAATTTGAGAC
TTAGTTTTTCGAAAAGAATGTATGATGAAAGTGTTTTGTCACCACTTTCGTCACCTATTCCTCCCTCACCATTAGTTCGTTAAGAC
TTAATTAAAAGGGAAGAATTTAATTTATGTTTTTTTATATTTTGAAAAAAATTTGTAAGAATAAGATTATAATAGGAAAAGAAA
ATAAGTATGTAGGATGAGGAGTATTTTCAGAAATAGTTGTTAGCGTATGTATTGACAACTGGTCTATGTACTTAGACATCATAA
TTTGTCTTAGCTAATTAATGAATGCAAAAGTGAAGTTATGTTATGACTCTT

Figure 4.5. *acs2-2* genomic sequence of *ACS2* gene. The genomic sequence was retrieved from SGN. The green and pink colored regions indicates the 5' and 3' UTR regions of the gene respectively whereas the blue colored regions corresponds to the four exons of the gene. Upstream to the 5' UTR is the promoter region. The red colored arrow heads indicating the change in nucleotide bases compared to WT after *acs2-2* sequencing.

A

WT Peptide seq 485

>Solyc01g095080.2.1

MGFEIAKTNSILSKLATNEEHGENSPYFDGWKAYDSDPFHPLKNPNGVIQMGLAENQLCLDLIEDWIKRNPKGSICSEGIKSFKAIAN
FQDYHGLPEFRKAIAKFMEKTRGGRVRFDPERVVMAGGATGANETIIFCLADPGDAFLVPSPYYPAFNRDLRWRTGVQLIPIHCESS
NNFKITSKAVKEAYENAQKSNIKVKGLILTNPSNPLGTTLDKDTLKSVLSFTNQHNIHLVCDEIYAATVFDTPQFVSIAEILDEQEMTYC
NKDLVHIVYSLSKDMGLPGFRVGIIYSFNDDVVNCARKMSSFGLVSTQTQYFLAAMLSDEKFVDNFLRESAMRLGKRHKHFTNGLE
VVGIKCLKNNAGLFCWMDLRPLLRESTFDSEMSLWRVIINDVKLNVSPGSSFECQEPGWFRVCFANMDDGTVDIALARIRRFVGVE
KSGDKSSSMEKKQQWKKNNLRLSFSKRMYDESVLSPLSSPIPPSPLVR*

B

***acs2-1* Peptide seq 485**

>Solyc01g095080.2.1

MGFEIAKTNSILSKLATNEEHGENSPYFDGWKAYDSDPFHPLKNPNGVIQMGLAENQLCLDLIEDWIKRNPKGSICSEGIKSFKAIAN
FQDYHGLPEFRRAIAKFMEKTRGGRVRFDPERVVMAGGATGANETIIFCLADPGDAFLVPSPYYPAFNRDLRWRTGVQLIPIHCESS
NNFKITSKAVKEAYENAQKSNIKVKGLILTNPSNPLGTTLDKDTLKSVLSFTNQHNIHLVCDEIYAATVFDTPQFVSIAEILDEQEMTYC
NKDLVHIVYSLSKDMGLPGFRVGIIYSFNDDVVNCARKMSSFGLVSTQTQYFLAAMLSDEKFVDNFLRESAMRLGKRHKHFTNGLEE
VGIKCLKNNAGLFCWMDLRPLLRESTFDSEMSLWRVIINDVKLNVSPGSSFECQEPGWFRVCFANMDDGTVDIALARIRRFVGVEK
SGDKSSSMEKKQQWKKNNLRLSFSKRMYDESVLSPLSSPIPPSPLVR*

C

***acs2-2* Peptide seq 485**

>Solyc01g095080.2.1

MGFEIAKTNSILSKLATNEEHGENSPYFDGWKAYDSDPFHPLKNPNGVIQMGLAENQLCLDLIEDWIKRNPKGSICSEGIKSFKAIAN
FQDYHGLPEFRKAIAKFMEKTRGGRVRFDPERVVMAGGATGANETIIFCLADPGDAFLVPSPYYPAFNRDLRWRTGVQLIPIHCESS
NNFKITSKAVKEAYENAQKSNIKVKGLILTNPSNPLGTTLDKDTLKSVLSFTNQHNIHLVCDEIYAATVFDTPQFVSIAEILDEQEMTYC
NKDLVHIVYSLSKDMGLPGFRVGIIYSFNDDVVNCARKMSSFGLVSTQTQYFLAAMLSDEKFVDNFLRESAMRLGKRHKHFTNGLE
VVGIKCLKNNAGLFCWMDLRPLLRESTFDSEMSLWRVIINDVKLNVSPGSSFECQEPGWFRVCFANMDDGTVDIALARIRRFVGVE
KSGDKSSSMEKKQQWKKNNLRLSFSKRMYDESVLSPLSSPIPPSPLVR*

Figure 4.6. ACS2 peptide sequences. **A** representing WT protein sequence, **B** representing ACS2-1 protein sequence, and **C** corresponds to ACS2-2 protein sequence respectively. The red colored arrow heads indicating the change in amino acids which was observed in ACS2-1 protein compared to WT after sequencing.

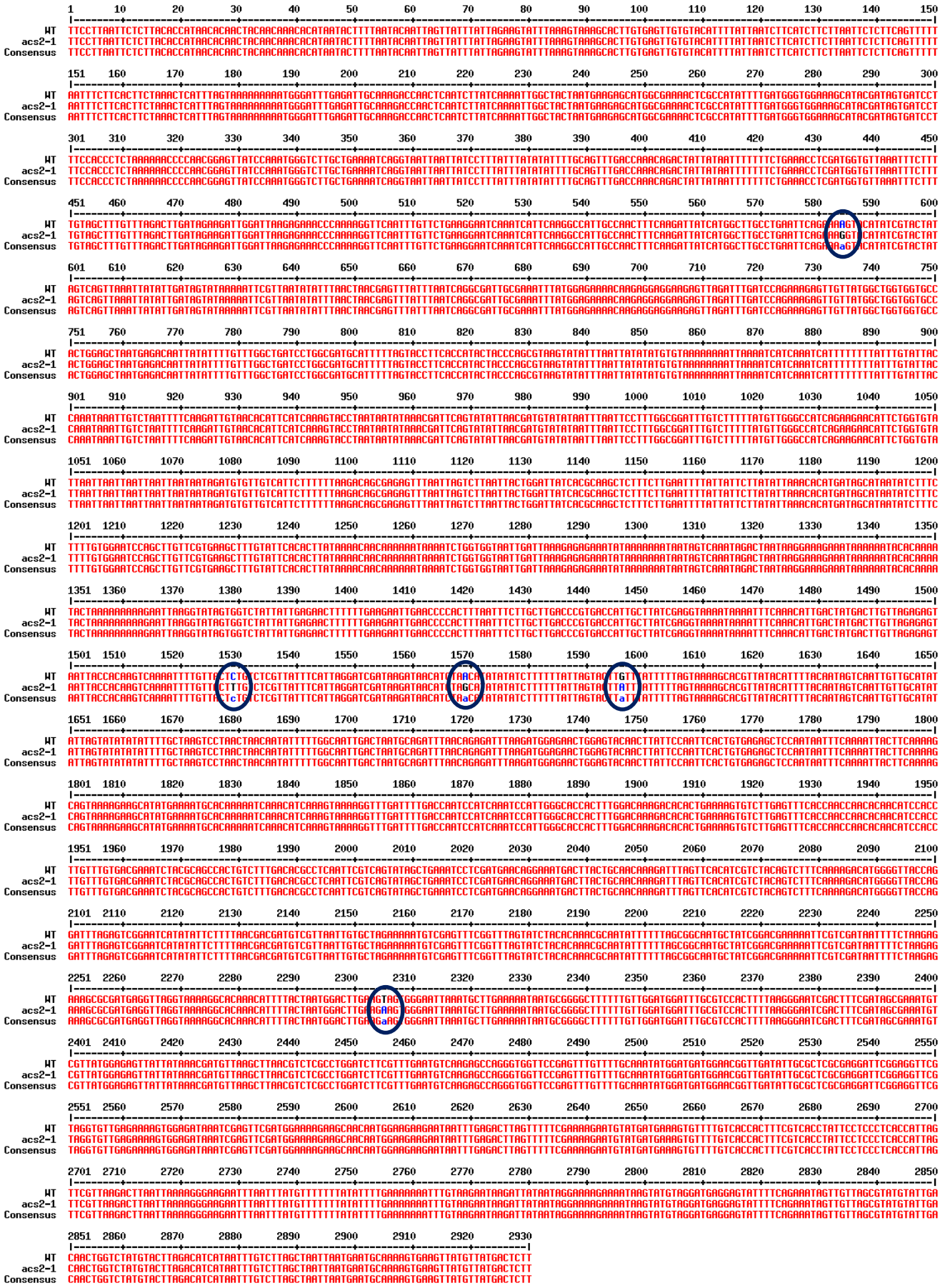

Figure 4.7. Multialign of genomic sequence of *acs2-1* with WT. The blue colored circle representing the changes in the nucleotide bases compared to WT.

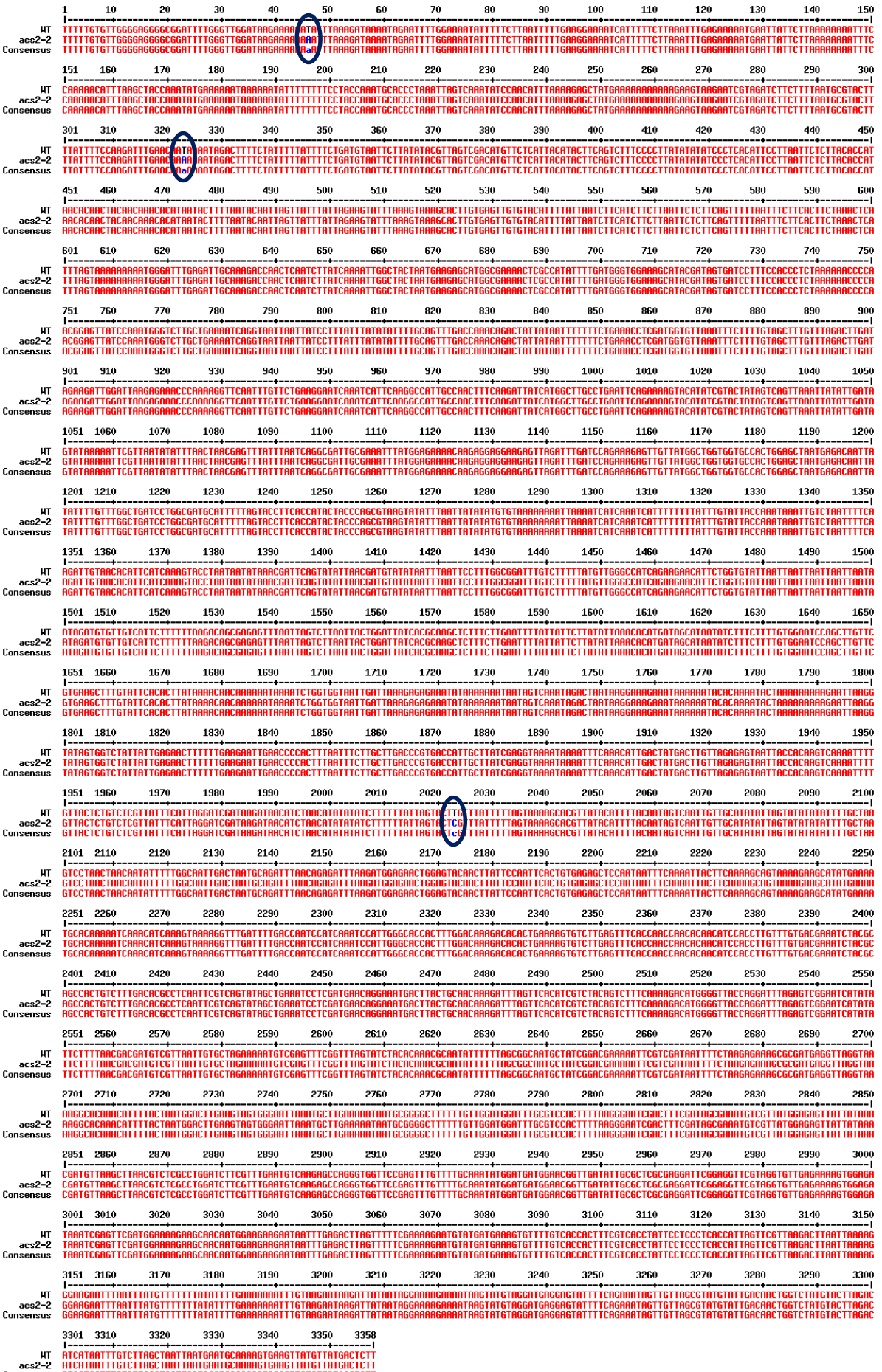

Figure 4.8. Multialign of genomic sequence of *acs2-2* with WT. The blue colored circle representing the changes in the nucleotide bases compared to WT.

A

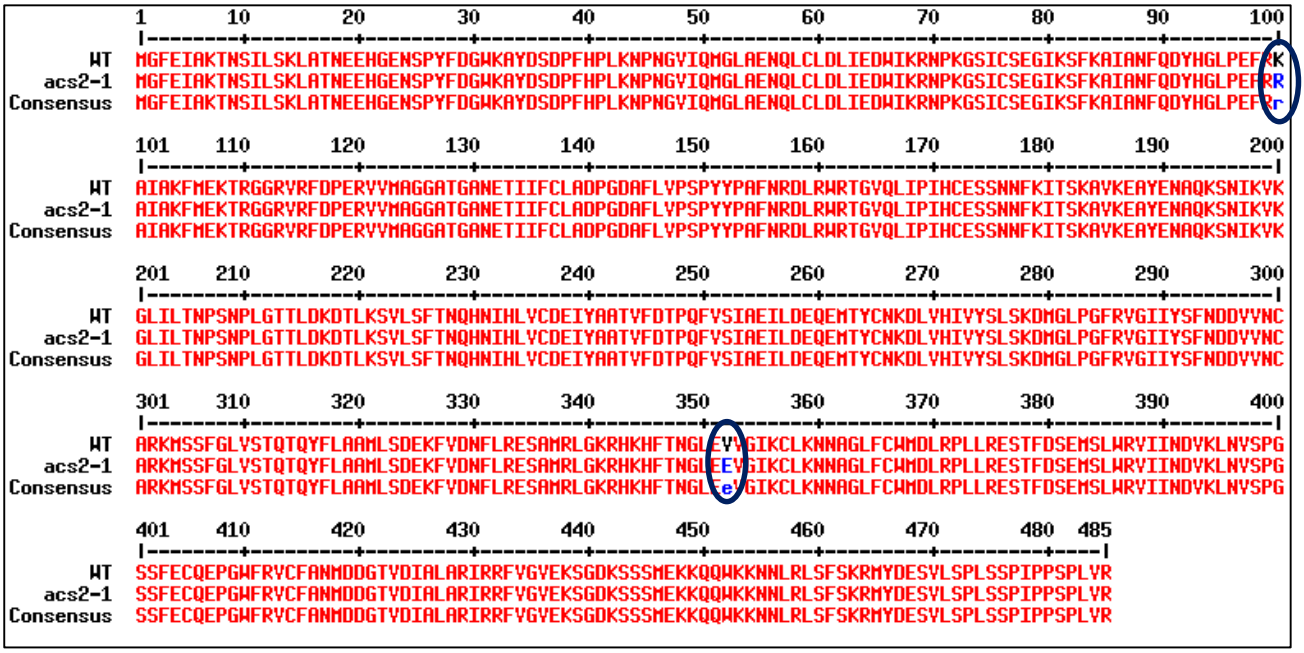

B

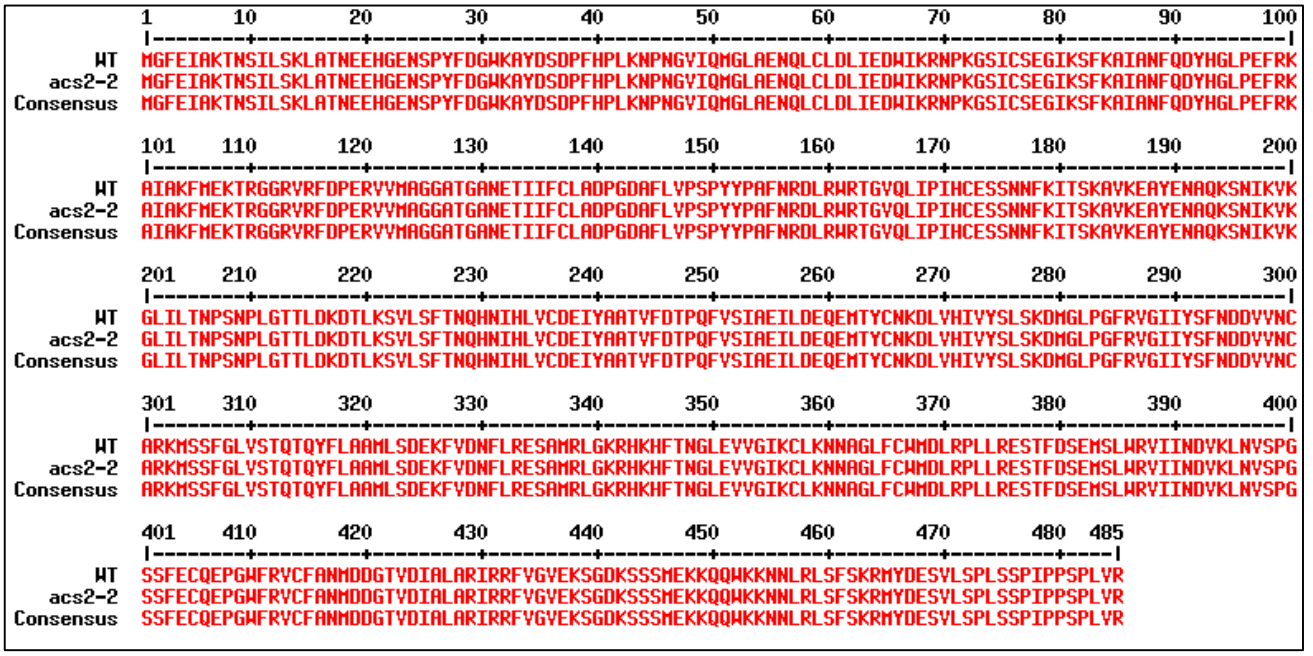

Figure 4.9. Multialign of protein sequence of ACS2-1 (A) and ACS2-2 (B) with WT. The blue colored circle representing the changes in the amino acids compared to WT.

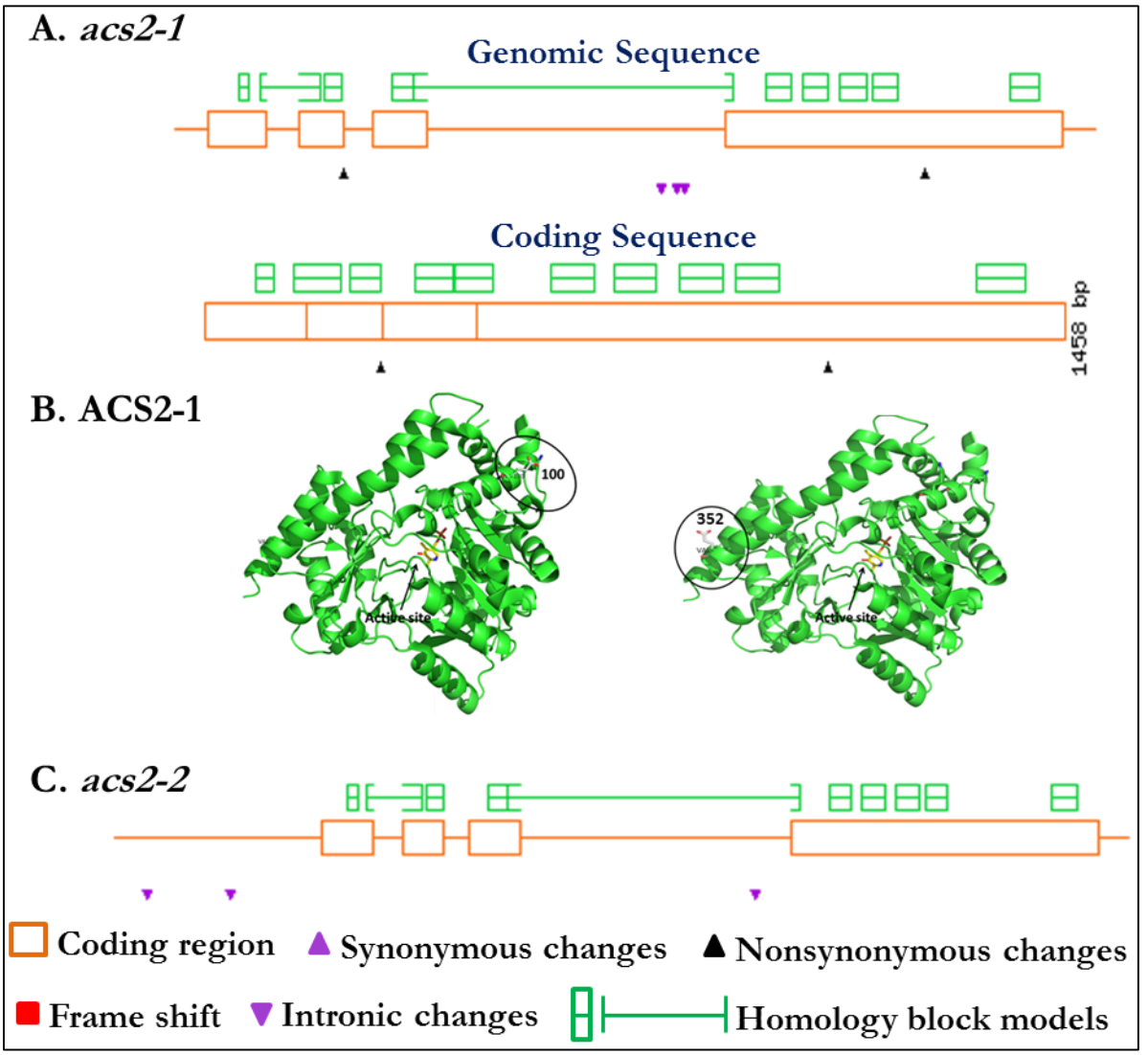

Figure 4.10. Confirmation of *acs2-1* and *acs2-2* mutations by sequencing. **(A)** Pictorial diagram of *ACS2* gene showing location of mutations in *acs2-1* mutant. *acs2-1* mutant has two missense mutations in exon 2 and exon 4 respectively and three intronic mutations. **(B)** Modeling of ACS2-1 mutant protein. Missense mutations resulted in amino acid substitutions from lysine to arginine and valine to glutamic acid at positions 100 and 352 respectively, in the ACS2 protein sequence. These mutations lies in α-chain of protein surface. **(C)** Pictorial diagram of *ACS2* gene showing location of mutations in *acs2-2* mutant. The *acs2-2* mutant exhibits two mutations in the promoter region and one mutation in the third intron.

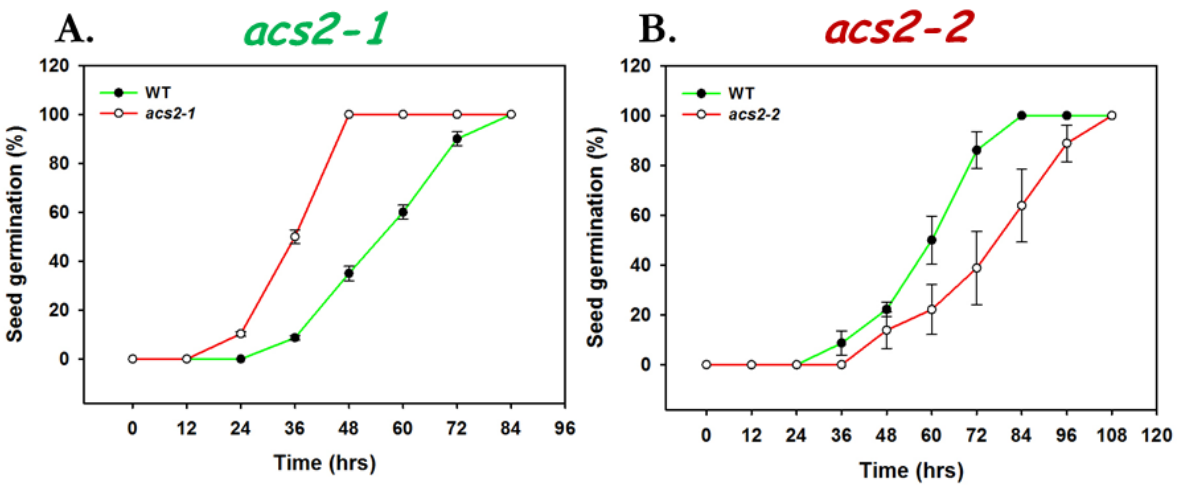

Figure 4.11. Time course of seed germination. Seeds were surface sterilized using 4% (v/v) sodium hypochlorite. After washing with water, seeds were germinated in plastic petri plates on premoistened filter paper and sealed with the parafilm. Three different sets of Petri plates (each set containing three such petri plates), for WT, *acs2-1* and *acs2-2* mutant seeds respectively, were kept in darkness. Seed germination was monitored at a fixed interval of time (12 hr.). **(A)** Represents *acs2-1* mutant seeds germination and **(B)** represents *acs2-2* mutant seeds germination. For seed germination profiling, seeds number, n= 30 ± SE.

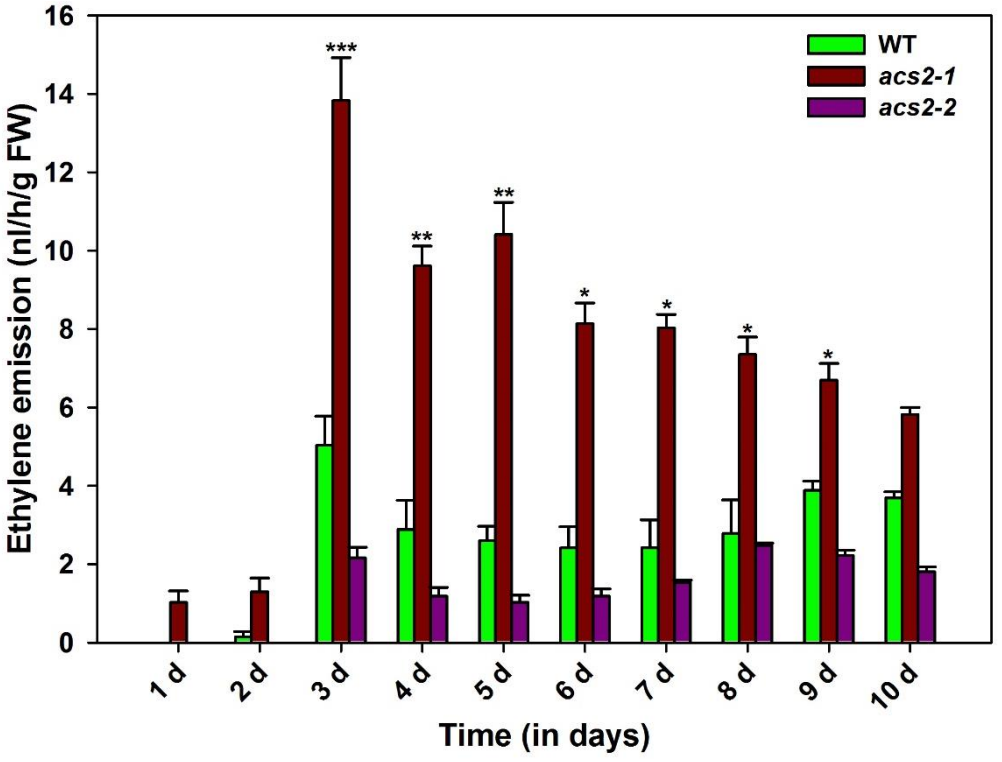

Figure 4.12. Ethylene emission from dark grown germinating seedlings of *acs2-1*, and *acs2-2* mutants. To monitor the ethylene emission from WT and mutant seedlings, surface sterilized seeds were sown in darkness in a tightly sealed 10 mL glass vial on 0.8% (w/v) agar. At 24 hr intervals one mL of the head space volume was withdrawn from the vial using an injection syringe. The head space was injected into a gas Chromatogram (model GC-17A, Shimadzu, Kyoto, Japan) fitted with a flame ionization detector and an activated "Porapack T" column to determine ethylene levels. Student's t-test; * for $P \leq 0.05$, ** for $P \leq 0.01$ and *** for $P \leq 0.001$.

4.2.8 The *acs2-1* mutant exhibits longer primary root and more lateral roots

To examine whether *acs2-1* mutation affected overall seedling growth and phenotype, seedling's phenotype was monitored under continuous white light. Among the few organs, the growth of roots was slightly accelerated in the *acs2-1* mutant. In addition *acs2-1* mutant displayed more number of lateral roots compared to WT. In contrast *acs2-2* mutant exhibited slightly higher number of lateral roots, whereas the primary root length was slightly smaller than the WT **(Fig. 4.13)**.

4.2.9 *acs2-1* and *acs2-2* mutant retain triple response to ethylene

To monitor whether ethylene receptors were functional or not in *acs2* mutants, WT and mutants seedlings after germination in normal air were grown in tightly sealed boxes containing different concentrations of externally applied ethylene in darkness. **Figure 4.14** depicts that *acs2-1* seedlings were more sensitive to the external ethylene than the wild type. Even at low ethylene concentration (2 mL), *acs2-1* mutant seedlings displayed triple response similar to WT control **(Fig. 4.14A and B)**. On the other hand, *acs2-2* mutant seedlings initiated triple response at higher dose (4 mL) of externally injected ethylene compared to WT **(Fig. 4.14A and C)**. Nonetheless, both *acs2-1*, *acs2-2* and WT seedlings exhibited distinct triple response with tightening of terminal hook, shortening and thickening of hypocotyl and root **(Fig. 4.14E and F)**.

4.2.10 The *acs2-1* and *acs2-2* mutations elicit pleiotropic effect on plant morphology

The effect of *acs2-1* and *acs2-2* mutations was not limited to the seedlings. The mutants exhibited altered ethylene responses throughout the life cycle of plants. The mutations also exerted a strong pleiotropic effect on all stages of plant development from seed germination to senescence. The specific variations in morphological features of mutants were compared with WT at different stages of development. The *acs2-1* plants displayed faster growth compared to WT **{Fig. 4.15A (a)}**. Though 45 days old both WT and *acs2-1* plants had the similar number of internodes, but *acs2-1* mutant plants are showing elongated internode and early flowering. Also the leaf has more length than the WT. After 1.5 months of growth in the green house, mutant plants were distinctly taller than the WT **{Fig. 4.15A (a)}**. The leaf of *acs2-1* plants harvested from 7th node was pale in color than corresponding WT leaves of the 45 days old plant from the same node **{Fig. 4.15A(b)}**. The *acs2-1* mutation also affected the development of reproductive organs. The mutant plant showed more number of flowers per truss in comparison to wild type **{Fig. 4.15A(c)}**. Most of these flowers set fruits after natural pollination which

resulted in increased fruit set. The number of fruits per truss in *acs2-1* mutant was (8±1), whereas each truss of WT had (5±1) fruits **{Fig. 4.8A (d, e)}**. One of the important feature is straight, long and less green fruit sepals of *acs2-1* mutant while WT fruit shows curly and green sepals **{Fig. 4.15A(d, e)}**. Taken together, above results indicate that *acs2-1* mutation accelerates the overall development of plants and has a beneficial effect on fruit yield.

On the other hand, *acs2-2* mutant plant exhibited slightly slower growth compared to WT **{Fig. 4.15B (a)}**. The leaf color of mutant was more dark green and curly compared to WT **{Fig. 4.15B (b)}**. The number of flowers per truss in mutant was almost similar as WT but flower is small with elongated sepals **{Fig. 4.15B(c, d)}**. However, the fruits of *acs2-2* mutant were somewhat larger in size than the WT fruits **{Fig. 4.15B (e)}**.

4.2.11 The *acs2-1* mutant leaves exhibit early senescence

Ethylene is known to promote leaf senescence in higher plants (Jing et al., 2005). Examination of senescence of leaves detached from the vine revealed that *acs2-1* mutant leaves senesced faster than the WT. The yellowing of *acs2-1* mutant leaves due to loss of green chlorophyll was faster than the WT both under continuous white light and also in darkness when kept for six days **(Fig. 4.16A)**. In contrast, the detached leaves of *acs2-2* mutant exhibited a delayed senescence compared with WT when kept for 12 days **(Fig. 4.16B)**.

4.2.12 The *acs2-1* mutant leaves emits high ethylene

The *acs2-1* mutant leaves harvested from plants showed higher level of ethylene emission compared to WT leaves **(Fig. 4.17A)**. In addition, the total amount of chlorophyll (Chl. A and Chl. B) and carotenoids in *acs2-1* mutant leaf was slightly lower than the WT leaf. The reduction in pigments level in the *acs2-1* mutant leaf may be due to influence of ethylene on degradation of chlorophyll pigments **(Fig. 4.17B)**.

In contrast *acs2-2* mutant leaves exhibited less ethylene emission compared to WT leaves **(Fig. 4.17A)**. The total chlorophyll and carotenoids content of *acs2-2* mutant leaf was slightly higher compared to WT leaf **(Fig. 4.17B)**.

4.2.13 The *acs2-1* mutation lowers carotenoid levels in leaf tissue

The influence of *acs2-1* mutation on total carotenoid level was also monitored by resolving individual carotenoids by U-HPLC coupled with PDA detector. A total of seven carotenoids (Violaxanthin, neoxanthin, lutein, α-carotene, β-carotene, 9'-cis α-carotene and 9'-cis β-carotene) were detected. The *acs2-1* mutant exhibited a slight

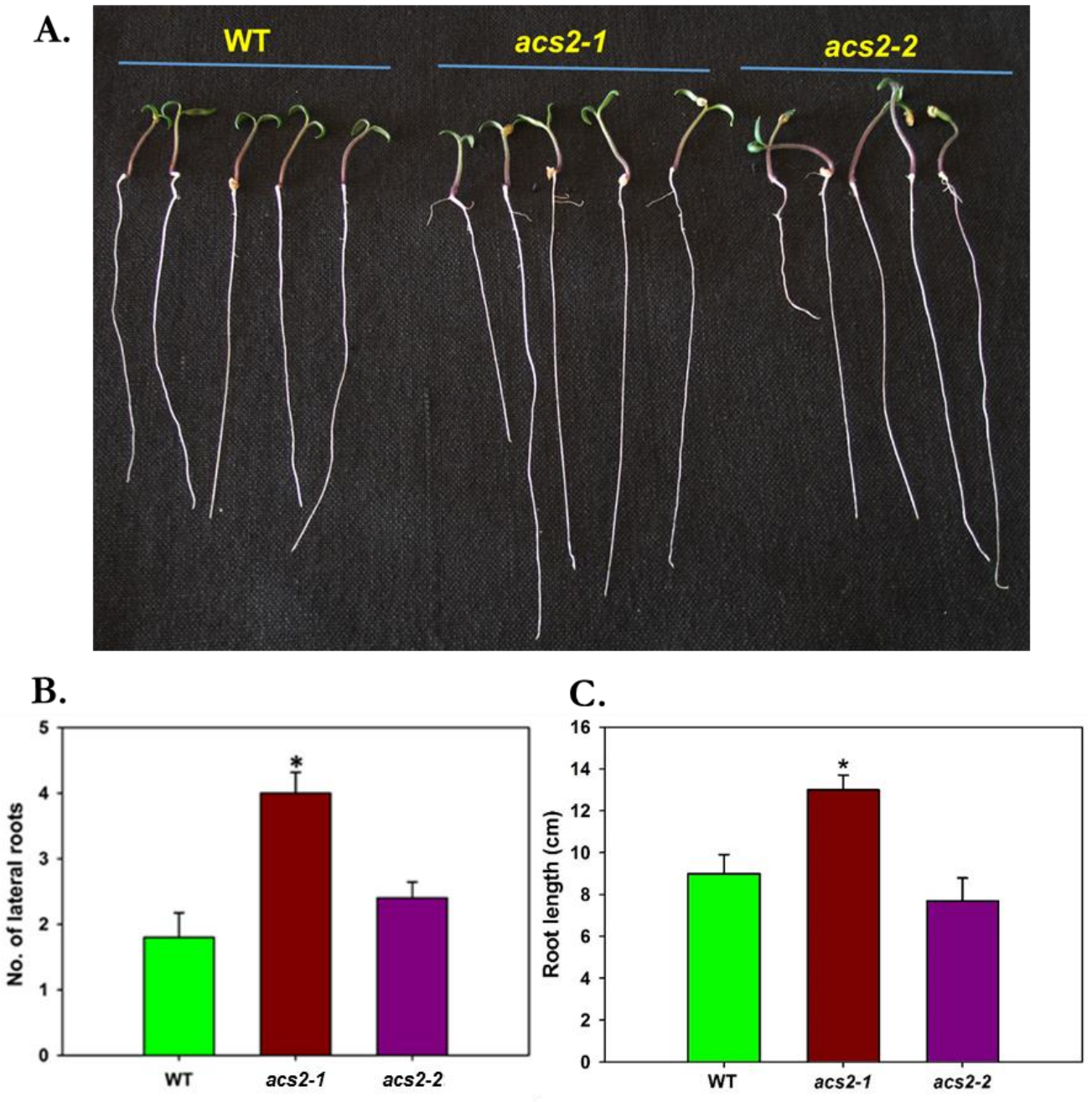

Figure 4.13. Phenotype of 5 days old light grown *acs2-1* and *acs2-2* seedlings. The length of the roots was measured and lateral roots were counted. Seedlings were grown on 0.8% (w/v) agar in three different sets of air-tight Petri plates. The plates were placed in vertical orientation under continuous white light (100 μmole m^{-2} s^{-1}) for five days. Each set consisted of three sets of biological replicates (A, B and C). (Student's t-test; * for $P \leq 0.05$, ** for $P \leq 0.01$ and *** for $P \leq 0.001$, for root length and lateral roots, seeds number, n= 36 ± SE).

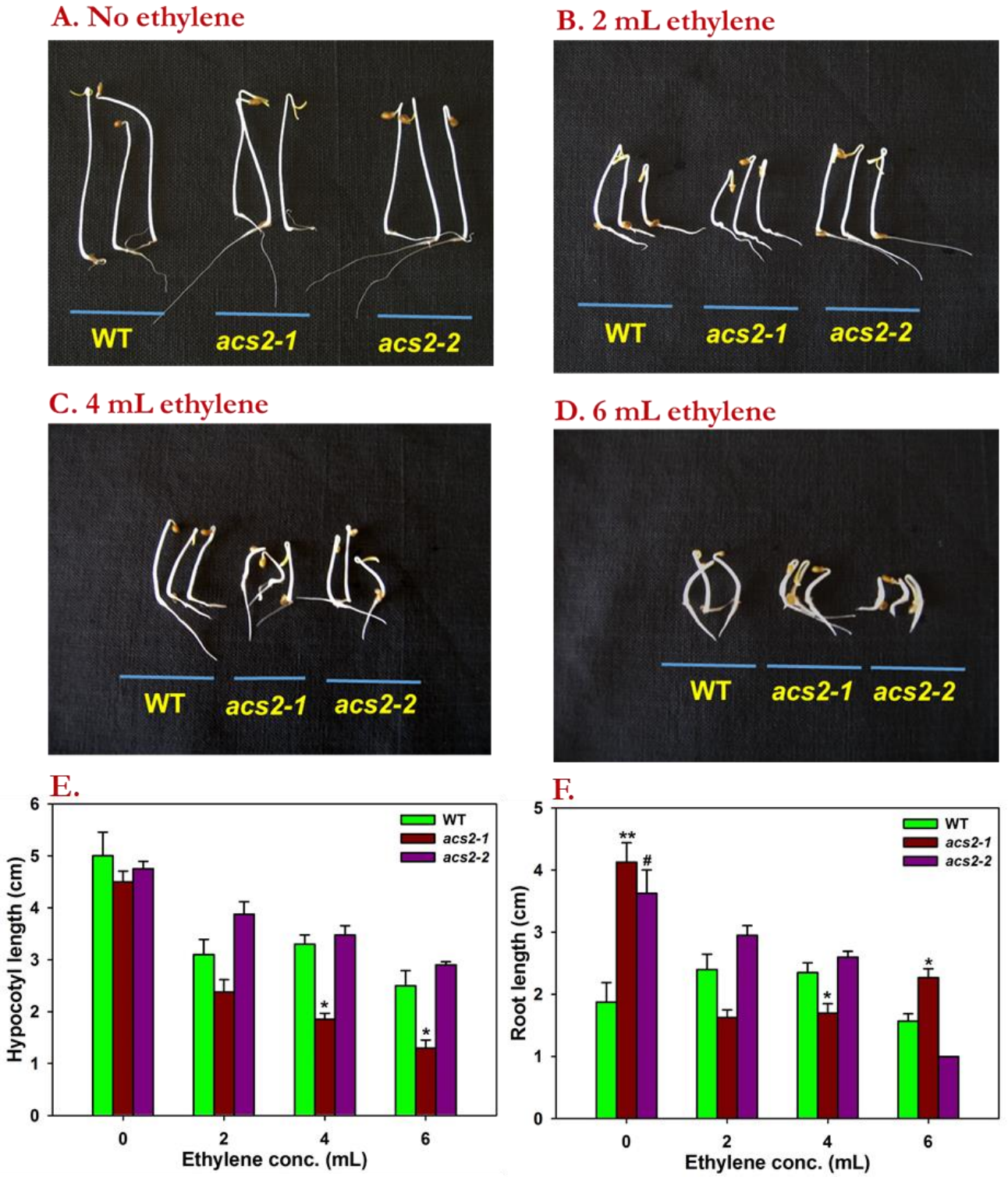

Figure 4.14. Induction of triple response in WT and mutant seedlings to ascertain the functioning of ethylene receptors. The seedlings of WT and mutants after seed germination were grown in an air-tight seed germination plastic box on 0.8% (w/v) agar, in the darkness for five days. A known volume of ethylene (indicated on top of the respective figures) was injected in each box. After five days, seedling's phenotype was monitored for the triple response and hypocotyls and roots length were measured. (Student's t-test; *, # for $P \leq 0.05$, ** for $P \leq 0.01$ and *** for $P \leq 0.001$, for ethylene response experiments, seedlings number, n= 30 ± SE).

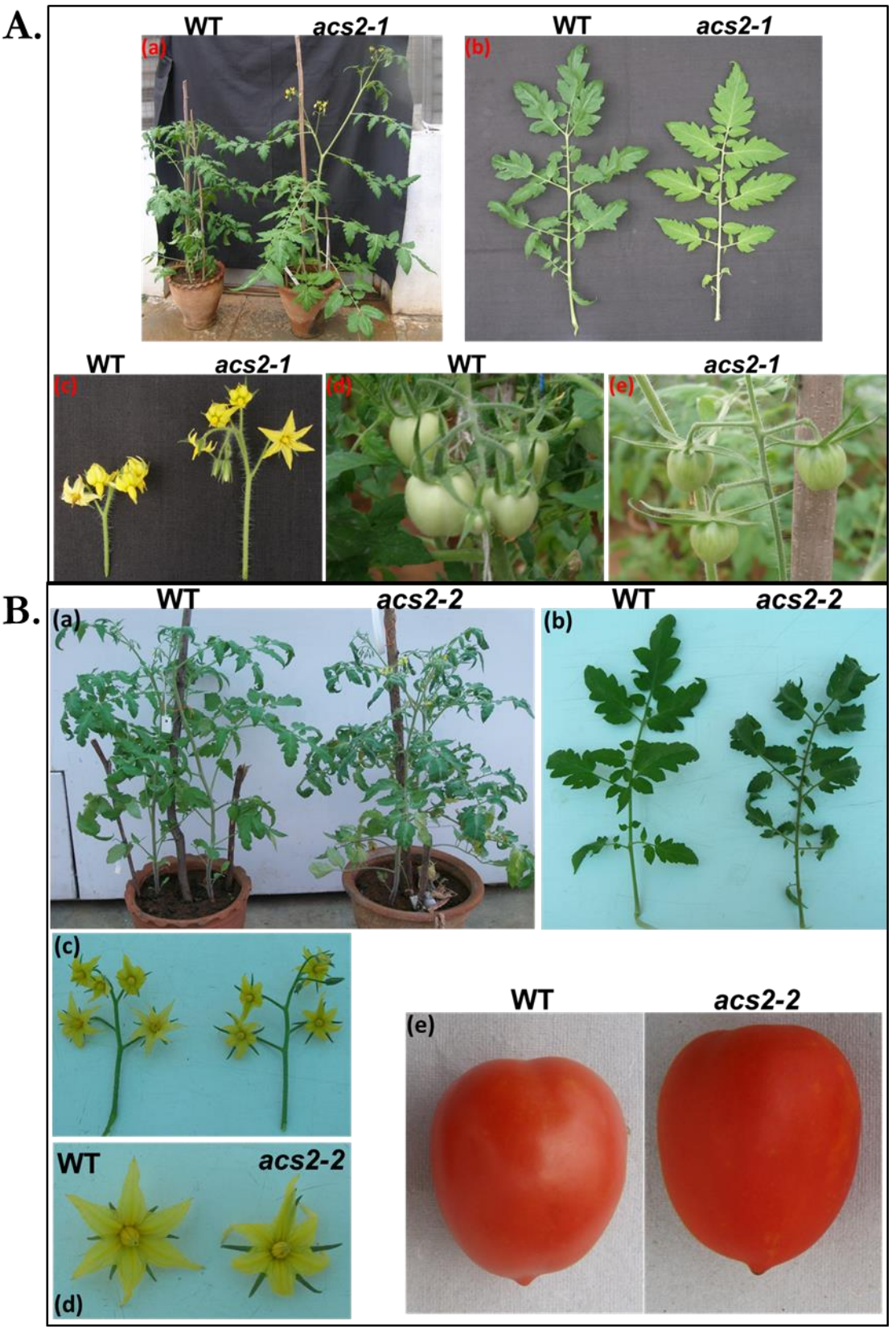

Figure 4.15. Comparisons of plant phenotype, leaf morphology and flower phenotype of 45-days-old WT, *acs2-1 (***A)**, and *acs2-2 (***B)** mutant plants. **A. (a)** and **B. (a)** Comparisons of plant phenotype. **A. (b)** and **B. (b)** Comparisons of leaf morphology between wild type and mutants. Leaves were taken from the 7th node of the wild-type and mutant plants. **A. (c)** and **B. (c and d)** Comparisons of inflorescences and flowers of WT and mutants. **A. (d and e)** and **B. (e)** Comparisons of fruit phenotype.

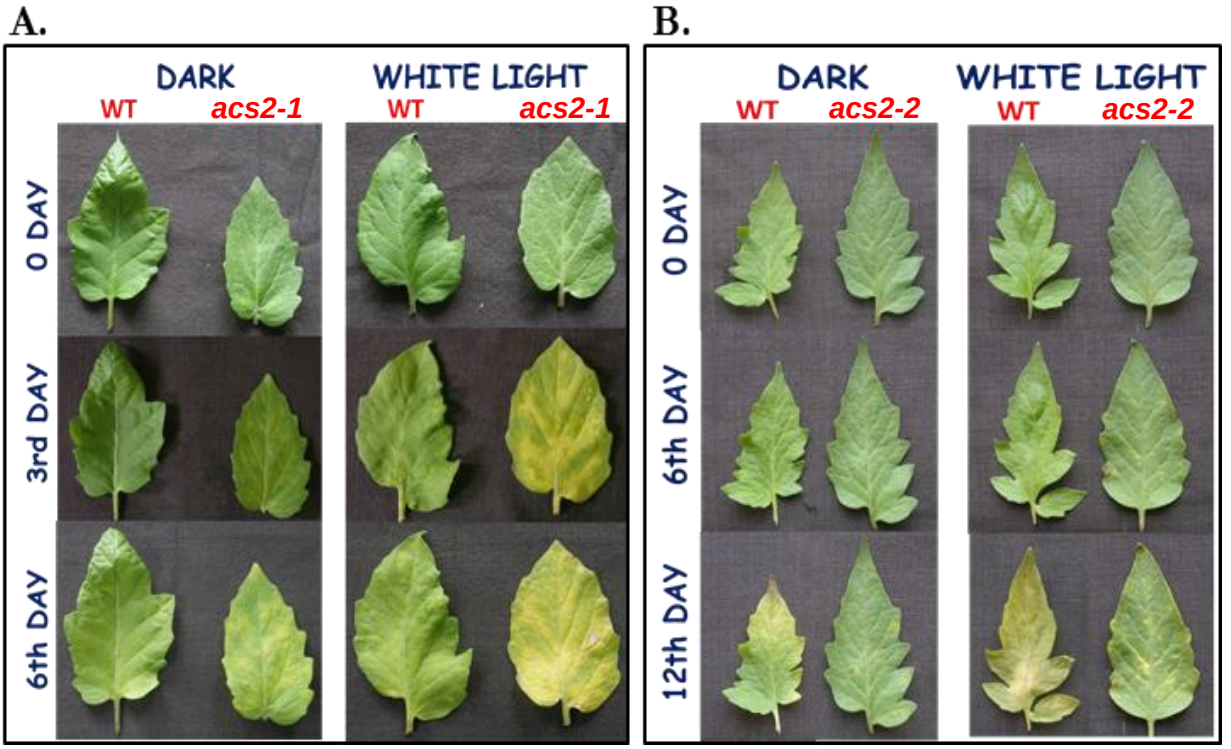

Figure 4.16. Senescence of detached leaves of WT, *acs2-1,* **(A)** and *acs2-2* **(B)** mutants. Leaves were harvested from the seventh node of both mutants and wild type plants of 45 days old. After harvesting, leaves were placed in petri plates on premoistened filter paper. The petri plates were kept either under continuous white light (100 µmole $m^{-2}s^{-1}$) or in darkness respectively to record leaf senescence. Each such set contained three biological replicates **(A-B)**.

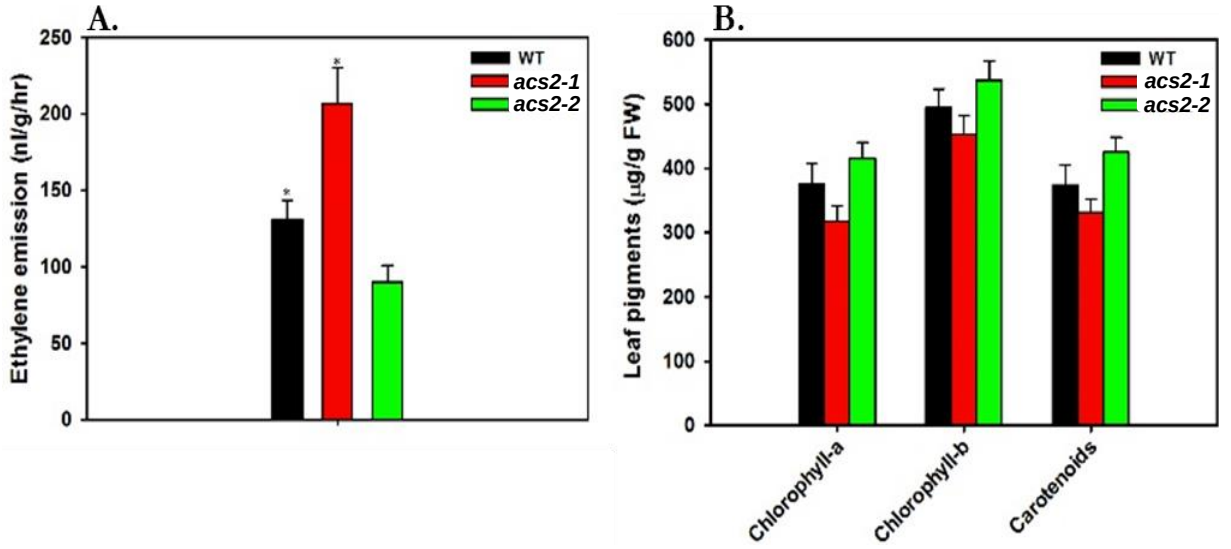

Figure 4.17. (A) Estimation of the ethylene emission from leaves of wild-type, *acs2-1,* and *acs2-2* mutant. Leaves were harvested from the 7th node of 45-days-old plants of wild-type and mutant lines. **(B)** Chlorophyll level in leaf tissue of wild type, *acs2-1,* and *acs2-2* mutant. Each value is the mean of three biological replicates.

decrease in the levels of xanthophyll and carotenoids compared to WT leaves **(Fig. 4.18)**. On the other hand a slight increase in levels of xanthophyll and carotenoids were observed in the leaf of *acs2-2* mutant compared to WT leaf **(Fig. 4.18)**.

4.2.14 The *acs2-1* mutation influences phytohormone levels in leaf tissue

A total of seven phytohormones viz. zeatin, indole-acetic acid (IAA), indole butyric acid (IBA), jasmonic acid (JA), methyl jasmonic acid (MeJA), abscisic acid (ABA) and salicylic acid (SA) were detected in tomato leaf tissue **(Fig. 4.19)**. Out of seven phytohormones, the levels of three phytohormones namely JA, and ABA and MeJA increased in *acs2-1* mutant leaves compared to WT **(Fig. 4.19)**. On the other hand, zeatin, IAA, IBA and SA levels declined in *acs2-1* mutant leaves compared to WT **(Fig. 4.19)**.

On the other hand, the *acs2-2* mutant leaves exhibited low level of SA but zeatin level is high compared to WT while the levels of other phytohormones were comparable to the WT leaves **(Fig. 4.19)**.

4.2.15 The *acs2-1* mutation affected primary metabolites accumulation

Considering that *ACS2* mutation influences leaf morphology, pigments and hormone levels, the influence of mutation on overall profile of primary metabolites was examined. A total of 140 primary metabolites, as a whole, were detected in tomato leaf and fruits. Detected primary metabolites were categorized in different groups like amino acids, organic acids, alcohols, sugars, fatty acids and their derivatives **(Table 4.4A)**. Comparisons of metabolites levels revealed that the levels of major primary metabolites like amino acids, organic acids, sugars and alcohols in *acs2-1* mutant leaves were significantly different compared to WT and *acs2-2* mutant leaves respectively **(Fig. 4.20A)**. PCA analysis of primary metabolites corresponding to leaves of WT and mutants (*acs2-1*, *acs2-2*), revealed that the primary metabolites of mutant leaves show different patterns compared to WT **(Fig. 4.20B)**.

4.2.16 *acs2-1* mutant shows accelerated fruit ripening and senescence

Traditionally, on-vine ripening of tomato fruit is categorized into four distinct phases; mature green (MG), turning (TUR) characterized by development of red color at the distal end of fruit, red ripe (RR), and fruit senescence/abscission (FA). The effect of *acs2-1* and *acs2-2* mutations on the on-vine developmental process of fruits was monitored by measuring the size of fruits from the date of anthesis till red ripe stage. While the *acs2-1* fruits exhibited smaller in size compared to WT fruit **(Fig. 4.21A),** the *acs2-2* fruits size was little larger to WT fruits **(Fig. 4.21B)**. During on-vine ripening of

acs2-1 and WT fruits, the transition between different stages of ripening were recorded by visual observation of fruit color development. The *acs2-1* mutation affected all transition phases of ripening as a result the fruits showed early ripening and senescence **(Fig. 4.22)**. In contrast, the *acs2-2* mutant fruits exhibited a significant delay in fruit ripening and senescence. Both *acs2-2* and WT fruits reached breaker stage at almost same time (39-40 DPA) **(Fig. 4.23B)**. In contrast *acs2-1* mutant fruits attained breaker (32 DPA) stage 7-8 days earlier then WT fruit. After breaker stage, transition to subsequent ripening stages was slower in *acs2-2* mutant fruits compared to wild type and *acs2-1* fruits. The wild type fruits attained red ripe stage in 9-12 days while during same time interval *acs2-2* fruits reached only to orange stage and required additional 8-10 days to reach the fully red ripe stage **(Fig. 4.23A, B)**. In contrast, the *acs2-1* mutant fruits attained red ripe stage within 4-5 days from breaker stage **(Fig. 4.23A, B)**. In total, post-breaker stage, *acs2-1* fruit attained the red ripe stage in five days.

Apart from the accelerated ripening, the *acs2-1* mutation also affected the senescence process of fruit. The on-vine fruit senescence was significant faster in *acs2-1* mutant compared to WT and *acs2-2* fruits. The *acs2-1* mutant fruits stayed on vine 10-15 days after attaining red ripe stage, while WT fruits remained on vine for 20-25 days from the red ripe stage **(Fig. 4.22)**. Contrastingly, *acs2-2* fruits stayed on-vine for a longer duration of 35-45 days from the red ripe stage without a visible sign of senescence **(Fig. 4.22)**. Above results indicated that the *acs2-1* mutation accelerated both onset of ripening and senescence of fruits, and *acs2-2* mutation delayed fruit ripening.

4.2.17 The *acs2-1* mutant shows higher ethylene emission and reduced firmness of fruits

Comparison of ethylene emission showed a distinct influence of *acs2-1* and *acs2-2* mutation during the fruit ripening. In general, ethylene emission gradually increases from the MG to TUR (turning) and then gradually declines in subsequent ripening stages. At MG stage in WT and mutant fruits, the ethylene emission was nearly similar except at the turning stage and red ripe stage of fruits **(Fig. 4.24A)**. At the turning stage, *acs2-1* fruits emitted a very high amount of ethylene compared to WT and *acs2-2* fruits. However, at RR stage ethylene emission declined and was slightly higher than WT. It is likely that increased ethylene emission at the turning stage of *acs2-1* fruits may be related to its accelerated ripening features. On the other hand, *acs2-2* fruits released lower ethylene emission then WT at TUR and at RR stages.

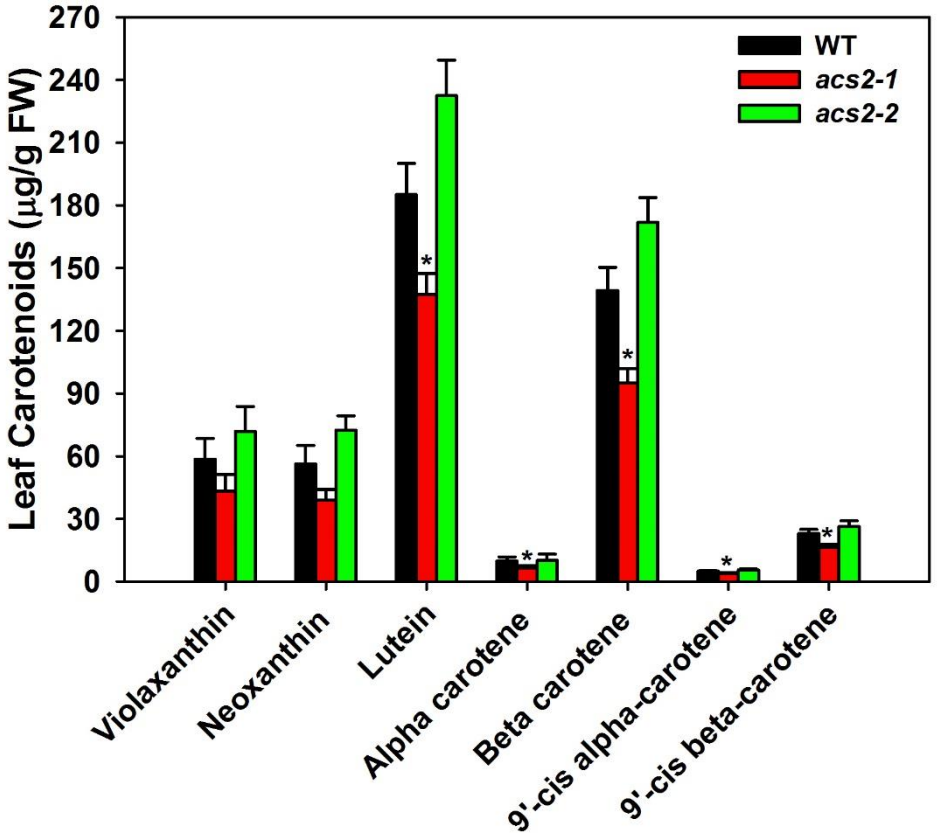

Figure 4.18. Carotenoids and xanthophylls levels in leaf tissues of *acs2-1*, *acs2-2* mutants and wild type. (Student's t-test; * for P ≤ 0.05, ** for P ≤ 0.01 and *** for P ≤ 0.001, for carotenoid estimation, sample number, n= 5 ± SE).

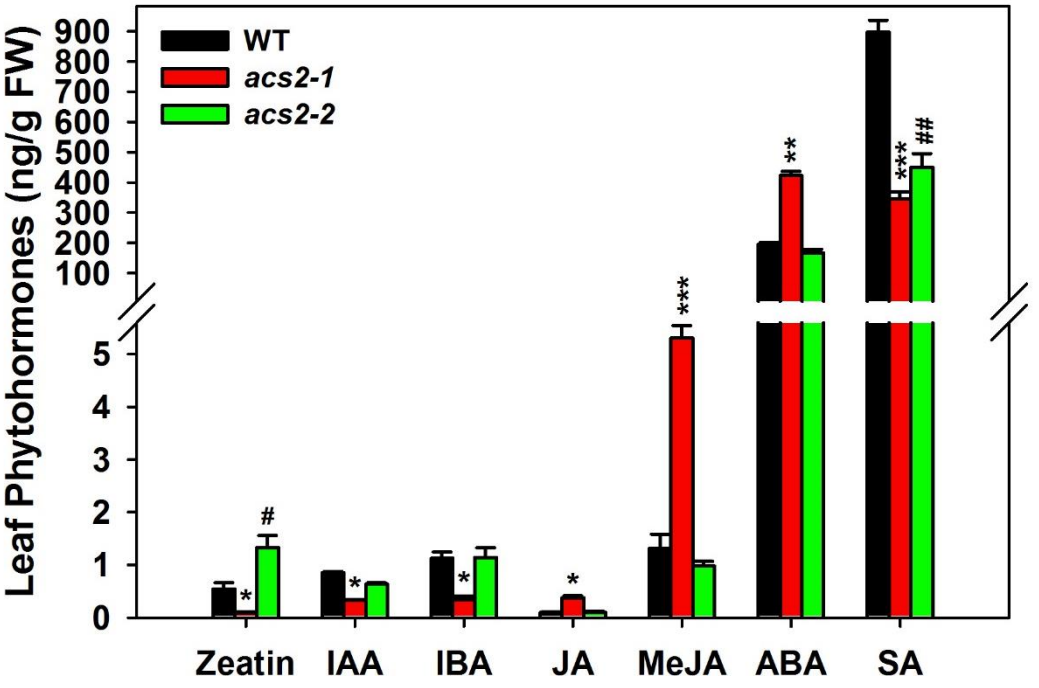

Figure 4.19. Phytohormones profiling of leaf tissue of WT, *acs2-1* and *acs2-2* mutants. Hormones were determined in 5 independent samples for each line. Quantification was done by the using calibration for each of the seven unlabeled hormones (SA, ABA, JA, MeJA, IAA, IBA, and Zeatin). (Student's t-test; *, # for P ≤ 0.05, **, # # for P ≤ 0.01 and *** for P ≤ 0.001).

Table 4.4 List of primary metabolites extracted from Leaf and Fruit tissue of tomato.

A. Leaf metabolites

Amino acids	Organic acids	Fatty acids	Sugars	Miscellaneous
I-alanine	Lactic acid	Pentanoic acid	Erythronic acid	Ethylene glycol
L-Valine	Glycolic acid	Myristate	Lyxofuranose	Propane-1,3-diol
Isoleucine	Pyruvic acid	Palmitic acid	Xylose,(anti)	Glycerol
Proline	Oxalic acid	Margarate	Xylose,(syn)	Hydroxylamine
Glycine	Benzoic acid	Linoleic acid	Arabinose	Uracil
Serine	Phosphoric acid	à-Linolenic acid	Ribose	Phenyl ether
L-Threonine	Nicotinic acid	Stearic acid	Levoglucosan	18-O-Feruloyloxyoctadec-9-enoic acid
L-Aspartic acid	Maleic acid	Arachidic acid	Tagatofuranose,(iso 2)	Threonic acid
L-Proline-5-oxo	Succinic acid	Borate	Ribonic acid	Hydroxypyridine
GABA	Glyceric acid	Dehydroabietic acid	Psicofuranose,(iso 2)	Thymol-á-d-glucopyranoside
Glutamic acid	Fumaric acid		Fructose,(anti)	UN1
Phe Alanine	Malic acid		Fructose,(syn)	UN2
L-Tyrosine	(E)-Aconitic acid		Mannose,(E)	UN3
L-Ornithine	Phosphoric acid,der		Galactose,(E)	UN4
	Isocitric acid		Glucose,(E)	UN5
	Citric acid		Mannose,(Z)	UN6
	2-Ketogluteric acid		Galactose,(Z)	UN7
	Cinnamic acid		Glucose(Z)	UN8
			Glucopyranose	UN9
			Sucrose	UN10
			Myo-Ionositol	

B. Fruit metabolites

Amino acids	Organic acids	Fatty acids	Sugars	Miscellaneous
ACC	Lactic acid	Pentanoic acid	Erythronic acid	Cyclopentenol
Acetyl glycine	Caproic acid	Nonanoic acid	Lyxose	Ethylene glycol
I-alanine	Glycolic acid	Myristate	Lyxofuranose	Propane-1,2-diol
L-Valine	Pyruvic acid	Palmitic acid	Xylose,(anti)	Propane-1,3-diol
Leucine	Oxalic acid	Margarate	Gluconic acid	Glycerol
Isoleucine	Malonic acid	Linoleic acid	Xylose,(syn)	1-Dodecanol
Proline	Benzoic acid	Oleic acid	Arabinose	Meso-erythritol
Glycine	Pipecolic acid	à-Linolenic acid	Arabinofuranose	Phloroglucinol
Serine	Phosphoric acid	Stearic acid	Ribose	
L-Threonine	Nicotinic acid	Arachidic acid	Levoglucosan	Ethylbisamine
b-Alanine	Maleic acid	Docosanoic acid	Rhamnose,(anti)	1-Propanamine
Pyroglutamic acid	Succinic acid	Octadecatrienoic acid	Tagatofuranose,(iso 2)	Hydroxylamine
L-Methionine	Methyl Succinic acid	Borate	Ribonic acid	Ethyl amine
L-Aspartic acid	Glyceric acid		Psicofuranose,(iso 2)	Cadaverine
L-Proline-5-oxo	Fumaric acid		Fructopyranose,(iso 2)	Uracil
GABA	Methylmaleic acid		Fructose,(anti)	Uridine
L-Cystene	Pipecolinic acid		Fructose,(syn)	Adenosine
Glutamic acid	Itaconic acid		Mannose,(E)	Phenyl ether
Phe Alanine	Malic acid		Galactose,(E)	18-O-Feruloyloxyoctadec-9-enoic acid
L-Asparagine	Parabanic acid		Glucose,(E)	Morpholine
I-Glutamine	2-Pyrrolidone-5-carboxylic acid		Mannose,(Z)	Threonic acid
L-Tyrosine	L-(+)-Tartaric acid		Galactose,(Z)	Hydroxypyridine
L-Ornithine	(E)-Aconitic acid		Glucose(Z)	Thymol-á-d-glucopyranoside
	Phosphoric acid,der		Gulonic acid	UN1
	Isocitric acid		Glucopyranose	UN2
	Citric acid		N-Acetyl-D-Glucosamine	UN3
	2-Ketogluteric acid		Galacturonic acid	UN4
	Isocitric acid lactone		Fructose-6-phosphate	UN5
	L-Ascorbic acid		Sucrose	UN6
	Cinnamic acid		Myo-Ionositol	UN7

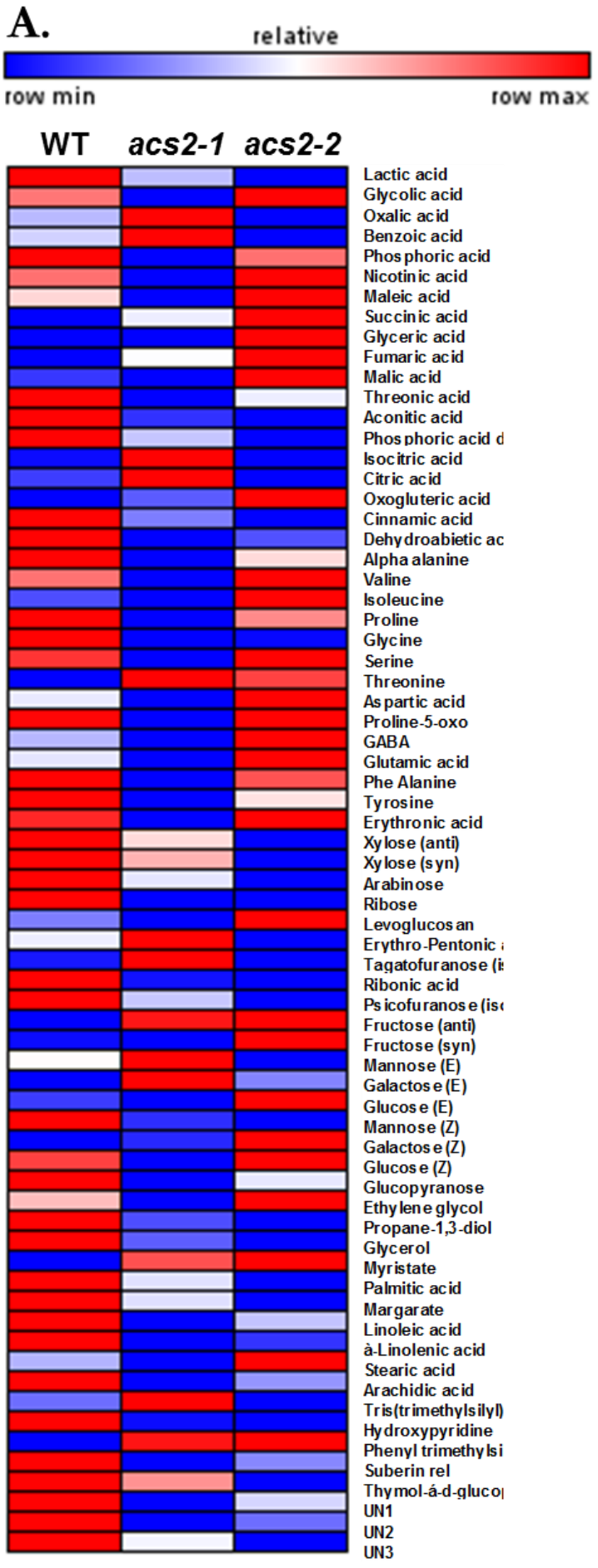
A.
relative
row min
row max
WT
acs2-1
acs2-2
Lactic acid
Glycolic acid
Oxalic acid
Benzoic acid
Phosphoric acid
Nicotinic acid
Maleic acid
Succinic acid
Glyceric acid
Fumaric acid
Malic acid
Threonic acid
Aconitic acid
Phosphoric acid d
Isocitric acid
Citric acid
Oxogluteric acid
Cinnamic acid
Dehydroabietic ac
Alpha alanine
Valine
Isoleucine
Proline
Glycine
Serine
Threonine
Aspartic acid
Proline-5-oxo
GABA
Glutamic acid
Phe Alanine
Tyrosine
Erythronic acid
Xylose (anti)
Xylose (syn)
Arabinose
Ribose
Levoglucosan
Erythro-Pentonic
Tagatofuranose (i
Ribonic acid
Psicofuranose (is
Fructose (anti)
Fructose (syn)
Mannose (E)
Galactose (E)
Glucose (E)
Mannose (Z)
Galactose (Z)
Glucose (Z)
Glucopyranose
Ethylene glycol
Propane-1,3-diol
Glycerol
Myristate
Palmitic acid
Margarate
Linoleic acid
à-Linolenic acid
Stearic acid
Arachidic acid
Tris(trimethylsilyl)
Hydroxypyridine
Phenyl trimethylsi
Suberin rel
Thymol-á-d-glucop
UN1
UN2
UN3

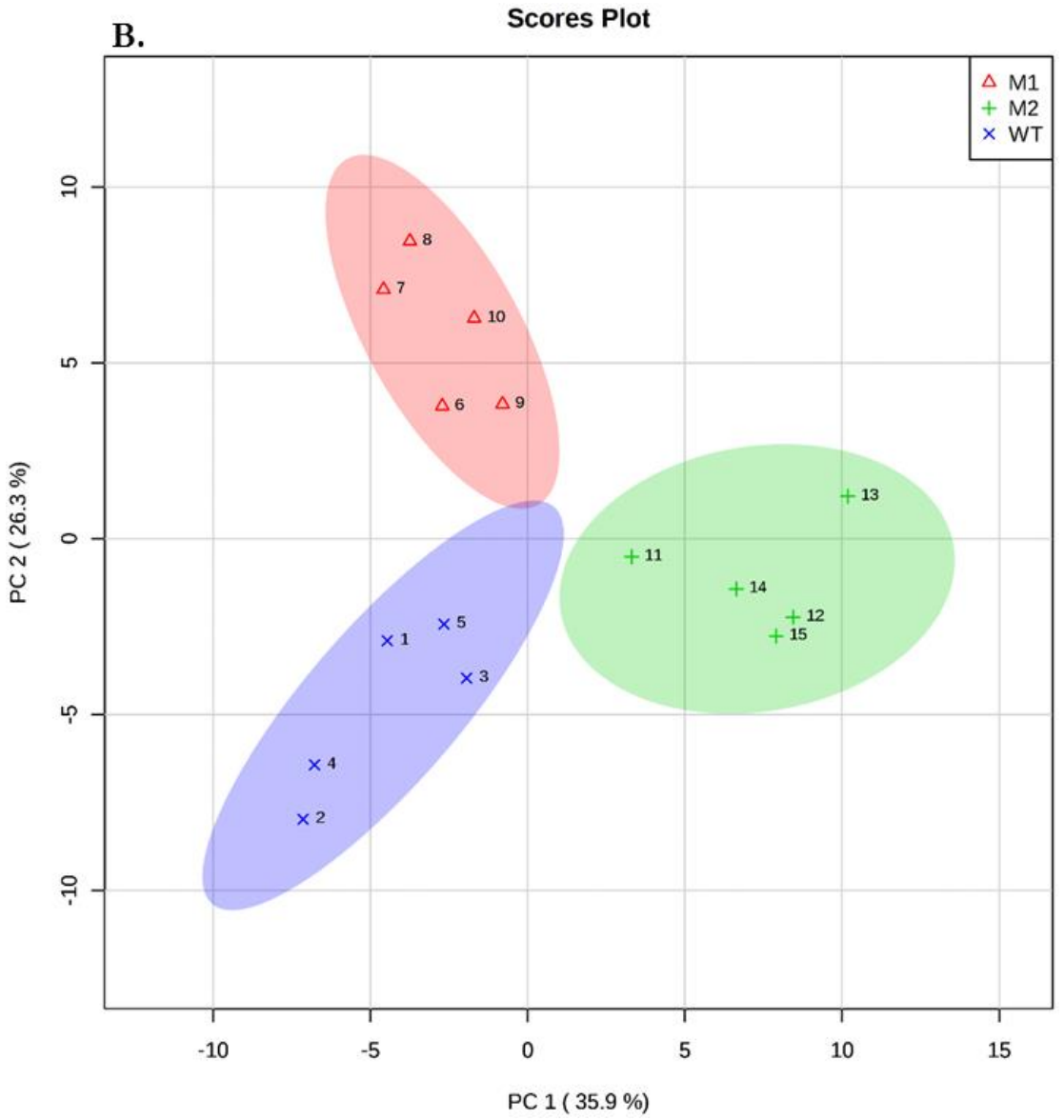

Figure 4.20. Primary metabolite profiling of leaf tissue. **(A)** Heat map representing the difference in metabolites level in different biological replicates (1-15) of leaf tissue of WT (M82) and mutants (*acs2-1*, *acs2-2*). Blue color corresponds to low level while red color denotes high level of particular metabolite. **(B)** Principal component analysis (PCA) score plot for metabolites levels in different biological replicates (1-15) of leaf tissue of WT (M82) and mutants (*acs2-1*, *acs2-2*). Metabolites of different leaf tissue were analyzed and the correlation variances explained by the PC1 and PC2 components are 35.9% and 26.3% respectively. Blue ellipse represents WT while red ellipse represents *acs2-1* and green ellipse corresponds to *acs2-2* mutant. In figures, M1 represents *acs2-1* mutant leaves and M2 represents *acs2-2* mutant leaves.

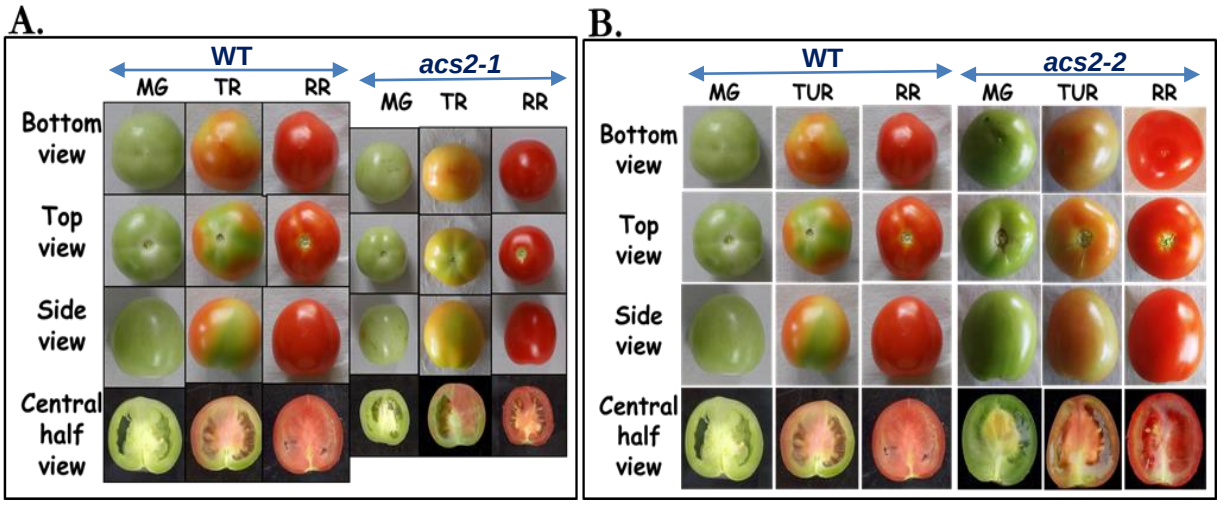

Figure 4.21. Comparisons of morphology of WT and mutant (*acs2-1, acs2-2*) fruits at different maturity stages. Fruits were harvested from the second truss of the vine. The transition between different stages of ripening was visually monitored by the changes in fruit color.

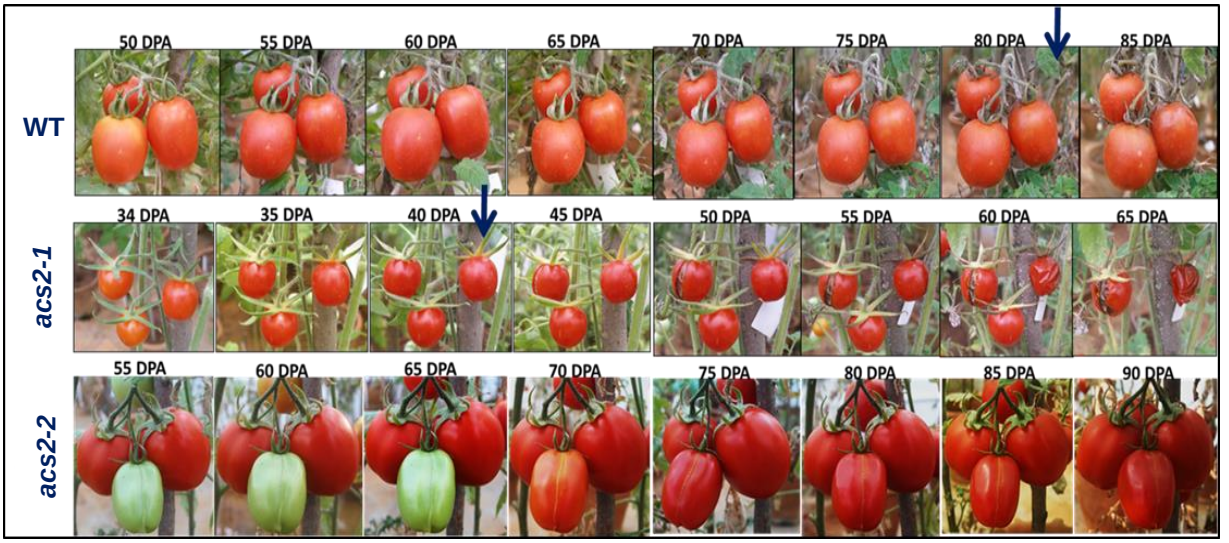

Figure 4.22. On-vine fruit ripening and senescence of wild-type (M82), *acs2-1,* and *acs2-2* mutants. Photographs were taken at a five-day interval to depict fruit ripening and senescence of second fruit truss. The transition between different stages of ripening was visually monitored by the changes in fruit color. To precisely determine the age of fruits, flowers were tagged at anthesis and this time point was considered as zero DPA (Days Post Anthesis). Pictures were taken from mature green + four days stages. Blue arrow mark indicates the day when cracking of fruits in *acs2-1* or rotting of fruits in WT started.

A.

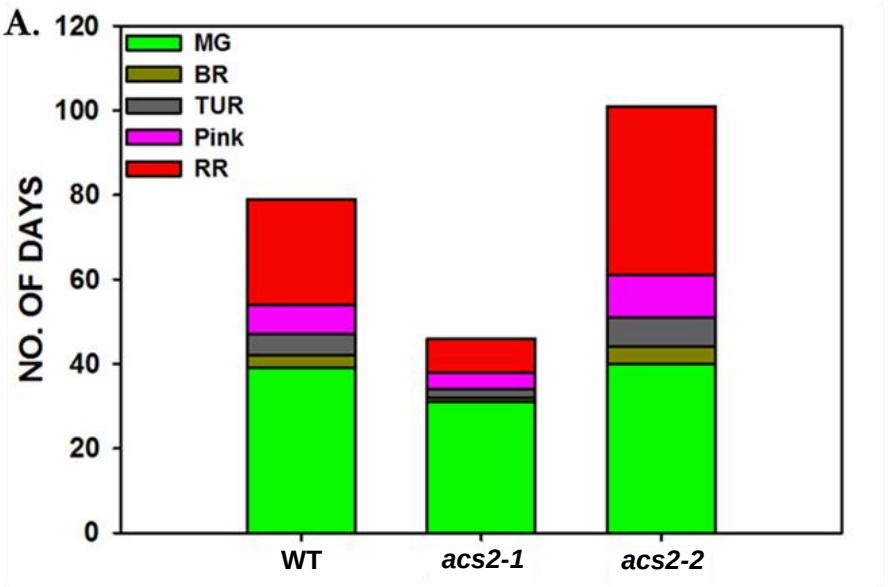

B.

Plant accession	No. of flowers/ truss	Total no. of flowers/ plant	Total no. of fruit set/truss	BR DPA	Pink DPA	RR DPA	No. of locules
WT	6-8	50-70	6-7	39	47	55	2-3
acs2-1	7-10	60-80	6-9	32	35	37	2-3
acs2-2	5-7	45-65	3-5	40	50	60	2-3

Figure 4.23. Comparison of ripening promotion of wild type and *acs2* mutant fruits. The fruit development was monitored on vine from post-anthesis (days post-anthesis - DPA) through different stages of ripening: mature green (MG), breaker (BR), Turning (TUR), Pink (P), red ripe (RR). The transition between different stages of ripening was visually monitored by the changes in fruit color. In addition to fruit ripening, no. of flower per truss, total no. of flowers per plant at a particular time point, total no. of fruit set per truss and no. of locules per fruit, was also monitored.

An important determinant of fruit quality is firmness. The impact of *acs2-1* and *acs2-2* mutation was also examined on the firmness of fruit during the ripening. On comparing the fruit firmness of WT and mutants, *acs2-2* fruits were firmer at MG, TUR and RR stage compared to WT fruits **(Fig. 4.24B)**. On the other hand, the *acs2-1* mutant fruits at TUR and RR stages were less firm compared to WT fruits. Nevertheless, the firmness of *acs2-1* mutant fruits at MG stage was similar to WT fruits **(Fig. 4.24B)**.

4.2.18 Mutation in *acs2-1* leads to increased ACC levels, ACS, and ACO activities

In plant ethylene synthesis is mediated by two enzymes ACC synthase (ACS) and ACO oxidase (ACO). The ACS generates ethylene precursor ACC from the S-Adenosine Methionine (SAM) and ACO oxidase coverts ACC to the final end-product ethylene (Yang and Hoffman, 1984). To determine whether increased ethylene production in *acs2-1* mutant fruits was associated with increased formation of ACC, its level was estimated in fruits at different maturity stages of WT, *acs2-1* and *acs2-2* mutant by a modified protocol of Bulens et al. (2011) **(Fig. 4.25)**. Consistent with the increased ethylene production, the in *acs2-1* mutant free ACC level increased by 1.5 fold compared to WT **(Fig. 4.25A)**. Above result indicated that increased ethylene production in *acs2-1* mutant fruits was likely due to increased level of ACC. Compared to *acs2-1* mutant, at RR stage the *acs2-2* mutant fruits exhibited two-fold decrease in free ACC level compared to WT fruits **(Fig. 4.25D)**.

Though the formation of ACC is the rate limiting step of ethylene biosynthesis, it is also regulated by changes in the amount of conjugated ACC, 1-malonylamino cyclopropane-1-carboxylic acid (MACC). In addition to the conversion of ACC to ethylene, a part of ACC is also converted to MACC by ACC N-malonyl transferase. To examine the relative conversion between ACC and MACC, the MACC level was measured in WT, *acs2-1*, and *acs2-2* mutant fruits. Consistent with the increased production of ethylene, the level of MACC also increased by two-fold in *acs2-1* fruits at RR stage compared to WT **(Fig. 4.25B)**. In contrast, the *acs2-2* mutant fruit exhibited half the level of MACC at RR stage compared to WT **(Fig. 4.25E)**. The total ACC content of fruits was determined by adding free ACC and MACC, displayed same trend. Here too, the level of total ACC in *acs2-1* mutant fruit was two-fold higher compared to WT **(Fig. 4.25C)**. Whereas, the total ACC level was half in *acs2-2* fruits compared to WT **(Fig. 4.25F)**.

The possibility that ACS2-1 mutant enzyme may more effectively convert SAM to ACC was also examined. Since *acs2-1* fruits emit increased ethylene, it could reflect

higher ACS2 activity and concentrations. Similarly *acs2-2* fruits emit less ethylene than WT perhaps due to reduced ACS2 activity. To ascertain this, ACS enzyme activity was estimated *in-vitro* in the fruits of WT and the mutants. Similar to increase in ethylene, ACS activity showed two-fold increase in the fruits of *acs2-1* mutant, whereas fruits of *acs2-2* mutant exhibited 50% lower ACS activity compared to WT **(Fig. 4.26A, B)**. Together these results suggest that *acs2-1* mutation likely affect the conversion of SAM to ACC through alteration of ACS enzyme.

We next examined whether increase in ACS activity also stimulates ACO activity in *acs2-1* mutant. ACO is the penultimate enzyme in the ethylene biosynthetic pathway, which convert ACC to ethylene. *In-vitro* ACO enzyme activity was measured using a modified protocol of Bulens et al. (2011). Interestingly, *acs2-1* mutant also showed a significant increase in ACO activity in fruits whereas *acs2-2* mutant fruits exhibit a slight decrease in ACO activity compared to WT fruits at different stages of ripening **(Fig. 4.26C, D)**.

4.2.19 Production of polyclonal antibodies specific for ACS2 peptide

The ACS2 specific peptide was identified and synthesized by a USA based company, PEPTIDE 2.0 **(Fig. 4.27A, B)**. The synthesized peptide with carrier protein was intramuscularly injected into an albino rabbit to raise antibodies against ACS2 peptide. After each booster dose, the titer value for antibody response was checked by a dot-blot assay. The assay showed that with every booster injection the titer of antibody increased in rabbit **(Fig. 4.27C-F)**. After 4th booster injection the antigen (2 µg) could be detected even with 1/50,000 dilution of antibody on dot blot. While dot blot are not specific for a particular antigen, and can have error. Nevertheless, the assay indicated that antibody titer, again identified ACS2 peptide, was higher after 4th booster dose.

4.2.20 Purification of antibody fractions and immunoprecipitation of ACS2 protein

The usage of crude enzyme preparation from tomato fruits without any purification did not reveal any ACS specific band on western blot from both WT and mutant. This could be due to possibility that ACS2 protein abundance in the crude extract of tomato fruit is very low and was below the limit of detection **(Fig. 4.28A)**. Considering this limitation, IgG and IgM fractions were purified from ACS2 antiserum by DEAE (Diethyl Amino Ethane) Sepharose CL-6B beads to further estimate the ACS2 antibody titer. To visualize the ACS2 protein specific bands on PVDF membrane, western blot analysis was performed using RR fruit crude extract. A clear protein bands of size 55 kDa, specific to ACS2 protein were detected on PVDF membrane using

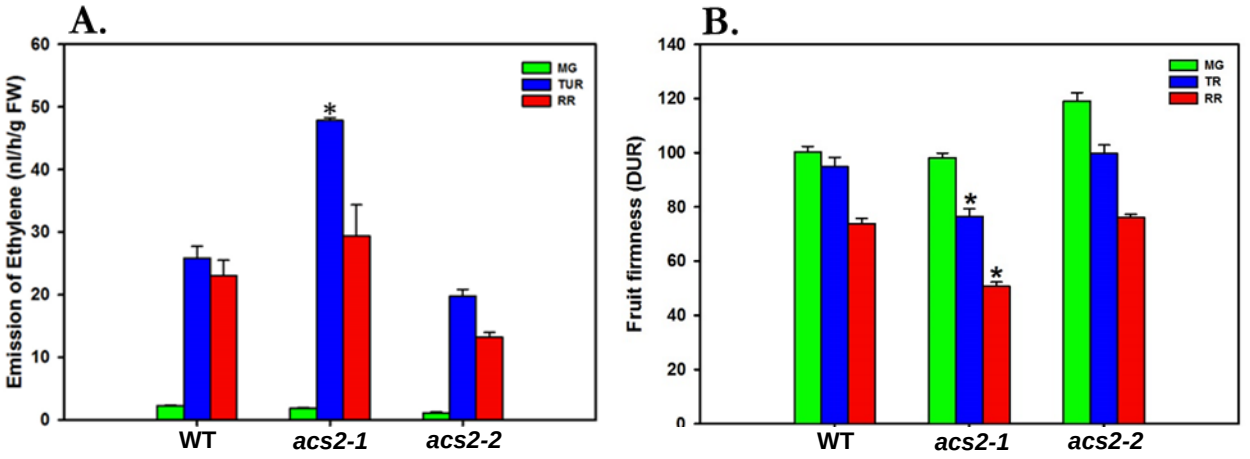

Figure 4.24. (A) Comparisons of the ethylene emission from fruits of wild type and mutants at different stages of ripening- mature green (MG), turning (TUR), red ripe (RR). The fruits of wild type and different mutant lines were harvested from the second truss of the vine and ethylene emission was determined as described in methods. Each value is the mean of three biological replicates. **(B)** Measurement of fruit firmness. The firmness of fruits was measured using Durofel DFT 100. Firmness value was recorded by measuring each fruit at equatorial plane two times. Three-four fruits of each wild-type (M82) and mutants were used for measurements. **Note:** 1 DUR unit is equal to 9 kg/cm^2 pressure.

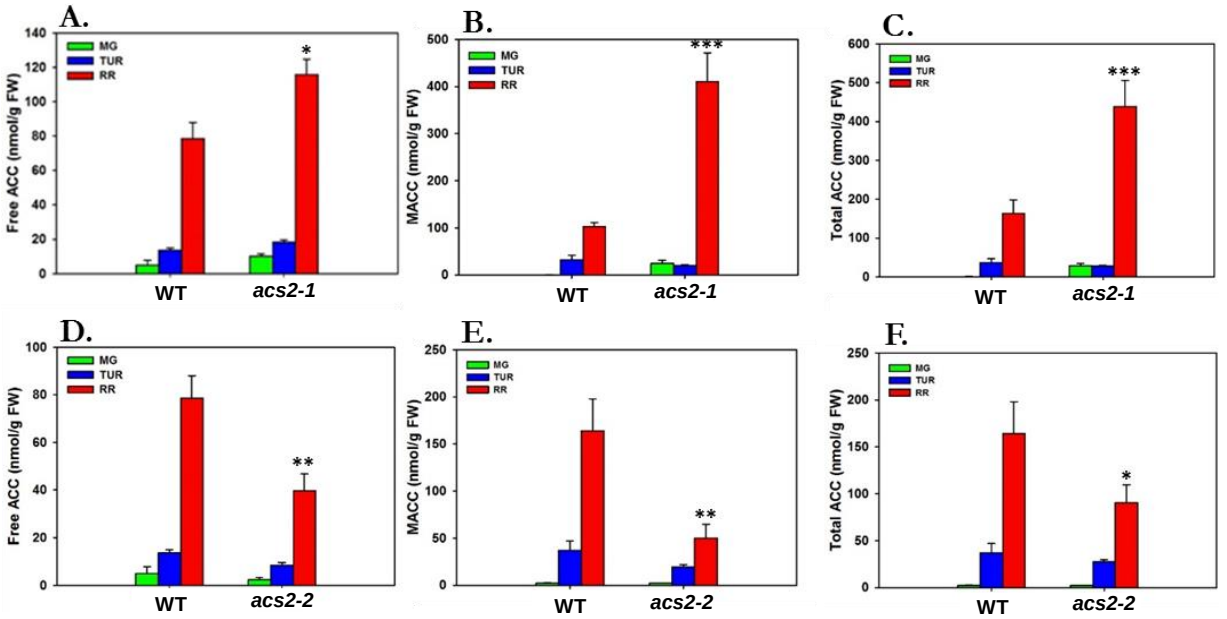

Figure 4.25. Estimation of 1-aminocyclopropane-1-carboxylic acid (ACC) in WT and mutant fruits at different stages of ripening. **A** and **D** represent amount of free ACC, **B** and **E** represent bound ACC in the form of MACC whereas **C** and **F** corresponds to total ACC in mature green, turning and red ripe fruits of WT and mutant respectively. (Student's t-test; * for P ≤ 0.05, ** for P ≤ 0.01 and *** for P ≤ 0.001, for each fruit maturity stage, n=3 ± SE).

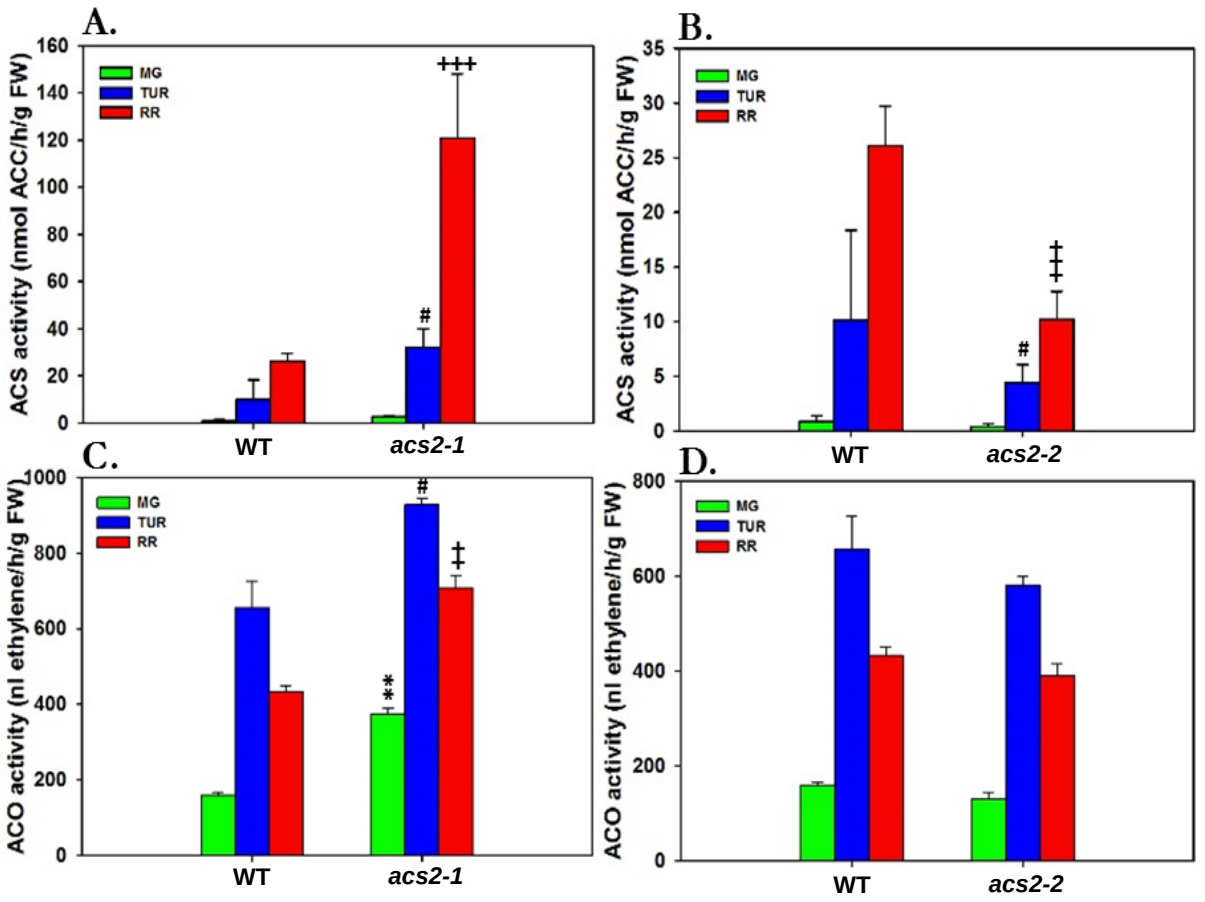

Figure 4.26. Determination of ACS and ACO enzyme activities in WT and mutant fruits. **A** and **B** represent ACS activity while **C** and **D** represent ACO activity. (Student's t-test; *, #, and + for P ≤ 0.05; **, ##, and ++ for P ≤ 0.01; and ***, ###, and +++ for P ≤ 0.001, for each fruit maturity stage, n=3 ± SE).

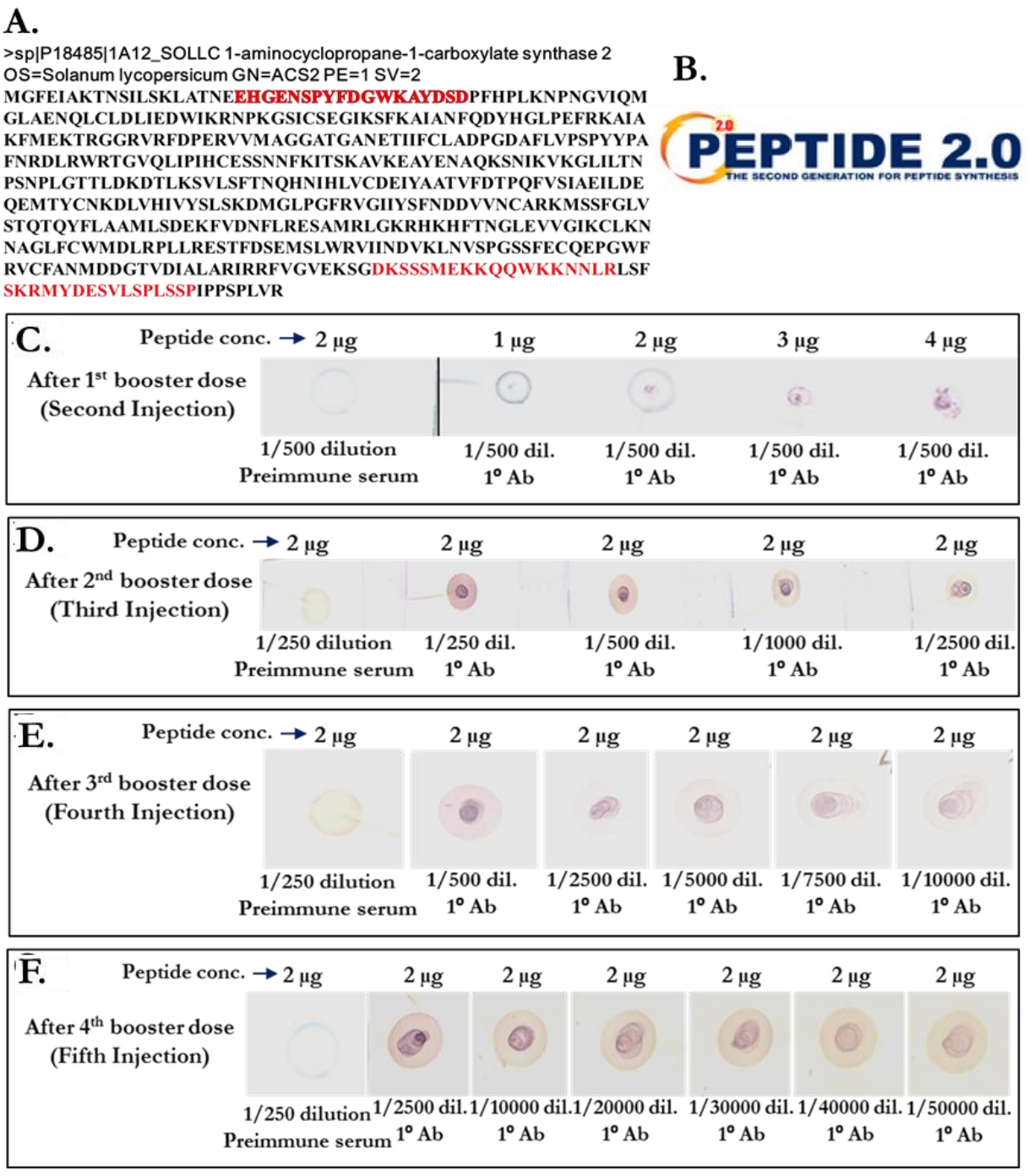

Figure 4.27. Production of polyclonal antibodies specific for ACS2 protein. Three antigenic peptides specific to ACS2 protein was predicted by PEPTIDE 2.0 **(A)**. Out of three peptides, N-terminal region peptide "EHGENSPYFDGWKAYDSD" specific to ACS2 protein was selected to be synthesized by PEPTIDE 2.0 **(B)**. Collected the polyclonal antisera after 1st, 2nd, 3rd, and 4th booster dose and checked for titer value by DOT BLOT assay **(C-F)**.

purified IgG fraction **(Fig. 4.28B)**. To check whether the antibody raised against ACS2 protein specifically reacted only to ACS2 protein, the immunoprecipitation (IP) of ACS activity was carried out. It is expected that in assay of ACS2 interacting with antibody, it can be precipitated by binding complex to protein-A Sepharose. The residual enzyme activity left in the supernatant was reflected the loss of ACS2 protein by binding to antibody. The effect of IP was compared by using preimmune serum and IgG fraction at different dilutions (1/25, 1/300 and 1/800). A maximum reduction in ACS activity was observed with IgG at 25 fold dilution. At higher dilution (1/800), ACS activity was similar to control. There was no effect of pre-immune serum at all dilutions **(Fig. 4.29)**.

Interestingly, a significant reduction in ACS activity (3 fold) was observed in the the supernatant of RR fruits of WT after pelleting the immunoprecipitates. In case of *acs2-1* the supernatent showed the 4 fold reduction in the activity after incubation with 25 fold diluted IgG and immunoprecipitation. Similarly the *acs2-2* mutant fruit extracts after immunoprecipitation showed 3 fold reduction in activity **(Fig. 4.29)**.

4.2.21 The *acs2-1* mutant RR fruits exhibit increased level of ACS2 protein

The immunoprecipitated ACS2 protein was denatured with SDS-PAGE sample loading buffer and subjected to Western blot analysis to check the levels of ACS2 protein in WT and mutant fruits (*acs2-1* and *acs2-2*). The blot showed no detectable ACS2 bands for MG and BR (TUR) fruits of mutants and WT. The intensity of ACS band in RR fruits was highest in *acs2-1* mutant compared to WT and *acs2-2* mutant **(Fig. 4.30A)**. The western analysis of serial dilutions of WT and mutants extracts from RR fruits indicated that the intensity of 5 µg protein band of *acs2-1* mutant was equal to 20 µg protein of WT. Therefore, the level of ACS protein in RR fruits of *acs2-1* mutant may be four times higher than the WT **(Fig. 4.30A-B)**. On the other hand, the serial dilutions indicated that the level of ACS protein in *acs2-2* mutant fruit was about one fourth compared to WT fruits **(Fig. 4.30A-C)**.

4.2.22 Genetic analysis confirmed that *acs2-1* is a recessive mutation

The *acs2-1* mutant (♂) was crossed with the parental WT M82 (♀), and the resultant F_2 progenies were analyzed for the pattern of segregation of *acs2-1* mutant loci and inheritance of the mutant phenotype. Genomic DNA from BC_1F_1 plants was subjected to mismatch-specific CEL I endonuclease assay for mutation **(Fig. 4.31)**. The morphological traits of BC_1F_1 like fruit size, fruit color, leaf color, and plant height were similar to WT (M82) phenotype **(Fig. 4.32)**. The BC_1F_2 progenies from the selfing of BC_1F_1 {*acs2-1* (♂) x WT (♀)} were examined for its segregation ratio of mutant versus

WT and heterozygous seedlings. The mutations were confirmed for BC_1F_2 plants by using CEL I mismatch assay, which involved analysis of two sets, the original genomic DNA isolated from each F_2 plant and the genomic DNA of F_2 plants mixed with WT parent DNA. Among these two sets only the sets with heteroduplexes would show the cut DNA fragments **(Fig. 4.33)**. Out of 140 BC_1F_2 lines screened, 29 plants were homozygous for *acs2-1* mutation, 61 plants were in heterozygous condition, and 30 plants were WT homozygous while remaining 20 plants were not confirmed due to failure of PCR reactions. The segregation ratio of F_2 plants was 1(WT): 2(Het): 1(mutant). The p-value for calculated (chi-square) $\chi 2$ (0.244) was $p = 0.62$, suggesting that the mutation is monogenic and segregating in 3(WT): 1(*acs2-1*) ratio **(Table 4.5, 4.6)**. The genotypic screening of mutant homozygous F_2 plants showed the true *acs2-1* progenies while the plants with WT phenotype showed both homozygous (WT) and heterozygous nature.

4.2.23 Co-segregation of F_2 (mutant homozygous) phenotype with genotype

4.2.23.1 The F_2 (M) plants exhibit accelerated fruit ripening and early senescence

As mentioned above the *acs2-1* mutation accelerates the on-vine ripening process of fruits. To ascertain genotype and phenotype co-segregation, the homozygous mutant fruits along with earlier reported WT control in section no. 4.2.16, F_2 (Mutant) plants were analyzed for on-vine fruit ripening. The F_2 (M) fruits exhibited comparatively similar diameter to *acs2-1* mutant fruit **(Fig. 4.34)**. During the on-vine ripening the transition between different stages of ripening of F_2 (M) fruits were recorded by visual observation of fruit color development. The F_2 (M) fruits showed early ripening and as well as senescence of fruit similar to parental *acs2-1* fruits **(Fig. 4.35)**. The on-vine fruit senescence process was significantly early in F_2 (M) compared to WT fruits. The F_2 (M) fruits stayed on vine 11-16 days after attaining red ripe stage that was almost similar to *acs2-1* fruits **(Fig. 4.35)**.The F_2 (M) mutant fruit attained turning stage earlier than the WT fruit (33 DPA). The F_2 (M) fruits also attained red ripe stage within four to five days from TUR stage **(Fig. 4.36A, B)**. In total, post-turning stage, F_2 (M) fruit attained the red ripe stage in four days. These results indicated that the F_2 (M) fruits showed an accelerated onset of ripening and faster senescence like parental *acs2-1* fruits.

4.2.23.2 The F_2 (M) plants exhibit an increase ethylene emission and lesser firmness of fruits

At the turning stage, the F_2 (M) fruits emitted higher amount of ethylene similar to the earlier reported parent *acs2-1* fruits. It is likely that increased ethylene emission at the turning stage of F_2 (M) and parent *acs2-1* fruits may be correlated with accelerated

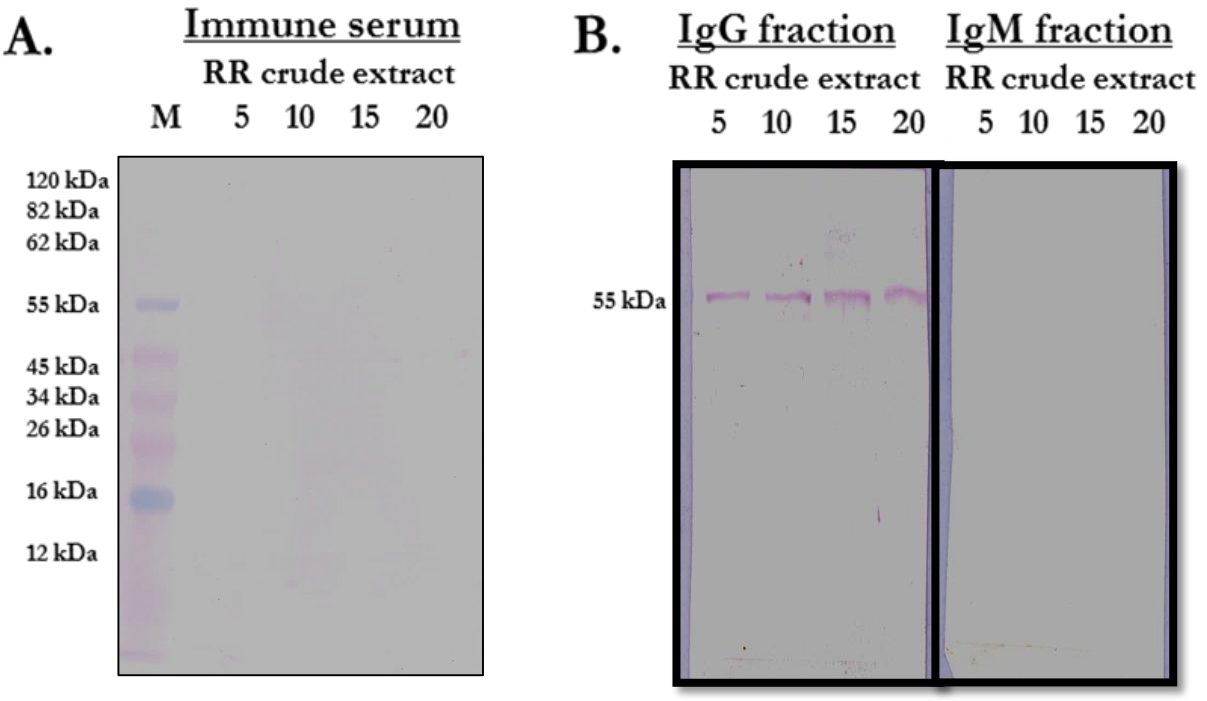

Figure 4.28. Western blot from ACS2 antiserum and purified polyclonal IgG and IgM fractions. **(A)** Different concentration (5-20 µg) of crude extract of RR fruits of WT (M82) was loaded on gel with protein marker (M) and western blot assay was performed by immune serum. **(B)** Purification of IgG and IgM isotype was carried out on DEAE (Diethyl Amino Ethane) Sepharose CL-6B chromatography (weak anion exchanger). Analyzed the different fractions of Igs obtained after elution for the specificity of the ACS2 protein by western blot. On 12% SDS-PAGE gel different concentration (5-20 µg) of crude extract of RR fruits of WT (M82) was loaded and confirmed the ACS2 specific bands of 55 kDa using molecular weight size marker, by IgG and IgM fractions by western blot.

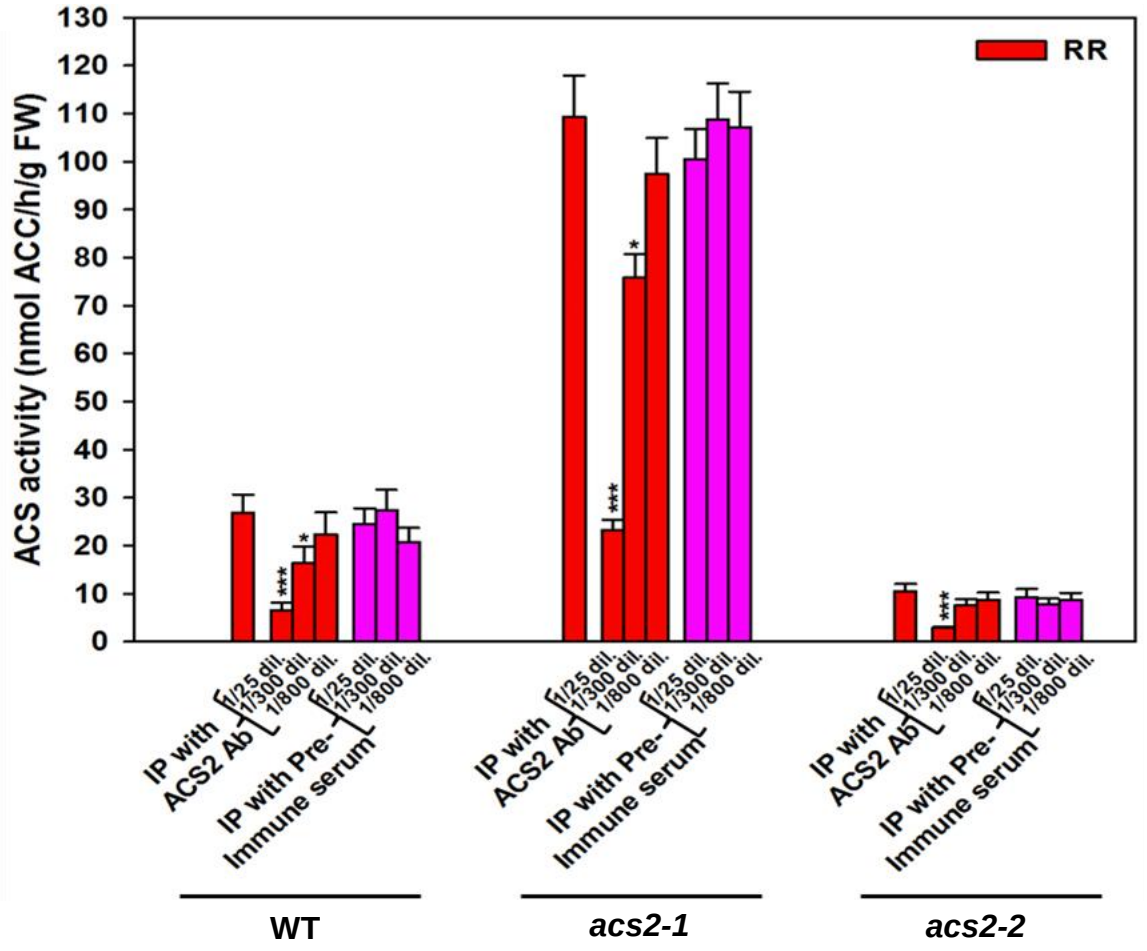

Figure 4.29. Immunoprecipitation (IP) of ACS2 protein from the enzyme extract by polyclonal IgG fractions of ACS2 antiserum. ACS activity in the RR fruits of WT and mutants was determined. Immunoprecipitation of ACS protein was carried out by different dilutions of IgG antibodies (1/25, 1/300 and 1/800) and protein-A Sepharose beads. After pelleting of antigen-antibody complex the supernatants were analyzed for the ACS activity. (Student's t-test; * for $P \leq 0.05$, ** for $P \leq 0.01$ and *** for $P \leq 0.001$, for each fruit maturity stage, n=3 ± SE).

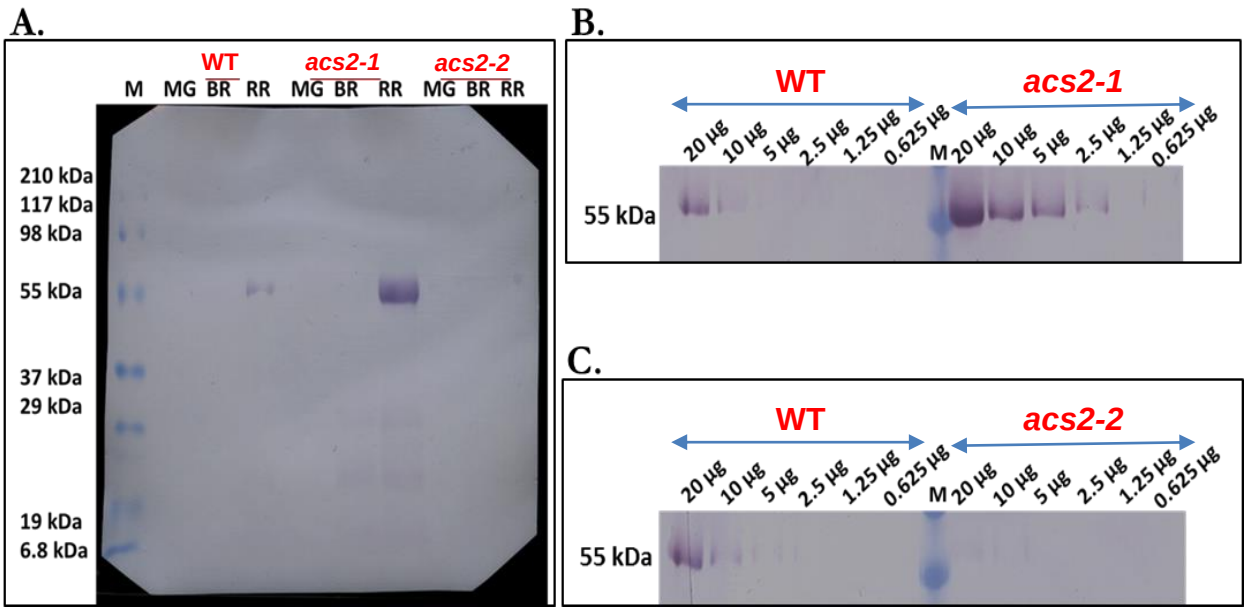

Figure 4.30. Western blot analysis of immunoprecipitated ACS2 protein at different stages of tomato fruit ripening. **(A)** IgG-mediated, immunoprecipitated ACS2 protein content was quantified by Bradford's assay. An equal amount (20 µg) of IP proteins from different maturity stages of tomato fruits of WT and mutants after boiling in SDS-PAGE buffer was loaded on 12% SDS-PAGE gel. To check the ACS2 protein levels at RR stage in WT and mutants (*acs2-1*, *acs2-2*), the IP proteins were serially diluted and western blot analysis was carried out **(B-C)**.

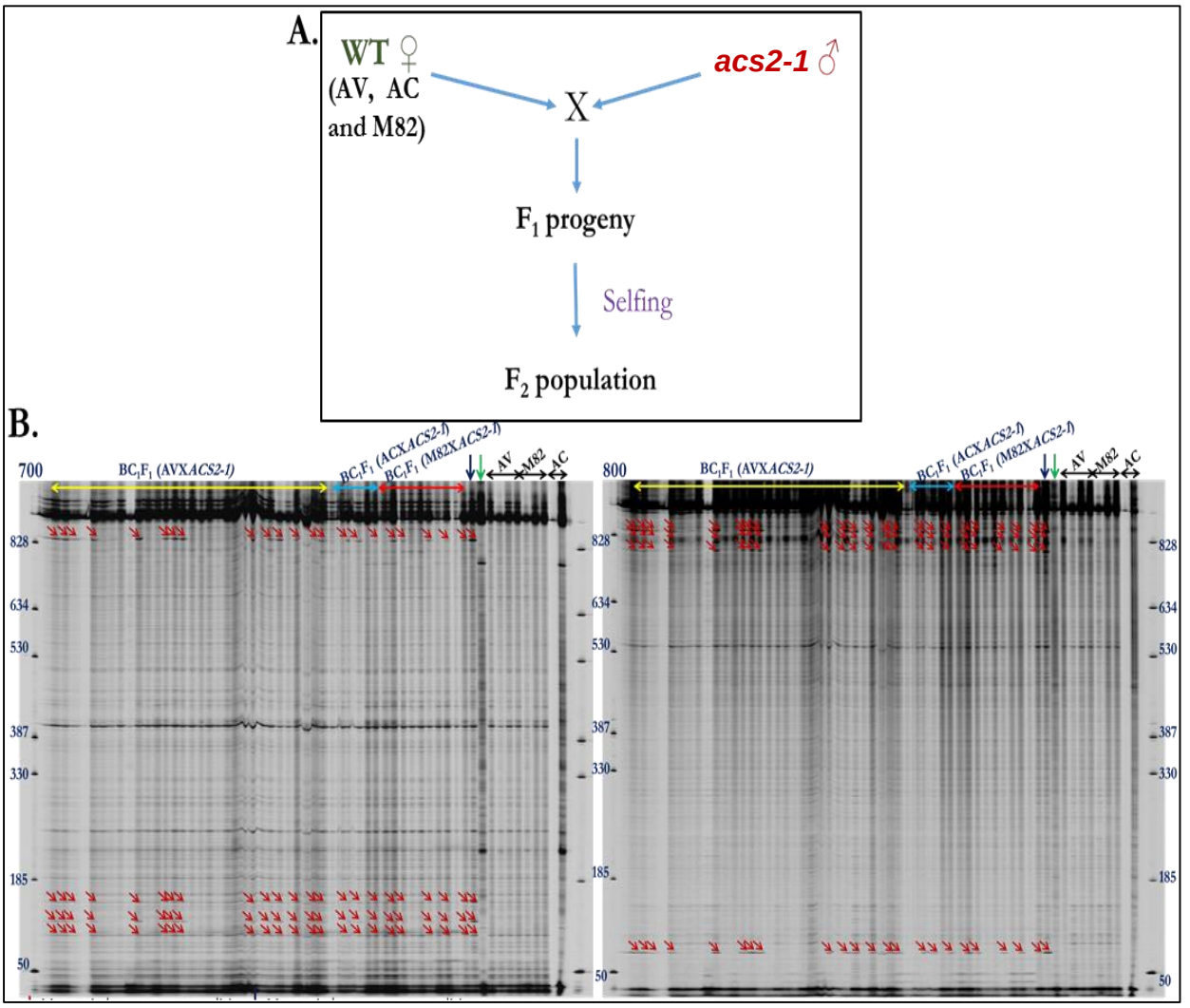

Figure 4.31 (A). Schematic representation of backcross of *acs2-1* mutant and **(B)** Confirmation of mutation in BC_1F_1 plants on Li-COR gel. Amplified and digested one Kb PCR product using end labelled (IR dye) Subset I of Set II primers **(Table 3.2)** of F_1 plants, mutant (*acs2-1*) and WT (AV, AC, and M82) was loaded on Li-COR gel. The cut fragments at 700 channel for mutation were approximately 90 bp, 140 bp, 170 bp, and 930 bp respectively whereas at complementary 800 channel were 70 bp, 830 bp, 860 bp, and 910 bp respectively, represented by red arrow heads. The lanes indicated by blue and green arrow heads represents the *acs2-1* mutations in heterozygous and in homozygous condition respectively.

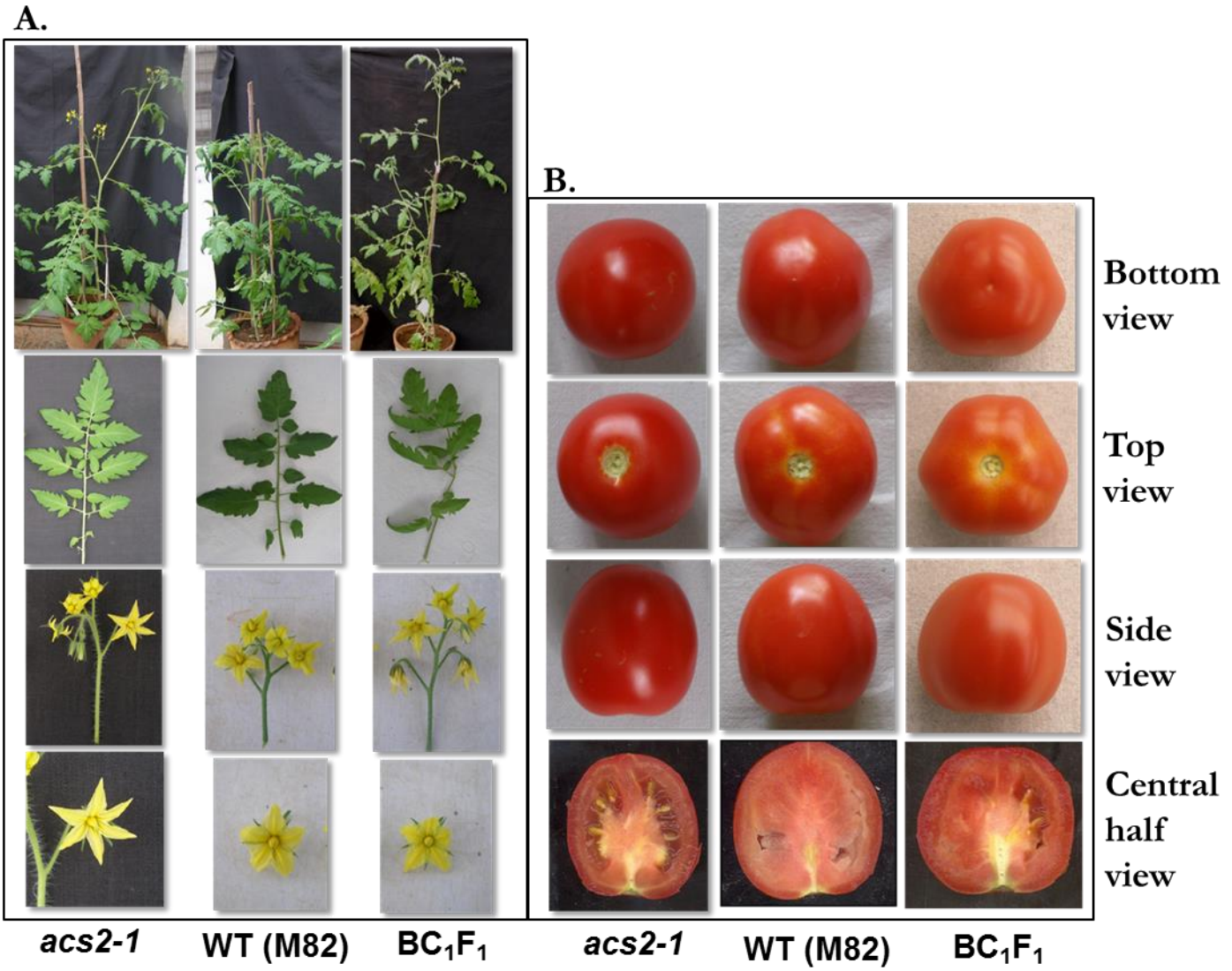

Figure 4.32 (A-B). Comparisons of plant phenotype (45 days old), leaf morphology, flower and fruit phenotype of WT, *acs2-1* mutant and BC_1F_1 plants. Leaves were taken from the 7th node of the wild-type and mutant plants (45 days old). Flower inflorescence and fruits were taken from the second truss of the 90 days old tomato vine for comparisons. The bottom, side top and cut halves of fruits are shown.

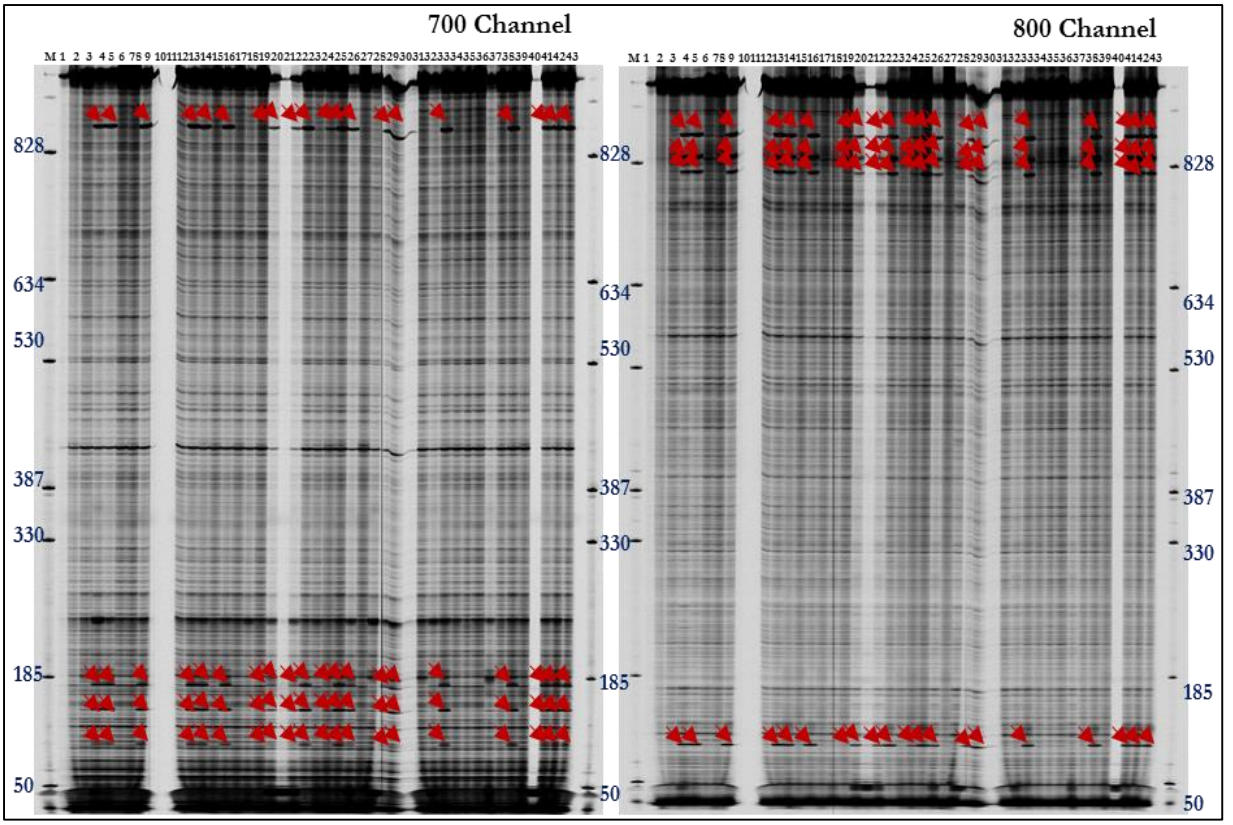

Figure 4.33. Confirmation of mutation in BC_1F_2 plants on Li-COR gel. The CEL I digested one Kb PCR product (using Subset I of Set II primers) **(Table 3.2)** amplified from genomic DNA of BC_1F_2 plants, mutant (*acs2-1*) and WT (M82) plants was loaded on Li-COR gel. The cut fragments at 700 channel for mutation were approximately 90 bp, 140 bp, 170 bp, and 930 bp respectively whereas at complementary 800 channel were 70 bp, 830 bp, 860 bp, and 910 bp respectively, represented by red arrow heads. M represents molecular weight ladder, lane 2 corresponds to WT (M82) sample, and lane 3 corresponds to mutant homoduplex. Lane no. 4, 5, 8, 12, 13, 15, 18, 19, 21, 22, 24, 25, 26, 29, 30, 34, 40, 43, 44, and 45 corresponds to heteroduplex digested PCR product of BC_1F_2. Remaining lanes do not show any mutations.

Table 4.5 BC_1F_2 segregation ratio.

Crosses	F_2 population size	Mutant (Homozygous)	Heterozygous	WT (Homozygous)	Not confirmed	χ^2	P-Value
WT (M82) ♀ X *ACS2-1*♂	**140**	**29**	**61**	**30**	**20**	**0.244 (1:3) 0.254 (1:2:1)**	**0.62 (1:3) 0.88 (1:2:1)**

Table 4.6 Table for calculation of chi-square value.

df	$\chi^2_{.995}$	$\chi^2_{.990}$	$\chi^2_{.975}$	$\chi^2_{.950}$	$\chi^2_{.900}$	$\chi^2_{.100}$	$\chi^2_{.050}$	$\chi^2_{.025}$	$\chi^2_{.010}$	$\chi^2_{.005}$
1	0.000	0.000	0.001	0.004	0.016	2.706	3.841	5.024	6.635	7.879
2	0.010	0.020	0.051	0.103	0.211	4.605	5.991	7.378	9.210	10.597
3	0.072	0.115	0.216	0.352	0.584	6.251	7.815	9.348	11.345	12.838
4	0.207	0.297	0.484	0.711	1.064	7.779	9.488	11.143	13.277	14.860
5	0.412	0.554	0.831	1.145	1.610	9.236	11.070	12.833	15.086	16.750

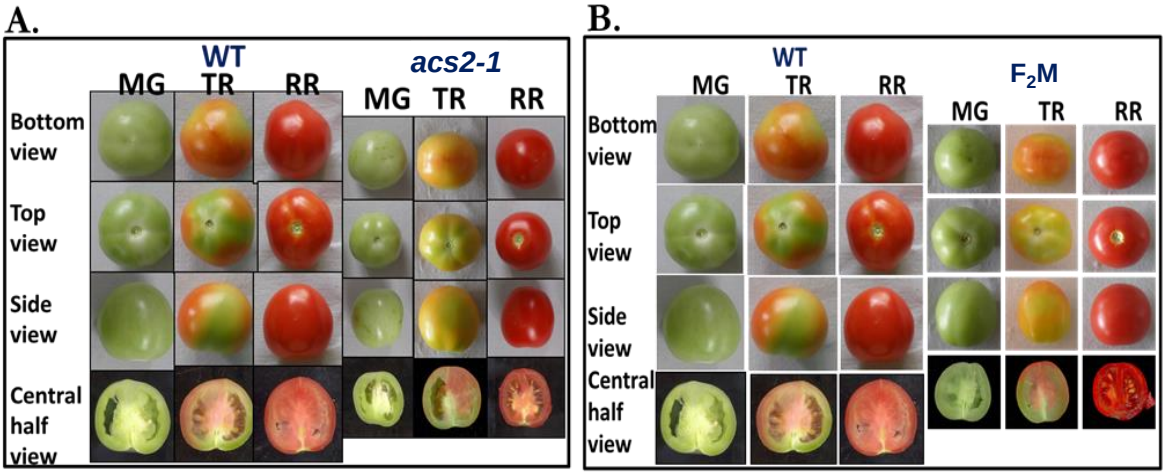

Figure 4.34 (A-B). Comparison of variations in fruit morphology between wild-type, mutant and F_2 (M). Fruits were harvested from the second truss of the vine. The transition between different stages of ripening was visually monitored by the changes in fruit color.

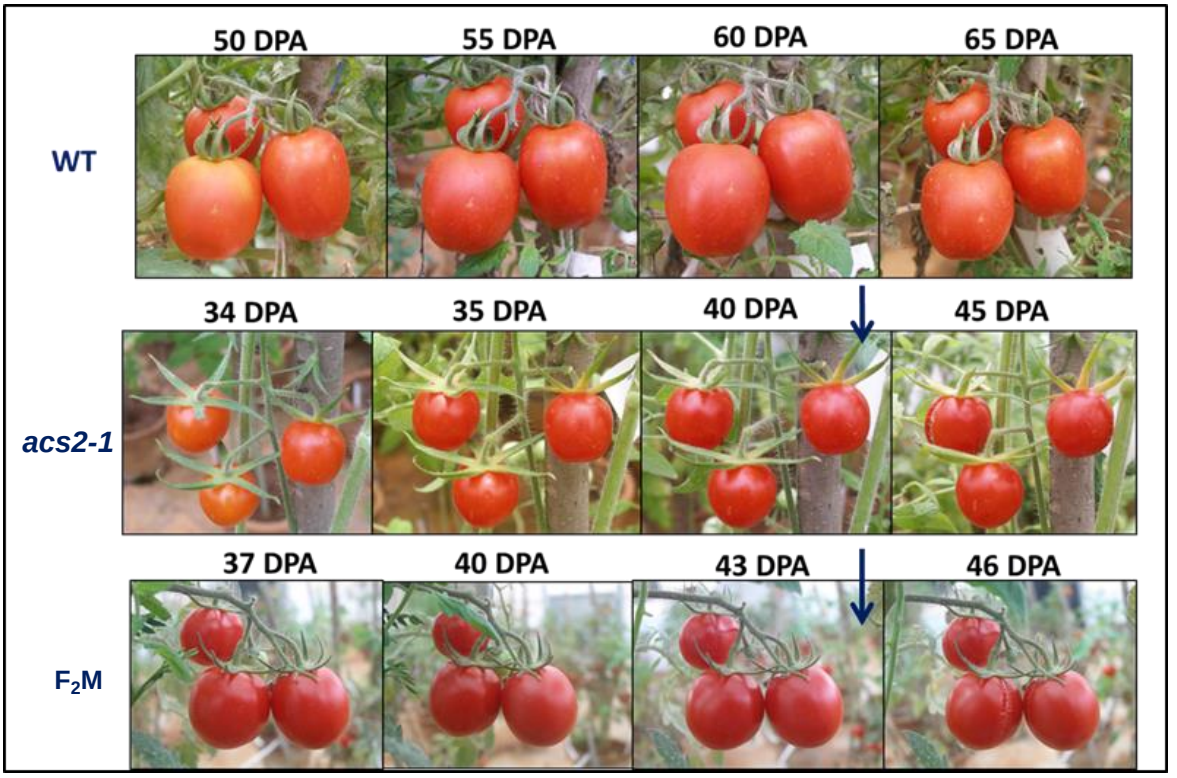

Figure 4.35. On-vine fruit senescence study. For on-vine fruit senescence study we have selected second fruit truss of reported parent wild type (M82), reported parent mutant (*acs2-1*) and F_2 (M) respectively in greenhouse grown tomato plants. Pictures were taken from orange/pink stages. The blue arrow heads represented the days (42 DPA in *acs2-1* mutant and 44 DPA in F_2M) on which cracking of fruits initiated.

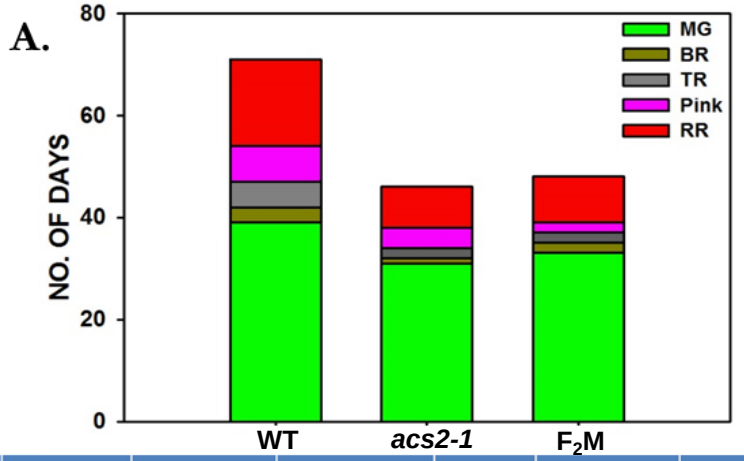

B.

Plant accession	No.of flowers /truss	Total no. of flowers/ plant	Total no. of fruit set/truss	BR DPA	Pink DPA	RR DPA	No. of locules
WT	6-8	90-100	6-7	39	47	55	2-3
acs2-1	7-10	60-80	6-9	32	34	35	2-3
F_2M	5-7	70-90	4-6	33	35	37	2-3

Figure 4.36. Comparison of ripening of BC_1F_2 (M) fruits with earlier reported wild-type parent (M82) and mutant parent (*acs2-1*) in Figure 4.23. **(A)** Stacked bar graph represents the on-vine fruit development through different stages of ripening: mature green (MG), breaker (BR), Turning (TUR), Pink (P), red ripe (RR). **(B)** Table shows few other monitored features like number of flower per truss, total number of flowers per plant at a particular time point, total number of fruit set per truss and number of locules per fruit, of parent mutant, BC_1F_2 compared with parent WT.

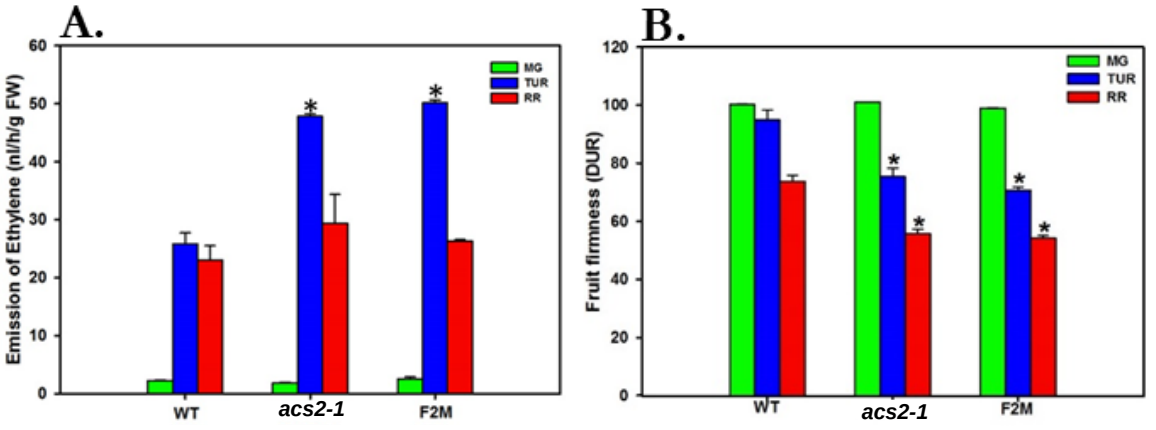

Figure 4.37. Measurement of ethylene emission from fruit and fruit firmness. **(A)** The bar graph represents the comparisons of ethylene level at mature green (MG), turning (TUR), red ripe (RR) stages of parent wild-type (M82), parent mutant (*acs2-1*) and F_2 (M) fruits. **(B)** Comparisons of fruit firmness of parent wild-type (M82), parent mutant (*acs2-1*) and F_2 (M) at different fruit maturity. Each value is the mean of three biological replicates. Firmness value was recorded by measuring each fruit at equatorial plane two times. (Student's t-test; * for $P \leq 0.05$, ** for $P \leq 0.01$ and *** for $P \leq 0.001$, for each fruit maturity stage, n=3 ± SE).

ripening features **(Fig. 4.37A)**. On comparing the fruit firmness with the earlier reported parent WT and *acs2-1,* the F_2 (M) fruits had firmness similar to parent *acs2-1* fruits at MG, TUR and RR stage **(Fig. 4.37B)**.

4.2.23.3 Brix and pH values of F_2 (M) fruits were similar to *acs2-1* fruits

The influence of mutations was also examined on the pH and Brix content of F_2 (M) fruits during the ripening. The parent *acs2-1* and F_2 (M) RR fruits showed slightly higher Brix level than *acs2-2* and parent WT (M82) fruits **(Fig. 4.38)**. On comparing the fruit pH value at RR stage of parent WT (M82), parent *acs2-1*, F_2 (M) and *acs2-2* mutant, the *acs2-2* fruits were less acidic at RR stage compared to parent WT, parent *acs2-1*, and F_2 (M) fruits **(Fig. 4.38)**.

4.2.24 The *acs2-1* mutation alters phytohormone levels in fruits

To identify the effect of mutations in *ACS2* gene on phytohormones, the hormone profile of fruits of parent WT, parent *acs2-1,* F_2, and *acs2-2* mutants was examined at different maturity stages viz., MG, TUR and RR. Hormones level in fruits extract were quantified by using UPLC/ESI-MS. Out of nine examined hormones, a total of six phytohormones viz. zeatin, indole-acetic acid (IAA), jasmonic acid (JA), methyl jasmonic acid (MeJA), abscisic acid (ABA) and salicylic acid (SA) were detected **(Fig. 4.39)**. Out of six phytohormones, the levels of zeatin, JA, MeJA, ABA and SA were high at all the three stages of fruits of *acs2-1* and also in its F_2 (M) progeny compared to WT fruits **(Fig. 4.39A-R)**. In contrast, the IAA level was nearly 50% in *acs2-1* and F_2 (M) compared to WT fruits **(Fig. 4.39D-F)**. The JA level in the MG and TUR tissue of F_2 (Het) of *acs2-1* mutant was below the limit of detection **(Fig. 4.39J-K)**. On the other hand, the *acs2-2* mutant fruits exhibit a significant low levels of ABA (at RR stage), zeatin, MeJA and SA compared to WT fruits in all the three stages. The levels of other phytohormones like IAA and JA were similar to the WT fruits **(Fig. 4.39)**.

4.2.25 The *acs2-1* mutation enhances carotenoids accumulation in fruits

One of the main characteristics of tomato (*Solanum lycopersicum*) fruit ripening is a massive accumulation of carotenoids (mainly lycopene), which contribute to the nutrient quality of tomato fruit. Previous studies indicated that ethylene plays a central role in promoting fruit ripening. However, some recent studies indicated that jasmonic acid plays a positive role in lycopene biosynthesis independently of ethylene as well as in the presence of ethylene (Liu et al., 2012). The profiles of fruits carotenoids and xanthophyll were examined at different maturity stages. A total of 12 carotenoids (phytoene, phytofluene, ζ-carotene, lycopene, δ-carotene, α-carotene, lutein, ϒ-carotene, β-carotene,

zeaxanthin, antheraxanthin and neoxanthin) were detected **(Fig. 4.40A-O)**. Only a few carotenoids (phytoene, lycopene, lutein, and β-carotene) were detected in all the three stages (MG, TUR, and RR) of fruits. Zeaxanthin, antheraxanthin, and neoxanthin were detected only in MG and TUR stages of fruits **(Fig. 4.40-L)**. The levels of most of the carotenoids like phytoene, phytofluene, ζ-carotene, lycopene, δ-carotene, β-carotene and neoxanthin, were higher in RR fruit of *acs2-1* and its F_2 (M) progeny compared to WT fruits **(Fig. 4.40)**. The *acs2-2* mutant fruits exhibit relatively low levels of carotenoids except lycopene, compared to WT fruits. However *acs2*-2 fruits have overall higher total carotenoids level at TUR and RR stages due to higher accumulation of lycopene **(Fig. 4.40N-O)**. The total carotenoids levels were higher in *acs2-1* and its F_2 (M) progenies in all the three maturity stages of fruits compared to WT **(Fig. 4.40M-O)**.

4.2.26 The *acs2-1* mutant fruits have higher level of folates

Folate is an essential compound belonging to vitamin B_9 group that mediate transfer of one-carbon (C1) units in reactions involved in C_1 metabolism (Hanson and Roje 2001, Scott et al., 2000). Chemically, folate molecules are composed of a pterin ring, a p-aminobenzoic acid, and a glutamate. The cellular folate pool is represented by a complex mixture of tetrahydrofolate, (THF) and its derivatives, which differ in the oxidation state of the pterin ring or in the oxidation state of the carried C_1 unit and in the number of glutamate moieties ranging from one to approximately eight γ -linked glutamates.

The *acs2-1* mutant fruit emits high ethylene as well as increased ACS2 activity and elevated level of ACC. The precursors for ACC are methionine and adenosine nucleotide respectively. Due to the involvement of folates as a co-factor in various important biochemical reactions specially, in amino acids (methionine) metabolism and nucleotide (adenosine) biosynthesis, the folate levels were examined in *ACS* fruits. The RR fruits of *acs2-1* mutant exhibited 1.5 fold increase in total folate level compared to WT while *acs2-2* fruits exhibited a folate level similar to WT fruits **(Fig. 4.41)**. Tetrahydrofolate (THF) moiety was not detected at RR stage of fruits. Only the derivatives of THF like 5-Methylene-THF, 5, 0-Methenyl-THF and 5-Formyl-THF, were detected **(Fig. 4.41)**.

4.2.27 The *acs2-1* mutation affects primary metabolites levels in fruits

It has been reported that during on-vine ripening in tomato, the levels of major hexoses, glucose and fructose, cell wall components such as galacturonic acid, and for amino acids such as aspartic, glutamic acid, and methionine increases. Major changes

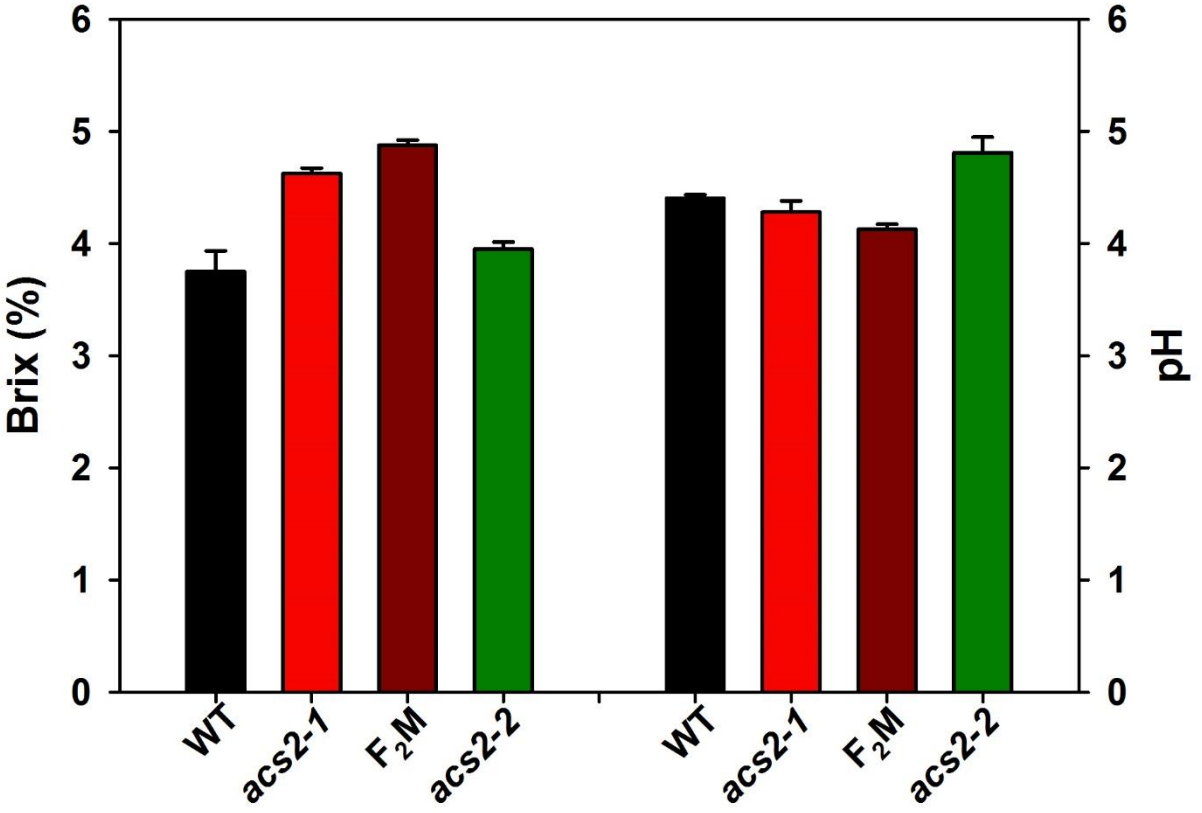

Figure 4.38. Estimation of total soluble solids (Brix value) and pH of fruits of parent WT (M82), parent mutant (*acs2-1*) and F_2 (M) at RR stages. Error bar graph corresponds to the difference in the Brix values and pH values of RR tomato fruits. (Student's t-test; * for $P \leq 0.05$, ** for $P \leq 0.01$ and *** for $P \leq 0.001$, for each fruit, n=3 ± SE).

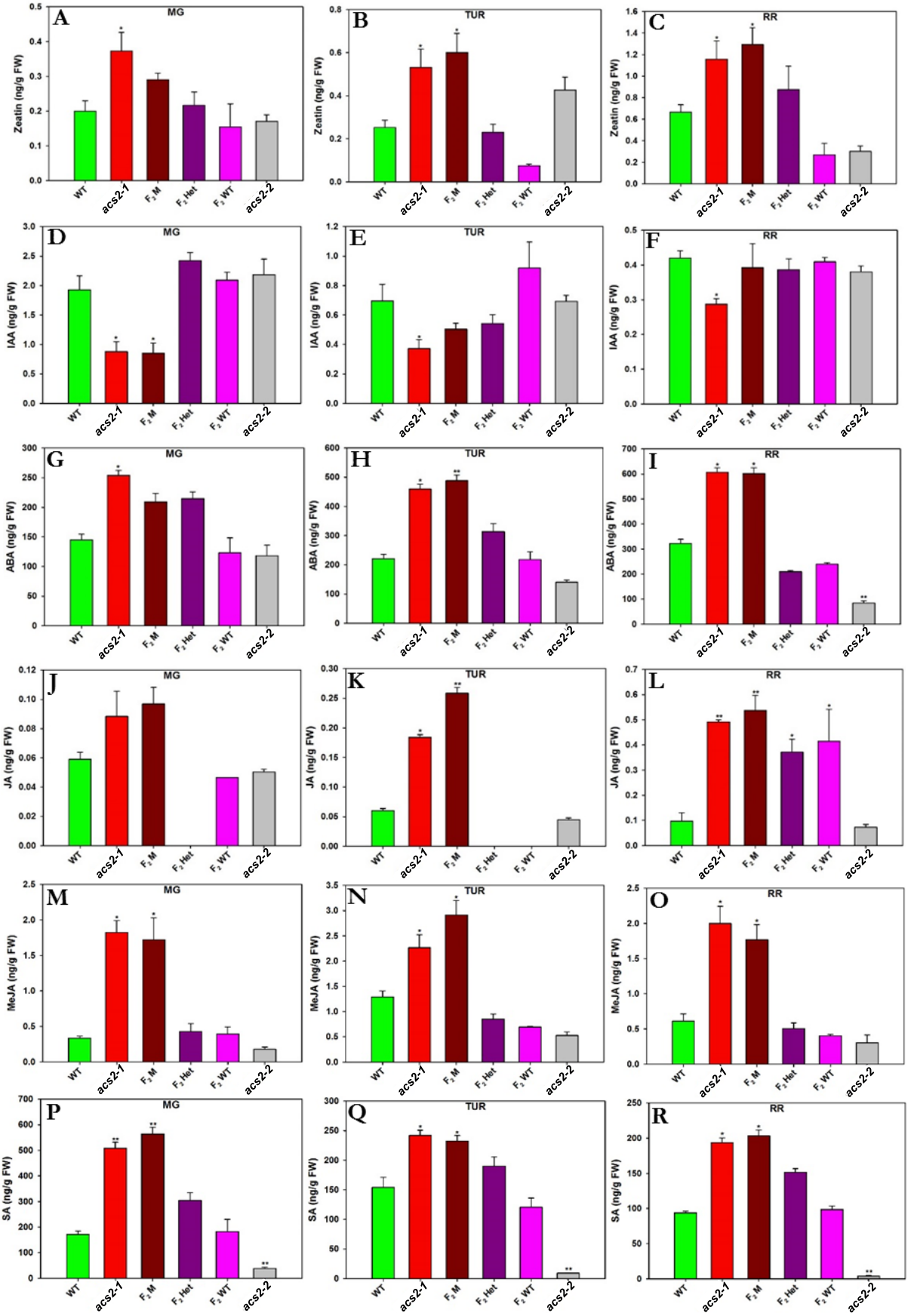

Figure 4.39. Phytohormones profiling of fruits of WT (M82), mutants (*acs2-1*, *acs2*-2), and F_2 progenies of *acs2-1*. **(A-R)** The bar graphs compare phytohormones (SA, ABA, JA, MeJA, IAA, and Zeatin) levels at different fruit maturity (MG, TUR and RR). (Student's t-test; * for $P \leq 0.05$, ** for $P \leq 0.01$ and *** for $P \leq 0.001$, for each fruit maturity stage, n=5 ± SE).

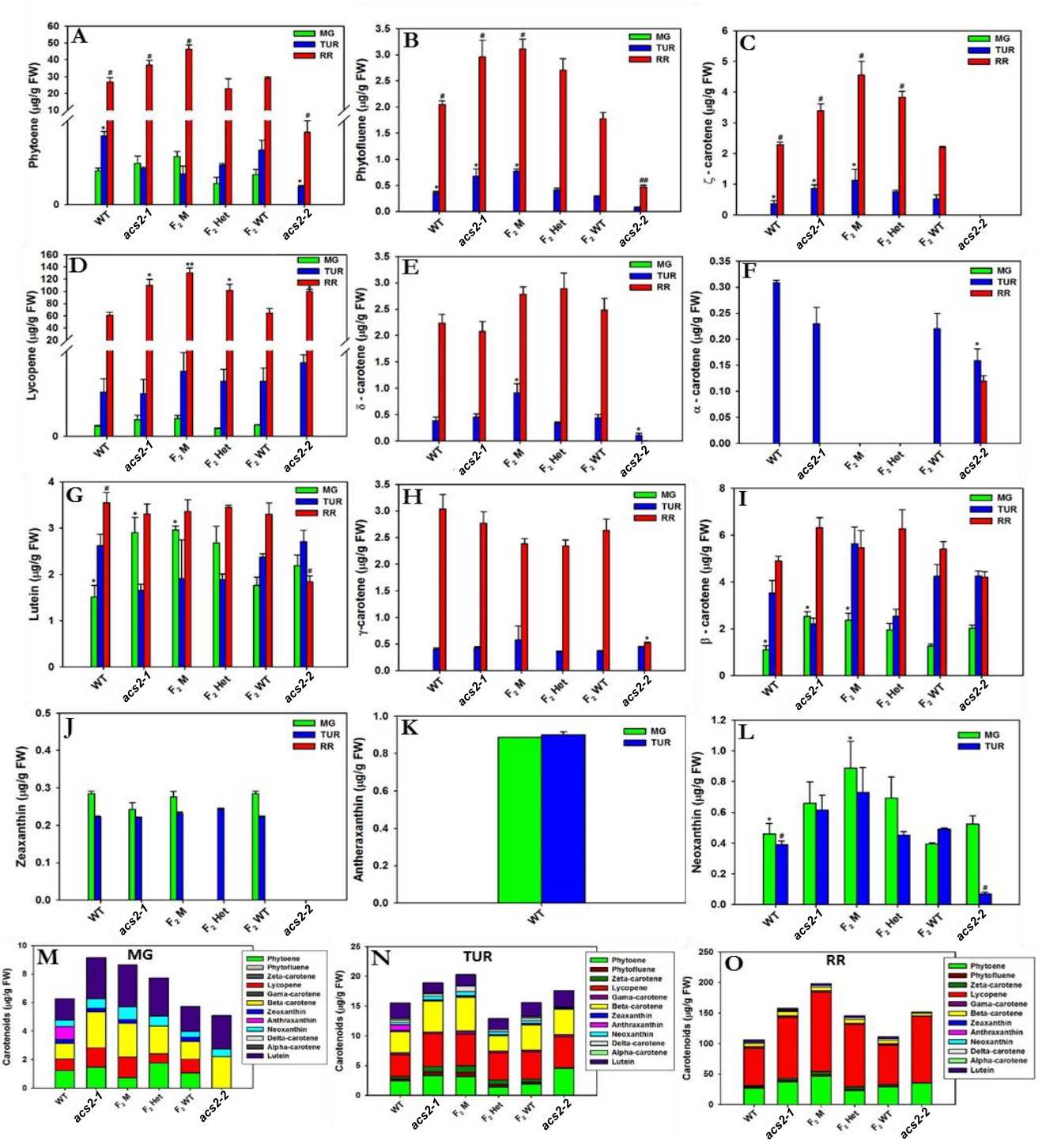

Figure 4.40. Carotenoids and xanthophyll profiling. **(A-L)** The bar plots compare the carotenoids levels in fruits of WT (M82), mutants (*acs2-1*, *acs2-2*), and F_2 progenies of *acs2-1* at different fruit maturity stages. **(M-O)** Stacked bar graph represent the total carotenoids present in WT, mutants and F_2 progenies at each fruit maturity stage. Each value is the mean of five biological replicates. (Student's t-test; * for $P \leq 0.05$, ** for $P \leq 0.01$ and *** for $P \leq 0.001$).

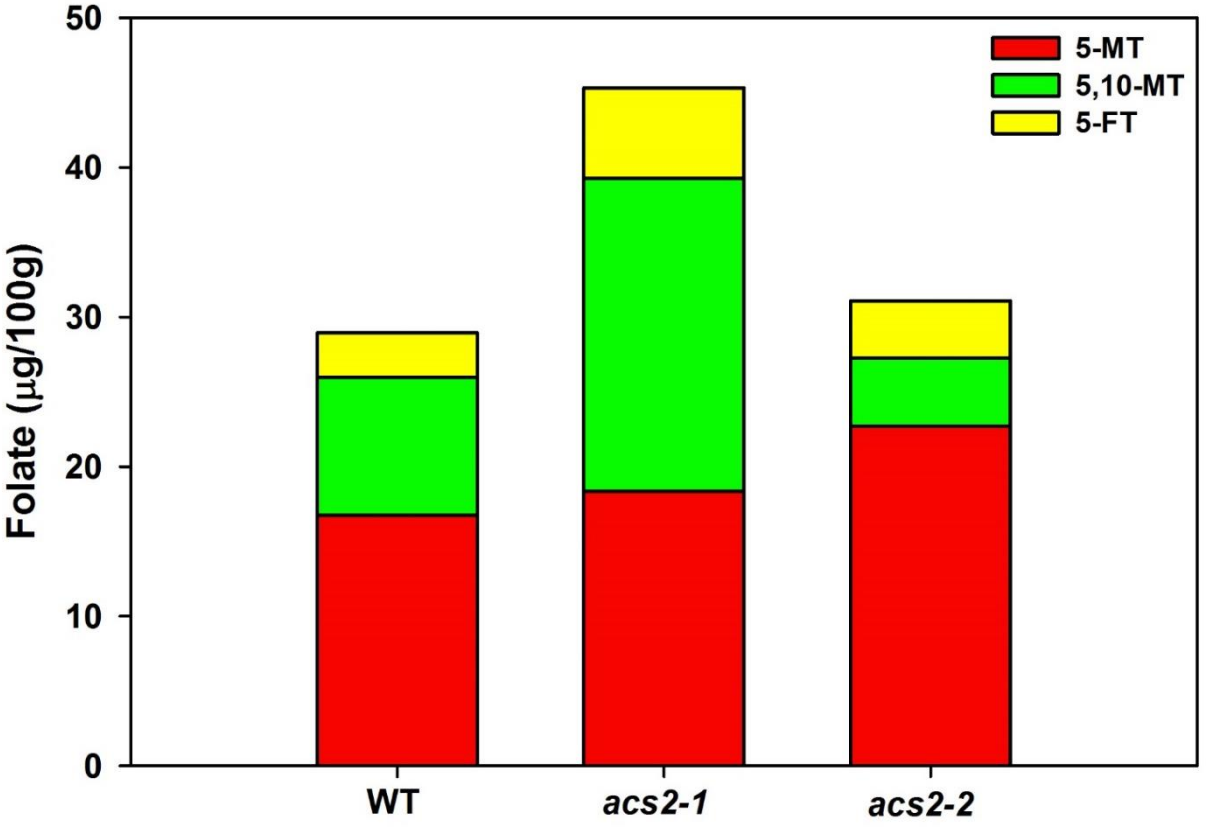

Figure 4.41. Comparison of total folate in RR fruit of WT and mutants. Stacked bars show different folate forms detected in red ripe fruits. Three folate forms, 5-CH_3-THF, 5-CHO-THF, and 5,10-CH^+THF are detected at RR stage. Results are average of five biological replicates.

were also observed at the components of TCA cycle, showing a decrease in malic acid, fumaric acids, and accumulation of citric acid (Oms-Oliu et al., 2011).

A total of 140 primary metabolites were detected in tomato fruit and leaf respectively. Detected primary metabolites were categorized in different groups like amino acids, organic acids, alcohols, sugars, fatty acids and their derivatives **(Table 4.3B)**. Comparisons of metabolites level revealed that the levels of major primary metabolites like amino acids, organic acids, sugars and alcohols in *acs2-1* mutant fruits were significantly different compared to WT and *acs2-2* mutant at different maturity stages of fruits respectively **(Fig. 4.42A)**. The PCA analysis (the correlation variances explained by the PC1 and PC2 components are 13.8% and 19.9% respectively) of primary metabolites corresponding to fruits of WT and mutants (*acs2-1*, *acs2-2*), revealed that the primary metabolites of WT fruits shows different pattern compared to mutants **(Fig. 4.42B)**.

Interestingly in RR fruits of *acs2-1* mutant ACC accumulate at a level high enough to be detected. To best of our knowledge, ACC has not been detected by GC-MS along with primary metabolites in normally maturing tomato fruits. Identification of ACC in primary metabolites also support our result of showing elevated ACC levels in *acs2-1* mutant fruits **(Table. 4.4B) (Fig. 4.42E)**. In contrast, ACC level in WT and *acs2-2* mutant fruits was below the limit of detection. Levels of major hexose sugars like glucose, fructose and galactose, and some organic acids like citric acid, ascorbic acid, and some amino acids such as aspartic acid, pyroglutamic acid, glutamic acid and methionine were very high at all the stages of *acs2-1* mutant fruits than the WT and *acs2-2* fruits **(Fig. 4.42C-K)**. On the other hand the levels of some metabolites like malic acid, GABA (gamma amino butyric acid), proline, 5-Oxoproline and phosphoric acid was higher in *acs2-2* mutant fruits compared to WT and *acs2-1* fruits **(Fig. 4.42C-K)**.

The heat map of metabolites corresponding to different fruit maturity of WT, *acs2-1* mutant, and *acs2-1* F_2 progenies showed the very different pattern of metabolite accumulation. As indicated by yellow circle, the expression pattern of few metabolites was similar in SS stages of *acs2-1*, F_2M, and F_2het fruit **(Fig. 4.43A)**. PCA analysis indicated that the primary metabolites of WT fruit shows different pattern than *acs2-1* mutant and F_2 homozygous mutant fruits. On the other hand the metabolome of F_2 heterozygous mutant fruits is intermediate between WT and *acs2-1* mutant **(Fig. 4.43B)**. This suggests the co-segregation of metabolite trait (phenotype) with the genotype of

acs2-1 F_2 populations and also shows that the *acs2-1* mutation may have affected even in heterozygous state.

4.2.28 1-MCP treatment delays on-vine ripening and revert primary metabolite expression in *acs2-1* mutant fruits

At standard temperature and pressure, 1-MCP (1-Methylcyclopropene) is a gas with a molecular weight of 54 and a formula of C_4H_6. It is believed that 1-MCP occupies the ethylene receptors thus blocking ethylene action. After 1-MCP binds to receptors, the ethylene cannot bind and elicit its action. Sisler and Serek (1997) proposed a model of how 1-MCP reacts with the ethylene receptor. The affinity of 1-MCP for the receptor is approximately ten times greater than that of ethylene. Compared with ethylene, 1-MCP is active at much lower concentrations. 1-MCP also influences ethylene biosynthesis in some species through feedback inhibition. Examination of the effect of 1-MCP on *acs2-1* mutant and WT fruits under on-vine condition **(Fig. 4.44A, B)** revealed that the 1-MCP application significantly delayed ripening by (8 days in WT fruits and three days in *acs2-1* fruits. When a single fruit of a truss is enclosed in bag with 1-MCP, the fruits show differential regulation of ripening. However this differential regulation occurs due to the slowing down the autocatalytic ripening by ethylene **(Fig. 4.44C)**. The expression levels of few primary metabolite like pyruvic acid, oxalic acid, malic acid, citric acid, methionine, glutamic acid, GABA, glycine, tyrosine, glucose, mannose, fructose etc. was also different in 1-MCP treated fruits of WT and *acs2-1* mutant compared to untreated one **(Fig. 4.44D-E)**.

Interestingly ACC level in the 1-MCP treated fruits of *acs2-1* mutant was below detection limit **(Fig. 4.45A-C)**. Compared to the untreated tissue, the levels of major hexose sugars like glucose, fructose and galactose, and some organic acids like citric acid, ascorbic acid, and some amino acids such as aspartic acid, pyroglutamic acid, glutamic acid was found very low in *acs2-1* fruits. Moreover, we did not detect methionine in the treated tissue of *acs2-1* fruits **(Fig. 4.45)**. On the other hand the expression level of some metabolites like malic acid, GABA (gamma amino butyric acid), proline, 5-Oxoproline and phosphoric acid was found increased in 1-MCP treated tissue of WT and *acs2-1* fruits **(Fig. 4.45A-I)**.

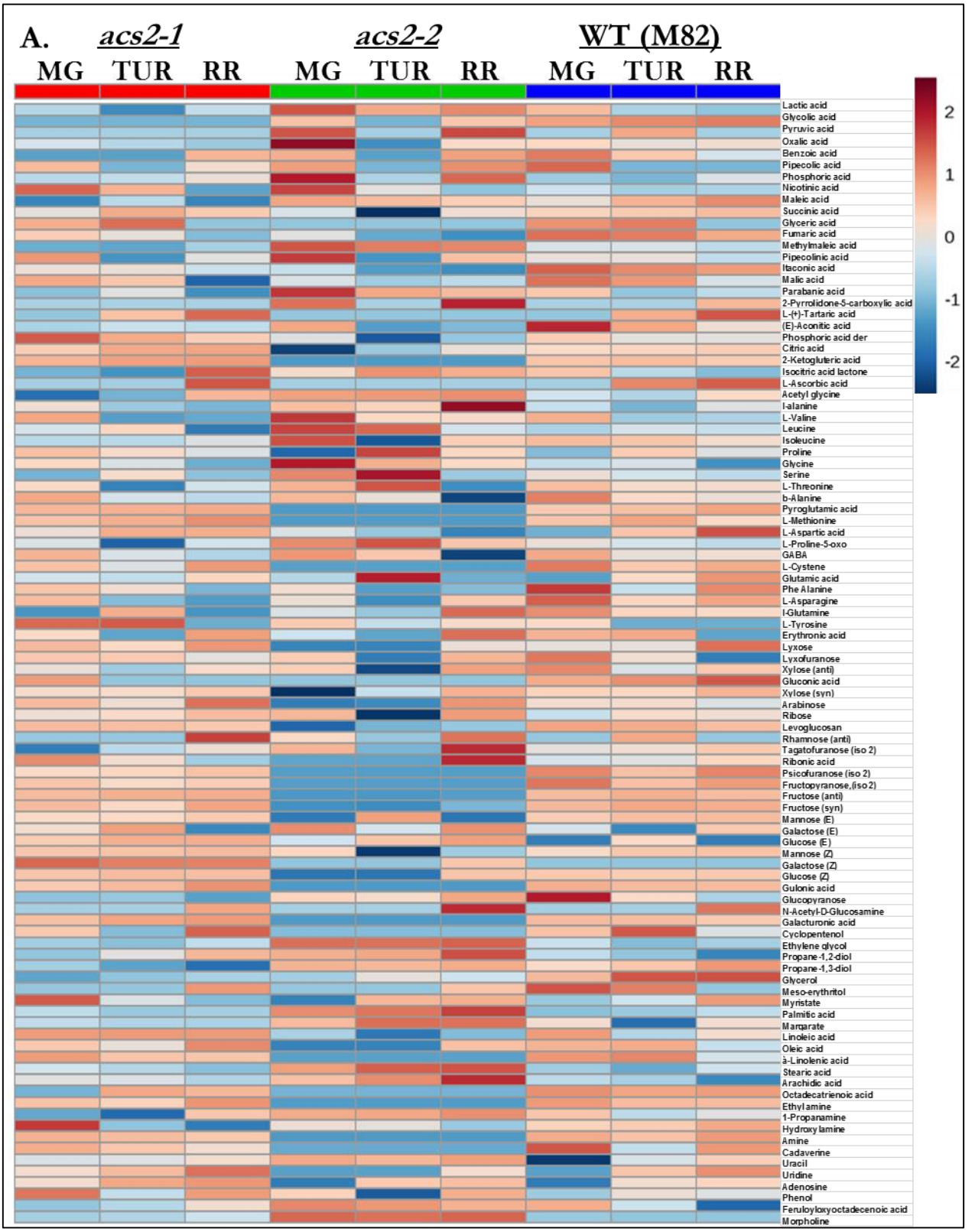
A.
acs2-1
acs2-2
WT (M82)
MG
TUR
RR
MG
TUR
RR
MG
TUR
RR
2
1
0
-1
-2
Lactic acid
Glycolic acid
Pyruvic acid
Oxalic acid
Benzoic acid
Pipecolic acid
Phosphoric acid
Nicotinic acid
Maleic acid
Succinic acid
Glyceric acid
Fumaric acid
Methylmaleic acid
Pipecolinic acid
Itaconic acid
Malic acid
Parabanic acid
2-Pyrrolidone-5-carboxylic acid
L-(+)-Tartaric acid
(E)-Aconitic acid
Phosphoric acid der
Citric acid
2-Ketogluteric acid
Isocitric acid lactone
L-Ascorbic acid
Acetyl glycine
l-alanine
L-Valine
Leucine
Isoleucine
Proline
Glycine
Serine
L-Threonine
b-Alanine
Pyroglutamic acid
L-Methionine
L-Aspartic acid
L-Proline-5-oxo
GABA
L-Cystene
Glutamic acid
Phe Alanine
L-Asparagine
l-Glutamine
L-Tyrosine
Erythronic acid
Lyxose
Lyxofuranose
Xylose (anti)
Gluconic acid
Xylose (syn)
Arabinose
Ribose
Levoglucosan
Rhamnose (anti)
Tagatofuranose (iso 2)
Ribonic acid
Psicofuranose (iso 2)
Fructopyranose,(iso 2)
Fructose (anti)
Fructose (syn)
Mannose (E)
Galactose (E)
Glucose (E)
Mannose (Z)
Galactose (Z)
Glucose (Z)
Gulonic acid
Glucopyranose
N-Acetyl-D-Glucosamine
Galacturonic acid
Cyclopentenol
Ethylene glycol
Propane-1,2-diol
Propane-1,3-diol
Glycerol
Meso-erythritol
Myristate
Palmitic acid
Margarate
Linoleic acid
Oleic acid
à-Linolenic acid
Stearic acid
Arachidic acid
Octadecatrienoic acid
Ethylamine
1-Propanamine
Hydroxylamine
Amine
Cadaverine
Uracil
Uridine
Adenosine
Phenol
Feruloyloxyoctadecenoic acid
Morpholine

B.

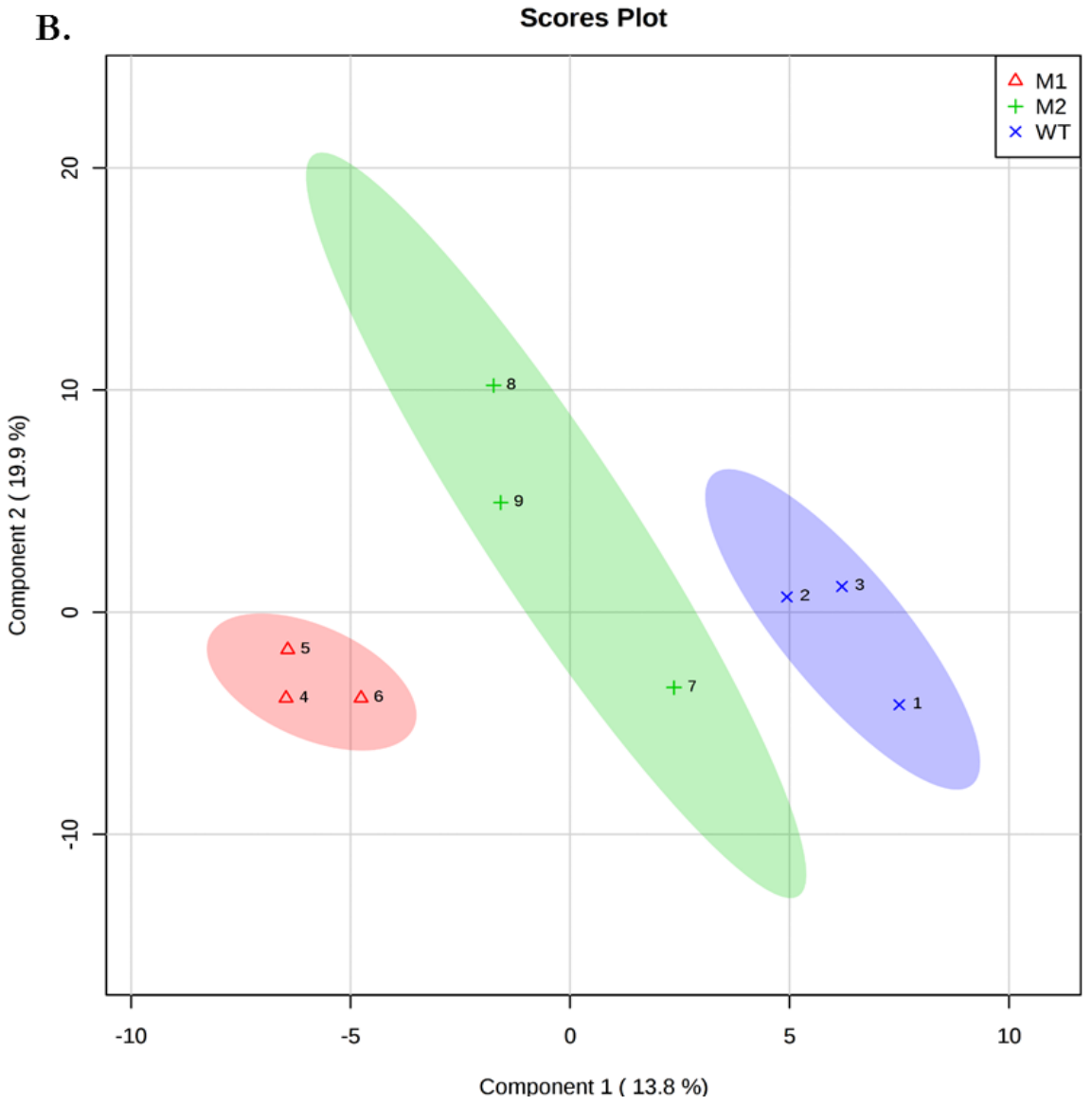
Scores Plot
M1
M2
WT
Component 2 (19.9 %)
Component 1 (13.8 %)
20
10
0
-10
-10
-5
0
5
10
8
9
2
3
5
4
6
7
1

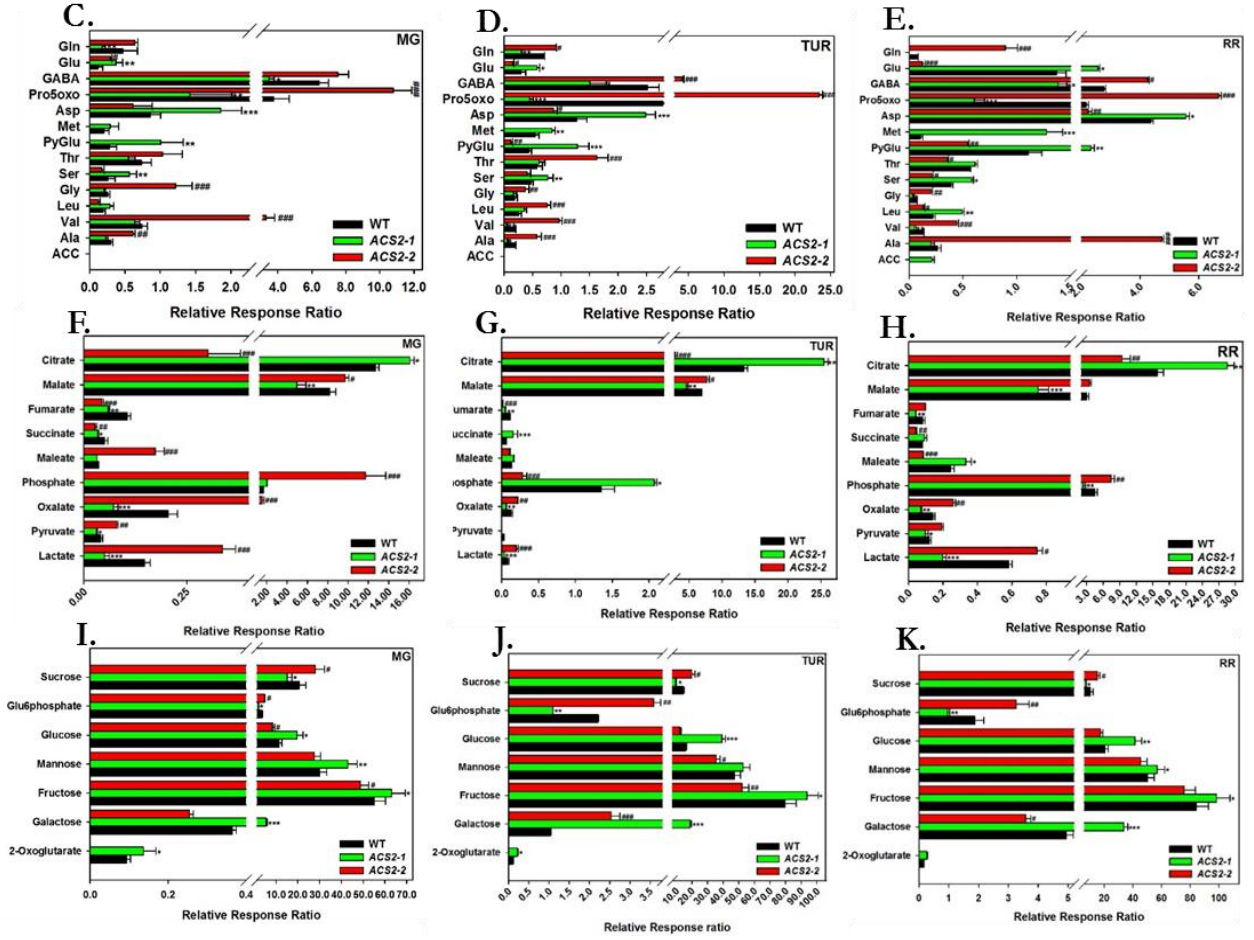

Figure 4.42. Relative metabolite accumulation in wild type and mutants (*acs2-1*, *acs2-2*) fruits at different maturity stages. **(A)** Heat map representing the difference in metabolites level in MG, TUR, and RR fruits of WT (M82) and mutants (*acs2-1*, *acs2-2*). Blue color corresponds to low level while red color denotes high level of particular metabolite. **(B)** Principal component analysis (PCA) score plot for metabolites levels in different maturity stages of fruits of WT (M82) and mutants (*acs2-1*, *acs2-2*). Metabolites of different fruits were analyzed and the correlation variances explained by the PC1 and PC2 components are 13.8% and 19.9% respectively. Blue ellipse represents WT, while red ellipse represents *acs2-1,* and green ellipse corresponds to *acs2-2* mutant. In score plot, the numbers 1, 4 and 7 corresponds to the MG stages, 2, 5 and 8 corresponds to TUR stage and 3, 6 and 9 represents RR stages of fruits of WT as well as mutants. In score plot, M1 represents *acs2-1* mutant and M2 represents *acs2-2* mutant. **(C-E)** Bar graphs comparing relative response ratio of amino acids in fruits at different stages. **(F-H)** Bar graphs comparing relative response ratio of major organic acids in fruits at different stages. **(I-K)** Bar graphs comparing relative response ratio of major sugars in fruits at different stages. (Student's t-test; * for $P \leq 0.05$, ** for $P \leq 0.01$ and *** for $P \leq 0.001$).

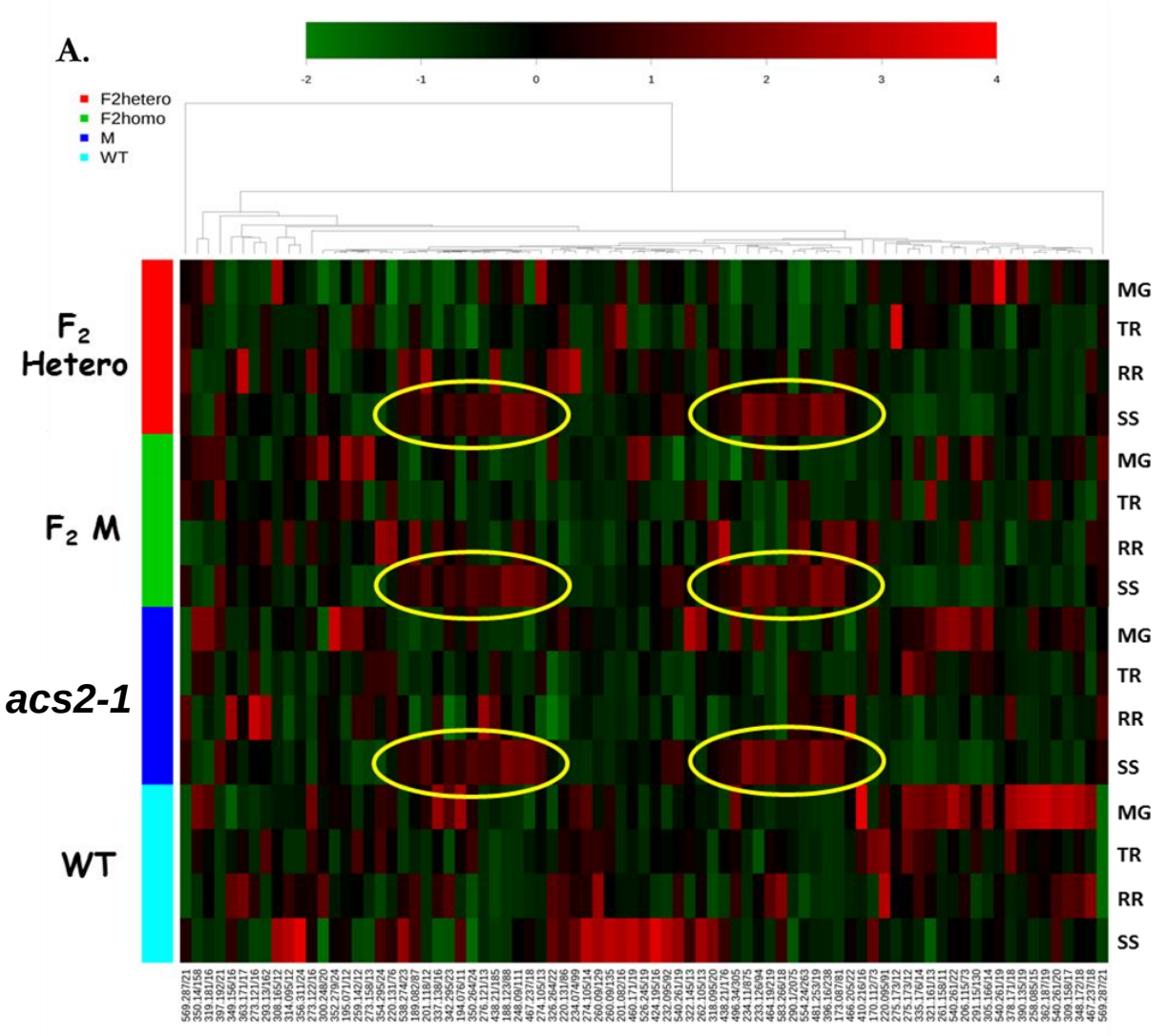
A.
-2
-1
0
1
2
3
4
F2hetero
F2homo
M
WT
F2 Hetero
F2 M
acs2-1
WT
MG
TR
RR
SS

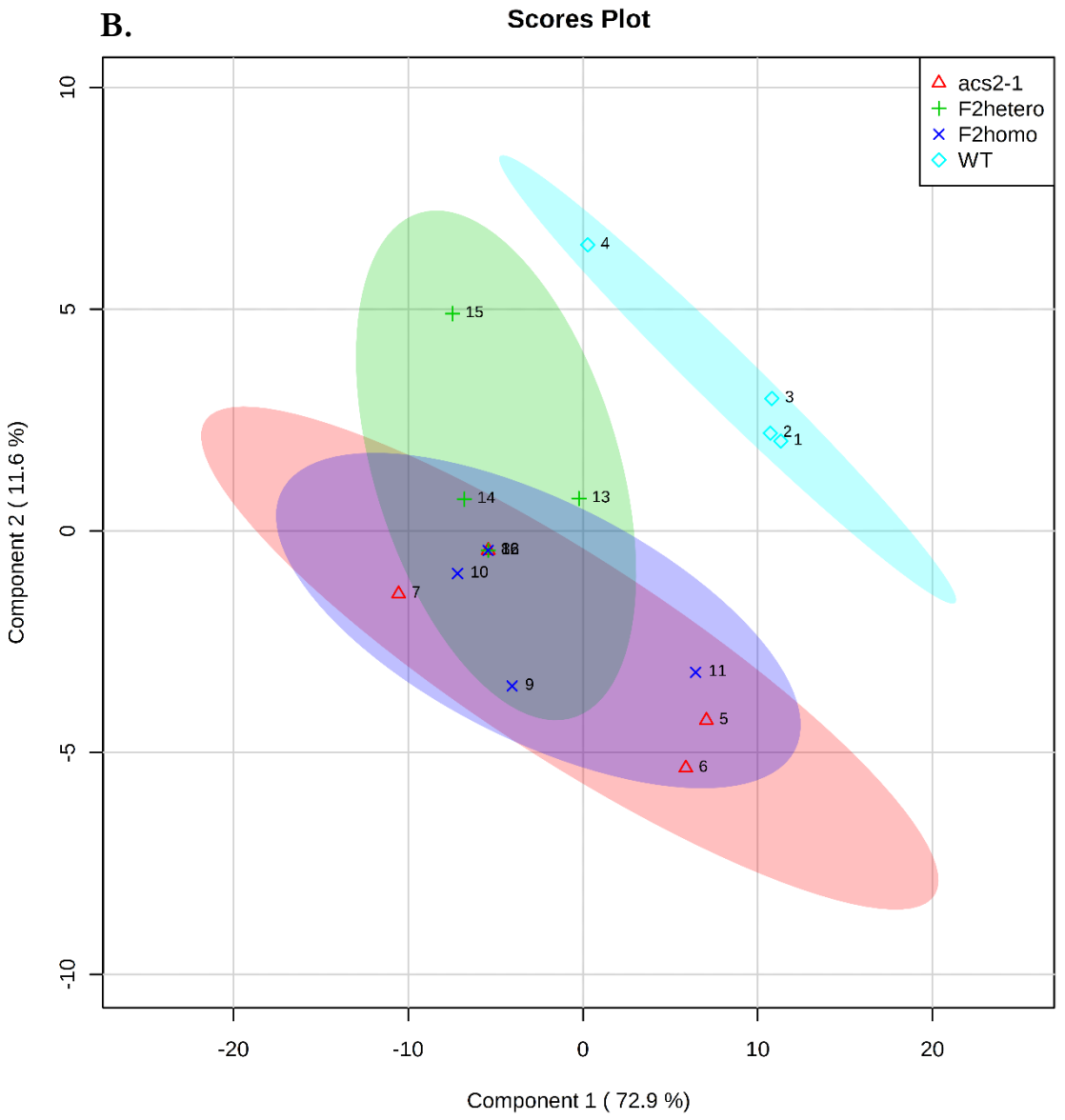

Figure 4.43. Relative metabolite accumulation and clustering in wild type, *acs2-1* mutant, and F_2 fruits at different maturity stages. **(A)** Heat map representing the comparison of metabolites accumulation in fruits of WT, *acs2-1* mutant and its F_2 progenies at different fruit maturity. Yellow circles indicates the group of metabolites wit the similar expression profile in senescing fruits of *acs2-1*, F_2 homozygous mutant, and F_2 heterozygous. Green color corresponds to low level while red color denotes high level of particular metabolite. The numbers representing the exact mass/retention time of the corresponding metabolites. **(B)** Principal component analysis (PCA) score plot for metabolites levels at different maturity stages of fruits of WT (M82), mutants (*acs2-1*), and mutant F_2 progenies. The correlation variances explained by the PC1 and PC2 components are 72.9% and 11.6% respectively. Cyan ellipse represents WT, red ellipse represents *acs2-1* mutant, blue ellipse corresponds to mutant F_2 in homozygous, and green ellipse representing the metabolites in F_2 heterozygous fruits. The no. 1, 5, 9, 13 correspond to MG stages, 2, 6, 10, 14 correspond to TUR stages, 3, 7, 11, 15 correspond to RR stages, and 4, 8, 12, 16 represent the SS stages of respective fruits.

A.

1-MCP solution
(200 mg/5 ml water)

B.

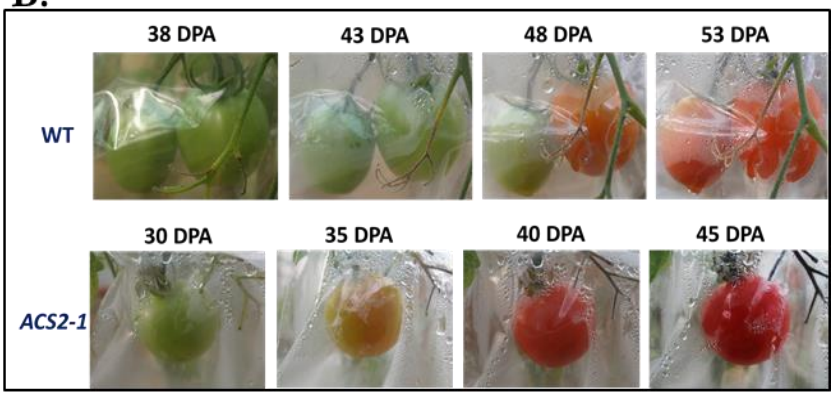

C.

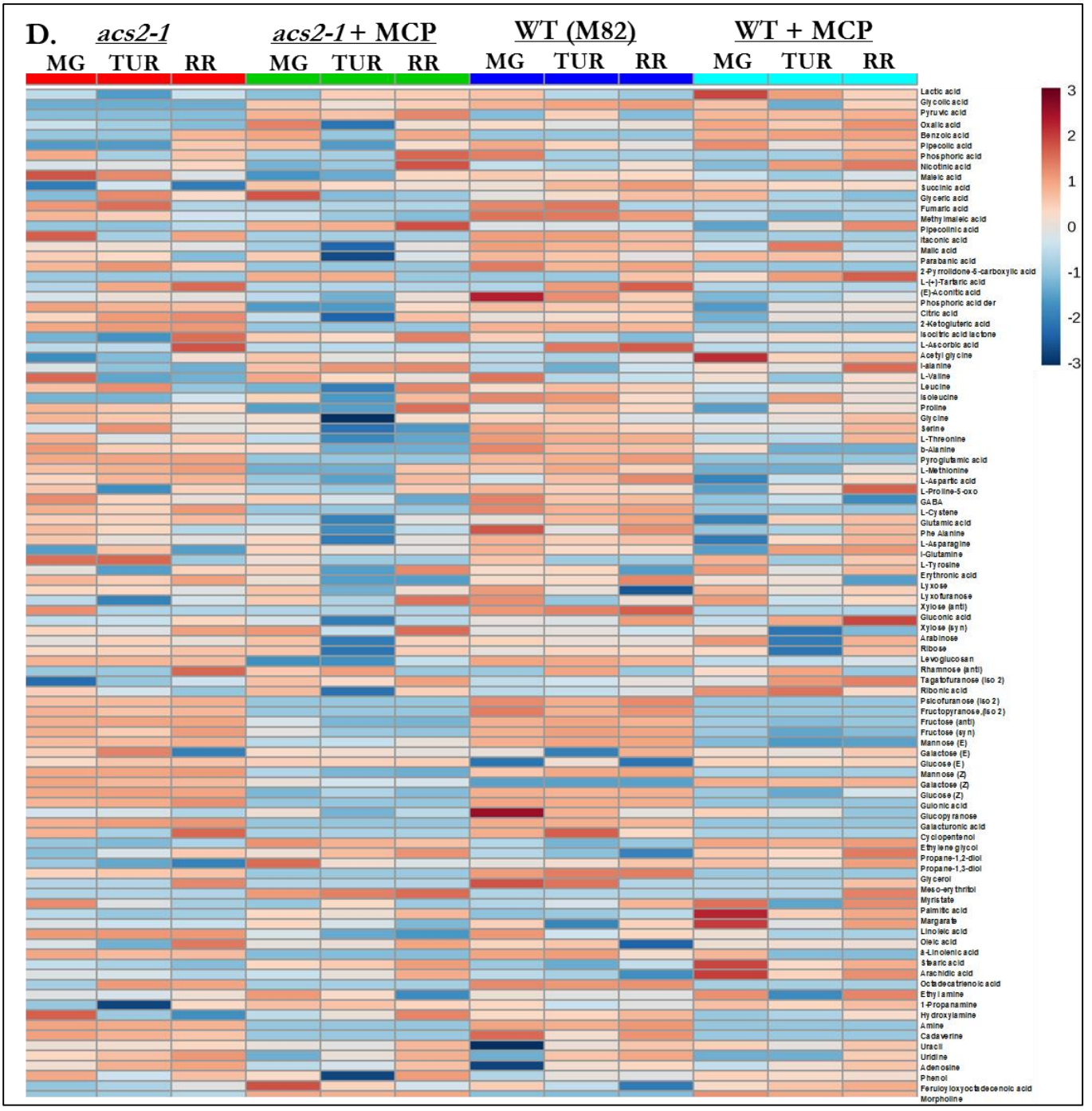
D.
acs2-1
acs2-1 + MCP
WT (M82)
WT + MCP
MG TUR RR MG TUR RR MG TUR RR MG TUR RR
Lactic acid
Glycolic acid
Pyruvic acid
Oxalic acid
Benzoic acid
Pipecolic acid
Phosphoric acid
Nicotinic acid
Maleic acid
Succinic acid
Glyceric acid
Fumaric acid
Methylmaleic acid
Pipecolinic acid
Itaconic acid
Malic acid
Parabanic acid
2-Pyrrolidone-5-carboxylic acid
L-(+)-Tartaric acid
(E)-Aconitic acid
Phosphoric acid der
Citric acid
2-Ketoglutaric acid
Isocitric acid lactone
L-Ascorbic acid
Acetyl glycine
l-alanine
L-Valine
Leucine
Isoleucine
Proline
Glycine
Serine
L-Threonine
b-Alanine
Pyroglutamic acid
L-Methionine
L-Aspartic acid
L-Proline-5-oxo
GABA
L-Cystene
Glutamic acid
Phe Alanine
L-Asparagine
l-Glutamine
L-Tyrosine
Erythronic acid
Lyxose
Lyxofuranose
Xylose (anti)
Gluconic acid
Xylose (syn)
Arabinose
Ribose
Levoglucosan
Rhamnose (anti)
Tagatofuranose (iso 2)
Ribonic acid
Psicofuranose (iso 2)
Fructopyranose,(iso 2)
Fructose (anti)
Fructose (syn)
Mannose (E)
Galactose (E)
Glucose (E)
Mannose (Z)
Galactose (Z)
Glucose (Z)
Gulonic acid
Glucopyranose
Galacturonic acid
Cyclopentenol
Ethylene glycol
Propane-1,2-diol
Propane-1,3-diol
Glycerol
Meso-erythritol
Myristate
Palmitic acid
Margarate
Linoleic acid
Oleic acid
a-Linolenic acid
Stearic acid
Arachidic acid
Octadecatrienoic acid
Ethylamine
1-Propanamine
Hydroxylamine
Amine
Cadaverine
Uracil
Uridine
Adenosine
Phenol
Feruloyloxyoctadecenoic acid
Morpholine
3
2
1
0
-1
-2
-3

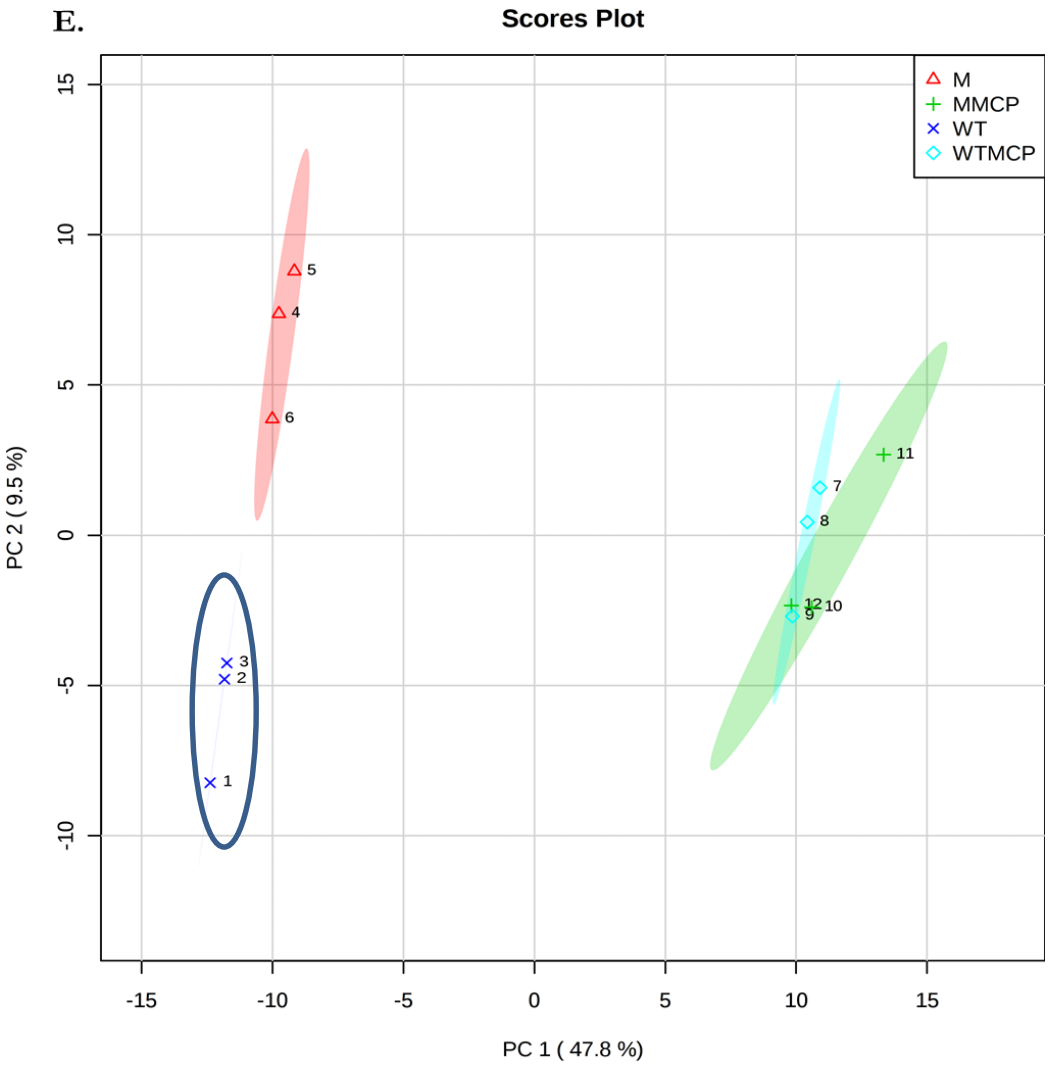

Figure 4.44. On-vine treatment of 1-MCP to mature green fruits of WT and *acs2-1* mutant plants. **(A)** represents experimental setup for the treatment of 1-MCP on MG fruits. **(B)** corresponds to the delayed in ripening of WT as well as mutant fruits after treatment of 1-MCP. **(C)** represents the difference in ripening of same truss fruits after treatment of 1-MCP. Five biological replicates were considered for the experiment. **(D)** Heat map representing the difference in metabolites level in 1-MCP treated and untreated MG, TUR, and RR fruits of WT (M82) and mutants (*acs2-1*). Blue color corresponds to low level while red color denotes high level of particular metabolite. **(E)** Principal component analysis (PCA) for metabolites levels at different maturity stages of 1-MCP treated and untreated fruits of WT (M82) and mutant (*acs2-1*). The correlation variances explained by the PC1 and PC2 components are 47.8% and 9.5% respectively. Blue crosses represents untreated WT, and red ellipse represents untreated *acs2-1*. Green and cyan ellipse corresponds to MCP treated *acs2-1* mutant and WT respectively. In score plot, the numbers 1, 4, 7, and 10 corresponds to the MG stages, 2, 5, 8, and 11 corresponds to TUR stage and 3, 6, 9, and 12 represents RR stages of fruits of WT as well as mutants. In score plot, M represents *acs2-1* mutant.

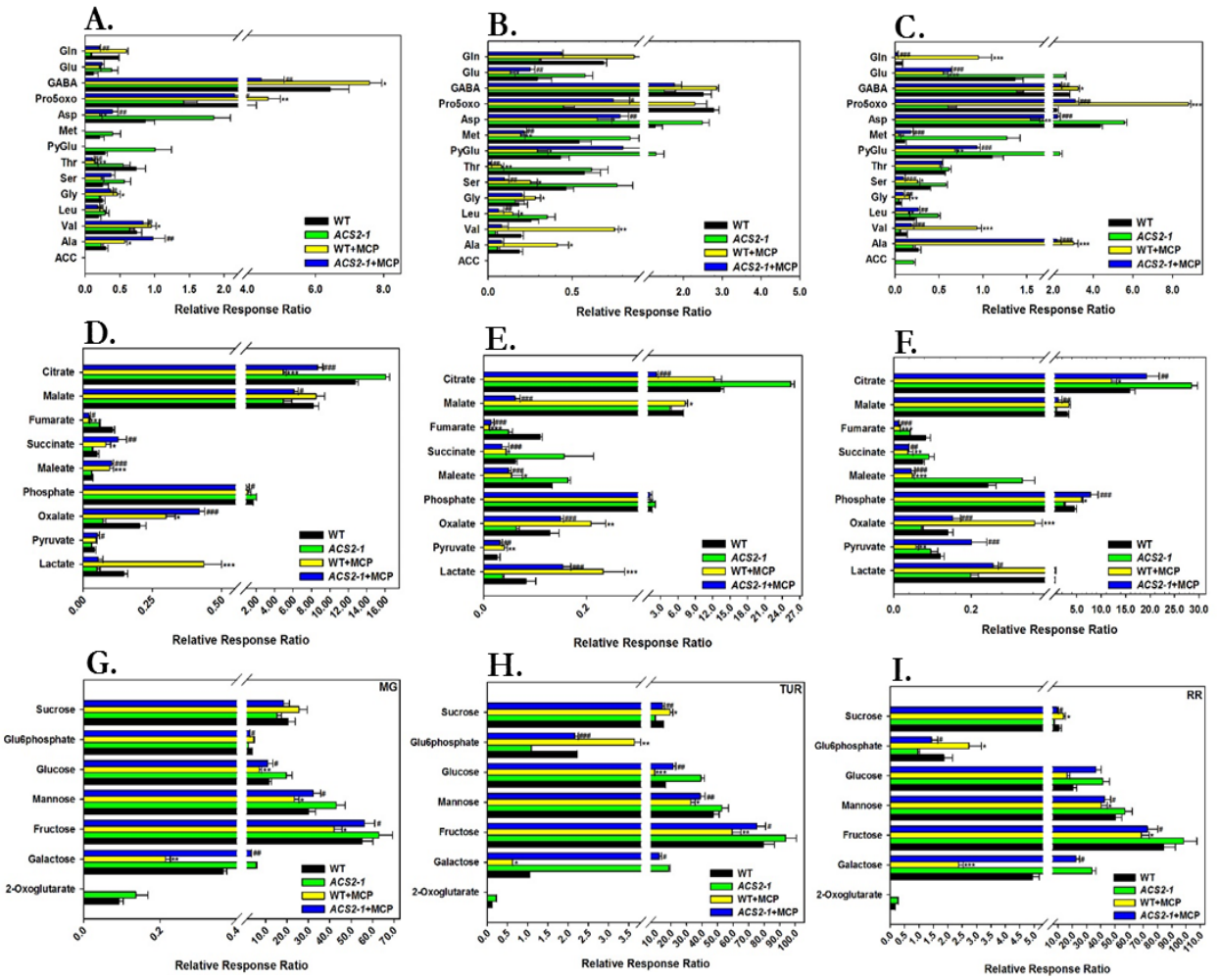

Figure 4.45. Relative accumulation of primary metabolites (Amino acids, Organic acids, and Sugars) in fruits of WT and *acs2-1* mutant after on vine treatment with 1-MCP (1-Methylcyclopropene). The histogram (group error bars) were plotted by placing amino acids **(A-C)**, organic acids **(D-F)** and sugar's **(G-I)** on y-axis and their corresponding relative response ratio value on X-axis using Systat.SigmaPlot.v11.0 software. The relative response ratio value is obtained by dividing the metabolite peak area by reference (ribitol) peak area. (Student's t-test; * for $P \leq 0.05$, ** for $P \leq 0.01$ and *** for $P \leq 0.001$).

4.3 Discussion

4.3.1 The *acs2-1* and *acs2-2* are novel mutant alleles

To improve shelf life of tomato, till date, major focus has been on the manipulation of ethylene production, perception and action employing either sense or antisense technology (Hamilton et al., 1990; Oeller et al., 1991; Theologis et al., 1993; Ye et al., 1996; Xiong et al., 2003, 2005). All these attempts have been largely successful in obtaining low ethylene producing tomatoes, displaying an extended shelf life but with compromised fruit quality traits. Gupta et al. (2013) delayed ripening in tomatoes by silencing three homologs (*ACS1A*, *ACS2*, and *ACS6*) of the 1-aminocyclopropane-1-carboxylate synthase (ACS) gene during ripening using RNAi technology. The chimeric RNAi-ACS construct designed to target ACS homologs effectively repressed the ethylene production in tomato fruits. Fruits from such lines exhibited delayed ripening and extended shelf life for ~45 days, with improved juice quality. So far in tomato, only one ethylene receptor mutant *Nr* (*Never ripe*) has been identified that confers insensitivity to ethylene (Lanahan et al., 1994; Wilkinson et al., 1995). The homologs of ethylene signaling components similar to Arabidopsis have also been identified in tomato (Tomato Genome Consortium, 2012; Lashbrook et al., 1998; Zhou, 1996).

In contrast, till date, there is no natural mutant in ethylene biosynthesis pathway in tomato has been identified. In tomato the *ACS2* mutant alleles (*acs2-1* and *acs2-2*) were isolated from EMS-mutagenized M_3 seeds of M82 cultivar. ACS carries out the rate-limiting step in ethylene biosynthesis (Yang and Hoffman, 1984) and in tomato it is a part of multi-gene family, comprising nine homologs, which are differentially expressed (Cara and Giovannoni, 2008). ACS2 and ACS4 are responsible for the climacteric burst of ethylene production at the onset of ripening (termed System-2). Sequencing of mutant alleles revealed nucleotide changes at positions A3452 to G and T5174 to A in exon 2 and 4 respectively, leads to the amino acid changes K100 to R and V352 to E respectively, in the ACS2-1 protein. On the other hand in the *acs2-2* mutant, two mutations were in the promoter region and one mutation was located in intron three. Unlike *acs2*-1 mutant, the mutation in *acs2*-2 may not have a direct effect on protein structure and function.

4.3.2 The *acs2-1* is an ethylene overproducer while the *acs2-2* is an ethylene under producer mutant

The classic ethylene-mediated "triple response" phenotype of etiolated seedlings has been used to isolate several mutants that are defective in ethylene response in

Arabidopsis (Guzman and Ecker, 1990). The triple response is characterized by exaggerated apical hook, shortening of hypocotyl and root length and radial swelling at the base of hypocotyl of etiolated seedlings. The seedlings that failed to display above characters in the presence of ethylene were selected as ethylene insensitive mutants. Etiolated seedlings of *acs2-1* mutant were more sensitive to external ethylene compared to *acs2-2* seedlings. At a very low concentration of ethylene, the *acs2-1* seedlings exhibited the triple response. The retention of triple response indicated that ethylene signaling pathway in both mutant seedlings was not affected due the mutations in the *ACS2* gene.

In Arabidopsis it is reported that the ethylene stimulates seed germination (Bleecker et al., 1988; Wilson et al., 2014) whereas seeds of ethylene insensitive *etr1-1* mutants show sluggish germination (Chiwocha et al., 2005). The *asc2-1* mutant seeds germinated earlier than WT and while *acs2-2* mutant showed delayed germination. The contrasting behavior of these two mutants with respect to the seed germination indicated that the mutations may have affected the overall ethylene production from the seeds and also the germinating seedlings. The examination of ethylene emission from the germinating seedlings of WT and the mutants confirmed above presumption. A time course analysis of ethylene emission from the germinating seeds and during seedling growth revealed that the *acs2-1* seedlings emitted high amount of ethylene than the WT. It can be assumed that enhanced synthesis of the ethylene from above mutant may have stimulated the seed germination. In contrast the *acs2-2* seedlings emitted low amount of ethylene compared to WT seedlings during the course of seed germination and seedling growth. Since ethylene is needed for seed germination, the block in ethylene emission may have contributed to the delayed seed germination of the *acs2-2* mutant.

The post-germination phenotype of the seedlings of mutants was largely similar to the wild type yet it revealed few subtle differences. Recent studies reported that the ethylene negatively regulates the lateral root formation in Arabidopsis (Ivanchenko et al., 2008) and tomato (Negi et al., 2008, 2010). Contrary to this the light-grown *acs2-1* mutant though produced more ethylene (in dark grown condition) showed higher number of lateral root formation than the WT. On the other hand the *acs2-2* mutant also showed slightly higher number of lateral roots. However, it is possible that the increased lateral root in the mutants may be due to secondary mutations and may not be related to the *ACS2* mutations. However this can only be ascertained by genetic analysis after crossing with the WT parent. In addition Negi et al. (2010) grew tomato seedlings on the nutrient agar that is supplemented with the minerals. In this study we grew the seedlings on the

agar without any nutritional supplement. It is known that the mineral nutrient and sugars strongly influences the lateral root formation (López-Bucio et al., 2003; Gupta et al., 2015). The other difference could be the genetic background of M82 (used in this study) and Ailsa Craig (used by Negi et al., 2008), which may have contributed to the difference in the lateral root numbers. Evidently the differences between this study and earlier study indicate that a more detailed analysis is needed to ascertain why *acs2*-1 mutant initiated more lateral roots than the wild type. This is analysis is also important considering that *epi* mutant of tomato that overproduces ethylene and have some degree of constitutive ethylene signaling show reduced numbers of lateral roots (Negi et al., 2008). A comparison of *epi* mutant with that of *acs2-1* would be interest to see influence to these two loci on plant phenotype.

It is known that while ethylene or its precursor ACC inhibits hypocotyl elongation in dark-grown seedlings, in light-grown seedlings ethylene or ACC stimulates the hypocotyl elongation (Smalle et al., 1997; Vandenbussche et al., 2003). Likewise, the light grown *acs2-1* seedlings show longer root and hypocotyl length compared to WT and *acs2-2*.

Another intriguing result was that the ethylene is reported to inhibit the root elongation in the light-grown seedlings (Ruzicka et al., 2007), however the root of acs2-1 mutant was slightly longer than the WT, while those of *acs2-2* were shorter than WT. However, in this case too, the growth conditions used in this study, where seedlings were grown on nutrient free agar may have contributed to above phenotypes.

It is of interest to note that the primary root of the both *acs2-1* and *acs2-2* dark-grown seedlings were much longer than the WT. It is in contrast with the action of the ethylene as during triple response ethylene induces shortening of the primary root of the seedlings. It is also in contrast to tomato *epi* mutant that show some amount of constitutive triple response with its dark-grown seedlings display much shorter hypocotyl and root than the parent seedling (Barry et al., 2001). Though *acs2-1* seedling show slightly shorter hypocotyl, its primary root is nearly double in length than the WT control. On exposure to ethylene the roots of both mutants become shorter than the corresponding wild type control.

4.3.3 The *acs2-1* and *acs2-2* mutations shows the pleiotropic effect on plant morphology

The phenotypic characterization of *ACS2* mutants indicated that mutation affect the several developmental process of plants. The *acs2-1* mutant exhibited light green

color phenotype in the seedlings stage as well as of foliage compared to WT, while the *acs2-2* mutant leaf are dark green compared to WT. It is not known whether the Arabidopsis *eto1* mutant (Guzman and Ecker, 1990) and tomato *epi* mutant also has pale green color in the seedlings. However, the pale color of cotyledons and of primary leaf of one-week-old light-grown seedlings of *acs2-1* was similar to Arabidopsis *cytokinin resistant1* (*cyr1)*, a cytokinin signaling mutant (Deikman and Ulrich, 1995). However, a remarkable difference between *acs2-1* and *cyr1* mutants is that *cyr1* mutant exhibits incomplete cotyledons and leaf expansion, consistent with the observed phenotype of cytokinin insensitive plants (Cary et al., 1995) whereas *acs2-1* mutant exhibits fully expanded cotyledons and leaf. The pale green phenotype of the *acs2-1* mutant is displayed throughout the vegetative development, compared to WT and *acs2-2* mutant

The *acs2-2* mutants show dark-green leaves compared to its wild type parent. Similar to this mutant, the maize *ZmACS6* mutant also produces less ethylene similar to *acs2-2* mutant, and exhibit increased chlorophyll content in the leaf (Young et al., 2004). It can be surmised that the ethylene production from plants have an effect on the chlorophyll accumulation, where more ethylene inhibits chlorophyll production and less ethylene promotes the chlorophyll accumulation.

It is reported that normally in the adult plant ethylene suppress the elongation of the plants except in flooding resistant plants (Abeles et al 1992). However in this study we observed that the *acs2-1* mutant plants grew faster than the WT control. The information about role of ethylene in growth of adult plant is incomplete and also most often the action on vegetative growth takes place by a combined action of several plant hormones (Vandenbussche et al 2012). The promotive effect of ethylene is well document for hypocotyl elongation and ethylene also promotes elongation growth for shade avoidance (Vandenbussche et al 2012).

4.3.4 The *acs2-1* mutation affects the ACS2 activity

Since ACS is the key enzyme in regulation of ethylene biosynthesis considerable information has been collected about its regulation and function. The activity of ACS proteins are regulated by several different mechanisms such as phosphorylation, ubiquitin mediated protein degradation, dimerization etc. In ripening tomato fruits ACS levels are regulated not only transcriptionally but also post-translationally. Tatsuki and Mori (2001) showed that ACS2 protein in the extract of wounded tomato fruits fed with [^{32}P] inorganic phosphate was phosphorylated at Serine 460 located at the C-terminal region. However, another isoform ACS4 was not phosphorylated *in-vitro*, indicating that different

ACS isozymes have different post-translational regulatory mechanisms, such as phosphorylation. This observation is in conformity with existence of three different types of ACS enzymes in plants and tomato ACS2 and ACS4 belong to different classes with respect to their phosphorylation.

A complete inactivation of ACS2 protein was observed on deletion of the C-terminus of protein through Arg 429. In contrast, a deletion of 46–52 amino acids from the C-terminus increased the substrate (SAM) affinity of truncated enzyme by nine-fold higher than the wild-type enzyme (Li and Mattoo, 1994). The truncation also caused the loss of dimerization of ACS2 protein, which in WT exists as dimer. These studies highlighted the importance of non-conversed C-terminus of ACS protein indicated that the deletion in this region affects its enzymatic function as well as dimerization.

Huai et al. (2001) analyzed the crystal structure of ACS protein of tomato and found that in dimeric form N-terminal amino acid 11-19 interact with the C-terminal region helix H14. Further, biochemical studies indicated that this interaction is important for conformation, stabilization, and catalytic activity of ACS protein (Li and Mattoo, 1994; Li et al., 1996). Evidently, the C-terminus residues of ACS protein differentially regulate its catalytic activity either by stabilizing the protein or by enhancing the activity of the enzyme.

Considering above, it is evident that the mutation in C-terminus of ACS2 protein can have affect the function of protein. Several studies have indicated that turnover of ACS protein also plays an important role in regulating ethylene emission from plants (Chae and Kieber 2005). The *acs2-1* mutant carried five mutations of which two caused distinct change in the amino acids. The nucleotide changes at positions A3452 to G and T5174 to A in exon 2 and four respectively, lead to the amino acid changes K100 to R and V352 to E respectively, in the ACS2-1 protein. The use of PARESNP predicted that these non-synonymous changes may not be deleterious in the nature. The changes lead to SIFT scores of 0.12 (K100 to R) and 0.85 (V352 to E) units respectively, and PSSM differences were 7.6 and -9.7 respectively. These values indicated that the mutation would not affect the function of ACS2 protein as for a loss of function the SIFT score should be less than 0.05 unit and PSSM difference should be more than 10 units (Beckstette et al., 2006; Huang et al., 2010; Sim et al., 2012). The 3-D model indicated that the amino acid changes were located in the α-helix of protein surface and most likely did not affect the active site interface.

However the prediction from the SIFT score and PSSM value are tentative as it does not account for a specific features of protein which may be related to the post-translational modification of the proteins. One of the important regulators of ACS activity is the turnover of the protein that is regulated by the C-terminus of the protein (Chae and Kieber 2005). Tomato ACS2 is phosphorylated by a CDPK at a conserved serine residue Ser-460 at c-terminal of the protein (Tatsuki and Mori 2001). Importantly, it is believed that above phosphorylation of ACS protein blocks binding of the ETO1/EOL proteins. That in turn inhibits the ubiquitination of the ACS proteins and protects ACS from degradation by the 26S proteasome. In addition to this ACS stability is also regulated by action of MAP kinases (Liu and Zhang 2004). However it remains to be established whether the two mutations in ACS2-1 protein changed its capacity for the phosphorylation.

In addition to potential changes in protein phosphorylation, there are other mechanisms that may have increased the stability of ACS2-1 protein. In-vivo ACS protein exists in homodimeric as well as heterodimeric form (Yamagami et al. 2003; Tsuchisaka and Theologis, 2004). The two amino acid changes in α-helix of ACS2 protein may interfere with protein folding as valine (V), a neutral non-polar amino acid at position 352 in amino acid chain is converted to glutamic acid (E), an acidic polar amino acid while lysine (K), a basic polar amino acid is changed to arginine (R), a basic polar amino acid. The change in polarity and the functional group present in amino acids can alter the bonding pattern with different amino acids, molecules, etc. As a result alteration in the folding pattern of protein, it may stimulate higher degree of phosphorylation that may make protein more stable.

While the molecular basis of regulating protein stability is not known and at the best can be guessed, the data obtained in this study favors that the mutations increased the stability of the ACS2-1 protein. First, the *acs2*-1 mutant seedlings show higher emission of ethylene and similar high emission is also seen in the fruits and also in the leaves. Second, Several phenotype of the plant such as early seed germination, enhanced senescence and accelerated fruit ripening and the senescence are consistent with higher ethylene biosynthesis from the *acs2-1* mutant plants. Third, the *acs2-1* mutant show higher accumulation of ACC than the WT at RR stage of the fruits, which is also supported by detection of ACC in the primary metabolites of the mutant fruits. The immunoblots of ACS2-1 protein isolated from red ripe fruit of *acs2-1* mutant and the WT parent show 4 fold higher level of ACS2-1 protein in the fruit than the WT. Taken together these

evidences indicated the higher emission from *acs2*-1 mutant most likely results from the increased stability of the protein.

Among the two ACS mutant isolated in this study, the *acs2-2* mutant lacked any mutation in the ORF of the protein. It had two mutations in the promoter region and one mutation in intron three, which being not the part of the coding region; would not affect the function of ACS2-2 protein. However due to mutations in the promoter sequence it may affect the affinity for binding of regulatory transcription factors to the promoter region may be altered. The evidence indicated that the *acs2-2* mutation reduced the expression of ACS2 protein in the mutant. Its properties were opposite to that discussed above for *acs2-1* mutant. The *acs2-2* mutant showed lower emission of ethylene, delayed seed germination, slower leaf senescence, delayed fruit ripening and longer shelf life of the fruits. Contrary to *acs2-1* mutant the *acs2-2* mutant showed reduced amount of on immunoblots of ACS2 protein isolated from red ripe fruits compared to the WT parent. It remains to be determined whether the transcripts of ACS2 were also lower in the *acs2-2* mutant, which may have contributed to the reduced amount of ACS2 protein.

4.3.5 The *acs2-1* and *acs2-2* mutations affect the ripening and shelf life of fruit

The *acs2-1* and *acs2-2* mutations affect all the phase of fruit development and ripening, however their action were contrastingly opposite. The development of *acs2-1* mutant fruit was accelerated at all stages of the ripening. Consequently all the ripening related phases were much shorter in *acs2-1* mutant compared to wild type after attaining MG phase. The mutant fruits also attained MG stage earlier than the WT. Likewise *acs2-1* fruits reached BR stage seven days earlier than WT. From post-breaker stage, ripening was accelerated in *acs2-1* fruits and fruits reached RR stage in stage while WT fruits took 15 days to attain RR Stage. Contrarily, all ripening phases were longer in *acs2-2* mutant. The *acs2-2* mutant fruit attained MG and BR stage with somewhat closer days. However post-breaker stage ripening was very slow in *acs2-2* mutant fruits. The mutant *acs2-2* fruits attained the red ripe stage in 20 days compared to 15 days for WT.

The observed ripening behavior of these two mutants was consistent with ethylene being prime regulator of tomato fruit ripening. The *acs2-1* fruits emit almost two-fold higher ethylene than the WT fruits while the *acs2-2* fruits emit 25% less ethylene than WT fruits. In tomato it is well established that during fruit ripening ethylene regulates the climacteric rise of respiration and associated biochemical and physiological change such as softening, color and aroma production (Oeller et al., 1991; Giovannoni, 2007). During system II rise of ethylene during in tomato fruit ripening it is believed that

increase in the levels of *ACS2* and *ACS4* activity is responsible for the burst of ethylene at the onset of ripening. However, above conclusions is basically derived from analysis of transcript level of these genes and directly correlation to respective enzyme activity of *ACS2* and *ACS4* has not been demonstrated.

The transgenic evidences favors role of ACS enzyme in regulating tomato ripening. Oeller et al. (1991) demonstrated that silencing of *ACS2* exhibited a marked inhibition in the ethylene production and delay in onset of fruit ripening and silenced fruits never turned red and soft. Similarly Gupta et al. (2013) demonstrated that silencing of three ACS isoform *ACS1A*, *ACS2* and *ACS6* substantially delayed the ripening. Several other evidences indicated that manipulation in ethylene biosynthesis or manipulation in perception and action of ethylene enhances the shelf-life of fruits (Oeller et al., 1991, Hamilton et al., 1990; Theologis et al., 1993; Xiong et al., 2005; Xie et al., 2006; Giovannoni, 2007). Our results are in conformity with these reports and provide additional evidence that mutations in *ACS2* affect the ripening attributes of tomato fruits. Till date no mutations in tomato *ACS* gene have been identified. The correlation of fruit ripening with reported *ACS2* mutations is first such report in tomato and add new perspectives to regulation of fruit ripening.

Consistent being an overproducer of ethylene, the *acs2-1* mutant fruits on-vine after attaining RR stage showed shorter life. The fruit skin after few days of RR stage started cracking on vine a mark of early senescence of on-vine ripened fruits. The cracking caused the loss of water and fruits underwent spoilage. Even the fruits without cracking of skin started losing water after 10 days of attaining RR Stage. On the other hand *acs2-2* mutant showed prolonged on-vine shelf-life of fruits compared to WT. The progress in softening of *acs2-2* fruits was very slow, and fruit remained firm and fresh up to 50 days after the breaker stage. Similarly, Gupta et al. (2013) reported that silencing of three ACS homologs *ACS2*, *ACS1A*, *ACS6* substantially increased the off-vine shelf life of fruits for ~45 days.

During ripening, a distinct change occurs in composition and texture in the cell wall of fruit. The up-regulation of genes regulating the cell wall disassembly such as *EXP1* (*Expansin1*), *PG* (*Polygalacturonase*), *TBG4* (*β-galactosidase4*) and *XTH5* (*a-xyloglucan endotransglucosylase/hydrolase5*) is associated with tomato fruit softening. The up-regulation of these genes is dependent on ethylene and induced during ripening (Brummell, 2006). Considering that expression of *EXP1*, *TBG4*, and *XET* is down regulated in ripening mutants such as *rin*, *nor*, and *Nr* fruits which are more firm confirm that the expression

of these genes are associated with fruit ripening (Smith et al., 2002; Brummell 2006). The reduced expression of *PG*, *EXP1*, *TBG4* and *XTH5* was also observed in chimeric RNAi lines of *ACS2-ACS1A-ACS6* genes (Gupta et al., 2013) consistent with reduced production of ethylene and enhanced shelf life of fruits. Though we have not examined it is likely that while in *acs2-1* mutant the cell wall disassembly is promoted, it is inhibited in *acs2-2* mutant. The decreased firmness in *acs2-1* mutant that minimized the shelf life of fruits might be due to up-regulation in activities of the cell wall modifying genes. On the other hand, in the *acs2-2* mutant reduction in activities of the cell wall modifying enzymes increased the firmness and enhanced the shelf life of fruits.

4.3.6 The *acs2-1* mutant shows increase in the levels of several phytohormones

Fruit ripening involves well-orchestrated coordination of several regulatory steps, which brings about subtle changes to the metabolic and physiological traits in ripening fruits (Klee and Giovannoni, 2011; Seymour et al., 2013). The ripening process involves the initiation of multiple genetic and biochemical pathways, however the molecular hierarchy of these regulators is not well understood. Many of these changes during ripening may be brought about changes in response to various hormones other than ethylene. Among the hormones the major ripening control seems to be achieved predominantly by ethylene and recent evidences favors a role for ABA too (Giovannoni, 2004; McAtee et al., 2013). In tomato and peach fruits, the maximum ABA content precedes the climacteric ethylene production. It has been shown that ABA promotes ripening by promoting ethylene biosynthesis through up-regulation of ethylene biosynthesis genes (Sun et al., 2012a). The *acs2-1* fruits showed increased levels of ABA and several of its phenotype may have relationship with increase in ABA level. In transgenic plants with RNAi silenced NCED shows 20% reduction in ABA levels which in turn leads to reduction in expression of several cell wall modifying enzymes (Sun et al., 2012a) and enhanced shelf life of fruit. It is likely that increase in ABA level in the *acs2-1* mutant promotes the activity of these enzymes and thus reduces the on-vine life of fruits. Likewise the lower level of ABA in *acs2-2* mutant fruit may have contributed to increase in the on-vine life of the mutant fruit. Alternately there seems to be interplay between ethylene and ABA during tomato fruit ripening and together these may have contributed to regulation of shelf life in *acs2-1* and *acs2-2* mutant fruit.

Few studies have reported that GA application delay fruit ripening in tomatoes, peach mango, sapota etc. (Dostal and Leopold, 1967; Martínez-Romero et al., 2000; Singh et al., 2007; Sudha et al., 2007). However GA reportedly plays a role during early tomato fruit development (De jong et al., 2009, Serrani et al 2007). In apple, mangoes, pears and tomatoes fruits the endogenous level of methyl jasmonate (MJ) increases with the progression of ripening (Fan et al., 1998). However in this study the GA level in the tomato fruit was below the detection level at all stages of ripening in both mutants and the wild type.

In tomato fruits, it is reported the jasmonates can regulate the lycopene formation independently of ethylene (Liu et al., 2012). In JA-deficient *def1* and *spr2* mutants, the lycopene content is significantly lower in the fruits, while overexpression of prosystemin that increases level of JA in turn enhances lycopene level. In this study the *acs2-1* mutant showed higher level of both JA and MeJA, which may have also influenced observed higher levels of lycopene and other carotenoids in the fruits.

The *acs2-1* mutant also show increase in the zeatin level at all stages of ripening. While cytokinin and ethylene can interact with each other at several levels, one of the levels is the regulation of ACS5 activity. In etiolated Arabidopsis seedlings though cytokinin induce the ethylene synthesis (Vogel et al. 1998) it is mediated not by increase in transcript levels rather by increasing the stability of ACS5 protein (Chae et al. 2003). The cytokinin likely block targeting of ACS5 protein for rapid degradation by the 26S proteasome (Wang et al. 2004). Though ACS2 protein is stable in *acs2-1* mutant, whether such a mechanism operates in *acs2-1* mutant remains to be investigated.

The role of hormones like salicylic acid has not been investigated in details in relation to fruit ripening. In the industry pre-treatments with methyl salicylate is used as a postharvest handling tool to reduce chilling injury of tomato fruit (Zhang et al., 2011). The available information on salicylic acid is limited to application of exogenous salicylic to MG or ripening fruits (Ding and Wang 2003), where the observed effects can be artefactual. The observed increase in salicylic acid level is first report in ripening tomato fruits. Though there is no direct evidence, but it can be speculated that the increase in endogenous salicylic acid in *acs2-1* mutant may have advantage as *acs2-1* tomato mutant lines would be less sensitive to chilling injury.

The observed increase in the hormonal level was specifically related to the *acs2-1* mutation and also showed a strong genetic linkage. For all the observed hormonal levels in *acs2-1* mutant were also similarly observed in the F_2 progeny of a genetic cross. The

homozygous F_2 mutant lines showed similar increase in the phytohormone levels, whereas homozygous wild type F_2 lines did not show such increase. It is therefore clearly evident that *acs2-1* mutation affects the levels of other hormones too and observed effect on ripening in addition to ethylene may involve other hormones too.

The influence of the *acs2-2* mutant on the phytohormone levels was largely opposite to that of *acs2-1* mutant. It can be assumed that the effect of *acs2-1* mutation on the physiological responses would be also opposite to those observed for *acs2-1* mutant and therefore are not discussed in details. Both mutations also influenced the levels of auxin but the RR stage the differences are not apparent with respect to the wild type and appears that IAA effect on the metabolism is mainly restricted at MG stage and diminishes during ripening.

4.3.7 The *acs2-1* mutant shows increased carotenoids levels in fruits

During tomato fruit ripening, development of red color is associated with the conversion of chloroplast to chromoplast with a concomitant increase in carotenoids levels consisting of mainly lycopene and β-carotene. An association between ethylene action and carotenoid accumulation is evident in *Nr* mutant of tomato that due to a dominant mutation in ETR3 ethylene receptor show reduced amount carotenoid accumulation in fruits (Lanahan et al., 1994). Several reports have indicated that during the ripening burst of ethylene is associated with increased expression of *PSY1,* which may contribute to increase in lycopene accumulation via phytoene and phytofluene (Bramley, 2002; Giovannoni, 2007). Oeller et al. (1991) reported that antisense suppression of *ACS2* gene in tomato inhibited the development of red color due to which reduced accumulation of lycopene. The reduction in the production of ethylene in fruits of chimeric RNAi ACSs line (*ACS2, ACS6, ACS1A*) was associated with reduced lycopene accumulation and expression of *PSY1* gene (Gupta et al., 2013). In addition to ethylene jasmonic acid also induces lycopene biosynthesis independently as well as in presence of ethylene (Liu et al., 2012).

Interestingly, in the *acs2-1* mutant fruit along with overproduction of ethylene and jasmonic acid levels are also upregulated. The *acs2-1* mutant also shows increased accumulation of carotenoids (especially lycopene) in *acs2-1* fruits than WT. It is likely that both ethylene and also JA may have contributed to above increase in the lycopene level. It is also likely that increase in the levels of carotenoids in this mutant may have contributed to the increase in ABA levels, as carotenoids serves as precursor for ABA (Nambara and Marion-Poll, 2005). The influence of *acs2-1* mutant on lycopene formation

is evident on all steps of precursor formation, which show increased accumulation of phytoene, phytofluene and ζ-carotene in the RR fruits.

Unexpectedly the fruits of *acs2-2* mutant also showed increased level of the lycopene in the fruits and thus had more carotenoid content in the RR fruits. On the other hand unlike *acs2-1* mutant it did not show any elevated levels of carotenoid precursors. The reason for the carotenoid accumulation in *acs2-2* mutant is not known but can be speculated. One of the reasons could be that the RR stage in *acs2-2* mutant is attained after nearly 20 days after BR stage. During this period the carotenoid synthesis continues and due to longer transition time from BR to RR stage it accumulate more carotenoids especially lycopene as in RR fruits of tomato preferentially accumulates lycopene. It is also reported the transgenic reduction of ABA level in tomato fruits improves the shelf life of fruits and also enhances the accumulation of carotenoids. This is consistent with the hormonal profiles of *acs2-2* mutant that shows reduced amount of ABA in the RR fruits.

Interestingly, lycopene content while substantially increased in *acs2-2* fruits, but no differences were observed in the accumulation of β-carotene in *acs2-2* fruits compared to WT. It is an intriguing observation that increased lycopene is usually associated with increased β-carotene level. The exact cause of this is not known. The climacteric increase in ethylene may arise from the interplay of various phytohormones. In a recent research Liu et al. (2012) reported that jasmonates (JA) induce the lycopene biosynthesis independently of ethylene formation in tomato fruits. This ethylene independent formation of carotenoids is restricted only to the formation of lycopene, not on the β-carotene. Since *acs2-1* mutant and also F_2 (M) plants emit high levels of ethylene and has high level of JA, it is likely that these two hormones may combinedly may have contributed to very high levels of carotenoids (lycopene) biosynthesis in our mutant fruit might be mediated by jasmonic acid (ethylene-dependent). Since lycopene is the most abundant carotenoid found in tomatoes it is regarded as the bioactive component alternative for the remedy of chronic diseases (Ford and Erdman Jr, 2012). Considering this the *acs2-1* mutant might be potentially useful for developing early maturing variety of tomato with high carotenoid content in fruit.

4.3.8 The total folate level is high in *acs2-1* mutant fruit

Folates represent all forms of vitamin B found in biological systems while folic acid is the synthetic form found in dietary supplements and fortified foods (Tamura et al., 2006). Iniesta et al. (2009) investigated the level of 5-methyltetrahydrofolate in

commercial raw tomato cultivar harvested in Murcia (Spain). They found the maximum level in Ronaldo cultivar, equal to 31.5 µg/100 g FW. In particular, folates have a role in various one-carbon transfer reactions, including purine and pyrimidine biosynthesis, amino acid metabolism, methylation of nucleic acids, proteins, and lipids (Lucock, 2000).

Due to the involvement of folates as a co-factor in various important biochemical reactions specially, in amino acids (methionine) metabolism and nucleotide (adenosine) biosynthesis, the folate levels were examined in *ACS* fruits. Interestingly the RR fruits of *acs2-1* mutant exhibited 1.5 fold increase (46-48 µg/100 g) in total folate level compared to WT while *acs2-2* fruits exhibited a folate level similar to WT fruits. The high folate level in *acs2-1* mutant fruits is correlating with high ethylene as well as increased ACS2 activity and elevated level of ACC.

4.3.9 The *acs2-1* mutation increases the flux of primary metabolites coupled to ethylene biosynthesis and respiration in fruit

The fruit ripening represent a critical period whereby traits, such as organoleptic composition are established and ultimately dictate the final quality of the fruit. Water, organic acids (primarily citrate and malate), and minerals accumulate inside the vacuole of expanding cells (Coombe, 1976) while starch accumulates transiently and is converted subsequently to reducing sugars (Wang et al., 1993). Organic acids are important components in tomatoes that strongly influence fruit taste and overall quality. Citric acid is the major fruit acid, followed by malic acid and several less abundant acids such as ascorbic acid, dehydroascorbic acid, citramalic, shikimic, fumaric, isocitric, succinic, lactic, maleic, saccharic, gluconic, gulonic and tartaric acids (Oms-Oliu et al., 2011). Shikimic acid, which is only detected and is highly abundant in very young fruit, is also a precursor for the biosynthesis of tryptophan, phenylalanine and tyrosine (Carrari and Fernie, 2006). Citric acid content increases with maturation up to a maximum during the postharvest stage, whereas malic acid concentration decreases during maturation and ripening (Oms-Oliu et al., 2011).

The major sugar and sugar alcohols in tomato fruit are glucose, fructose, sucrose, galactose and inositol, whereas maltose, raffinose, glucose-6-phosphate, mannitol and sorbitol are only present in minor concentrations (Oms-Oliu et al., 2011). As ripening commences, plastid-stored starch is converted to sugars such as d-glucose and d-fructose, which accumulate to levels above those required for respiration (Tucker, 1993). Both glucose and fructose occur in equal quantities in fruit during ripening (Oms-Oliu et al., 2011), which is generally attributed to invertase activity responsible for breaking down

sucrose (Richardson et al., 1990). As a result, ripe tomatoes have increased levels of fructose, glucose whereas sucrose levels decrease progressively during maturation and ripening of fruit. Galactose, galacturonic acid, and mannose have been identified as primary cell wall components associated with ripening-related softening. Their levels increase throughout maturation and ripening in parallel to the decreasing firmness (Oms-Oliu et al., 2011), indicating a breakdown of the cell wall complex (Oms-Oliu et al., 2011).

Oms-Oliu et al. (2011) demonstrated that concentrations of amino acids vary with different stages of maturity and ripening. Significant increases in glutamic and aspartic acid, methionine, phenylalanine and threonine are visible, whereas, at the same time, a reduction in levels of GABA, β-alanine, glycine and valine is shown throughout maturation and ripening. Other amino acids, such as asparagine, glutamine, leucine, isoleucine and serine increase at the breaker stages and decrease at subsequent postharvest stages. Besides fatty acids, free amino acids provide an important source of precursors for various aroma volatiles in tomato fruit, such as 2-phenylethanol, 2-isobutylthiazole, and phenyl acetaldehyde (Buttery and Ling, 1993). Finally, an increase in methionine is observed at the onset of ripening (Oms-Oliu et al., 2011). This can be understood given methionine is an important ethylene precursor (Adams and Yang, 1977). However, methionine levels continue to increase during postharvest storage when ethylene production drops again (Oms-Oliu et al., 2011).

An exhaustive study of primary metabolites in *nor*, *rin*, and *Nr* mutant of tomato was done by Osorio et al. (2011) and concluded that the levels of major sugars like glucose, fructose, and sucrose were reduced during development of fruit ripening in these mutants. During ripening the levels of few amino acids like Phe, Asp, Ile, Glu, and Ala were increased in these mutants whereas the levels of GABA, b-Ala, Thr, Ser, Gly, and Val were decreased during ripening. All three mutants displayed no alteration in their levels of malate and succinate across the studied period. Furthermore, levels of citrate and isocitrate changed significantly only in *nor*.

Interestingly, we reported the ACC as a primary metabolite in normal maturing *acs2-1* mutant fruit that is the clear indication of elevated level of ACC in our mutant, because till now nobody has reported ACC as a primary metabolite in normally maturing tomato fruits. After fine analysis and comparison of metabolites, it was observed that the level of major hexose sugars like glucose, fructose and galactose, and some organic acids like citric acid, ascorbic acid, and some amino acids such as aspartic acid, pyroglutamic

acid, glutamic acid and methionine was very high in red ripe stage of *acs2-1* mutant fruits than WT. But the expression level of some metabolites like malic acid, GABA (gamma amino butyric acid), serine, proline, 5-Oxoproline and phosphoric acid levels were found low to moderate in *acs2-1* mutant fruit as compared to WT. On the other hand, we did not detect ACC and methionine in *acs2-2* mutant fruits, and additionally the levels of malic acid, GABA (gamma amino butyric acid), serine, proline, and 5-Oxoproline were high compared to WT.

On the basis of primary metabolite expression level in our mutant we propose a model indicates the high expression level of intermediates related to ethylene biosynthesis resulted in the high ethylene emission from *acs2-1* mutant fruits. High ethylene level activates the TCA cycle and respiration rate that ultimately leads to early senescence in mutant compared to WT.

4.3.10 On-vine 1-MCP treatment reverting the primary metabolites levels in fruit

1-Methylcyclopropene (1-MCP) radically inhibits ripening of tomato fruit. The increase in ethylene production and internal ethylene concentration associated with the climacteric stage of ripening are delayed by 1-MCP treatment (Hoeberichts et al., 2002; Krammes et al., 2003; Opiyo & Ying, 2005). Other ripening processes that are inhibited include respiration (Colleli et al., 2003; Wills & Ku, 2002), color change and softening (Mir et al. 2004; Mostofi et al., 2003; Opiyo & Ying, 2005). Generally, 1-MCP treatment influences physicochemical changes of tomato fruit, as well as a reduction in decay, weight loss and extends storage life of the fruit. 1-MCP treatment of tomato fruit cv. Faustine F_1 significantly reduced respiration rate and ethylene production during storage, reduced natural weight loss during the storage period compared to the untreated fruit, and also showed storage potential and market value of tomato fruit depended on the treatment with 1-MCP, stage of maturity and storage temperature (Wrzodak and Gajewski, 2015).

On the basis of results obtained by on-vine treatment of 1-MCP on fruits, we can conclude that the treatment of 1-MCP can overcome the expression level of intermediates related to ethylene biosynthesis resulted in the low ethylene emission from *acs2-1* mutant fruits. Low ethylene level slowly down the TCA cycle and respiration rate that ultimately leads to delay ripening of fruits in the *acs2-1* mutant as well as in WT.

In this study, we reported the isolation of two mutant alleles of *ACS2* gene. The two missense mutations in *acs2-1* (Lys 100 to Arg) and (Val 352 to Glu) in α-helix of protein polypeptide chain likely increased stability of the ACS2-1 protein, leading to

higher ACS activity. The accumulation of ACS2 protein in mutant fruits resulted in an elevated level of ACC and ethylene emission as well as increase in ACS and ACO enzyme activities. *acs2-1* fruits also showed elevated levels of carotenoids and citric acid that accelerated fruit ripening and also resulted in accelerated senescence of fruits. Since *acs2-1* mutant ripens earlier, this allele can be used for developing early maturing tomato variety with high carotenoid content in fruit. *acs2-2* is a novel mutant with no mutation in the coding region but has two mutations in the promoter region and one mutation in the third intron. The mutations in promoter appear to reduce the accumulation of ACS2 protein in fruits, and mutant fruits emit a lower amount of ethylene. The lower level of ACS2 protein appeared to leads to lower ACC level and decreased ACS enzyme activity in fruits. In *acs2-2* mutant, the accumulation of carotenoids was higher than WT. Due to the high level of malic acid, the *acs2-2* mutant fruits showed delayed ripening and senescence with the long on-vine life of fruits. Taking this into account, the *acs2-2* mutant is an excellent allele for developing tomato with long shelf life and high lycopene content in the fruit.

CHAPTER 5

IDENTIFICATION AND CHARACTERIZATION OF NATURAL VARIANTS IN *ACS2* GENE BY ECOTILLING

5.1 Introduction

EcoTILLING is a modified TILLING strategy that is widely used for the detection of polymorphisms in target genes in natural populations (Comai et al., 2004). Similar to the pooling of DNA from a mutagenized population used for TILLING, the DNA from different natural accessions are pooled and examined for polymorphism by EcoTILLING against a reference cultivar. The DNA from natural accessions can be either mixed with reference cultivar DNA, or it can be mixed with different lines.

Similar to TILLING, EcoTILLING also employs cleavage of heteroduplex formed at the point of polymorphism by the action of mismatch specific endonucleases CEL I. The cut fragments are detected by any standard electrophoresis method such as agarose gel or polyacrylamide gel; capillary electrophoresis; HRM etc. EcoTILLING is a cost-effective technique as pooling and later de-convolution of samples is less critical, and also the number of individuals to be sequenced for each representative haplotype can be minimized.

Like TILLING, EcoTILLING has been widely employed in various plant species from Arabidopsis to the orphan crops for which genome sequences are not available like cassava, ground nut, millets, etc. (Till et al., 2007). EcoTILLING has been extensively used to identify the genetic variability in *Arabidopsis thaliana* (Comai et al., 2004), *Populus trichocarpa* (Gilchrist et al., 2008), *Vigna radiata* (Barkley et al., 2008), *Phaseolus vulgaris* (Galeano et al., 2009), *Musa* spp. (Till et al., 2010) etc. In addition to the identification of genetic variation, this technique has also been applied to detect new alleles that conferred biotic and abiotic stress in *Hordeum vulgare* (Mejlhede et al., 2006), *Oryza sativa* (Kadaru et al., 2006; Negrao et al., 2011), *Cucumis* spp (Nieto et al., 2007), *Solanum tuberosum* (Elias et al., 2009). In tomato, EcoTILLING has been used to identify novel alleles for *eIF4E* gene that confers resistance to viruses (Rigola et al., 2009) and also for improving the fruit quality (Bauchet et al., 2012).

Tomato though it is a new world crop plant, it is presently grown and consumed in almost all parts of the world. Domestication of tomato has led to the development of a large number of tomato cultivars and varieties differing in many morphological characters from leaf to fruit. Since tomato fruit is a rich source of health-promoting nutrients like lycopene and β-carotene (Paiva et al., 1999; Omoni et al., 2005) considerable efforts have been directed towards development of nutrient-rich tomato cultivars.

Notwithstanding the wealth of information generated using tomato mutants to date, majority of studies were conducted using either spontaneous mutants (that can be introgressed into local cultivars by repeated backcrosses to generate a pure line) or using transgenic lines for a set of genes of interest (which requires regulatory body approval and also has ethical issues). To avoid issues with genetically modified organisms (GMOs), high throughput techniques like EcoTILLING can be applied to natural accessions to identify alleles that can lead to the production of nutrient-rich tomatoes. The identification of a natural accession with high total soluble sugar content (Brix value) in tomato fruit (Bauchet et al., 2012) has set an example for improving the fruit quality using EcoTILLING.

EcoTILLING was first successfully applied in Arabidopsis ecotypes (Comai et al., 2004) and later was adopted for several species for analyzing natural variation such as in black cotton wood (Gilchrist et al., 2006), variation in resistance genes of barley (Mejlhede et al., 2006) and in Cucumis species (Nieto et al., 2007). Ibiza et al. (2010) reported identification of five new eIF4E variants related to potato virus Y-resistance responses through identification of SNPs in *eIF4E* genes in Capsicum. EcoTILLING in promoter sequences of 24 transcription factors in rice led to identification of genes associated with the drought tolerance index and level (Yu et al., 2012) and identification of three SNPs in two *FAE1* paralogs that were associated with low erucic acid (LEA) content in *Brassica rapa*, (Wang et al., 2010). In addition to its advantage of high throughput screening, multiple SNPs in an amplicon can also be detected through EcoTILLING.

In the present study, a large collection of natural accessions of tomato was examined to identify allelic variants. Our data provide the evidence for the functional relevance of *ACS2* in tomato fruit ripening and is also relevant for tomato breeding. This study also furthers our understanding of the role of *ACS2* in regulating fruit ripening and carotenoid accumulation in tomato.

5.2 Results

Taking in account the importance of *ACS2* gene in ethylene biosynthesis and in other morpho-physiological and developmental process, the nucleotide diversity for the gene was evaluated in a population comprising of 391 accessions (Appendix I).

5.2.1 EcoTILLING of tomato *ACS2* gene

A total of four primer sets **(Table 3.2)** were used to assess the natural variation in *ACS2* gene. All four primer sets were optimized for PCR amplification by touchdown PCR. PCR products were analyzed on polyacrylamide gel on Li-COR based system and polymorphisms were manually scored in accessions **(Fig. 5.1)**. Some of the accessions showed similar cleavage pattern while others were different. Multiple cleavage bands were detected in some lanes representing several polymorphic sites in an individual accession. Each SNP is defined as a unique fragment visible on the polyacrylamide gel, and the prominent bands were considered for haplotype classification.

5.2.1.1 Genotyping and sequencing of natural variants

Based on the similarities and differences observed on Li-COR gels, the *ACS2* variants were categorized into 30 haplotypes with the reference accession WT (AV) designated as HT0. The accessions showing similar SNP pattern were grouped into one haplotype. Each haplotype included a variable number of accessions exhibiting identical SNP pattern for *ACS2* gene. As expected, most accessions were similar to the reference cultivar and thus were included in the haplotype HT0. The accessions included in each haplotype are listed in **Table 5.1**. Haplotype 7 and 23 were represented by the maximum number (4) of accessions while the rest of the haplotypes were represented by 1-3 accessions. One representative genotype for each unique haplotype was sequenced on both the strands. The raw sequences were analyzed using the Chromas 2.4 software. Alignment of the variant sequences with reference cultivar helped in the identification of the exact position of the SNPs.

5.2.1.2 SNP data analysis of *ACS2* gene

Approximately 2.3 million bp (no. of individuals screened x total amplicon size) were screened using EcoTILLING. A total of 30 unique haplotypes were detected for *ACS2* gene using four amplicons covering complete *ACS2* gene. The PARSESNP analysis of the 30 haplotypes epresented the position of single nucleotide polymorphisms, insertions, and deletions. Most of the SNPs identified were present in the promoter and intronic region (**Fig. 5.2)**. All the polymorphisms in coding region were categorized into two categories- synonymous SNPs (S), that do not cause any

change in the amino acid by corresponding nucleotide encoded by the target gene and nonsynonymous SNPs (NS), which cause a change in the amino acid sequence. The haplotypes 7 and 15 shares maximum (10) number of nonsynonymous base change while haplotype 5, 10, 20, 22, 25 and 30 contains least (1) number of nonsynonymous base change. The SIFT scores for all the nonsynonymous changes were predicted to be tolerated except haplotypes 1 and 2; therefore, the function of ACS2 protein may not be affected drastically by these SNPs **(Table 5.2)**.

Apart from these observed nonsynonymous changes, we could identify a maximum of 12 synonymous SNPs in HT13 and a minimum of one synonymous SNP in HT6 respectively. The details of the position of the base change and the unaltered amino acids are listed in **Table 5.2**. In total, 264 SNPs and 11 INDELS were detected with a mean of 1 SNP/8.8 Kb and 1 INDEL/212.7 Kb. A total number of 99 nonsynonymous and 73 synonymous SNPs were identified upon EcoTILLING of *ACS2* gene. The number of SNPs observed for each possible base change was calculated including the INDELS **(Fig. 5.3A)**. The observed SNPs were categorized according to nucleotide substitution as either transition (C/T or G/A) or transversions (C/A or T/G). The percent of transitions was more than that of transversion **(Fig. 5.3B)**. Phylogenetic analysis of haplotype protein sequences was performed using ClustalX v2.1 and FigTree v1.3.1 software. After analysis, the haplotypes 1, 2, 4, 6, 16, 7, 3, 30 and 17 are very close relatives to reference cultivar AV compared to other haplotypes during the course of evolution **(Fig. 5.4)**.

5.2.1.3 Physiological and biochemical characterization of *ACS2* variant fruits

5.2.1.3.1 Fruit phenotyping of *ACS2* natural variants

The molecular and genetic studies in tomato suggest that *ACS2* and its isoform has a key role in ethylene biosynthesis and climacteric fruit ripening (Barry et al., 2000; Van de Poel et al., 2012; Gapper et al., 2013). Studies have also shown that manipulating tomato *ACS* and *ACO* isoforms can result in altered fruit ripening (Oeller et al., 1991; Gupta et al., 2013). To examine whether *ACS2* gene affects fruit morphology and ripening, the chronology of the fruit development of *ACS2* variants was examined in open field and the variations in fruit morphology were recorded using Tomato Analyzer compared to the reference **(Fig. 5.5)**. A total of nine fruit morphometric attributes like Fruit perimeter, Fruit area, Fruit max height, Fruit max width, Lobedness degree, Distal end protrusion, Shoulder height, Fruit shape triangle, and Fruit shape index were recorded by Tomato analyzer **(Fig. 5.6)**. **Figure 5.6** show that the perimeter and area of

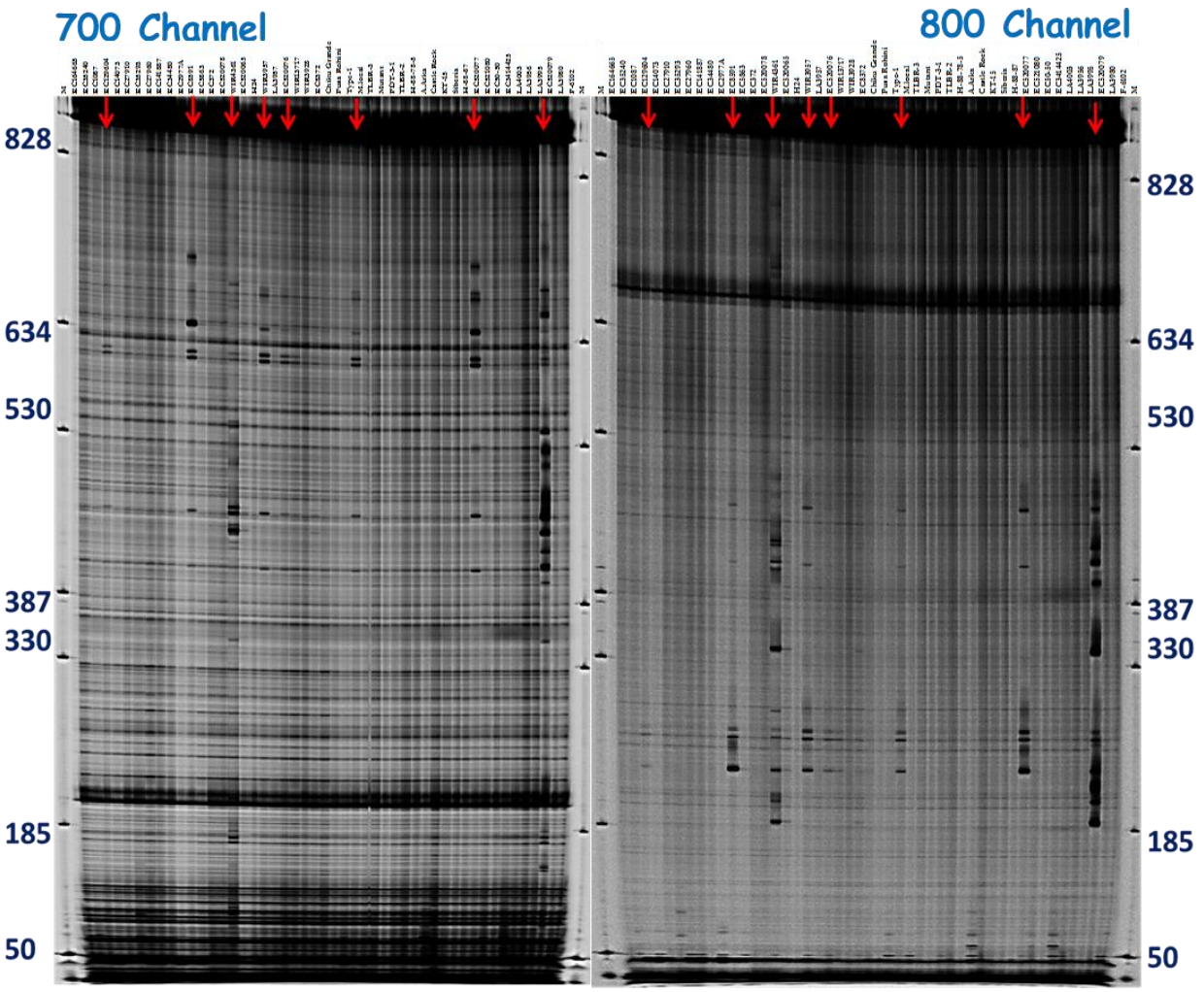

Figure 5.1. Detection of SNPs of *ACS2* gene in tomato accessions using EcoTILLING. The Li-COR gel analyzer images in IRD700 nm and IRD800 nm channel are shown for an 844 bp region of Exon 1-3 of *ACS2* gene. Each lane in a 48 well gel was loaded with CELI digested DNA from a unique accession. The accession lanes harboring SNPs are marked by red arrow heads. Complementary bands, one in IRD700 and another in IRD800 were observed for each polymorphism. The both sides of the image show DNA markers with respective sizes.

Table 5.1 The *ACS2* haplotypes in tomato accessions. The SNPs identified by EcoTILLING were confirmed by sequencing the *ACS2* gene. Based on the gene sequences, the polymorphisms were sorted into haplotypes.

Haplotypes	Accessions
HT0	Arka vikas (reference cultivar) and genotypes similar to reference
HT1	EC 487
HT2	EC 8936
HT3	EC 1087, EC 520076, Type 1
HT4	EC 520078
HT5	H 24, EC 520077, EC 520079
HT6	EC 528367
HT7	EC 546727, EC 529083, EC 528365, EC 520046
HT8	EC 1129
HT9	EC 26150, EC 27995
HT10	Azad No. 1
HT11	B7-120
HT12	DVKT-1
HT13	EC 252
HT14	EC 492
HT15	EC 2630
HT16	EC 2977
HT17	EC 3176
HT18	EC 3736
HT19	EC 20639
HT20	EC 25563, EC 521080
HT21	EC 89248
HT22	EC 326146
HT23	EC 520052, EC 521039, EC 529085, IIVR 164
HT24	EC 529086
HT25	EZ 521076, WIR 3768
HT26	IIHR 2201
HT27	IIVR 93
HT28	LA 0500
HT29	LA 2133
HT30	N 4241, Sankranti

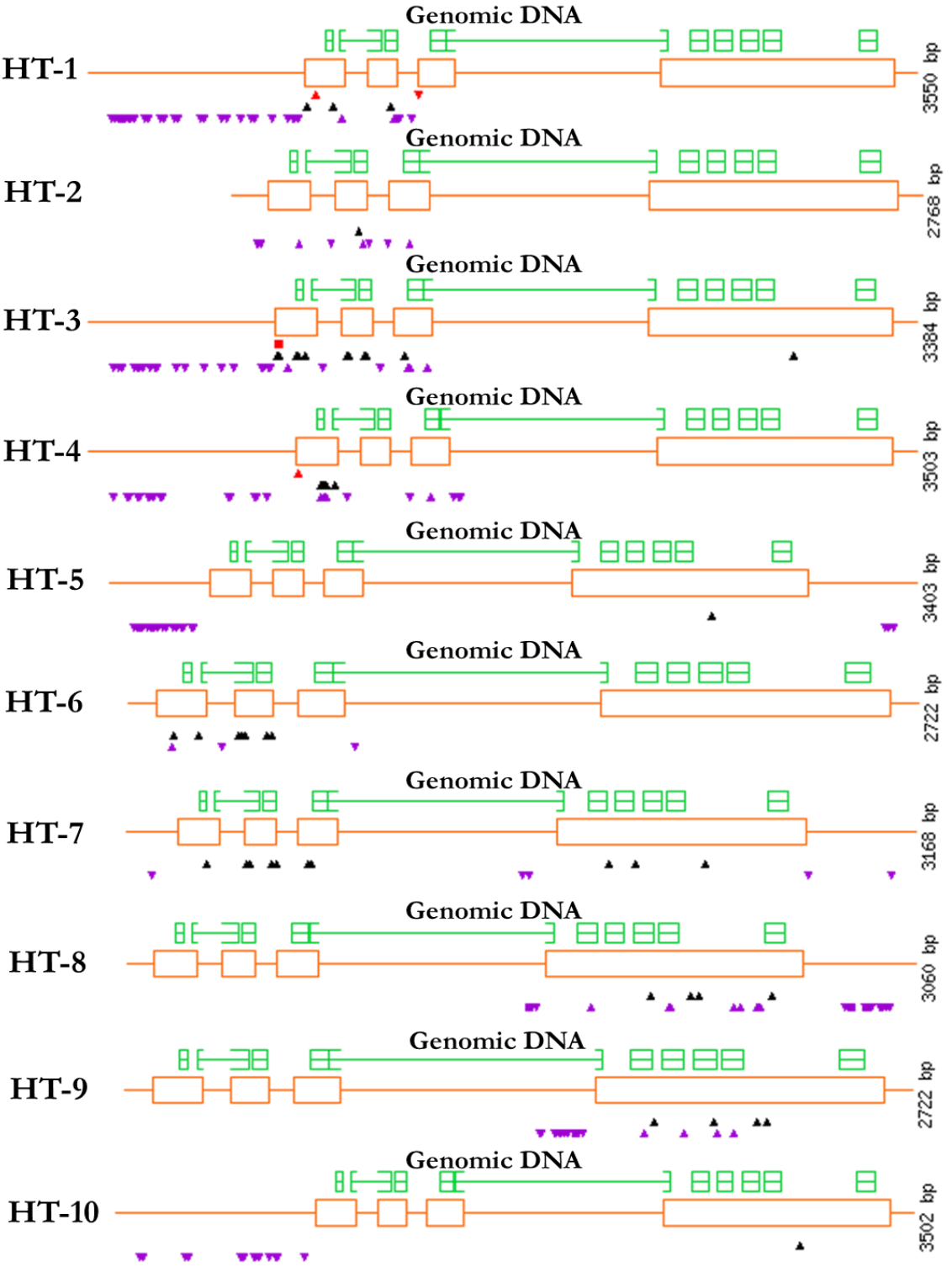
Genomic DNA
HT-1
3550 bp
Genomic DNA
HT-2
2768 bp
Genomic DNA
HT-3
3384 bp
Genomic DNA
HT-4
3503 bp
Genomic DNA
HT-5
3403 bp
Genomic DNA
HT-6
2722 bp
Genomic DNA
HT-7
3168 bp
Genomic DNA
HT-8
3060 bp
Genomic DNA
HT-9
2722 bp
Genomic DNA
HT-10
3502 bp

Continued…..

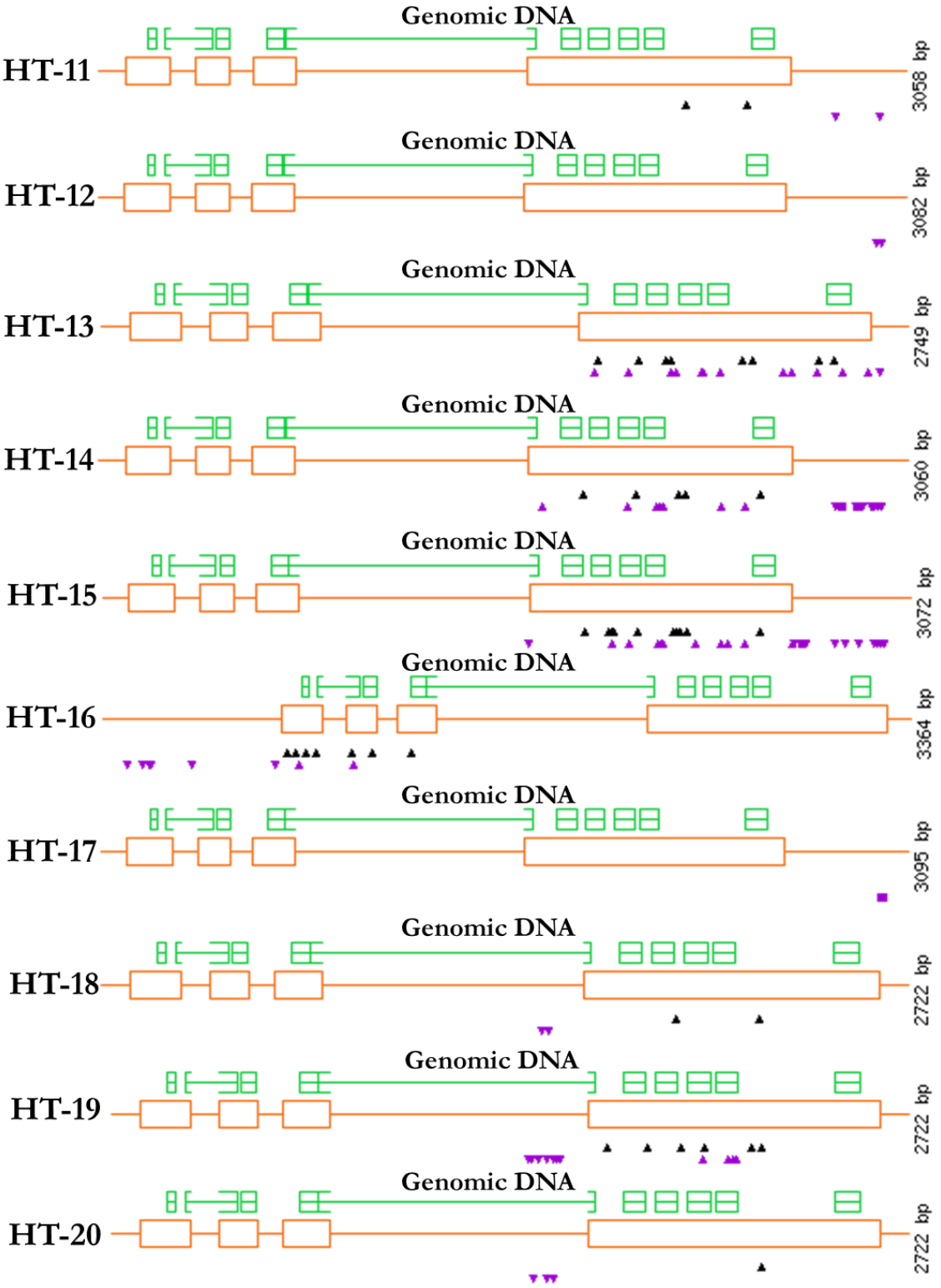
Genomic DNA
HT-11
3058 bp
Genomic DNA
HT-12
3082 bp
Genomic DNA
HT-13
2749 bp
Genomic DNA
HT-14
3060 bp
Genomic DNA
HT-15
3072 bp
Genomic DNA
HT-16
3364 bp
Genomic DNA
HT-17
3095 bp
Genomic DNA
HT-18
2722 bp
Genomic DNA
HT-19
2722 bp
Genomic DNA
HT-20
2722 bp

Continued…..

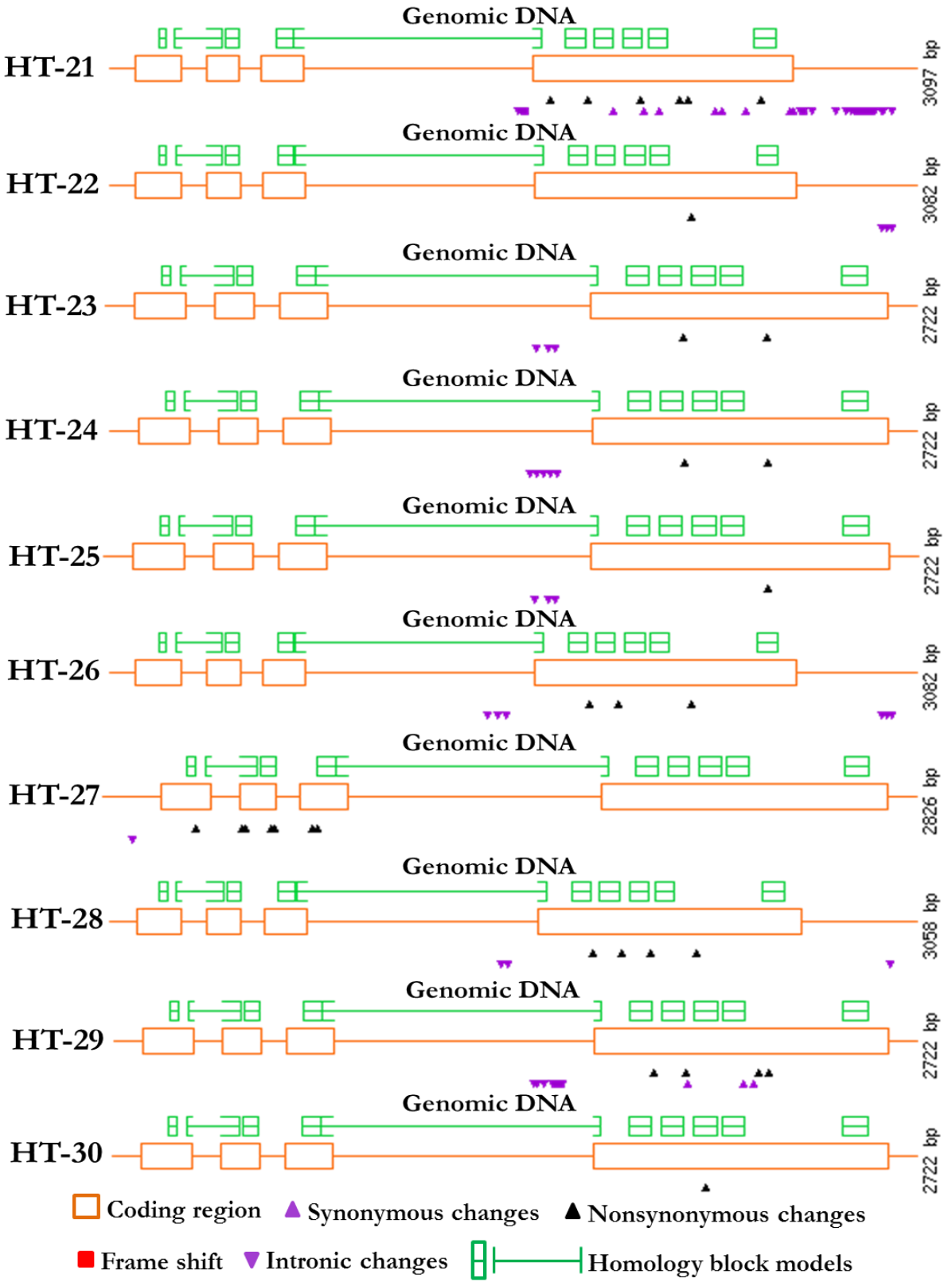

Figure 5.2. PARSESNP output files of the *ACS2* haplotypes. Open orange boxes denote exons interconnected with introns (solid line). A black upright triangle indicates NS changes in the DNA sequence that affect the amino acid s in the protein . A purple upright triangle indicates S changes that do not affect the amino acid. Purple downward triangles indicate nucleotide changes in introns. Red boxes represent the insertions or deletions. INDELs when present in coding region lead to the change in the reading frame.

Table 5.2 The *ACS2* haplotypes identified with the respective nucleotide and amino acid changes.

Haplotype	No. of SNPs	Base change	Amino acid change	Sift score	Accessions Harbouring SNPs	Nature of the SNPs
HT0	-	-	-	-	-	-
HT1	Multiple	G3058A T3099A A3174C T3214C T3418C C3435A A3458G A3508G A3537T	M1I L15* H40P L53= F89L G94= Intron Intron Splice junction	0	1	NS NS S NS S
HT2	Multiple	T3178C G3305A T3418C C3435A A3458G A3533T T3622C	P41= Intron F89L G94= Intron Intron T128=	0	1	S NS S S
HT3	Multiple	T3063C A3068G T3070: T3109C T3138G T3146G C3179A T3247A A3345T T3353G C3417A A3428T T3484A A3583T A3598G T3604G A3676G T5174A	F3S I5V Frameshift N18= F28C W31G L42I Intron E64D I67S N88K Y92F Intron R115S R120= V122= L146= V352E	0.32 0.60 0.73 0.93 0.59	3	NS NS S NS NS NS NS NS NS NS NS S S S NS
HT4	Multiple	G3059T C3157T A3159G A3165T C3168T C3172T A3174C T3178C C3179T C3216A A3268C A3533T T3622C T3715C A3736G A3742T	G2* Y34= D35G D37V P38L F39= H40P P41= L42= A54D Intron Intron T128= Intron Intron Intron	0.52 0.38 0.34 0.28	1	S NS NS NS S NS S S NS S

Continued…..

Haplotype	No. of SNPs	Base change	Amino acid change	Sift score	Accessions Harbouring SNPs	Nature of the SNPs
HT5	1	T5174A	V352E		3	NS
HT6	Multiple	T3106A G3113A G3197T T3276A G3334A G3346A G3359A T3432G G3449A A3733T	T17= E20K V48F Intron D61N D65N R69K H93Q R99K Intron	 0.21 0.41 1.00 0.68 0.28	1	S NS NS NS NS NS NS NS
HT7	Multiple	A3174C G3334A G3346A T3432G G3449A G3576A G3593A A4437G G4465A G4786C A4895C T5174A	H40P D61N D65N H93Q R99K R113K E119K Intron Intron V223L E259A V352E	0.21 0.41 0.68 0.28	4	NS NS NS NS NS NS NS NS NS NS
HT8	Multiple	T4513TTT A4518G T4539G G4752A A4987G A5055T G5061T G5138C T5174A T5304C T5334C T5394C G5403T A5413C T5452G	Intron Intron Intron L211= I290V T312= T314= G340A V352E L395= C405= I425= A428= R432= S445A	 1.00 0.32	1	 S NS S S NS NS S S S S S NS
HT9	Multiple	T4389A T4393C A4437G T4443C T4456A G4465A G4476A G4486A T4513TTT A4518G T4539G G4752A G4786C C4887T A4987G C5004T G5061T G5138C T5174A	Intron Intron Intron Intron Intron Intron Intron Intron Intron Intron Intron L211= V223L I256= I290V D295= T314= G340A V352E	 1.00	2	 S NS S NS S S NS NS

Continued…..

Haplotype	No. of SNPs	Base change	Amino acid change	Sift score	Accessions Harbouring SNPs	Nature of the SNPs
HT10	1	T5174A	V352E		1	NS
HT11	2	T5174A C5410T	V352E R431W		1	NS NS
HT12	-	-	-	-	1	-
HT13	Multiple	C4632T A4645G G4752A G4786C A4876G T4893C C4897A C4911T C5001T C5004T G5061T G5138C T5174A A5274G T5304C T5394C G5395A T5452G G5478A T5566C	H171= N176D L211= V223L I253V D258= Q260K Y264= N294= D295= T314= G340A V352E L385= L395= I425= A426T S445A K453= L483=	0.65 0.32 	1	S NS S NS NS S NS S S S S NS NS S S S NS NS S S
HT14	Multiple	C4632T G4786C A4953G A4987G G5061T G5076C A5085G A5149G T5174A T5304C T5394C T5452G	H171= V223L K278= I290V T314= A319= L322= K344E V352E L395= I425= S445A	1.00 0.32	1	S NS S NS S S S NS NS S S NS

Continued…..

Haplotype	No. of SNPs	Base change	Amino acid change	Sift score	Accessions Harbouring SNPs	Nature of the SNPs
HT15	Multiple	G4570A G4786C A4876G C4887T G4891A C4897A A4953G A4987G G5061T G5076C A5085G G5125T G5138C A5149G T5174A G5205T T5304C A5331G T5394C T5452G A5577G	Intron V223L I253V I256= D258N Q260K K278= I290V T314= A319= L322= A336S G340A K344E V352E A362= L395= E404= I425= S445A *486=	0.65 1.00 0.32	1	NS NS S NS NS S NS S S S NS NS NS NS S S S S NS S
HT16	Multiple	A3081G G3113A G3130C G3158A G3197T G3346A G3357A T3432G G3593A	N9S E20K S25= D35N V48F D65N K68= H93Q E119K	0.48 0.41 0.68	1	NS NS S NS NS NS S NS NS
HT17	-	-	-	-	1	-
HT18	Multiple	A4437G G4465A A4895C T5174A	Intron Intron E259A V352E		1	 NS NS
HT19	Multiple	C4378T T4389A T4410C A4437G A4442G C4462G G4465A G4476A T4488A A4645G G4786C C4897A T4974C G4978A G5061T G5076C A5085G G5138C T5174A	Intron Intron Intron Intron Intron Intron Intron Intron Intron N176D V223L Q260K F285= V287I T314= A319= L322= G340A V352E	0.53	1	 NS NS NS S NS S S S NS NS

Continued…..

Haplotype	No. of SNPs	Base change	Amino acid change	Sift score	Accessions Harbouring SNPs	Nature of the SNPs
HT20	Multiple	C4396T A4437G G4465A T5174A	Intron Intron Intron V352E		2	 NS
HT21	Multiple	A4523T A4548CT A4645G G4786C C4887T A4987G C5004T G5061T G5138C T5174A A5274G T5304C T5394C T5452G T5566C A5577G	Intron Intron N176D V223L I256= I290V D295= T314= G340A V352E L385= L395= I425= S445A L483= *486=	 1.00 0.32 	1	 NS NS S NS S S NS NS S S S NS S S
HT22	1	T5174A	V352E		1	NS
HT23	Multiple	T4397C A4437G G4465A A4895C T5174A	Intron Intron Intron E259A V352E		4	 NS NS
HT24	Multiple	A4371G C4396T G4418A A4437G G4465A A4895C T5174A	Intron Intron Intron Intron Intron E259A V352E		1	 NS NS
HT25	Multiple	C4396T A4437G G4465A T5174A	Intron Intron Intron V352E		2	 NS
HT26	Multiple	C4396T A4437G G4465A G4786C A4895C T5174A	Intron Intron Intron V223L E259A V352E		1	 NS NS NS

Continued…..

Haplotype	No. of SNPs	Base change	Amino acid change	Sift score	Accessions Harbouring SNPs	Nature of the SNPs
HT27	Multiple	A3174C	H40P			NS
		G3334A	D61N	0.21		NS
		G3346A	D65N	0.41		NS
		T3432G	H93Q	0.68	1	NS
		G3449A	R99K	0.28		NS
		G3576A	R113K			NS
		G3593A	E119K			NS
HT28	Multiple	A4437G	Intron			
		G4465A	Intron			
		G4786C	V223L		1	NS
		A4895C	E259A			NS
		G5002A	D295N			NS
		T5174A	V352E			NS
HT29	Multiple	A4379C	Intron			
		T4389A	Intron			
		T4410C	Intron			
		C4412T	Intron			
		A4437G	Intron			
		T4456:	Intron			
		T4457:	Intron			
		G4465:	Intron			
		T4466:	Intron		1	
		T4467:	Intron			
		G4476A	Intron			
		G4786C	V223L			NS
		G4894C	E259Q			NS
		G4899A	Q260=			S
		G5088A	S323=			S
		A5121G	E334=			S
		G5138C	G340A			NS
		T5174A	V352E			NS
HT30	1	G4960C	G281R	0.23	2	NS

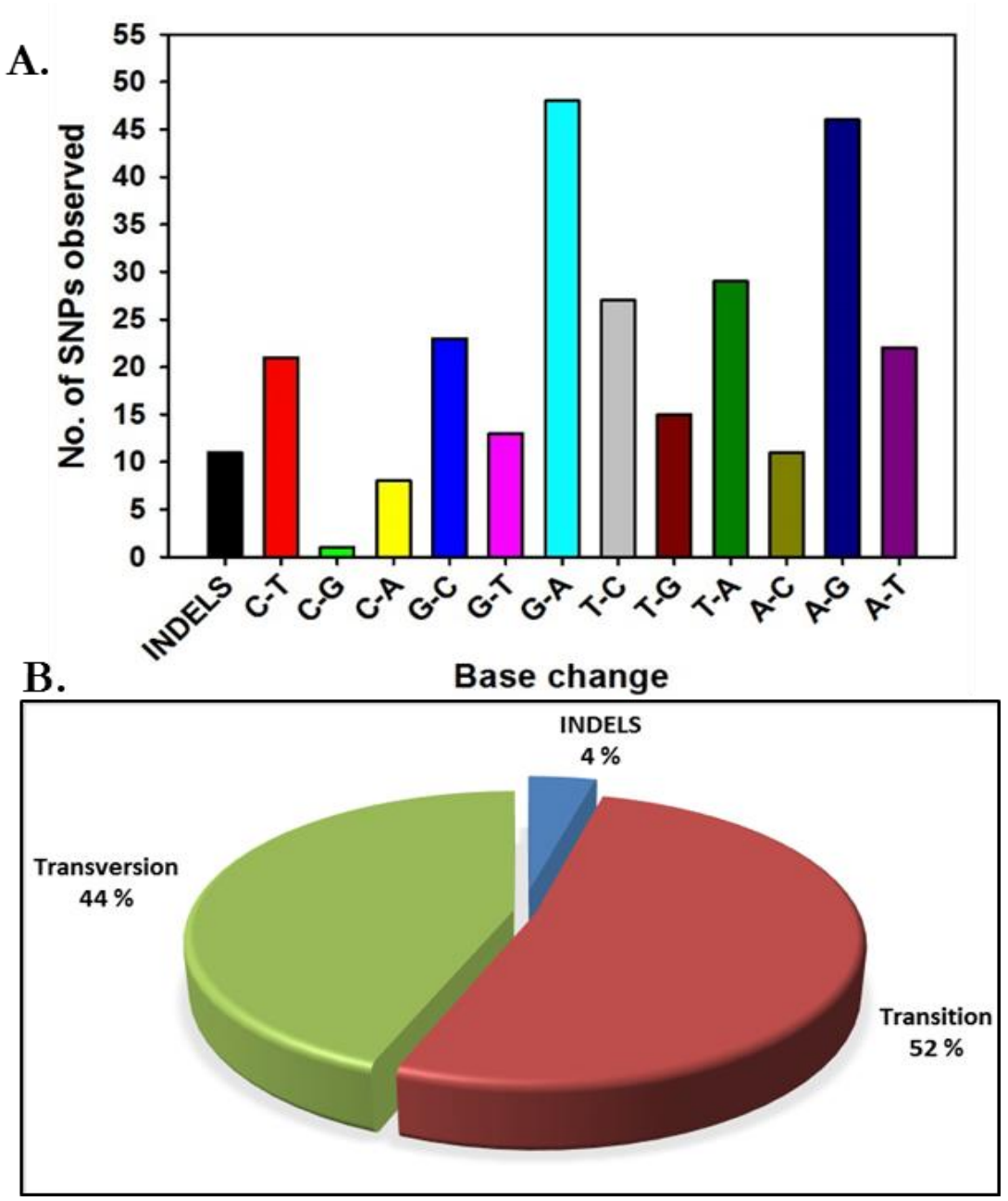

Figure 5.3. The distribution of SNPs in *ACS2* gene. **A**, frequency of the type of nucleotide base changes observed and **B**, frequency of different types of base changes.

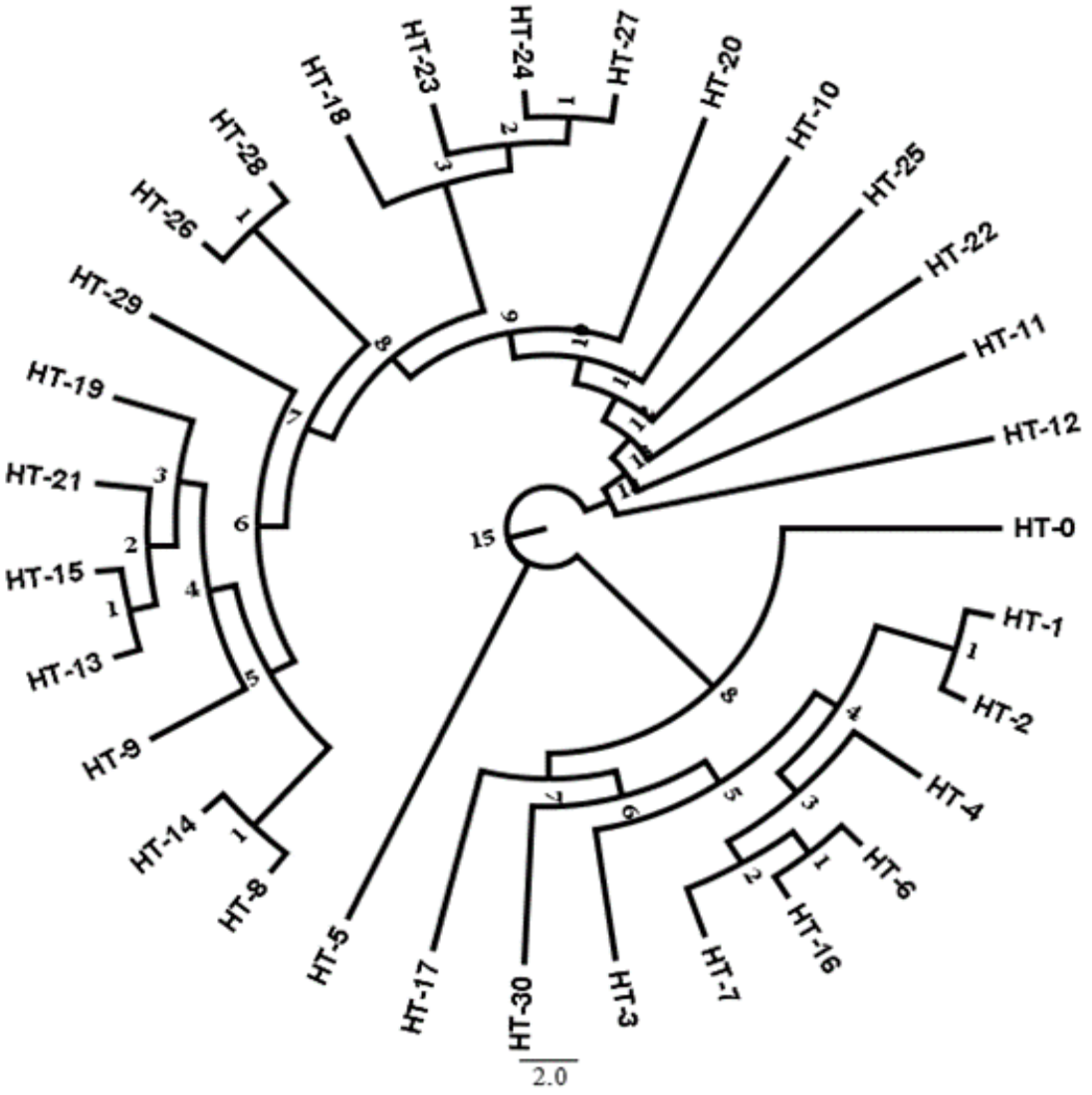

Figure 5.4. Phylogram representing the clustering of different haplotypes of ACS2 protein. The phylogram combines the phylogenetic relationships between the *ACS2* haplotypes and reference cultivar analyzed which were obtained by maximum likelihood. Branch lengths are not in proportion to evolutionary times.

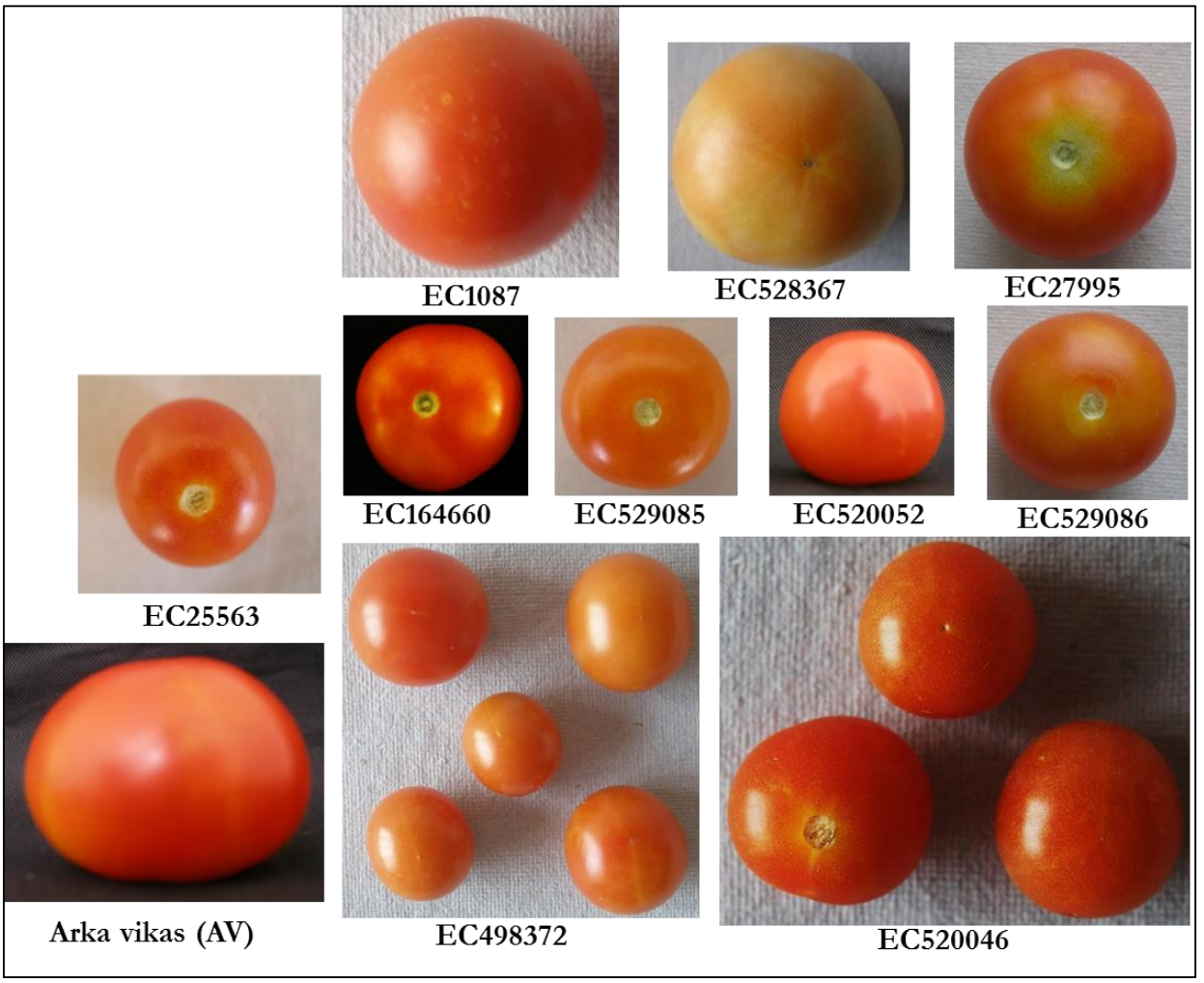

Figure 5.5. Comparison of fruit morphology of different *ACS2* natural variants with reference AV. Fruits were harvested from the second truss of the vine.

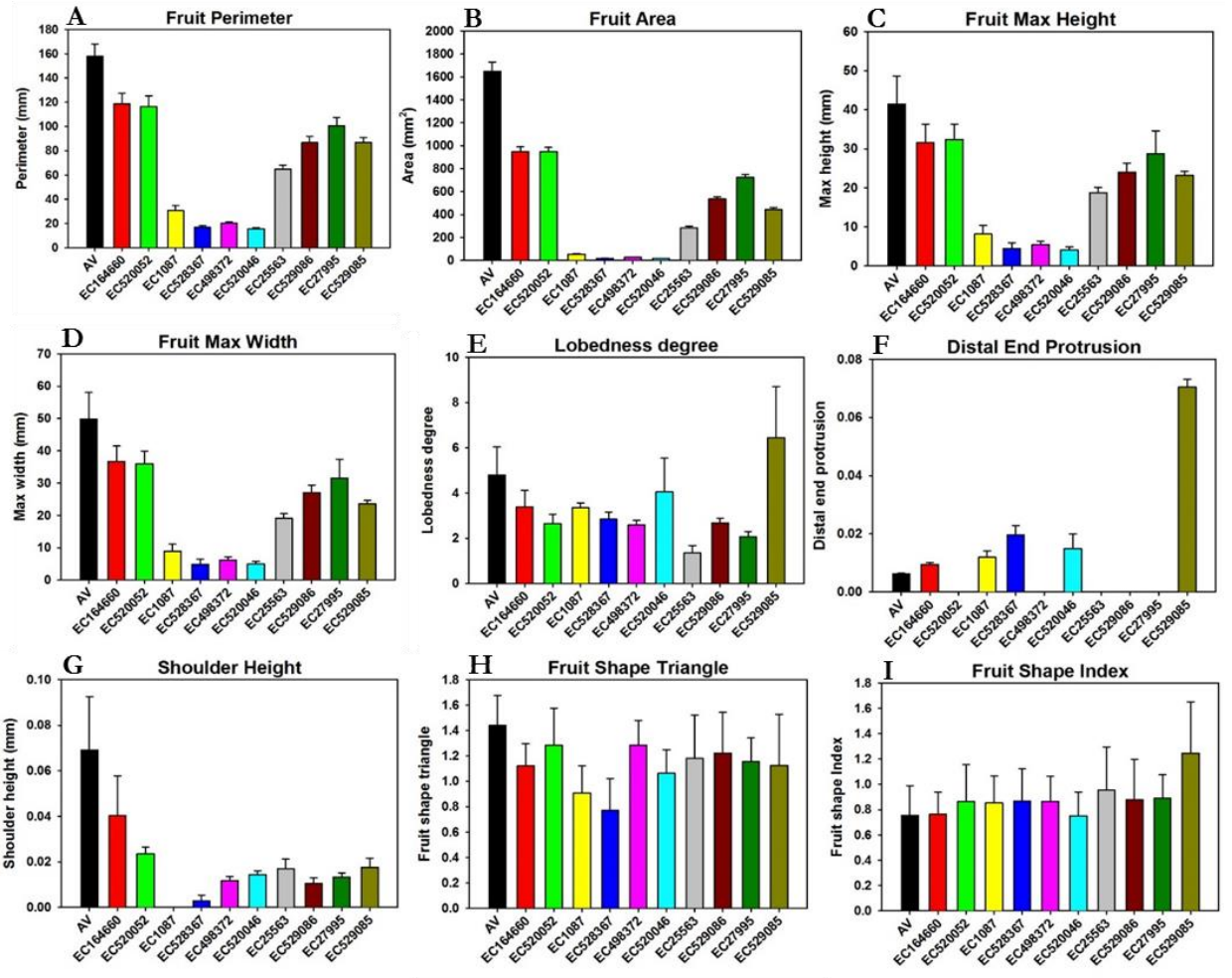

Figure 5.6. Comparisons of fruit morphometric attributes of *ACS2* natural variants using Tomato Analyzer. Fruits were harvested at RR stage, cut longitudinally into two halves and cut surfaces was scanned. Scanned JPEG images of tomato were opened in Tomato Analyzer software and various fruit morphometric attributes were calculated.

fruits of EC1087, EC526367, EC498372, and EC520046 lines were less than half compared to AV. The fruit shape index for EC25563 is close to one which resulted in the round nature of the fruit compared to AV **(Fig. 5.6I)**.

5.2.1.3.2 Ethylene estimation of *ACS2* variant fruits

ACS2 is a key gene responsible for ethylene emission and climacteric ripening of tomato fruits. To examine the effect of SNPs in ACS2 activity of natural variants, we measured the ethylene emission from the RR fruits of variants. The fruits of accessions EC20639, EC1087, EC520046, and EC498372 showed higher level of ethylene emission compared to AV. On the other hand, the fruits of EC6875 and EC529086 emitted comparatively decreased ethylene **(Fig. 5.7)**.

5.2.1.3.3 Carotenoids profiling of *ACS2* variant fruits

One of the main characteristics of tomato (*Solanum lycopersicum*) fruit ripening is a massive accumulation of carotenoids (mainly lycopene), which may contribute to the nutrient quality of tomato fruit and its role in chemoprevention. Previous studies have shown that ethylene plays a central role in promoting fruit ripening. Recent studies indicate that jasmonic acid also plays a positive role in lycopene biosynthesis independently of ethylene as well as in presence of ethylene (Liu et al., 2012). Fruit carotenoids and xanthophyll profiling was done at different maturity stages. A total of seven carotenoids (phytoene, phytofluene, lycopene, lutein, ϒ-carotene, β-carotene, and violaxanthin) were detected in RR fruits **(Fig. 5.8)**. The RR fruits of EC520076 and EC529085 variants exhibit significant increased level of total carotenoids, especially lycopene, compared to reference AV fruits **(Fig. 5.8)**.

5.2.1.3.4 Folate profiling of *ACS2* variant fruits

Folates represent all forms of vitamin B found in biological systems while folic acid is the synthetic form found in dietary supplements and fortified foods (Tamura et al., 2006). Iniesta et al. (2009) investigated the level of 5-methyltetrahydrofolate in commercial raw tomato cultivar harvested in Murcia (Spain). They found the maximum level in Ronaldo cultivar, equal to 31.5 μg/100 g FW. In particular, folates have a role in various one-carbon transfer reactions, including purine and pyrimidine biosynthesis, amino acid metabolism, methylation of nucleic acids, proteins, and lipids (Lucock, 2000). Based on the previous study we were intended to check the folate levels in our *ACS2* variants fruits. Using LC-MS, we estimated the total folates in green and red tomato fruits of variants and AV **(Fig. 5.9)**. A significantly increased level of total folate was observed in EC27995, EC520046, IIHR2201, and Sankranti variant lines compared to

AV fruits. Out of these lines, EC520046 and IIHR2201 fruits also exhibit more than two-fold of total carotenoids level in MG and RR stages compared to AV fruits **(Fig. 5.9)**.

5.3 Discussion

We established EcoTILLING using a collection of 391 tomato accessions representing the natural gene pool of *Sonalum lycopersicum*. In this study, we screened the allelic variation in *ACS2* gene that is a component of ethylene biosynthesis pathway. Further, we identified haplotypes that may be associated with altered ethylene emission, enhanced fruit carotenoids and folate content, which in turn might be useful for the development of nutritionally enriched tomato cultivar.

5.3.1 Detection of polymorphisms by EcoTILLING

EcoTILLING protocols for SNP detection was similar to that used for TILLING. Since EcoTILLING identifies SNPs across genes, plants bearing the unique fragments with their complementary fragments in another channel (considered as a SNP) were grouped according to size and pattern. While the pattern of fragments could be used for grouping of haplotype, a single accession/few accessions confirm precise location of SNPs in the accessions, were sequenced to know the exact number and position of the SNPs. Occasionally, due to mispriming, weak fluorescence towards top of each lane and sometimes due to increased noise at the bottom of the gel, false positives may also show up in EcoTILLING (Till et al., 2006a; Till et al., 2010). With a 1:1 (reference DNA: DNA from the natural accession) pooling strategy for EcoTILLING, the errors could be minimized and improving the stringency of detecting SNPs. Several accessions showed multiple cleavage patterns that could have arisen by the presence of nearby polymorphic sites, insertions and deletions. Though LI-COR analysis of some accessions showed only one cleaved product, however, sequencing of such accessions revealed the presence of more than one SNP. This may be due to the possibility that if bands were cleaved at both ends, they would not fluoresce and, therefore, cannot be detected on LI-COR system (Liang, 2011). In spite of these minor drawbacks in LI-COR based detection of SNPs, results showed that EcoTILLING is a suitable and cost effective method for identification of SNPs in tomato.

5.3.2 Single Nucleotide Polymorphisms in tomato *ACS2* gene

Nearly 44 tomato accessions showed polymorphisms for *ACS2* gene. Based on the cleavage pattern of PCR products on the LI-COR gel, these accessions were classified into 30 haplotypes. Interestingly, most of the SNPs were observed in the

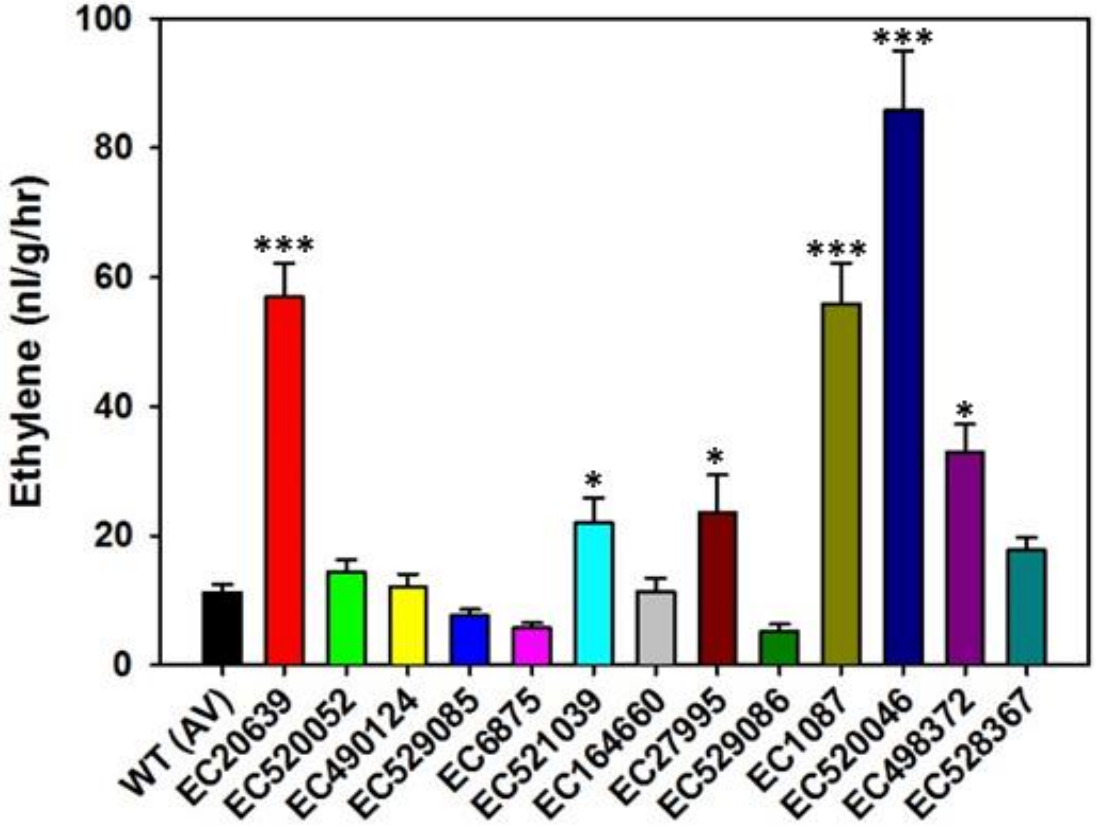

Figure 5.7. Comparisons of the ethylene emission at red ripe (RR) stages of fruits of AV and *ACS2* variants. The fruits of AV and different variants were harvested from the second truss of the vine. Each value is the mean of three biological replicates. (Student's t-test; * for $P \leq 0.05$, ** for $P \leq 0.01$ and *** for $P \leq 0.001$).

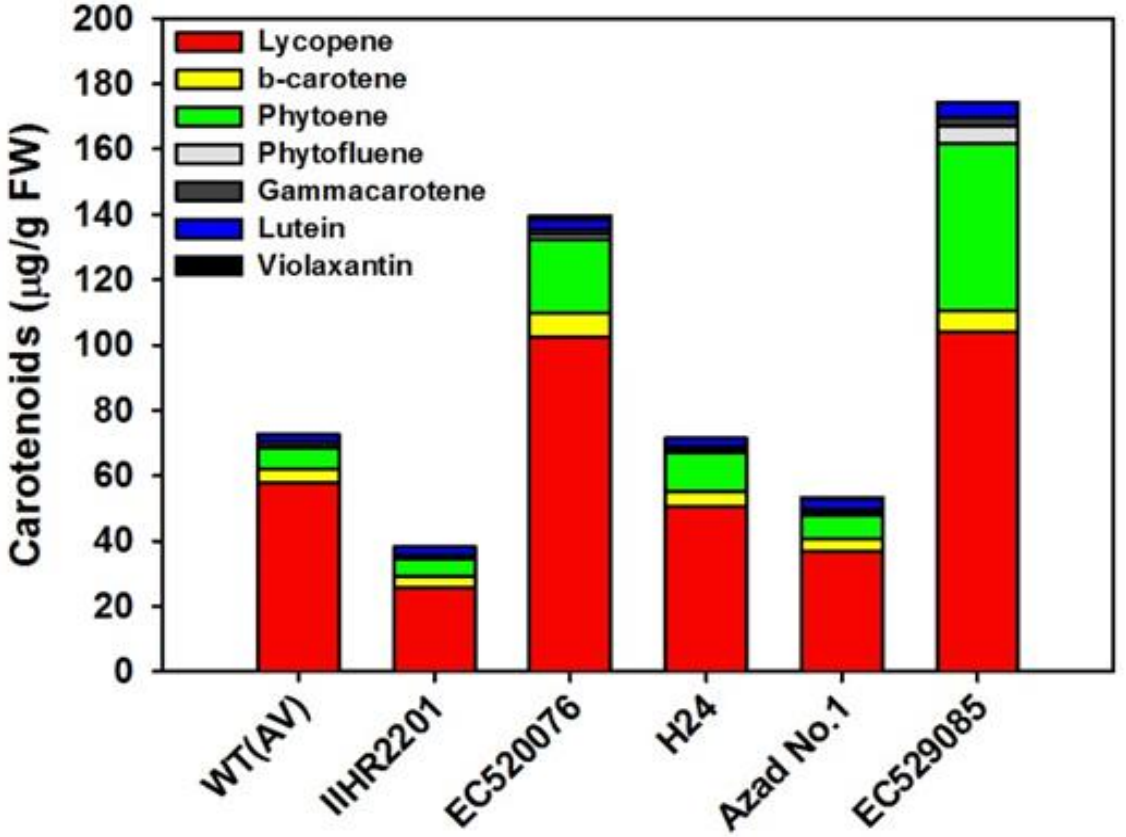

Figure 5.8. Carotenoids and xanthophyll profiling of RR fruit tissue of AV and *ACS2* variants. Stacks bar graph representing the comparison between total carotenoids content of WT (AV) and different EcoTILLING lines of tomato. Each value is the mean of five biological replicates.

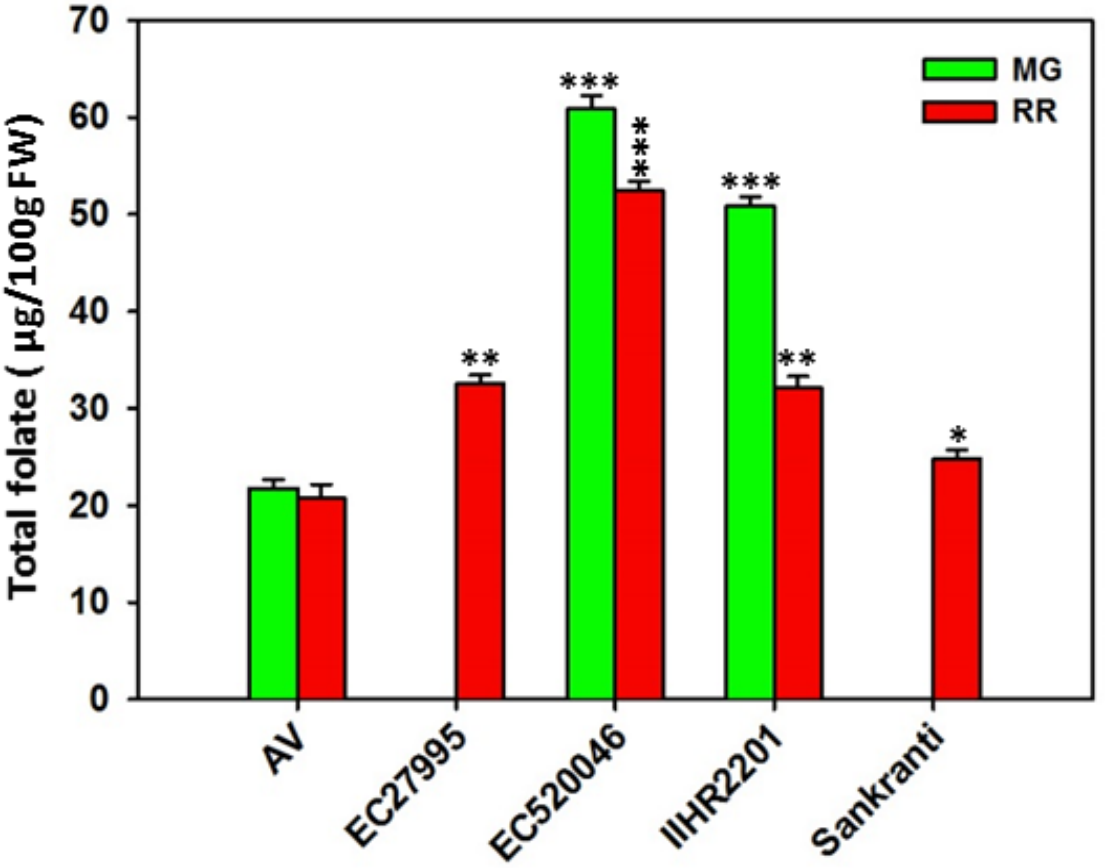

Figure 5.9. Total folate quantification at MG and RR fruit tissue of AV and variants using LC-MS. Results are average of three to five biological replicates. (Student's t-test; * for $P \leq 0.05$, ** for $P \leq 0.01$ and *** for $P \leq 0.001$).

promoter and introns. In the coding region, only 99 nonsynonymous and 73 synonymous SNPs were identified. Above result is consistent with that obtained from sequencing of large number cultivars, where only 10% SNPs are located in the coding region (Aflitos et al., 2014). The SIFT scores for the nonsynonymous SNPs were not appreciable, signifying that these changes do not alter the protein drastically.

Two accessions of *ACS2* gene (EC520076 and EC529085) showed a significant increase in total carotenoid content and EC520046 and IIHR2201 variants exhibited increased total folate level at the red ripe stage. It is known that manipulations in *ACS2* gene can affect the nutritive value of tomato fruits (Oeller et al., 1991; and Gupta et al., 2013). Among the accession analyzed, *ACS2* variants, EC520076, EC529085, EC520046 and IIHR2201 appear to be potential candidates to improve the tomato fruit quality.

5.3.3 The *ACS2* variants - a functional relevance for fruit ripening

Fruit ripening is a complex process regulated by many regulators. Ethylene biosynthesis and signaling confer a major regulation apart from the genetic hierarchy that has been elucidated to be controlled by transcription factors like RIN/MADS or SBP/CNR. Tomato fruit ripening is associated with the accumulation of carotenoids- which are health promoting compounds. Many transgenic approaches were used to characterize the biosynthetic genes of the carotenoid pathway (Just et al., 2007; Zhu et al., 2008). The availability of natural ripening mutants in tomato had facilitated the molecular understanding of fruit ripening process (Osorio et al., 2011; Gapper et al., 2013). It is a complex process regulated by many regulators. The phenotype may come from other genes too, as these are natural accessions. To confirm genotype and phenotype relationship we have to make crosses.

In spite of nucleotide diversity of 1 SNP/8.8 Kb for *ACS2* gene in EcoTILLING, only few alleles were identified with promising phenotypes. Gady et al., 2012 studied 258 tomato lines for the genes involved in sugar metabolism. The frequency of polymorphism observed in this study was low, i.e. out of 20 targeted genes; only 6 of them were found to harbor SNPs. Another study by Rigola et al. (2009) also found a low level of polymorphism in tomato lines from EU-SOL collection. In consistent with the low frequency of polymorphisms observed in tomato, our study also showed that the natural diversity for the *ACS2* gene is low. This low frequency might be due to the recalcitrance of tomato genome to polymorphisms or due to the importance of the genes that were considered for the study. More particularly, the ACS2 is a key enzyme in ethylene biosynthesis pathway and is important for fruit ripening and plant development.

Nevertheless, we identified novel alleles for the *ACS2* that can be useful for the development of an elite tomato cultivar with enhanced carotenoid and folate contents.

CHAPTER 6

NUCLEOTIDE DIVERSITY ANALYSIS OF *ACS2* GENE IN WILD RELATIVES OF TOMATO

6.1 Introduction

Wild relatives of a crop species are the ancestors or closely related taxa that originated at distinct geographic locations but share a common gene pool. These wild species grow in different habitats that endow them with special features to tolerate a myriad of environmental and climatic changes. Latest estimates report that there are between 50,000-60,000 crop wild relatives in the wild (Maxted and Kell, 2009), and their genetic potential remains to be utilized for crop improvement.

A significant increase in crop production was brought about by the green revolution in the 1960s and 1970s. It was largely based on the discovery of new genes in the traditionally grown landraces. Presently, with increasing concerns about climate change and its effects on agriculture, there is a high demand for ensuring food security. It has been stated that the development of new crop varieties or cultivars is required to achieve this goal (Lobell et al., 2008). This demand has promoted the quest for the search of novel genes and gene systems present in the wild relatives. The studies on wild relatives also provide us information about the evolutionary relationships of the genes and the different changes that have taken place as a part of natural selection.

Traditionally, wild relatives contributed significantly to improve food production through conventional breeding programs. Development of Asian rice with resistance to grassy stunt virus is one of such examples of unlocking the potential of wild relatives coupled with biotechnology (Prischmann et al., 2009). The gene responsible for resistance from *Oryza nivara*, a wild rice species was introgressed into many rice cultivars (Prischmann et al., 2009). A similar survey for disease resistance against western corn rootworm in maize and fusarium wilt in banana identified wild relatives that possessed the resistance trait that were successfully introgressed (Hajjar and Hodgkin, 2007). Apart from disease resistance, wild relatives have been used to enhance the tolerance to drought and salinity in barley, wheat and sunflower (Nevo and Chen, 2010; Miller and Seiler, 2003). In broccoli and pearl millet, the quality and yield were enhanced by crossing with wild relatives that harbored these particular traits (Sarikamis et al., 2006 and Hajjar and Hodgkin, 2007). However, conventional breeding is not easy in all crop species due to self-incompatibility problems. Therefore, developing novel cultivars needs a good crop model system that can be exploited for more benefits.

Tomato clade has 9 closely related species or subspecies: the wild or weedy forms of cherry tomato (*S. lycopersicum cerasiformae*) (Peralta et al., 2008), and the wild species- *S. chilense*, *S. chmielewskii, S. galapaganse*, *S. habrochaites*, *S. neorikii*, *S. pennellii*, *S. peruvianum* and

S. pimpinellifolium **(Table 6.1)**. Many useful traits found in wild tomato species such as tolerance to drought and salinity (*S. pennellii*) (Dehan et al., 1978, Shalata et al., 1998), accumulation of health-promoting phytochemicals (*S. habrochates*) and resistance to multiple pathogens (*S. galapaganse*, *S. lycopersicoides*, *S. neorickii* and *S. chilense*) have been introgressed into cultivated tomato (Robert, 2001; Rick et al., 1994). It is estimated that cultivated tomato contains less than 5% of the genetic variation of the wild relatives (Miller et.al., 1990) and this genetic potential can be exploited to improve many agronomic traits in tomato.

Tomato fruit is abundant in health promoting phytochemicals. The fruit of modern tomato or the domesticated tomato is large and red in color due to the accumulation of lycopene and β-carotene. On the contrary, the fruits of all the wild relatives are round and much smaller in size than tomato. On the basis of the accumulation of carotenoids during development and ripening of fruits, two categories are distinguished. Green fruited species are characterized by purplish green fruit color during maturation (Alexander and Grierson, 2002). The second group is characterized by the accumulation of carotenoids that impart orange or red color to the fruit (Bauchet and Causse, 2012) in the later stages of ripening. The biosynthesis of carotenoids begins with the conversion of IPP (isopentenyl diphosphate) to produce the precursor GGPP (geranylgeranyl diphosphate) via the plastid-localized MEP pathway (Giuliano, 2014). Further, a series of enzymes catalyze the conversion of GGPP to end product lycopene. In tomato, most of the carotenoid biosynthetic enzymes are well characterized and are under tight transcriptional and translational regulation. In addition to genetic regulation, internal (hormonal regulation) and external stimuli (e.g., light, wounding, pathogen attack and temperature shift) also regulate fruit ripening. Among these factors light is known to play an important role to regulate carotenoid biosynthesis in tomato fruits via a post-transcriptional modification of phytoene synthase enzyme (Thomas and Jen, 1975; Gupta et al., 2014). Consequently, fruits of phytochrome mutants of tomato ripened under darkness showed differences in the accumulation of lycopene (Gupta et al., 2014).

Tomato lacks mutants defective in *ACS2* gene. To gain better insight into ethylene regulation of tomato fruit ripening and improvement of ripening quality, *ACS2* mutants were isolated by reverse genetics techniques- TILLING and EcoTILLING. In addition, for *ACS2* gene, the sequence diversity was examined in five wild relatives of tomato. The coding regions of the *ACS2* gene from these wild relatives were sequenced and in-silico analysis of the single nucleotide polymorphisms was carried out to

Table 6.1 Principal features of the *Lycopersicon* subsection (*Solanum sect. Lycopersicon*).

Species new nomenclature/(old nomenclature)	TGRC Accession Number	Geographic distribution and habitat	Mating system	Fruit color	Genetic polymorphism
S. neorickii/ (*L. parviflorum*)	LA2133	South Equador, South central Peru native, 1500 - 3000 m, rocky humid and well drained areas	SC, highly AT/reciprocal	Green with dark green stripes	Low
S. pennellii/ (*L. pennellii*)	LA0716	Peruvian coast native, 0-2000 m, dry and rocky hill side	SI usually, SC populations in southern parts/reciprocal	Green	High
S. habrochaites/ (*L. hirsutum*)	LA1777	South west Equador to South central Peru native, 500 – 3300 m, forest regions	SI/SC populations in southern parts/UI	Green with darker green stripes	High
S. chilense/ (*L. chilense*)	LA1969	South Peru to north Chile, 0 – 3000 m, dry river bed	SI, AL/UI, EL	Green to whitish green with purple	High
S. galapagense/ (*L. cheesmanii f. minor*)	LA0483	Galapagos islands endemic species, 0 - 1300 m from sea shore to volcanic areas	SC, AT/reciprocal	Yellow orange	Low
S. pimpinellifolium/ (*L. pimpinellifolium*)	LA1589	South west Equador – northern Peru native, under 1000 m, South valleys of the pacific coast	SC, AT facultative AL/reciprocal	Red	Intermediate
S. lycopersicum/ (*L. esculentum*)	Arka Vikas (reference cultivar)	South India	SC	Red	Very low

*****Data is compiled from Peralta et al., (2007), Moyle et al., (2008), Grandillo et al., (2011). SI- Self-incompatible, SC- Self-compatible, AI- Allogamous, AT- Autogamous, UI- Unilateral incompatibility, EL-Embryo lethality.

understand the frequency of natural diversity of the gene at both nucleotide and protein level.

6.2 Results

The structural genomic data of the *ACS2* candidate gene was examined and compared for single nucleotide polymorphisms in the selected wild species using tomato as reference plant. The overall number and nature of SNPs such as synonymous and nonsynonymous and their distribution can reflect on the selection pressures for the functional diversity of these genes and provide an idea of the evolutionary conserved ness of the loci.

6.2.1 Sequence analysis of *ACS2* gene

The distribution of nucleotide variations found among the *ACS2* gene in different wild relatives considered was represented by PARSESNP output result file. The aligned length, including coding and non-coding regions of the *ACS2* gene, was 3869 nucleotides **(Fig. 6.1)**. Notably, the frequency of nucleotide variations in *ACS2* was 3-4 times higher in introns than in coding sequences. The number of SNPs was greater than the number of INDELs, with a total of 70 SNPs in the coding region resulting in an average of 1 SNP for 0.28 Kb of genomic DNA **(Fig. 6.2)**. Relatively fewer SNPs (16) and INDELs (5) were found in red colored fruit species than in the green colored fruit species (90 SNPs and 49 INDELs). On analyzing the polymorphism data per species, it was observed that the number of nucleotide polymorphisms observed for *ACS2* was highest in *S. pennellii* (green fruited) and least in the red fruited *S. pimpinellifolium* **(Fig. 6.2)**.

The nucleotide diversity analyzes showed that the nucleotide diversity of green fruited varieties was much higher (π = 0.01444) than the colored fruit species (π = 0.00072). The DnaSP analysis of the *ACS2* gene revealed high nucleotide diversity in the region located at 1000 to 2500 bp of the gene in green fruited species **(Fig. 6.3)**. According to this plot, low nucleotide diversity was also observed in the regions 100 to 900 bp of the gene. This analysis further showed that polymorphic sites were mainly located at the middle and the end of the gene, with most being in the introns **(Fig. 6.3)**.

6.2.1.1 Analysis of Nucleotide Base Changes

The observed SNPs were categorized according to the type of nucleotide substitution- either as transitions (C/T or G/A) or transversions (A/T, G/C, C/A, or T/G). The point substitution analysis showed that the A/G transition is the most frequent substitution in *ACS2* gene with 12% frequency. We observed that T/C

substitution is the next prevalent base change with a frequency of 10% **(Fig. 6.4A)**. A total of 105 INDELs were detected with an INDEL length ranging from 1 to 14 nucleotides.

Among 70 polymorphisms observed in the coding region, 25 were silent or synonymous, and the rest were nonsynonymous **(Fig. 6.4B)**. The details of the SNPs, position on the gene and the corresponding amino acid change are listed in **Table 6.3**. Some of the polymorphisms were common in the green-fruited species.

6.2.1.2 Variations in ACS2 protein sequence

The effects of genetic variation on amino acid sequence were evaluated by SIFT scores. All the five species used in the study showed different amino acid changes **(Table 6.3)**. The nonsynonymous changes observed in *ACS2* had no drastic effect on the protein function as the predicted SIFT values were higher than 0.05 except for *S. chilense*. Also, the PSSM score was found more than 10 in *S. chilense*. However, the nucleotide changes T3124 to G in *S. parviflorum* resulted in a premature stop codon at position L385. These changes might cause a truncation in the ACS2 protein thereby affecting the protein function in the species. The PRALINE alignment of the derived amino acids showed that the protein was highly conserved across the wild relatives **(Fig. 6.6)**. These possibilities have to be validated further to understand the role of *ACS2* in fruit ripening of green fruited species. Synonymous SNPs do not cause any change in amino acid and therefore presumably have no effect on the protein function. However, several studies in animal systems revealed that synonymous or silent changes can affect the protein function by altering the translation rates or altering the secondary structure of the mRNA (Kimchi-Sarfaty et al., 2007). On the contrary, in plants, very few studies have been conducted to understand the role of synonymous SNPs.

6.2.1.3 Phylogenetic analysis at the *ACS2* locus

To assess the evolutionary divergence between the five wild relatives of tomato at *ACS2* locus, we performed phylogenetic analysis using ClustalX v2.1 and FigTree v1.3.1 software respectively. A dendrogram was constructed based on the identified polymorphism in *ACS2* gene **(Fig. 6.5)**. The results showed the conserved topology of the phylogenetic tree, in which the colored tomato species were close to the domesticated tomato and the green-fruited species were represented as distant relatives at the bottom of the tree. Our results are consistent with the previous literature, and the following patterns of relationships could be deduced from the *ACS2* dendrogram: firstly, the red fruited wild relative *S. pimpinellifolium* is closely related to the domesticated *S.*

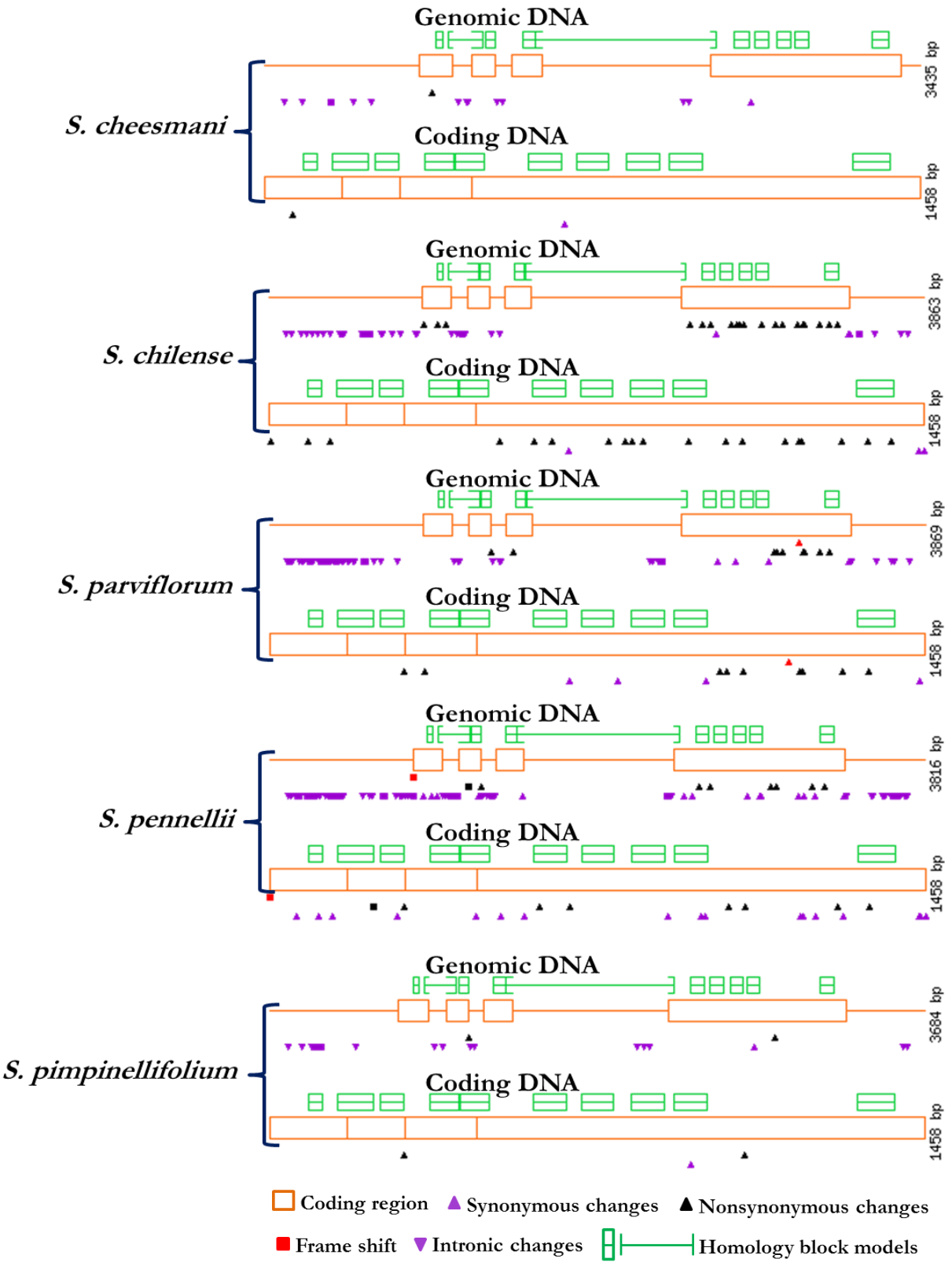

Figure 6.1. PARSESNP output file representing the distribution of SNPs for *ACS2* gene in wild relatives of tomato. Open orange boxes denote exons interconnected with a solid orange line indicating introns. A black upright triangle shows changes in the DNA sequence that affect the amino acid. A purple upright triangle indicates changes in the DNA sequence that do not change the amino acid. Purple downward triangles indicate changes in introns. Red boxes represent the frameshift changes.

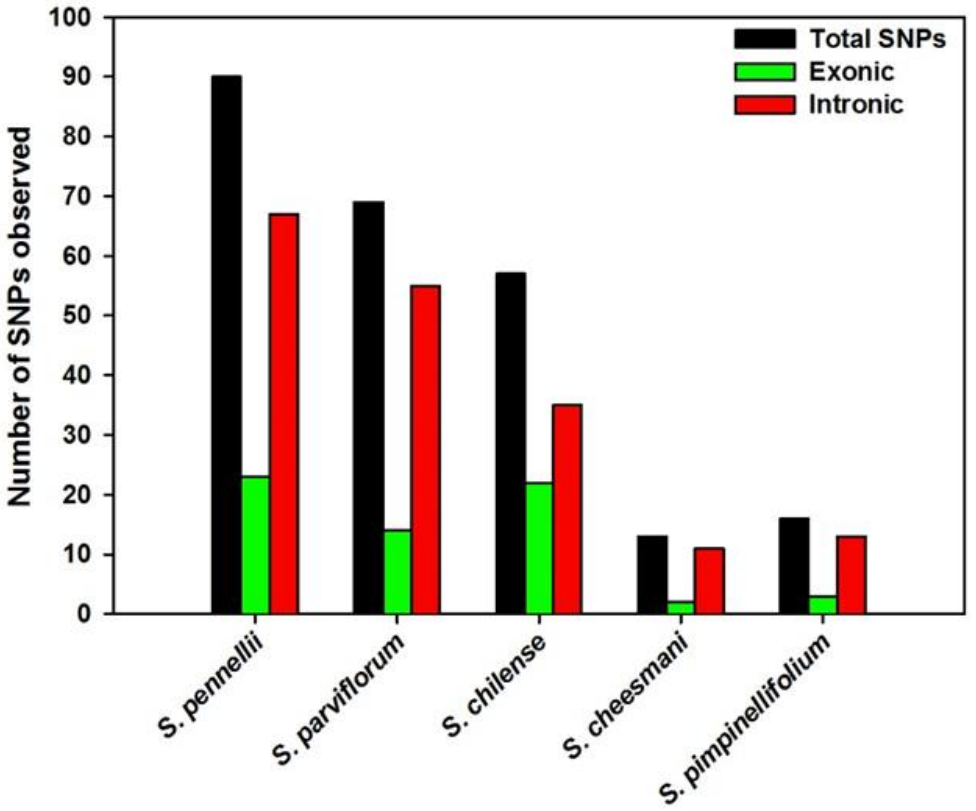

Figure 6.2. Number of exonic and intronic SNPs and the total number of SNPs present in *ACS2* gene of different wild relatives of tomato

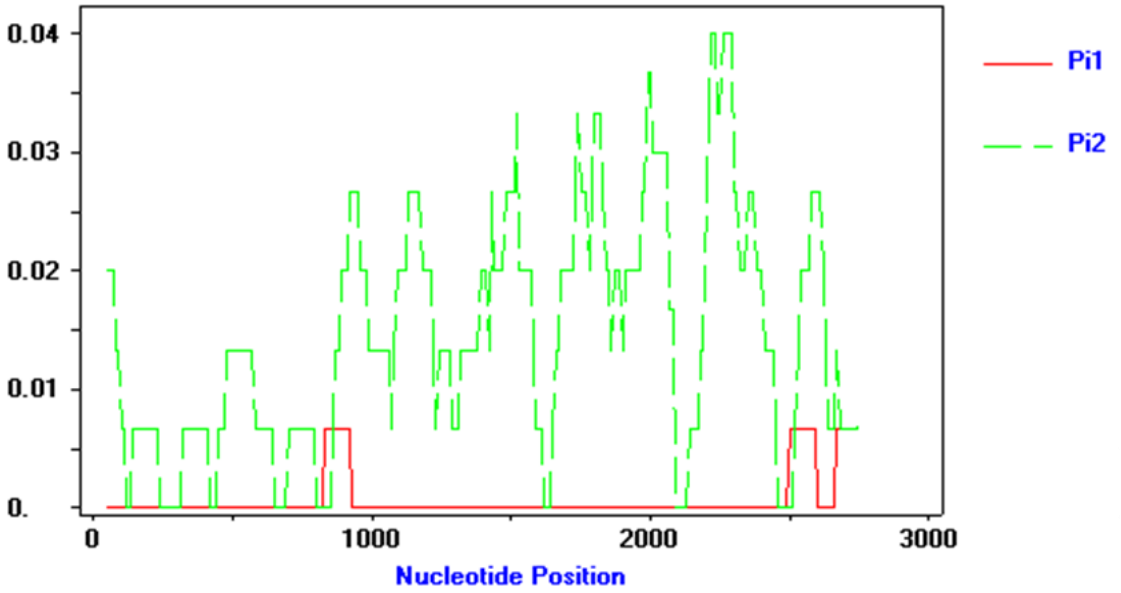

Figure 6.3. Nucleotide diversity (π) patterns along *ACS2* gene in sliding window among color fruited and green-fruited wild species. The analysis was performed using a window length of 100 bp in DNASP v 5.1. Pi1 (red color graph) and Pi2 (green colored graph) are the nucleotide diversities representing the colored fruited and green-fruited species respectively. **Note:** in the overlaid graph, Pi2 is high compared to Pi1 for the entire length of the *ACS2* gene indicating the high nucleotide diversity in green fruited species.

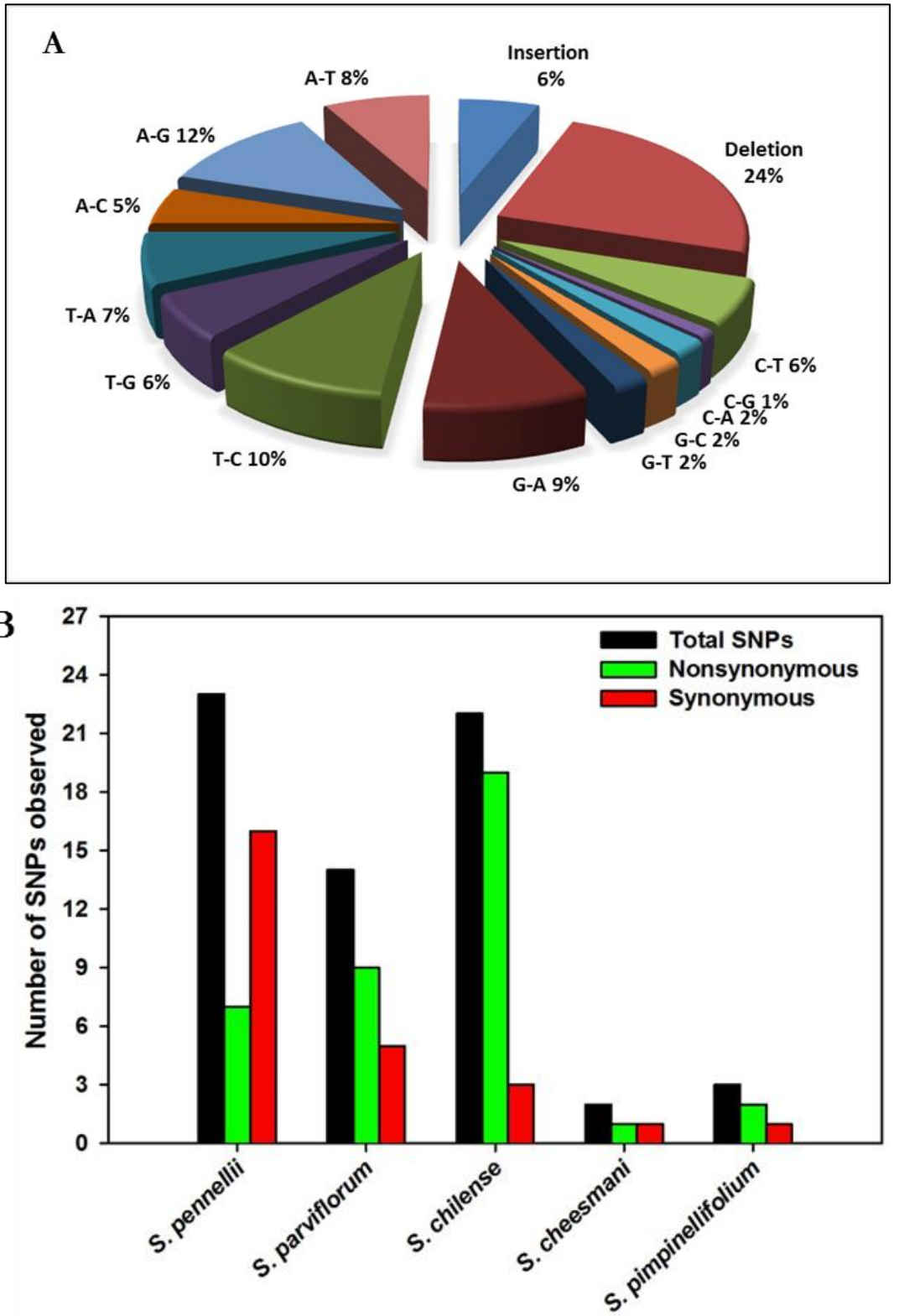

Figure 6.4. (A) Nucleotide substitution patterns observed in tomato *ACS2* gene. **(B)** Frequency of SNPs found in various wild relatives of tomato for *ACS2* gene.

Table 6.2 List of nucleotide polymorphisms in *ACS2* gene and their effect on amino acids.

S. No	Nucleotide change	Amino acid change	*S. pennellii*	*S. parviflorum*	*S. chilense*	*S. cheesmaniae*	*S. pimpinellifolium*	PSSM Difference	SIFT Score
1	G910T	G2V			+				
2	G892A	E20=	+						
3	A876G	H21R				+			
4	A990G	D29G			+				
5	T940C	S36=	+						
6	C970T	N46=	+						
7	A1041T	N46I			+				
8	C1160CCAA	S77SN	+						
9	C1212G	G94=	+						
10	A1117G	K100R					+		
11	A1229G	K100R	+	+					
12	G1433T	R115I		+					
13	A1474G	P153=	+						
14	C2409T	H171=	+						
15	A2480T	H171L			+				
16	A2460G	A188=	+						
17	A2557C	I197L			+			6.5	0.42
18	A2495G	K200R	+					2.7	0.46
19	T2599A	L211M			+			10.5	0.04
20	T2543C	S222=				+			
21	T2634C	S222=			+				
22	T2636C	S222=		+					
23	G2663C	V223L	+						
24	T2724G	S252R			+			12.2	0.05
25	T2744C	D258=		+					
26	A2759T	Y264F			+				
27	T2777A	V270D			+			19.0	0.03
28	A2801G	K278R			+			21.9	0.01
29	C2781T	D295=	+						
30	A2720G	T312=					+		
31	C2903T	T312I			+			10.9	0.15
32	G2853C	A319=	+						
33	A2862G	L322=	+						
34	G2939A	S323=		+					

S. No	Nucleotide change	Amino acid change	*S. pennellii*	*S. parviflorum*	*S. chilense*	*S. cheesmaniae*	*S. pimpinellifolium*	PSSM Difference	SIFT Score
35	A2971G	E334G		+					
36	G2986C	G340R			+				
37	G2988C	G340R		+					
38	G2989C	G340A	+						
39	T2839A	V352E					+		
40	G3022A	V352I			+				
41	G3024A	V352I		+					
42	T3037A	V352E	+						
43	T3116C	M383T			+				
44	T3124G	L385*		+					
45	T3075G	V393=	+						
46	T3148G	V393G		+					
47	T3146G	V393G			+				
48	T3081C	L395=	+						
49	T3152C	L395P			+				
50	T3154C	L395P		+					
51	A3108G	E404=	+						
52	G3158A	G421E	+						
53	T3171C	I425=	+						
54	T3242C	I425T			+				
55	T3244C	I425T		+					
56	T3300G	S444R			+			-8.2	0.44
57	T3302G	S444R		+					
58	T3229G	S445A	+					9.4	0.32
59	C3353T	S462L			+			1.0	0.66
60	A3339G	S481=	+						
61	A3414C	P482=			+				
62	A3416C	P482=		+					
63	T3343C	L483=	+						
64	A3425G	*486=			+				
65	A3354G	*486=	+						

+ indicates the presence of the SNPs in the wild relative.

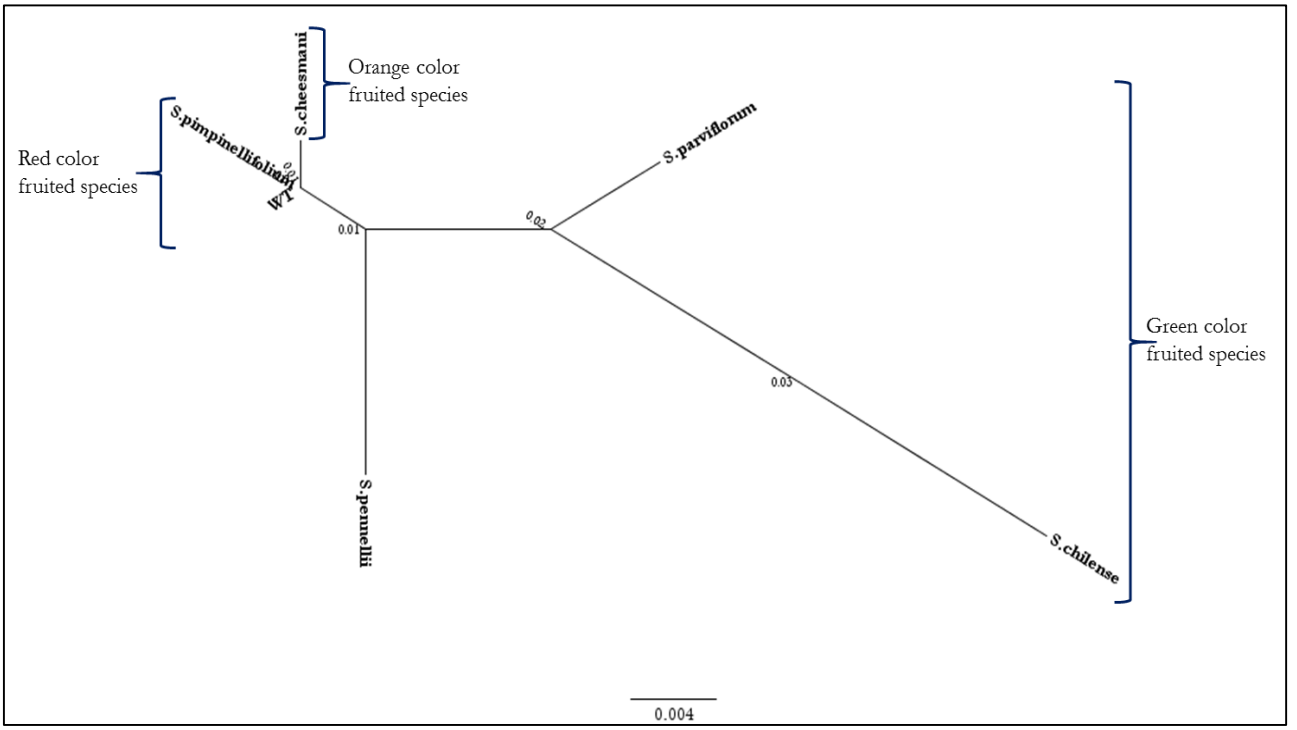

Figure 6.5. Dendrogram for five wild relatives and one domesticated species of tomato (WT AV) based on *ACS2* gene sequence.

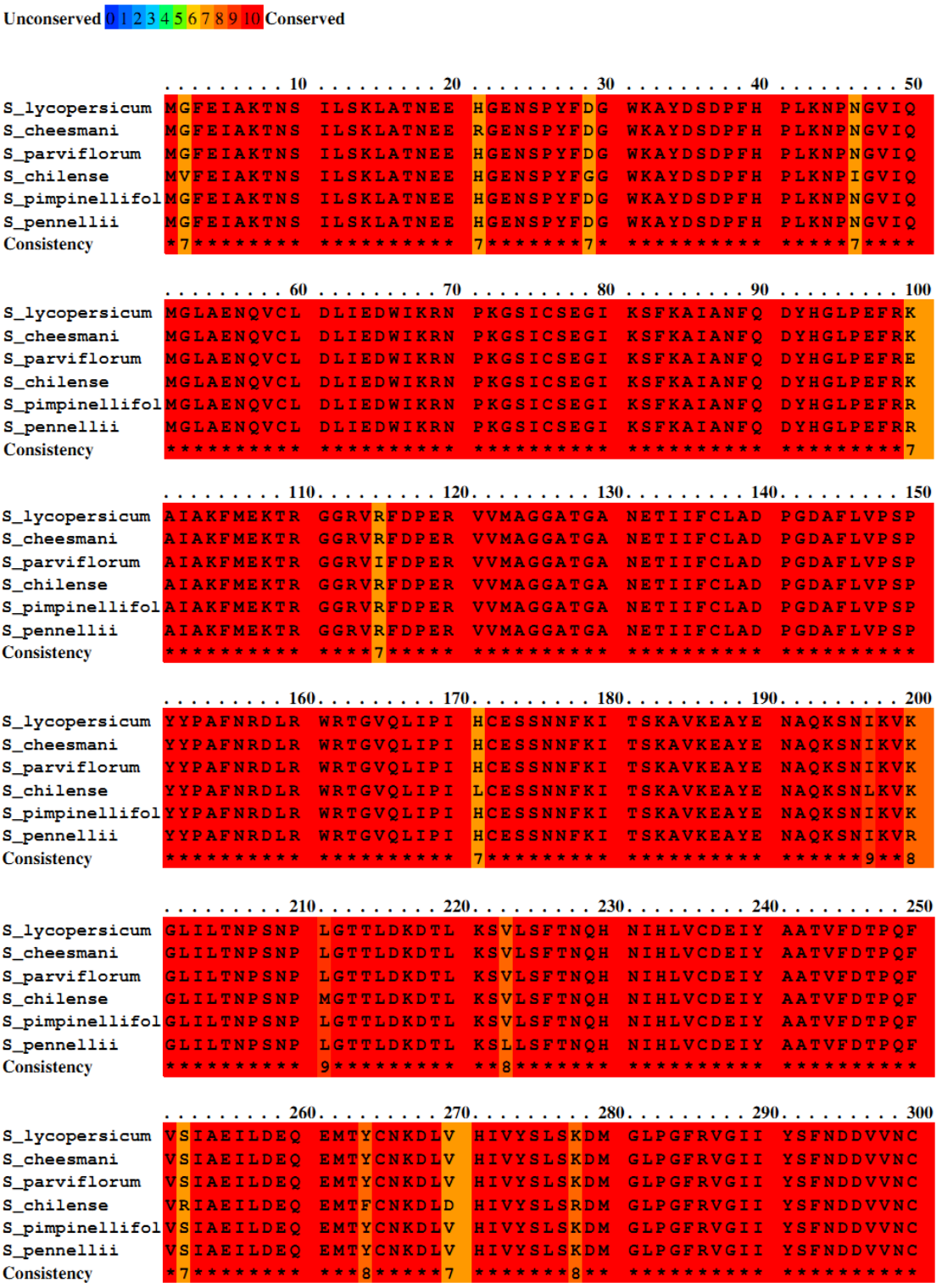
Unconserved 0 1 2 3 4 5 6 7 8 9 10 Conserved
10 20 30 40 50
S_lycopersicum MGFEIAKTNS ILSKLATNEE HGENSPYFDG WKAYDSDPFH PLKNPNGVIQ
S_cheesmani MGFEIAKTNS ILSKLATNEE RGENSPYFDG WKAYDSDPFH PLKNPNGVIQ
S_parviflorum MGFEIAKTNS ILSKLATNEE HGENSPYFDG WKAYDSDPFH PLKNPNGVIQ
S_chilense MVFEIAKTNS ILSKLATNEE HGENSPYFGG WKAYDSDPFH PLKNPIGVIQ
S_pimpinellifol MGFEIAKTNS ILSKLATNEE HGENSPYFDG WKAYDSDPFH PLKNPNGVIQ
S_pennellii MGFEIAKTNS ILSKLATNEE HGENSPYFDG WKAYDSDPFH PLKNPNGVIQ
Consistency *7******** ********** 7*******7* ********** *****7****
60 70 80 90 100
S_lycopersicum MGLAENQVCL DLIEDWIKRN PKGSICSEGI KSFKAIANFQ DYHGLPEFRK
S_cheesmani MGLAENQVCL DLIEDWIKRN PKGSICSEGI KSFKAIANFQ DYHGLPEFRK
S_parviflorum MGLAENQVCL DLIEDWIKRN PKGSICSEGI KSFKAIANFQ DYHGLPEFRE
S_chilense MGLAENQVCL DLIEDWIKRN PKGSICSEGI KSFKAIANFQ DYHGLPEFRK
S_pimpinellifol MGLAENQVCL DLIEDWIKRN PKGSICSEGI KSFKAIANFQ DYHGLPEFRR
S_pennellii MGLAENQVCL DLIEDWIKRN PKGSICSEGI KSFKAIANFQ DYHGLPEFRR
Consistency ********** ********** ********** ********** *********7
110 120 130 140 150
S_lycopersicum AIAKFMEKTR GGRVRFDPER VVMAGGATGA NETIIFCLAD PGDAFLVPSP
S_cheesmani AIAKFMEKTR GGRVRFDPER VVMAGGATGA NETIIFCLAD PGDAFLVPSP
S_parviflorum AIAKFMEKTR GGRVIFDPER VVMAGGATGA NETIIFCLAD PGDAFLVPSP
S_chilense AIAKFMEKTR GGRVRFDPER VVMAGGATGA NETIIFCLAD PGDAFLVPSP
S_pimpinellifol AIAKFMEKTR GGRVRFDPER VVMAGGATGA NETIIFCLAD PGDAFLVPSP
S_pennellii AIAKFMEKTR GGRVRFDPER VVMAGGATGA NETIIFCLAD PGDAFLVPSP
Consistency ********** ****7***** ********** ********** **********
160 170 180 190 200
S_lycopersicum YYPAFNRDLR WRTGVQLIPI HCESSNNFKI TSKAVKEAYE NAQKSNIKVK
S_cheesmani YYPAFNRDLR WRTGVQLIPI HCESSNNFKI TSKAVKEAYE NAQKSNIKVK
S_parviflorum YYPAFNRDLR WRTGVQLIPI HCESSNNFKI TSKAVKEAYE NAQKSNIKVK
S_chilense YYPAFNRDLR WRTGVQLIPI LCESSNNFKI TSKAVKEAYE NAQKSNLKVK
S_pimpinellifol YYPAFNRDLR WRTGVQLIPI HCESSNNFKI TSKAVKEAYE NAQKSNIKVK
S_pennellii YYPAFNRDLR WRTGVQLIPI HCESSNNFKI TSKAVKEAYE NAQKSNIKVR
Consistency ********** ********** 7********* ********** ******9**8
210 220 230 240 250
S_lycopersicum GLILTNPSNP LGTTLDKDTL KSVLSFTNQH NIHLVCDEIY AATVFDTPQF
S_cheesmani GLILTNPSNP LGTTLDKDTL KSVLSFTNQH NIHLVCDEIY AATVFDTPQF
S_parviflorum GLILTNPSNP LGTTLDKDTL KSVLSFTNQH NIHLVCDEIY AATVFDTPQF
S_chilense GLILTNPSNP MGTTLDKDTL KSVLSFTNQH NIHLVCDEIY AATVFDTPQF
S_pimpinellifol GLILTNPSNP LGTTLDKDTL KSVLSFTNQH NIHLVCDEIY AATVFDTPQF
S_pennellii GLILTNPSNP LGTTLDKDTL KSLLSFTNQH NIHLVCDEIY AATVFDTPQF
Consistency ********** 9********* **8******* ********** **********
260 270 280 290 300
S_lycopersicum VSIAEILDEQ EMTYCNKDLV HIVYSLSKDM GLPGFRVGII YSFNDDVVNC
S_cheesmani VSIAEILDEQ EMTYCNKDLV HIVYSLSKDM GLPGFRVGII YSFNDDVVNC
S_parviflorum VSIAEILDEQ EMTYCNKDLV HIVYSLSKDM GLPGFRVGII YSFNDDVVNC
S_chilense VRIAEILDEQ EMTFCNKDLD HIVYSLSRDM GLPGFRVGII YSFNDDVVNC
S_pimpinellifol VSIAEILDEQ EMTYCNKDLV HIVYSLSKDM GLPGFRVGII YSFNDDVVNC
S_pennellii VSIAEILDEQ EMTYCNKDLV HIVYSLSKDM GLPGFRVGII YSFNDDVVNC
Consistency *7******** ***8*****7 *******8** ********** **********

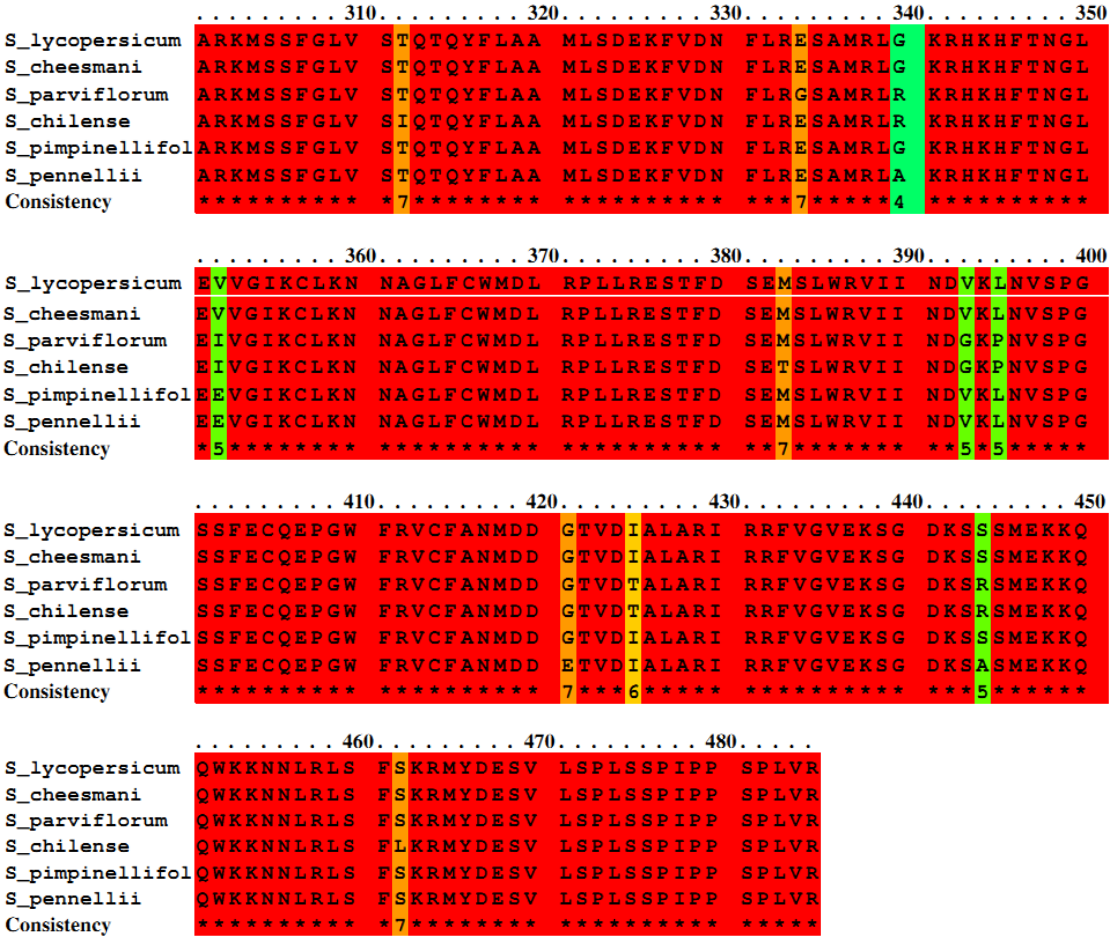

Figure 6.6. PRALINE multiple alignment output file of the derived ACS2 protein sequences of the five wild relatives. The conserved ness of the amino acids is denoted by a color code designed by the software. The highly unconserved moieties are indicated by dark blue color and, on the contrary, conserved moieties by deep red color.

lyopersicum. Secondly, all the green-fruited species were found to be the ancestors of present day tomato. However, *S. pennellii* was exceptionally placed in between the colored fruit and green fruit species in *ACS2* phylogram. This kind of discrepancy can be explained better by considering a large number of accessions of wild relatives where the phylogenetic trees can be computed more stringently.

6.3 Discussion

In general wild relatives of crop plants constitute an increasingly important resource for improving agronomic traits. With the recent improvements in tools available for molecular analysis, it is easier and quicker to identify useful traits in wild relatives to develop new and improved varieties. Despite the enormous promise they hold for improving crops, wild relatives are not thoroughly studied. *S. lycopersicum* is the domesticated species of tomato that is widely cultivated all over the world. Apart from the widely distributed domesticated species *S. lycopersicum*, the tomato has nine wild relatives (Peralta and Spooner, 2008). These wild relatives are adapted to different geographical conditions, vary in morphological traits like leaf shape, structure and fruit color (ranging from green to red) etc. conferring their genetic potential to adapt to the ever-changing environment. Understanding the genetic makeup of tomato wild relatives provides insights into evolutionary trends of different mechanisms underlying the agronomic traits (Bolger et al., 2014). In the present study, we analyzed the nucleotide diversity of *ACS2* genes in tomato wild relatives by direct sequencing of the PCR products.

The SNPs identified were found to be distributed throughout the length of the gene with a high frequency of intronic mutations in *ACS2*. As expected, the close wild relative of tomato, *S. pimpinellifolium* harbored fewer SNPs compared to the green-fruited species in *ACS2* genes. In a recent study on tomato by Aflitos et al., (2014), the estimated number of single nucleotide polymorphisms (SNPs) reported in wild relatives, especially in the green-fruited species was 20-fold higher than found in most of the tomato accessions. This high number of nucleotide variations observed in the green-fruited species like *S. pennellii*, *S. parviflorum* and *S. chilense* compared to the colored fruited (*S. pimpinellifolium* and *S. cheesmaniae*) species is an indicator of genetic potential of the wild species. Most probably, in the course of domestication, the variations were lost.

In terms of the overall density of polymorphisms across the regions considered for the study, an average of 1 SNP/0.28 Kb for *ACS2* gene was determined. As envisaged for any reverse genetic high-throughput technique for detecting mutations, the

frequency of naturally occurring variations might also depend on the length of the gene, number of exons and introns, length of the exons, GC content, gene function etc. The increased SNP frequency observed in tomato *ACS2* gene may be related to the functional importance of *ACS2* gene in ethylene biosynthesis pathway, as any spontaneous mutations could be resulted in alteration of the physiological and biochemical changes (as observed in our TILLING and EcoTILLING studies). Secondly, it may be attributed to the above-mentioned aspects of gene structure.

Nevertheless, the effect of genetic variations in the coding region can vary based on the position and nature of the SNPs or INDELs. Not necessarily all nucleotide changes affect the gene function. The change in nature of the amino acids determines the degree of loss of function or gain of function respectively. On the other hand, presence of INDELs in coding regions or regulatory domains leads to either truncation of the protein (due to stop codon), alter the binding sites (due to frameshifts) or affect the abundance and turnover (transcriptional regulation) of the protein, thus causing a loss of function. In spite of relatively high number of nonsynonymous changes **(Fig. 6.4)** observed for *ACS2* gene in wild relatives, the SIFT value for most of the changes was not significant to cause a drastic change in the function of the gene product. However, the nucleotide changes T3124 to G in *S. parviflorum* resulted in a premature stop codon at position L385. These changes might cause a truncation in the ACS2 protein. These changes may lead to loss of function of *ACS2* gene in the respective wild relatives.

Potential explanations for evolutionary pressure may include one or more recent genetic bottlenecks during domestication, a low mutation rate and a self-pollinating reproductive biology of *S. lycopersicum*. In corroboration with the studies of Peralta and Spooner. (2001) for *GBSSI* gene in tomato, the phylogenetic analyses of the two genes in wild relatives indicate the evolutionary trend of domesticated tomato i.e. from green fruited species to color fruited species.

In conclusion, our investigations demonstrate that the ethylene biosynthesis gene - *ACS2* is highly conserved in wild relatives of tomato in spite of the presence of nucleotide variations. In particular, though statistically significant signatures of selection were not detected in target gene *ACS2*. Notably, this study signifies the importance of *ACS2* gene in tomato fruit ripening and further investigations with the identification of multiple alleles or RNAi suppression lines or genome editing would shed light on the underlying mechanisms and identity of the interacting partners.

CHAPTER 7

SUMMARY AND CONCLUSIONS

Fruit ripening represents the final phase of plants development that is essential for the dispersal of seeds. The ripening confers both positive and negative attributes to the fruits. The positive attributes include enhancements of the organoleptic quality of fruits, whereas negative characteristics include an increase in the chance of perishability and pathogen attack. The negative attributes contribute the significant loss of commercial and economic importance of the fruits. The ripening is the consequence of several physiological, molecular, biochemical and metabolic changes that make the ripe fruits nutritious and palatable. In climacteric fruits, the ethylene serves as a primary hormone for ripening. The main aim of this work was to manipulate ripening particularly at the level of ethylene synthesis with an emphasis on improvement of shelf life of tomato fruits by isolating and characterizing the mutants compromised in ethylene biosynthesis. Although using the high throughput technologies and transgenic a tremendous progress has been made elucidating the mechanism of action and biosynthesis of ethylene and its regulation during the ripening, little is known about the detailed function of genes involved in ethylene biosynthesis. The identification and characterization of *ACS2* (key player of ethylene biosynthesis pathway) mutants is a strategy to gain further understanding of molecular mechanism involved in fruit ripening and to identify the novel function of a gene in ethylene response. Two *ACS2* mutants namely; *acs2-1* and *acs2-2* isolated from the EMS-mutagenized M_2 and M_3 lines of tomato were used for characterization in this study.

Nucleotide changes at positions A3452 to G and T5174 to A in exon 2 and four respectively, lead to the amino acid changes K100 to R and V352 to E respectively, in the ACS2-1 protein. By these changes, SIFT score results 0.12 and 0.85 units respectively and PSSM differences were 7.6 and -9.7 respectively. The 3-D models drawn with the software PyMOL (http://wwwpymol.org) indicated that the amino acid changes taken placed in α-helix of protein surface that do not take part in the formation of active site interface. In the *acs2-2* mutant, two mutations were in the promoter region and one mutation in intron three. All the three mutations are not the part of the coding region. Therefore, there is no structural alteration in the ACS2-2 protein.

The effect of mutations was examined on the vegetative and reproductive development of the plant. It was observed that mutation exerted the strong pleiotropic effect on all stages of plant development right from the seed germination, root elongation to fruit ripening in comparison with wild-type (M82).

Characterization of seed germination in mutants showed that *acs2-1* mutant seeds initiate sprouting approximately one day earlier than wild type (WT) seeds in darkness. On the other hand *acs2-2*, mutant seeds exhibited a slow germination compared to WT seeds. Germinating seedlings of *acs2-1* mutant emitted higher level of ethylene emission than WT whereas *acs2-2* mutant seedlings exhibited comparatively less ethylene emission. To check the effect of mutation on seedling phenotype, seedlings were grown under the continuous white light. Light grown seedlings showed accelerated root growth in the *acs2-1* mutant as well as more lateral roots than WT. In contrast, *acs2-2* mutant exhibited a comparatively lesser number of lateral roots while root length was not significantly prolonged compared to WT.

Examination of off-vine leaf senescence revealed that *acs2-1*mutant leaf senesced earlier than WT leaf both under continuous light as well as in darkness. Contrastingly, *acs2-2* mutant leaves exhibited the delayed senescence compared to WT. Since ACS is a crucial enzyme in the ethylene biosynthesis pathway, it is expected that the change in *ACS2* gene will cause in alteration in ethylene emission. The *acs2-1* mutant emitted higher level of ethylene in different plant organs like seedlings, leaf and fruits compared to WT. In contrast, *acs2-2* mutant exhibited decreased ethylene emission throughout life cycle including seedlings, foliage, and fruits.

The overproduction of ethylene in *acs2-1* mutant accelerated many life cycle processes showing early flowering, leaf senescence and early ripening of fruits. On-vine examination of fruit ripening study showed that the *acs2-1* mutant fruit ripened 15 ± 3 days earlier than WT. The fruit pericarp in *acs2-1* mutant was also thin which may have led to the early senescence of the mutant fruit compared to WT. The *acs2-1* mutant fruit was less firm than the WT. The reduced production of ethylene in the *acs2-2* mutant delayed developmental processes such as delayed leaf senescence and ripening of fruits (17 ± 3 days) respectively.

Yang cycle established that the emission of ethylene mainly depends on the activities of ACS and ACO enzymes (Yang and Hoffman, 1984). Measurement of In-vitro free, bound and total ACC (precursor of ethylene) at different maturity stages of WT and mutant fruits revealed that elevated levels of ACC in *acs2-1* mutant fruits than WT. Above enhanced level of ACC in *acs2-1* mutant fruits also correlates with the enhanced In-vitro activities of ACS and ACO enzymes compared to WT. Using immunoprecipitation of ACS2 protein with specific antibodies and western blot analysis showed that in *acs2-1* mutant fruits, the levels of ACS2 protein was four-fold higher than

WT. On the contrary, *acs2-2* mutant fruits at different maturity stages exhibited the lesser amount of ACC, ACS, and ACO enzyme activities. The level of ACS2 protein in *acs2-2* mutant fruits was observed one fourth of WT.

Multiple studies have showed that auxin, cytokinin, gibberellin, and brassinosteroid increases at fruit set, and auxin, gibberellin, and brassinosteroid are involved in fruit growth. During fruit maturation, there is an inhibition of auxin transport from the seed and increase in ABA level. The ripening/senescence leads to an increase in ABA and/or ethylene biosynthesis and response in the surrounding tissue (Gillaspy et al., 1993; Mariotti et al., 2011). Considering that phytohormones play major role during fruit growth and development, the levels of phytohormones were examined at different fruit maturity stages in mutants and WT. *acs2-1* mutant fruits showed higher levels of zeatin, ABA, jasmonic acid (JA), MeJA and salicylic acid (SA) and low level of IAA compared to WT. The *acs2-2* mutant fruits exhibited lower levels of zeatin, ABA, JA, MeJA and SA whereas level of IAA was comparable to WT.

One of the main characteristics of tomato (*Solanum lycopersicum*) ripening is a massive accumulation of carotenoids (mainly lycopene), which contribute to the nutrient quality of tomato fruit. Red ripe fruit of *acs2-1* mutant exhibited the higher accumulations of total carotenoids especially lycopene, phytoene, phytofluene, zeta-carotene, beta-carotene, and neoxanthin compared to WT. Contrastingly, *acs2-2* mutant fruit showed lower accumulation of phytoene, phytofluene, zeta-carotene, beta-carotene, lutein, zeaxanthin and neoxanthin but higher levels of lycopene accumulation compared to WT. However, total level of carotenoids was also higher in *acs2-2* mutant.

As *acs2-1* mutant fruit emits high ethylene as well as increased ACS2 activity and elevated level of ACC. The precursors for ACC are methionine amino acid and adenosine nucleotide. Since folates act as a co-factor in various important biochemical reactions specially, in amino acids (methionine) metabolism and nucleotide (adenosine) biosynthesis, the folate levels was examined in mutant fruits. Red ripe *acs2-1* mutant fruits exhibited 1.5 fold increase in total folate level compared to WT while *acs2-2* fruits exhibited less folate compared to WT.

On-vine ripening upregulates the major hexoses, glucose and fructose, as well as cell wall components such as galacturonic acid, and for amino acids such as aspartic, glutamic acid and methionine. In addition, massive changes are also observed in TCA cycle intermediates, indicating a decrease in malic and fumaric acids, and accumulation of citric acid (Oms-Oliu et al., 2011). In *acs2-1* fruit sugars like glucose, fructose and

galactose, and some organic acids like citric acid, ascorbic acid, and some amino acids such as aspartic acid, pyroglutamic acid, glutamic acid and methionine were very high in red ripe stage than WT. However, the level of metabolites like malic acid, GABA (gamma amino butyric acid), serine, proline, 5-Oxoproline and phosphoric acid levels was low to moderate in *acs2-1* mutant fruit than WT. Significantly, *acs2-1* mutant fruit also showed higher level of ACC which was below detection limit in WT fruit. In contrast, ACC and methionine were below detection limit in *acs2-2* mutant fruits, and the levels of malic acid, GABA (gamma amino butyric acid), serine, proline, and 5-Oxoproline were higher than WT.

Using different tomato accession, natural variants of *ACS2* gene were identified by EcoTILLING. EcoTILLING is a modified TILLING strategy that is widely used for the detection of polymorphisms in target genes in natural populations. For EcoTILLING, a collection of 391 *S. lycopersicum* accessions obtained from NBPGR (National Bureau of Plant Genetic Resources (http://www.nbpgr.ernet.in/), IIVR (Indian Institute of Vegetable Research, Varanasi, India (http://www.iivr.org.in/) Bejo Sheetal, Jalna, India and TGRC (Tomato Genetic Resource Center, University of California, Davis (http://tgrc.ucdavis.edu/) were used. To facilitate heteroduplex formation, genomic DNA of reference cultivar (AV) was used. Based on the similarities and differences observed on Li-COR gels, the *ACS2* variants were categorized into 30 haplotypes with the reference accession (AV) designated as HT0. The accessions showing similar SNP pattern were grouped into one haplotype. Each haplotype included a variable number of accessions exhibiting identical SNP pattern for *ACS2* gene. Haplotype 7 and 23 were represented by the maximum number (4) of accessions while the rest of the haplotypes were represented by one or more accessions.

Based on the phenotypic variation observed in the *ACS2* natural variants ethylene emission was examined in their variant, some natural accessions (EC520046, EC1087, and EC20639) showed high ethylene emission. Few accessions (EC520076, EC529085) exhibited enhanced the carotenoid content and few accessions showed high folate level (EC520046, IIHR2201) compared to control accession.

The nucleotide diversity of *ACS2* was analyzed among wild relatives of tomato. Wild relatives of a crop species are the ancestors or closely related taxa that originated at distinct geographic locations but share a common gene pool. These wild species grow in different habitats that endow them with special features to tolerate a myriad of environmental and climatic changes. Thus, the wild tomato species are important for

breeding, as a sources of desirable traits such as improved productivity, fruit quality and resistance to biotic and abiotic stresses, as well as for evolutionary studies (Kimura and Sinha, 2008). In the present study, coding regions of the *ACS2* gene was sequenced and performed in-silico analysis of the single nucleotide polymorphisms was carried out to understand the frequency of natural diversity of the *ACS2* gene at the nucleotide level.

The aligned length, including coding and non-coding regions of the *ACS2* gene, was 3869 nucleotides. A total of 105 INDELs were detected with an INDEL length ranging from 1 to 14 nucleotides. The distribution of nucleotide variations found among the sequenced regions of *ACS2* gene in different wild relatives considered was represented by PARSESNP output format. It is noteworthy that the frequency of nucleotide variations in *ACS2* is almost three times higher in introns than in coding sequences. The number of SNPs was found higher than the number of INDELs, with a total of 64 SNPs in the coding region. Relatively fewer SNPs (16) and INDELs (5) were found in red colored fruit species than in the green colored fruit species (90 SNPs and 49 INDELs).

In this study, we reported the isolation of two mutant alleles of *ACS2* gene. The two missense mutations in *acs2-1* in α-helix of protein polypeptide chain likely increased stability of the ACS2-1 protein, leading to higher ACS activity. The accumulation of ACS2 protein in mutant fruits resulted in an elevated level of ACC and ethylene emission as well as increase in ACS and ACO enzyme activities. *acs2-1* fruit also showed elevated levels of carotenoids and citric acid that accelerated fruit ripening and also resulted in accelerated senescence of fruits. Since *acs2-1* mutant ripens earlier, this allele can be used for developing early maturing tomato variety with high carotenoid content in fruit. On the other hand *acs2-2* is a novel mutant with no mutation in the coding region but has two mutations in the promoter region and one mutation in the third intron. The mutations in promoter appear to reduce the accumulation of ACS2 protein in fruits, and mutant fruits emit a lower amount of ethylene. The lower level of ACS2 protein appeared to leads to lower ACC level and decreased ACS enzyme activity in fruits. In *acs2-2* mutant, the accumulation of carotenoids was higher than WT. Due to the high level of malic acid; the *acs2-2* mutant fruits showed delayed ripening and senescence with the long on-vine life of fruits. Taking this into account, the *acs2-2* mutant is an excellent allele for developing tomato with long shelf life and high lycopene content in the fruit. Among the *ACS2* natural variants, the natural accessions (EC520046, EC1087, and EC20639) showed high ethylene emission, whereas few accessions (EC520076,

EC529085) exhibited enhanced carotenoid levels and few accessions (EC520046, IIHR2201) showed high folate when compared to Arka Vikas. Nucleotide diversity analysis of *ACS2* gene among wild relatives revealed that relatively fewer SNPs and INDELs were found in red colored fruit species than in the green colored fruit species.

REFERENCES

Abel S, Nguyen MD, Chow W, Theologis A (1995) ACS4, a primary indoleacetic acid-responsive gene encoding 1-aminocyclopropane-1-carboxylatesynthase in Arabidopsis thaliana. Structural characterization, expression in Escherichia coli, and expression characteristics in response to auxin. Journal of biological chemistry **270:** 19093-99

Abeles FB, Morgan PW, and Salveit ME (1992) Ethylene in Plant Biology. Academic Press, New York **2:** 145-156

Adams DO, Yang SF (1977) Methionine metabolism in apple tissue implication of S-adenosyl methionine as an intermediate in conversion of methionine to ethylene. Plant physiology **60:** 892-896

Adams DO, Yang SF (1979) Ethylene biosynthesis-identification of 1-aminocyclopropane-1-carboxylic acid as an intermediate in the conversion of methionine to ethylene. Proceedings of the National Academy of Sciences of the United States of America **76:** 170-174

Adams-Phillips L, Barry C, Giovannoni J (2004a) Signal transduction systems regulating fruit ripening. Trends in plant science **9:** 331-338

Adams-Phillips L, Barry C, Kannan P, Leclercq J, Bouzayen M, Giovannoni J (2004b) Evidence that CTR1-mediated ethylene signal transduction in tomato is encoded by a multigene family whose members display distinct regulatory features. Plant molecular biology **54:** 387-404

Aflitos S, Schijlen E, Jong H, Ridder D, Smit S, Finkers R, Wang J, Zhang G, Li N, Mao L (2014) Exploring genetic variation in the tomato (Solanum section *Lycopersicon*) clade by whole-genome sequencing. The plant journal **80:** 136-148

Agnieszka L, Agata C, Anna K-M, Filip M, Małgorzata T, Łukasz G, Ziółkowski PA, Piotr K, Arleta M, Aneta P (2014) Arabidopsis protein phosphatase 2C ABI1 interacts with type I ACC synthases and is involved in the regulation of ozone-induced ethylene biosynthesis. Molecular plant **7:** 960-976

Alcantara TP, Bosland PW, Smith DW (1996) Ethyl Methanesulfonate-Induced Seed Mutagenesis of Capsicum annuum. Journal of heredity **87**: 239-241

Alexander L, Grierson D (2002) Ethylene biosynthesis and action in tomato: a model for climacteric fruit ripening. Journal of experimental botany **53:** 2039-2055

Alonso JM, Hirayama T, Roman G, Nourizadeh S, and Ecker JR (1999) EIN2, a bifunctional transducer of ethylene and stress responses in Arabidopsis. Science **284:** 2148-2152

An F, Zhao Q, Ji Y, Li W, Jiang Z, Yu X, Zhang C, Han Y, He W, Liu Y, Zhang S, Ecker JR, Guo H (2010) Ethylene-induced stabilization of ETHYLENE INSENSITIVE3 and EIN3-LIKE1 is mediated by proteasomal degradation of EIN3 binding F-box 1 and 2 that requires EIN2 in Arabidopsis. The pant cell **22:** 2384-2401

Araujo WL, Tohge T, Osorio S, Lohse M, Balbo I, Krahnert I, Porzucek AS, Usadel B, Nesi AN and Fernie AR (2012) Antisense inhibition of the 2-Oxoglutarate Dehydrogenase complex in Tomato demonstrates its importance for Plant respiration and during leaf senescence and Fruit maturation. The plant cell **24**: 2328-2351

Arnaud N, Girin T, Sorefan K, Fuentes S, Wood TA, Lawrenson T, Sablowski R, Ostergaard L (2010) Gibberellins control fruit patterning in *Arabidopsis thaliana*. Genes and development **24:** 2127-2132

Atkinson RG, Sutherland PW, Johnston SL, et al. (2012) Down-regulation of *POLYGALACTURONASE1* alters firmness, tensile strength and water loss in apple (*Malus* × *domestica*) fruit. BMC plant biology **12:** 129-142

Azari R, Tadmor Y, Meir A, Reuveni M, Evenor D, Nahon S, Shlomo H, Chen L, Levin I (2010b) Light signaling genes and their manipulation towards modulation of phytonutrient content in tomato fruits. Biotechnology advances **28:** 108-118

Bakshi A, Shemansky J, Chang C, Binder B (2015) History of Research on the Plant Hormone Ethylene. Journal of plant growth regulation **34:** 809-827

Barba A.I.O, Hurtado MC, Mata MCS, Ruiz VF, Tejada MLS (2006) Application of UV-vis detection-HPLC method for a rapid determination of lycopene and β-carotene in vegetables. Food chemistry **95**: 328-336

Barkley NA, Wang ML, Gillaspie AG, Dean RE, Pederson GA, Jenkins TM (2008) Discovering and verifying DNA polymorphisms in a mung bean [V. radiata (L.) R. Wilczek] collection by EcoTILLING and sequencing. BMC research notes **1:** 28

Barry CS, Giovannoni JJ (2006) Ripening in the tomato *Green-ripe* mutant is inhibited by ectopic expression of a protein that disrupts ethylene signaling. Proceedings of the National Academy of Sciences, USA **103:** 7923-7928

Barry CS, Llop-Tous MI, Grierson D (2000) The regulation of 1-aminocyclopropane-1-carboxylic acid synthase gene expression during the transition from system-1 to system-2 ethylene synthesis in tomato. Plant physiology **123:** 979-986

Bauchet G, Causse M (2012) Genetic diversity in tomato (*Solanum lycopersicum*) and its wild relatives. Genetic diversity in plants**:** 133-162

Beckstette M. et al. (2006) "Fast index based algorithms and software for matching position specific scoring matrices". BMC bioinformatics **7**: 389.

Bidonde S, Ferrer MA, Zegzouti H, Ramassamy S, Latché A, Pech JC, Hamilton AJ, Grierson D, Bouzayen M (1998) Expression and characterization of three tomato 1-aminocyclopropane-1-carboxylate oxidase cDNAs in yeast. European journal of biochemistry **253:** 20-26

Binder BM, O'Malley RC, Wang W, Moore JM, Parks BM, Spalding EP, Bleecker AB (2004b) Arabidopsis seedling growth response and recovery to ethylene. a kinetic analysis. Plant physiology **136:** 2913-2920

Binder BM, Rodrı´guez FI, Bleecker AB (2010) The copper transporter RAN1 is essential for biogenesis of ethylene receptors in Arabidopsis. Journal of biological chemistry **285:** 37263-37270

Bleecker AB, Estelle MA, Somerville C, Kende H (1988). Insensitivity to ethylene conferred by a dominant mutation in *Arabidopsis thaliana*. Science **241:** 1086-1089

Bradford MM (1976) A rapid and sensitive method for the quantitation of microgram quantities of protein utilizing the principle of protein-dye binding. Analytical biochemistry **72**: 248-254

Binder BM, Walker JM, Gagne JM, Emborg TJ, Hemman G, Bleecker AB, Vierstra RD (2007) The Arabidopsis EIN3-Binding F-Box proteins, EBF1 and 2 have distinct but overlapping roles in regulating ethylene signaling. The plant cell **19:** 509-523

Bisson MMA, Bleckmann A, Allekotte S, Groth G (2009) EIN2, the central regulator of ethylene signalling, is localized at the ER membrane where it interacts with the ethylene receptor ETR1. Biochemical journal **424:** 1-6

Bisson MMA, Groth G (2010) New insight in ethylene signaling: autokinase activity of ETR1 modulates the interaction of receptors and EIN2. Molecular plant **3:** 882-889

Blancquaert D, De Steur H, Gellynck X, Van Der Straeten D (2014) Present and future of folate biofortification of crop plants. Journal of experimental botany **65:** 895-906

Bleecker A, Estelle M, Somerville C, Kende H (1988) Insensitivity to ethylene conferred by a dominant mutation in *Arabidopsis thaliana*. Science **241:** 1086–89

Bleecker AB, Kende H (2000) ETHYLENE A gaseous Signal Molecule in Plants. Annual. Review on cell and developmental biology **16**: 1-18

Bleecker AB, Patterson SE (1997) Last exit: senescence, abscission, and meristem arrest in Arabidopsis. The plant cell **9:** 1169-79

Boggio SB, Palatnik JF, Heldt HW, Valle EM (2000) Changes in the amino acid composition and nitrogen metabolizing enzymes in ripening fruit of *Lycopersicon esculentum* Mill. Plant science **159:** 125-133

Bolger ME, Weisshaar B, Scholz U, Stein N, Usadel B, Mayer KFX (2014) Plant genome sequencing - applications for crop improvement. Current opinion in biotechnology **26:** 31-37

Bradford KJ, Yang SF (1980) Xylem Transport of 1-Aminocyclopropane-1- carboxylic Acid, an Ethylene Precursor, in Water logged Tomato Plants. Plant physiology **65:** 322-326

Bradford MM (1976) A rapid and sensitive method for the quantitation of microgram quantities of protein utilizing the principle of protein-dye binding. Analytical biochemistry **72**: 248-254

Bramley PM (2002) Regulation of carotenoid formation during tomato fruit ripening and development. Journal of experimental botany **53:** 2107-2113

Brummell DA (2006) Cell wall disassembly in ripening fruit. Functional plant biology **33:** 103-119

Brummell DA, Harpster MH (2001) Cell wall metabolism in fruit softening and quality and its manipulation in transgenic plants. Plant molecular biology **47:** 311-340

Brummell DA, Harpster MH, Civello PM, Palys JM, Bennett AB, Dunsmuir P (1999) Modification of expansin protein abundance in tomato fruit alters softening and cell wall polymer metabolism during ripening. The plant cell **11:** 2203-2216

Brummell DA, Labavitch JM (1997) Effect of antisense suppression of endopoly- galacturonase activity on polyuronide molecular weight in ripening tomato fruit and in fruit homogenates. Plant physiology **115:** 717-725

Bulens I, Van de Poel B, Hertog M, De Proft M, Geeraerd A, Nicolaï B (2011) Protocol: An updated integrated methodology for analysis of metabolites and enzyme activities of ethylene biosynthesis. Plant methods **7:** 1-10

Buttery RG, Ling LC (1993) In: Teranishi, R., Buttery, R., Sugisawa, H. (Eds.), Volatiles of Tomato Fruit and Plant Parts: Relationship and Biogenesis Bioactive Volatile Compounds from Plants. ACS, Washington, pp. 23-34

Caldwell DG, McCallum N, Shaw P, Muehlbauer GJ, Marshall DF, Waugh R (2004) A structured mutant population for forward and reverse genetics in Barley (*Hordeum vulgare* L.). The plant journal **40:** 143-150

Camenisch TD, Brilliant MH, Segal DJ (2008) Critical parameters for genome editing using zinc finger nucleases. Mini Reciew of medical chemistry **8:** 669-676

Cancel JD, Larsen PB (2002) Loss-of-function mutations in the ethylene receptor ETR1 cause enhanced sensitivity and exaggerated response to ethylene in Arabidopsis. Plant physiology **129(4):** 1557-1567

Cara B, Giovannoni JJ (2008) Molecular biology of ethylene during tomato fruit development and maturation. Plant science **175:** 106-13

Carbonell-Bejerano P, Urbez C, Granell A, Carbonell J, Perez-Amador MA (2011) Ethylene is involved in pistil fate by modulating the onset of ovule senescence and the GA-mediated fruit set in Arabidopsis. BMC plant biology **11:** 84

Carrari F, Baxter C, Usadel B, Urbanczyk-Wochniak-Zanor MI, Nunes-Nesi A, Nikiforova V, Centero D, Ratzka A, Pauly M, Sweetlove LJ, Fernie AR (2006) Integrated analysis of metabolite and transcript levels reveals the metabolic shifts that underlie tomato fruit development and highlight regulatory aspects of metabolic network behaviour. Plant physiology **142:** 1380-1396

Carrari F, Fernie A (2006) Metabolic regulation underlying tomato fruit development. Journal of experimental botany **57:** 1883-1897

Carrari F, Nunes-Nesi A, Gibon Y, Lytovchenko A, Loureiro ME, Fernie AR (2003) Reduced expression of aconitase results in an enhanced rate of photosynthesis and marked shifts in carbon partitioning in illuminated leaves of wild species tomato. Plant physiology **133:** 1322-1335

Carrera E, Ruiz-Rivero O, Peres LE, Atares A, Garcia-Martinez JL (2012) Characterization of the *procera* tomato mutant shows novel functions of the SlDELLA protein in the control of flower morphology, cell division and expansion, and the auxin-signaling pathway during fruit-set and development. Plant physiology **160:** 1581-1596

Cary AJ, Liu W, Howell SH (1995) Cytokinin action is coupled to ethylene in its effects on the inhibition of root and hypocotyl elongation in *Arabidopsis thaliana* seedlings. Plant physiology **107:** 1075-1082

Causse M, Damidaux R, Rousselle P (2007) Traditional and enhanced breeding for quality traits in tomato. In: Razdan MK, Mattoo AK, editors. Genetic improve- ment of Solanaceous crops. TomatoEnfield, NH: Science Publishers;. p. 153-92

Chae HS, and Kieber JJ (2005) Eto Brute? Role of ACS turnover in regulating ethylene biosynthesis. Trends in plant science **10:** 291-296

Chae HS, Faure F, Kieber JJ (2003) The *eto1*, *eto2*, and *eto3* mutations and cytokinin treatment increase ethylene biosynthesis in Arabidopsis by increasing the stability of ACS protein. The plant cell **15:** 545-559

Chang C, Kwok SF, Bleecker AB, Meyerowitz EM (1993) Arabidopsis ethylene-response gene ETR1: similarity of product to two-component regulators. Science **262:** 539-544

Chao QM, Rothenberg M, Solano R, Roman G, Terzaghi W, Ecker JR (1997) Activation of the ethylene gas response pathway in Arabidopsis by the nuclear protein ETHYLENE-INSENSITIVE3 and related proteins. Cell **89:** 1133-1144

Cheema AA, Atta BM (2003) Radio sensitivity studies in basmati rice. Pak J Bot **35:** 197-207

Chen G, Alexander L, Grierson D (2004) Constitutive expression of EIL-like transcription factor partially restores ripening in the ethylene-insensitive Nr tomato mutant. Journal of experimental botany **55:** 1491-1497

Chen G, Hu Z, Grierson D (2008) Differential regulation of tomato ethylene responsive factor LeERF3b, a putative repressor, and the activator Pti4 in ripening mutants and in response to environmental stresses. Journal of plant physiology **165:** 662-670

Chen GP, Wilson ID, Kim SH, Grierson D (2001) Inhibiting expression of a tomato ripening associated membrane protein increases organic acids and reduces sugar levels of fruit. Planta **212:** 799-807

Chen R, Binder BM, Garrett WM, Tucker ML, Cooper B, Chang C (2011) Proteomic responses in *Arabidopsis thaliana* seedlings treated with ethylene. Molecular biosystems **7:** 2637-2650

Chen T, Liu J, Lei G, Liu Y-F, Li Z-G, Tao J-J, Hao Y-J, Cao Y-R, Lin Q, Zhang W-K, Ma B, Chen S-Y, Zhang J-S (2009) Effects of tobacco ethylene receptor mutations on receptor kinase activity, plant growth and stress responses. Plant cell and physiology **50:** 1636-1650

Chen Y-F, Gao Z, Kerris RJ 3rd, Wang W, Binder BM, Schaller GE (2010) Ethylene receptors function as components of high-molecular-mass protein complexes in Arabidopsis. PLoS one **5:** e8640

Chen Y-F, Randlett MD, Findell JL, Schaller GE (2002) Localization of the ethylene receptor ETR1 to the endoplasmic reticulum of Arabidopsis. Journal of biological chemistry **277:** 19861-19866

Chiwocha S, Cutler A, Abrams SR, Ambrose S, Yang J, Ross AR, et al. (2005) The etr1-2 mutation in *Arabidopsis thaliana* affects the abscisic acid, auxin, cytokinin and gibberellin metabolic pathways during maintenance of seed dormancy, moist-chilling and germination. Plant Journal **42:** 35-48

Christian M, Qi Y, Zhang Y, Voytas DF (2013) Targeted mutagenesis of *Arabidopsis thaliana* using engineered TAL effector nucleases. Genes genomes genetics **3:** 1697-1705

Christians MJ, Gingerich DJ, Hansen M, Binder BM, Kieber JJ, Vierstra RD (2009) The BTB ubiquitin ligases ETO1, EOL1, and EOL2 act collectively to regulate ethylene biosynthesis in Arabidopsis by controlling type-2 ACC synthase levels. The plant journal **57:** 332-345

Chuanli Ju, Bram Van de Poel, Endymion DC, James HT, Theodore RG,Charles FD Caren C (2015) Conservation of ethylene as a plant hormone over 450 million years of evolution. Nature plants **1:** 14004

Chung MC, Chou SJ, Kuang LY, Charng YY, and Yang SF (2002) Sub-cellular localization of 1-aminocyclopropane-1-carboxylic acid oxidase in apple fruit. Plant cell and physiology **43:** 549-554

Chung MY, Vrebalov J, Alba R, Lee J, McQuinn R, Chung JD, Klein P, Giovannoni J (2010) A tomato (*Solanum lycopersicum*) APETALA2/ERF gene, SlAP2a, is a negative regulator of fruit ripening. The plant journal **64:** 936-947

Clark KL, Larsen PB, Wang XX, Chang C (1998) Association of the Arabidopsis CTR1 raf-like kinase with the ETR1 and ERS ethylene receptors. Proceedings of the National Academy of Sciences, USA **95:** 5401-5406

Coenen C, Christian M, Luthen H, Lomax TL (2003) Cytokinin inhibits a subset of diageotropica-dependent primary auxin responses in tomato. Plant physiology **131:** 1692-1704

Colelli G, Sanchez M, Torralbo F (2003) Effects of treatment with 1- methylcyclopropene (1-MCP) on tomato. Alimentaria**:** 67-70

Comai L, Young K, Till BJ, Reynolds SH, Greene EA, Codomo CA, Enns LC, Johnson JE, Burtner C, Odden AR (2004) Efficient discovery of DNA polymorphisms in natural populations by Ecotilling. The plant journal **37:** 778-786

Coombe B (1976) The development of fleshy fruits. Annual review of plant physiology **27:** 507-528

Corbineau F, Xia Q, Bailly C, El-Maarouf-Bouteau H (2013) Ethylene, a key factor in the regulation of seed dormancy. Frontiers in plant science **5:** 539-539

Crane JC (1964) Growth substances in fruit setting and development. Annual review of plant physiology **15:** 303-326

D'Aoust MA, Yelle S, Nguyen-Quoc B (1999) Antisense inhibition of tomato fruit synthase decreases fruit setting and the sucrose unloading capacity of young fruit. The plant cell **11:** 2407-2418

de Jong M, Wolters-Arts M, Feron R, Mariani C, Vriezen WH (2009) The Solanum lycopersicum auxin response factor 7 (SlARF7) regulates auxin signaling during tomato fruit set and development. The plant journal **57:** 160-170

de Jong M, Wolters-Arts M, Garcia-Martinez JL, Mariani C, Vriezen WH (2011) The *Solanum lycopersicum* AUXIN RESPONSE FACTOR 7 (SlARF7) mediates cross-talk between auxin and gibberellin signalling during tomato fruit set and development. Journal of experimental botany **62:** 617-626

De Paepe A, Van Der Straeten D (2005) Ethylene biosynthesis and signaling: an overview. Vitamines and hormones **72:** 399-430

DeBolt S, Cook DC, Ford CM (2006) L-Tartaric acid synthesis from vitamin C in higher plants. Proceedings of the National Academy of Sciences of the United States of America **103:** 5608-5613

Dehan K, Tal M (1978) Salt tolerance in the wild relatives of the cultivated tomato: responses of *Solanum pennellii* to high salinity. Irrigation science **1:** 71-76

Deikman J (1997) Molecular mechanisms of ethylene regulation of gene transcription. Physiological plantarum **100:** 561-566

Deikman J, Ulrich M (1995) A novel cytokinin-resistant mutant of Arabidopsis with abbreviated shoot development. Planta **195:** 440-449

Denison FC, Paul A-L, Zupanska AK, Ferl RJ (2011) 14-3-3 proteins in plant physiology. Seminars in cell and developmental biology **22:** 720-727

Desikan R, Last K, Harrett-Williams R, Tagliavia C, Harter K, Hooley R, Hancock JT, Neill SJ (2006) Ethylene-induced stomatal closure in Arabidopsis occurs via AtrbohF-mediated hydrogen peroxide synthesis. The plant journal **47:** 907-916

Dolan L (1997) The role of ethylene in the development of plant form. Journal of eexperimental botany **48:** 201-10

Dong C-H, Jang M, Scharein B, Malach A, Rivarola M, Liesch J, Groth G, Hwang I, Chang C (2010) Molecular association of the Arabidopsis ETR1 ethylene eceptor and a regulator of ethylene signaling, RTE1. Journal of biological chemistry **285:** 40706-40713

Dong C-H, Rivarola M, Resnick JS, Maggin BD, Chang C (2008) Subcellular co-localization of Arabidopsis RTE1 and ETR1 supports a regulatory role for RTE1 in ETR1 ethylene signaling. The plant journal **53:** 275-286

Dong JG, Fernandezmaculet JC, and Yang SF (1992) Purification and characterization of 1-aminocyclopropane-1-carboxylate oxidase from apple fruit. Proc. Natl. Acad. Sci. U.S.A. **89:** 9789-9793

Dorcey E, Urbez C, Blazquez MA, Carbonell J, Perez-Amador MA (2009) Fertilization-dependent auxin response in ovules triggers fruit development through the modulation of gibberellin metabolism in Arabidopsis. The plant journal **58:** 318-332

Dostal HC, Leopold AC (1967) Gibberellin delays ripening of tomatoes. Science **158:** 1579-1580

Drake JW, Charlesworth B, Charlesworth D, Crow JF (1998) Rates of spontaneous mutation. Genetics **148:** 1667-1686

Durai S, Mani M, Kandavelou K, Wu J, Porteus MH, Chandrasegaran S (2005) Zinc finger nucleases: custom-designed molecular scissors for genome engineering of plant and mammalian cells. Nucleic acid research **33:** 5978-5990

Ecarnot M, Baczyk P, Tessarotto L, Chervin C (2013) Rapid phenotyping of the tomato fruit model, Micro-Tom, with a portable VIS-NIR spectrometer. Plant physiology and biochemistry **70:** 159-63

Ecker JR (1995) The ethylene signal transduction pathway in plants. Science **268:** 667–75

Egea I, Bian W, Barsan C, Jauneau A, Pech J-C, Latché A, Li Z, Chervin C (2011) Chloroplast to chromoplast transition in tomato fruit: spectral confocal microscopy analyses of carotenoids and chlorophylls in isolated plastids and time-lapse recording on intact live tissue. Annals of botany **108:** 291-297

Elshire RJ, Glaubitz JC, Sun Q, Poland JA, Kawamoto K, Buckler ES, Mitchell SE (2011) A robust, simple genotyping-by-sequencing (GBS) approach for high diversity species. PLoS one **6:** e19379

Emmanuel E, Levy AA (2002) Tomato mutants as tools for functional genomics. Current opinion of plant biology **5**: 112-117

Fan X, Mattheis JP, Fellman JK (1998) A role for jasmonates in climacteric fruit ripening. Planta **204:** 444-449

Fantini E, Falcone G, Frusciante S, Giliberto L, Giuliano G (2013) Dissection of tomato lycopene biosynthesis through virus-induced gene silencing. Plant physiology **163:** 986-98

Feng Z, Zhang B, Ding W, Liu X, Yang D-L, Wei P, Cao F, Zhu S, Zhang F, Mao Y (2013) Efficient genome editing in plants using a CRISPR/Cas system. Cell research **23:** 1229-1232

Fernie AR, Carrari F, Sweetlove LJ (2004) Respiratory metabolism: glycolysis, the TCA cycle and mitochondrial electron transport. Current. Opinion in. plant biology **7:** 254-261

Ford NA, Erdman Jr JW (2012) Are lycopene metabolites metabolically active? Acta Biochimica Polonica **59**: 1-4

Fraser PD, Pinto MES, Holloway DE, Bramley PM (2000) Application of high-performance liquid chromatography with photodiode array detection to the metabolic profiling of plant isoprenoids. The plant journal **24:** 551-558

Fraser PD, Truesdale MR, Bird CR, Schuch W, Bramley PM (1994) Carotenoid biosynthesis during tomato fruit development evidence for tissue-specific gene expression. Plant physiology **105:** 405-13

Fridman E, Carrari F, Liu YS, Fernie AR, Zamir D (2004) Zooming in on a quantitative trait for tomato yield using interspecific introgressions. Science **305:** 1786-1789

Fridman E, Pleban T, Zamir D (2000) A recombination hotspot delimits a wild-species quantitative trait locus for tomato sugar content to 484 bp within an invertase gene Proceedings of the National Academy of Sciences, USA **97:** 4718-4723

Fu DQ, Zhu BZ, Zhu HL, Jiang WB, Luo YB (2005) Virus-induced gene silencing in tomato fruit. The plant Journal **43:** 299-308

Fu FQ, Mao WH, Shi K, Zhou YH, Asami T, Yu JQ (2008) A role of brassinosteroids in early fruit development in cucumber. Journal of experimental botany **59:** 2299-2308

Fuentes S, Ljung K, Sorefan K, Alvey E, Harberd NP, Ostergaard L (2012) Fruit growth in Arabidopsis occurs via DELLA-dependent and DELLA-independent gibberellin responses. The plant cell **24:** 3982-3996

Fujisawa M, Nakano T, Shima Y, Ito Y (2013) A large-scale identification of direct targets of the tomato MADS box transcription factor RIPENING INHIBITOR reveals the regulation of fruit ripening. The plant cell **25:** 371-86

Gady AL, Hermans FW, Van de Wal MH, van Loo EN, Visser RG, Bachem CW (2009) Implementation of two high through-put techniques in a novel application: detecting point mutations in large EMS mutated plant populations. Plant methods **5:** 13

Gagne JM, Smalle J, Gingerich DJ, Walker JM, Yoo SD, Yanagisawa S, Vierstra RD (2004) Arabidopsis EIN3-binding F-box 1 and 2 form ubiquitin-protein ligases that repress ethylene action and promote growth by directing EIN3 degradation. Proceedings of the National Academy of Sciences, USA **101:** 6803-680

Galeano CH, Gomez M, Rodriguez LM, Blair MW (2009) CEL I nuclease digestion for SNP discovery and marker development in common bean (L.). Crop science **49:** 381-394

Gamble RL, Coonfield ML, Schaller GE (1998) Histidine kinase activity of the ETR1 ethylene receptor from Arabidopsis. Proceedings of the National Academy of Sciences, USA **95:** 7825-7829

Gamble RL, Qu X, Schaller GE (2002) Mutational analysis of the ethylene receptor ETR1. Role of the histidine kinase domain in dominant ethylene insensitivity. Plant physiology **128:** 1428-1438

Gane R (1934) Production of ethylene by some ripening fruits. Nature **134:** 1008-1008

Gao HY, Zhu BZ, Zhu HL, Zhang Y, Xie L, Li YH, Luo YCYB (2007) Effect of suppression of ethylene biosynthesis on flavour products in tomato fruits. Russ. Journal of plant physiology **54:** 80-88

Gao Z, Wen C-K, Binder BM, Chen Y-F, Chang J, Chiang Y-H, Kerris RJ III, Chang C, Schaller GE (2008) Heteromeric interactions among ethylene receptors mediate signaling in Arabidopsis. Journal of biological chemistry **283:** 23801-23810

Gao ZY, Chen YF, Randlett MD, Zhao XC, Findell JL, Kieber JJ, Schaller GE (2003) Localization of the raf-like kinase CTR1 to the endoplasmic reticulum of Arabidopsis through participation in ethylene receptor signaling complexes. Journal of biological chemistry **278:** 34725-34732

Gapper NE, McQuinn RP, Giovannoni JJ (2013) Molecular and genetic regulation of fruit ripening. Plant molecular biology **82:** 575-591

García-Martínez JL, Carbonell J (1980) Fruit-set of unpollinated ovaries of *Pisum sativum* L. Influence of plant-growth regulators. Planta **147:** 451-456

Gautier H, Diakou-Verdin V, Benard C, Reich M, Bourgard F, Poessel JL, et al (2008) How does tomato quality (sugar, acid, and nutritional quality) vary with ripening stage, temperature, and irradiance? Journal of agriculture and food chemistry **56:** 1241-1250

Gilchrist EJ, Haughn GW, Ying CC, Otto SP, Zhuang J, Cheung D, Hamberger B, Aboutorabi F, Kalynyak T, Johnson L (2008) Use of Ecotilling as an efficient SNP discovery tool to survey genetic variation in wild populations of Populus trichocarpa. Molecular ecology **15:** 1367-1378

Gilchrist EJ, O'Neil NJ, Rose AM, Zetka MC, Haughn GW (2006) TILLING is an effective reverse genetics technique for Caenorhabditis elegans. BMC genomics **7:** 262

Gillaspy G, Ben-David H, Gruissem W (1993) Fruits: a developmental perspective. The plant cell **5:** 1439-1451

Giovannoni JJ (2004) Genetic regulation of fruit development and ripening. The plant cell **16** Suppl, S170-180

Giovannoni JJ (2007) Fruit ripening mutants yield insights into ripening control. Current opinion in pant biology **10:** 283-289

Giovannoni JJ, DellaPenna D, Bennett AB, Fischer RL (1989) Expression of a chimeric polygalacturonase gene in transgenic *rin* (ripening inhibitor) tomato fruit results in polyuronide degradation but not fruit softening. The plant cell **1:** 53-63

Giovannoni J (2001) Molecular regulation of fruit ripening. Annual Review on plant physiology and plant molecular biology **52:** 725-749

Giuliano G (2014) Plant carotenoids: genomics meets multi-gene engineering. Current opinion in plant biology **19:** 111-7

Giuliano G, Bartley GE, Scolnik PA (1993) Regulation of carotenoid biosynthesis during tomato development. The plant cell **5:** 379-87

Goeschl J, Rappaport L, Pratt H (1966) Ethylene as a factor regulating the growth of pea epicotyls subjected to physical stress. Plant physiology **41:** 877-84

Goetz M, Hooper LC, Johnson SD, Rodrigues JC, Vivian-Smith A, Koltunow AM (2007) Expression of aberrant forms of AUXIN RESPONSE FACTOR8 stimulates parthenocarpy in Arabidopsis and tomato. Plant physiology **145:** 351–366

Goulao LF, Oliveira CM (2008) Cell wall modification during fruit ripening: when a fruit is not the fruit. Trends in food science and technology **19:** 4-25

Goulao LF, Santos J, de Sousa I, Oliveira CM (2007) Patterns of enzymatic activity of cell wall-modifying enzymes during growth and ripening of apples. Postharvest biology and technology **43:** 307-318

Gray JE, Picton S, Giovannoni JJ, Grierson D (1994) The use of transgenic and naturally-occurring mutants to understand and manipulate tomato fruit ripening. Plant, cell and environment **17:** 557-571

Gray WM (2004) Hormonal regulation of plant growth and development. PLoS biology **283:** e311

Greene EA, Codomo CA, Taylor NE, Henikoff JG, Till BJ, Reynolds SH, Enns LC, Burtner C, Johnson JE, Odden AR (2003) Spectrum of chemically induced mutations from a large scale reverse-genetic screen in Arabidopsis. Genetics **164:** 731-740

Guo HW, Ecker JR (2003) Plant responses to ethylene gas are mediated by SCF (EBF1/EBF2)-dependent proteolysis of EIN3 transcription factor. Cell **115:** 667-677

Gupta A, Pal RK, Rajam MV (2013) Delayed ripening and improved fruit processing quality in tomato by RNAi-mediated silencing of three homologs of 1-aminopropane-1-carboxylate synthase gene. Journal of plant physiology **170:** 987-995

Gupta A, Singh M, Laxmi A (2015) Interaction between glucose and brassinosteroid during the regulation of lateral root development in Arabidopsis. Plant physiology **168(1):** 307-320

Gupta S, Charakana C, Sreelakshmi Y, Sharma R (2011) Fluorescent dye labeled DNA size standards for molecular mass detection in visible/infrared range. BMC research notes **4:** 12

Gupta SK, Sharma S, Santisree P, Kilambi HV, Appenroth K, Sreelakshmi Y, Sharma R (2014) Complex and shifting interactions of phytochromes regulate fruit development in tomato. Plant cell and enviroment **37:** 1688-1702

Gutterson N, Reuber TL (2004) Regulation of disease resistance pathways by AP2/ERF transcription factors. Current opinion on plant biology **7:** 465-471

Guzman P, Ecker JR (1990) Exploiting the triple response of Arabidopsis to identify ethylene-related mutants. The plant cell **2:** 513-23

Hadfield KA, Bennett AB (1998) Polygalacturonases: many genes in search of a function. Plant physiology **117:** 337-343

Hajjar R, Hodgkin T (2007) The use of wild relatives in crop improvement: a survey of developments over the last 20 years. Euphytica **156:** 1-13

Hall AE, Bleecker AB (2003) Analysis of combinatorial loss-of-function mutants in the Arabidopsis ethylene receptors reveals that the *ers1 etr1* double mutant has severe developmental defects that are EIN2 dependent. The plant cell **15:** 2032-2041

Hall AE, Chen QHG, Findell JL, Schaller GE, Bleecker AB (1999) The relationship between ethylene binding and dominant insensitivity conferred by mutant forms of the ETR1 ethylene receptor. Plant physiology **121:** 291-299

Hall AE, Findell JL, Schaller GE, Sisler EC, Bleecker AB (2000) Ethylene perception by the ERS1 protein in *Arabidopsis*. Plant physiology **123:** 1449-1457

Hall BP, Shakeel SN, Amir M, Haq NU, Qu X, Schaller GE (2012) Histidine kinase activity of the ethylene receptor ETR1 facilitates the ethylene response in Arabidopsis. Plant physiology **159:** 682-695

Halliday LC, Artwohl JE, Ramakrishnan V, Bunte RM, Bennet BT (2004) Effects of Freund's Complete Adjuvant on Physiology, Histology and Activity of New Zealand white rabbits. Contemporary topics **43:** 8-13

Hamilton A, Lycett G, Grierson D (1990) Antisense gene that inhibits synthesis of the hormone ethylene in transgenic plants. Nature **346:** 284-287

Han L, Li G-J, Yang K-Y, Mao G, Wang R, Liu Y, Zhang S (2010) Mitogen-activated protein kinase 3 and 6 regulate Botrytis cinerea-induced ethylene production in Arabidopsis. The plant journal **64:** 114-127

Hanson AD, Gregory III JF (2011) Folate biosynthesis, turnover, and transport in plants. Annual review of plant biology **62**: 105-125

Harberd NP (2003) Botany. Relieving DELLA restraint. Science **299:** 1853-1854

Harker FR, Redgwell RJ, Hallet IC, Murray SH (1997) Texture of fresh fruit. Horticultural reviews **20:** 121-224

Hays DB, Do JH, Mason RE, Morgan G, Finlayson SA (2007) Heat stress induced ethylene production in developing wheat grains induces kernel abortion and increased maturation in a susceptible cultivar. Plant science **172:** 1113-1123

Henry IM, Nagalakshmi U, Lieberman MC, Ngo KJ, Krasileva KV, Vasquez-Gross H, Akhunova A, Akhunov E, Dubcovsky J, Tai TH (2014) Efficient Genome-Wide Detection and Cataloging of EMS-Induced Mutations Using Exome Capture and Next-Generation Sequencing. The plant cell **26:** 1382-1397

Heslot H (1977) Review of main mutagenic compound. In: Manual on mutation breeding. IAEA Technical reports series, No. **119:** 2nd ed, pp 51-58

Hetherington SE, Smillie RM, Davies W (1998) Photosynthetic activities of vegetative and fruiting tissues of tomato. Journal of eexperimental botany **49:** 1173-1181

Hileman LC, Sundstrom JF, Litt A, Chen M, Shumba T, Irish VF (2006) Molecular and phylogenetic analyses of the MADS-box gene family in tomato. Molecular biology evolution **23:** 2245-2258

Hirayama T, Kieber JJ, Hirayama N, Kogan M, Guzman P, Nourizadeh S, Alonso JM, Dailey WP, Dancis A, Ecker JR (1999) RESPONSIVE-TO-ANTAGONIST1, a Menkes/Wilson disease-related copper transporter, is require- ed for ethylene signaling in Arabidopsis. Cell **97:** 383-393

Hirschberg J (2001) Carotenoid biosynthesis in flowering plants. Current opinion in plant biology **4:** 210-8

Hoeberichts FA, Van Der Plas LH, Woltering EJ (2002) Ethylene perception is required for the expression of tomato ripening-related genes and associated physiological changes even at advanced stages of ripening. Postharvest Biology and Technology **26:** 125-133

Hohenlohe PA, Amish SJ, Catchen JM, Allendorf FW, Luikart G (2011) Next-generation RAD sequencing identifies thousands of SNPs for assessing hybridization between rainbow and west slope cutthroat trout. Molecular ecology research **11:** 117-122

Hua J, Chang C, Sun Q, Meyerowitz EM (1995) Ethylene insensitivity conferred by Arabidopsis *ERS* gene. Science **269:** 1712-1714

Hua J, Meyerowitz EM (1998) Ethylene responses are negatively regulated by a receptor gene family in *Arabidopsis thaliana.* Cell **94:** 261-271

Hua J, Sakai H, Nourizadeh S, Chen QHG, Bleecker AB, Ecker JR, Meyerowitz EM (1998) EIN4 and ERS2 are members of the putative ethylene receptor gene family in Arabidopsis. The plant cell **10:** 1321-1332

Huai Q, Xia Y, Chen Y, Callahan B, Li N, Ke H (2001) Crystal structures of 1-aminocyclopropane-1-carboxylate (ACC) synthase in complex with amino ethoxy-vinylglycine and pyridoxal-5'-phosphate provide new insight into catalytic mecha- nisms. Journal of .biological. chemistry **276:** 38210-38216

Huang T, Wang P, Ye Z-Q, Xu H, He Z, et al. (2010) Prediction of Deleterious Non-S ynonymous SNPs Based on Protein Interact ion Network and Hybrid Properties. PLoS one **5**: 0011900

Huang YF, Li H, Hutchison CE, Laskey J, Kieber JJ (2003) Biochemical and functional analysis of CTR1, a protein kinase that negatively regulates ethylene signaling in Arabidopsis. The plant journal **33:** 221-233

Hudgins JW, Ralph SG, Franceschi VR, and Bohlmann J (2006) Ethylene in induced conifer defense: cDNA cloning, protein expression, and cellular and subcellular localization of 1-aminocyclopropane-1-carboxylate oxidase in resin duct and phenolic parenchyma cells. Planta **224:** 865-877

Iniesta MD, P´erez-Conesa D, Garc´ıa-Alonso J, Ros G, Periago MJ (2009) "Folate content in tomato (*Lycopersicon esculentum*). Inluence of cultivar, ripeness, year of harvest, and

pasteurization and storage temperatures," Journal of agricultural and food chemistry **57:** 4739-4745

Ji K, Kai W, Zhao B, Sun Y, Yuan B, Dai S, Li Q, Chen P, Wang Y, Pei Y (2014) SlNCED1 and SlCYP707A2: key genes involved in ABA metabolism during tomato fruit ripening. Journal of experimental botany **288**

Jiao Y, Lau OS, Deng XW (2007) Light-regulated transcriptional networks in higher plants. Nature review on genetics **8:** 217-230

Jiménez-Bermúdez S, Redondo-Nevado J, Muñoz-Blanco J, Caballero JL, López-Aranda JM, Valpuesta V, Pliego-Alfaro F, Quesada MA, Mercado JA (2002) Manipulation of strawberry fruit softening by antisense expression of a pectate lyase gene. Plant physiology **128:** 751-759

Jing H-C, Schippers JH, Hille J, Dijkwel PP (2005) Ethylene-induced leaf senescence depends on age-related changes and OLD genes in Arabidopsis. Journal of experimental botany **56:** 2915-2923

Johnson PR, Ecker JR (1998) The ethylene gas signal transduction pathway: a molecular perspective. Annual review of genetics **32:** 227-254

Joo S, Liu Y, Lueth A, and Zhang S (2008) MAPK phosphorylation-induced stabilization of ACS6 protein is mediated by the non-catalytic C-terminal domain, which also contains the cis-determinant for rapid degradation by the 26S proteasome pathway. The plant journal. **54:** 129-140

Joy KW (1988) Ammonia, glutamine and asparagine: a carbon nitrogen interface. Canadian. Journal of botany **66:** 2103-2109

Ju C, Yoon GM, Shemansky JM, Lin D, Yin I, Chang J, Garrett W, Kessenbrock M, Groth G, Tucker ML, Cooper B, Kieber JJ, Chang C (2012) CTR1 phosphorylates the central regulator EIN2 to control ethylene hormone signaling from the ER membrane to the nucleus in Arabidopsis. Proceedings of the National Academy of Sciences, USA **109:** 19486-19491

Kadaru SB, Yadav AS, Fjellstrom RG, Oard JH (2006) Alternative Ecotilling protocol for rapid, cost-effective single-nucleotide polymorphism discovery and genotyping in rice (*Oryza sativa* L.). Plant molecular biology reporter **24:** 3-22

Kamiyoshihara Y, Iwata M, Fukaya T, Tatsuki M, and Mori H (2010) Turnover of LeACS2, a wound-inducible 1-aminocyclopropane-1-carboxylic acid synthase in tomato, is regulated by phosphorylation/dephosphorylation. The plant journal. **64:** 140-150

Kang C, Darwish O, Geretz A, Shahan R, Alkharouf N, Liu Z (2013) Genome-scale transcriptomic insights into early-stage fruit development in woodland strawberry *Fragaria vesca*. The plant cell **25:** 1960-1978

Karlova R, Rosin FM, Busscher-Lange J, Parapunova V, Do PT, Fernie AR, Fraser PD, Baxter C, Angenent GC, de Maagd RA (2011) Transcriptome and metabolite profiling show that APETALA2a is a major regulator of tomato fruit ripening. The plant cell **23:** 923-941

Kavanaugh CJ, Trumbo PR, Ellwood KC (2007) The U.S. Food and Drug Administration's evidence-based review for qualified health claims: tomatoes, lycopene, and cancer. Journal of national cancer institute **99:** 1074-1085

Kende H, Zeevaart J (1997) The Five "Classical" Plant Hormones. The plant cell **9:** 1197-1210

Kieber JJ, Rothenberg M, Roman G, Feldmann KA, Ecker JR (1993) CTR1, a negative regulator of the ethylene response pathway in Arabidopsis, encodes a member of the Raf family of protein kinases. Cell **72:** 427-4

Kilambi HV, Kumar R, Sharma R, Sreelakshmi Y (2013) Chromoplast-specific carotenoid-associated protein appears to be important for enhanced accumulation of carotenoids in *hp1* tomato fruits. Plant physiology **161:** 2085-2101

Kim CY, Liu Y, Thorne ET, Yang H, Fukushige H, Gassmann W, Hildebrand D, Sharp RE, Zhang S (2003) Activation of a stress-responsive mitogen-activated protein kinase cascade induces the biosynthesis of ethylene in plants. The plant cell **15:** 2707-2718

Kim H, Helmbrecht EE, Stalans MB, Schmitt C, Patel N, Wen C-K, Wang W, Binder BM (2011) Ethylene receptor ETR1 domain requirements for ethylene responses in Arabidopsis seedlings. Plant physiology **156:** 417-429

Kimchi-Sarfaty C, Oh JM, Kim I-W, Sauna ZE, Calcagno AM, Ambudkar SV, Gottesman MM (2007) A"silent" polymorphism in the *MDR1* gene changes substrate specificity. Science **315:** 525-528

Kimura S, Sinha N (2008) Tomato (Solanum lycopersicum): A model fruit-bearing crop. Cold spring harbour protocol **11:** 10.1101

Klee HJ (2004) Ethylene signal transduction. Moving beyond Arabidopsis. Plant physiology **135:** 660-667

Klee HJ, Giovannoni JJ (2011) Genetics and control of tomato fruit ripening and quality attributes. Annual review of genetics **45:** 41-59

Koorneef M, Meinke D (2010) The development of Arabidopsis as a model plant. The plant journal **61:** 909-921

Kornienko A, Butorina A (2013) Induced mutagenesis in Sugar Beet (Beta vulgaris L.): Obtained results and prospects for use in development of TILLING project. Biology bulletin review **3:** 152-160

Koshland DE (1993) The two-component pathway comes to eukaryotes. Science **262:** 532

Kousar Makeen, G. Suresh Babu, G.R. Lavanya and Grard Abraham (2007) Studies of Chlorophyll Content by Different Methods in Black Gram (*Vigna mungo* L.). International journal of agricultural research **2**: 651-654

Kramer M, Sanders R, Bolkan H, Waters C, Sheehy RE, Hiatt WR (1992) Postharvest evaluation of transgenic tomatoes with reduced levels of polygalacturonase: processing, firmness and disease resistance. Postharvest biology and technology **1:** 241-255

Krammes JG, Megguer CA, Argenta LC, Amarante CVTd, Grossi D (2003) Use of 1-methycyclopropene to delay fruit ripening of tomato. Horticultura Brasileira **21:** 611-614

Krieg DR (1963) Ethyl methane sulfonate-induced reversion of bacteriophage T4rII mutants. Genetics **48**: 561-580

Kumar R, Khurana A, Sharma AK (2014) Role of plant hormones and their interplay in development and ripening of fleshy fruits. Journal of experimental botany **65:** 4561-4575

Laemmli UK (1970) Cleavage of structural proteins during the assembly of the head of bacteriophage T4. Nature **227**: 680-685

Lanahan MB, Yen H-C, Giovannoni JJ, Klee HJ (1994) The never ripe mutation blocks ethylene perception in tomato. The plant cell **6:** 521-530

Lara I, Belge B, Goulao LF (2014) The fruit cuticle as a modulator of postharvest quality. Postharvest biology and technology **87:** 103-112

Lashbrook CC, Tieman DM, Klee HJ (1998) Differential regulation of the tomato ETR gene family throughout plant development. The plant journal **15:** 243-252

Le Gall G, Colquhoun IJ, Davis AL, Collins GJ, Verhoeyen ME (2003) Metabolite profiling of tomato (*Lycopersicon esculentum*) using 1H NMR spectroscopy as a tool to detect potential unintended effects following a genetic modification. Journal of. Agriculture and food chemistry **51:** 2447-2456

Lee JM, Joung JG, McQuinn R, Chung MY, Fei Z, Tieman D, Klee H, Giovannoni J (2012) Combined transcriptome, genetic diversity and metabolite profiling in tomato fruit reveals that the ethylene response factor SlERF6 plays an important role in ripening and carotenoid accumulation. The plant journal **70:** 191-204

Lelievre JM, Latche A, Jones B, Bouzayen M, Pech JC (1997) Ethylene and fruit ripening. Plant physiology **101:** 727-39

Leung H, Wu C, Baraoidan M, Bordeos A, Ramos M, Madamba S, Cabauatan P, Vera Cruz C, Portugal A, Reyes G (2001) Deletion mutants for functional genomics: progress in phenotyping, sequence assignment, and database Devlopment. rice genetics IV, 239-251

Li N, Huxtable S, Yang SF, Kung SD (1996) Effects of N-terminal deletions on 1-aminocyclopropane-1-carboxylate synthase activity. FEBS letters**378:** 286-290

Li N, Mattoo A (1994) Deletion of the carboxyl-terminal region of 1-aminocyclopropane-1-carboxylic acid synthase, a key protein in the biosynthesis of ethylene, results in catalytically hyperactive, monomeric enzyme Journal of biological chemistry **269:** 6908-6917

Li T, Liu B, Spalding MH, Weeks DP, Yang B (2012) High-efficiency TALEN-based gene editing produces disease-resistant rice. Nature biotechnology **30:** 390-392

Lieberman M, Mapson LW (1964) Genesis and biogenesis of ethylene. Nature **204:** 343-345

Liu L, Wei J, Zhang M, Zhang L, Li C and Wang Q (2012) Ethylene independent induction of lycopene biosynthesis in tomato fruits by jasmonates. Journal of experimental botany **10**: 1093

Liu Y, Schiff M, Dinesh-Kumar S (2002) Virus-induced gene silencing in tomato. The plant journal **31:** 777-786

Liu Y, Zhang S (2004) Phosphorylation of 1-aminocyclopropane-1-carboxylic acid synthase by MPK6, a stress-responsive mitogen-activated protein kinase, induces ethylene biosynthesis in Arabidopsis. The plant cell **16:** 3386-3399

Lobell DB, Burke MB, Tebaldi C, Mastrandrea MD, Falcon WP, Naylor RL (2008) Prioritizing climate change adaptation needs for food security in 2030. Science **319:** 607-610

López-Bucio J, Cruz-Ramírez A, Herrera-Estrella L (2003) The role of nutrient availability in regulating root architecture. Current opinion in plant biology **6(3)** 280-287

Lucock M (2000) "Folic acid: nutritional biochemistry, molecular biology, and role in disease processes," Molecular genetics and metabolism **71:** 121-138

Lytovchenko A, Eickmeier I, Pons C, Osorio S, Szecowka M, Lehmberg K, Arrivault S, Tohge T, Pineda B, Anton MT (2011) Tomato fruit photosynthesis is seemingly unimportant in primary metabolism and ripening but plays a considerable role in seed development. Plant physiology **157:** 1650-1663

Lyzenga WJ, Booth JK, and Stone SL (2012) The Arabidopsis RING-type E3 ligase XBAT32 mediates the proteasomal degradation of the ethylene biosynthetic enzyme, 1-aminocyclopropane-1-carboxylate synthase 7. The plant journal **71:** 23-34

Ma C, Ma B, He J, Hao Q, Lu X, Wang L (2011) Regulation of carotenoid content in tomato by silencing of lycopene β /ε -cyclase genes. Plant molecular biology report **29:** 117-24

Manning K, Tor M, Poole M et al (2006) A naturally occurring epigenetic mutation in a gene encoding an SBP-box transcription factor inhibits tomato fruit ripening. Nature genetics **38:** 948-952

Mariotti L, Picciarelli P, Lombardi L, Ceccarelli N (2011) Fruit-set and early fruit growth in tomato are associated with increases in indoleacetic acid, cytokinin, and bioactive gibberellin contents. Journal of plant growth regulation **30:** 405-415

Marsch-Martinez N, Reyes-Olalde JI, Ramos-Cruz D, Lozano-Sotomayor P, Zuniga-Mayo VM, de Folter S (2012) Hormones talking: does hormonal cross-talk shape the Arabidopsis gynoecium? Plant signaling and behavior **7:** 1698-1701

Martel C, Vrebalov J, Tafelmeyer P, Giovannoni JJ (2011) The tomato MADS-box transcription factor RIPENING INHIBITOR interacts with promoters involved in numerous ripening processes in a COLORLESS NONRIPENING-dependent manner. Plant physiology **157:** 1568-79

Marti C, Orzaez D, Ellul P, Moreno V, Carbonell J, Granell A (2007) Silencing of DELLA induces facultative parthenocarpy in tomato fruits. The plant journal **52:** 865-876

Martínez-Romero D, Valero D, Serrano M, Burló F, Carbonell A, Burgos L, Riquelme F (2000) Exogenous polyamines and gibberellic acid effects on peach (Prunus persica L.) storability improvement. Journal of food science **65:** 288-294

Mathieu S, Dal Cin V, Fei Z, Li H, Bliss P, Taylor MG, Klee HJ, Tieman DM (2009) Flavour compounds in tomato fruit: identification of loci and potential pathways affecting volatile composition. Journal of experimental botany **60:** 325-337

Matsuo S, Kikuchi K, Fukuda M, Honda I, Imanishi S (2012) Roles and regulation of cytokinins in tomato fruit development. Journal of experimental botany **63:** 5569-5579

Maxted N, Kell S (2009) Establishment of a global network for the in situ conservation of crop wild relatives: status and needs. FAO commission on genetic resources for food and agriculture, Rome, Italy**:** 266

McAtee P, Karim S, Schaffer R, David K (2013) A dynamic interplay between phytohormones is required for fruit development, maturation, and ripening. Front Plant science **4:** 79

McCallum CM, Comai L, Greene EA, Henikoff S (2000) Targeted screening for induced mutations. Nature biotechnology **18:** 455-457

McCarthy DL, Capitani G, Feng L, Gruetter MG, Kirsch JF (2001) Glutamate 47 in 1-aminocyclopropane-1-carboxylate synthase is a major specificity determinant. Biochemistry **40:** 12276-12284

McCollum J (1954) Effects of light on the formation of carotenoids in tomato fruits. Journal of food science **19:** 182-189

McSteen P, Zhao YK (2008) Plant hormones and signaling: common themes and new developments. Development and cell **14:** 467-473

Mejlhede N, Kyjovska Z, Backes G, Burhenne K, Rasmussen SK, Jahoor A (2006) EcoTILLING for the identification of allelic variation in the powdery mildew resistance genes mlo and Mla of barley. Plant breeding **125:** 461-467

Menda N, Semel Y, Peled D, Eshed Y, Zamir D (2004) In silico screening of saturated mutation library of tomato. The plant journal **38**: 861-872

Menu T, Saglio P, Granot D, Dai N, Raymond P, Ricard B (2004) High hexokinase activity in tomato fruit perturbs carbon and energy metabolism and reduces fruit and seed size. Plant, cell and environment **27:** 89-98

Mercado JA, Pliego-Alfaro F, Quesada MA (2011) Fruit shelf life and potential for its genetic improvement. In: Jenks MA, Bebeli PJ. eds. Breeding for fruit quality. **Oxford:** John Wiley & Sons, 81-104

Merchante C, Alonso JM, Stepanova AN (2013) Ethylene signaling: simple ligand, complex regulation. Current opinion of plant biology **16:** 554-560

Miedes E, Herbers K, Sonnewald U, Lorences (2010) Overexpression of a cell wall enzyme reduces xyloglucan depolymerization and softening of transgenic tomato fruits. Journal of agricultural food chemistry **58:** 5708-2713

Miedes E, Lorences EP (2009) Xyloglucan endotransglucosylase/hydrolases (XTHs) during tomato fruit growth and ripening. Journal of Plant Physiology **166:** 489-498

Miller J, Seiler G (2003) Registration of five oilseed maintainer (HA 429-HA 433) sunflower germplasm lines. Crop science **43:** 2313-2314

Miller J, Tanksley S (1990) RFLP analysis of phylogenetic relationships and genetic variation in the genus Lycopersicon. Theortical and applied genetics **80:** 437-448

Miller JM, and Conn EE (1980) Metabolism of hydrogen cyanide by higher plants. Plant physiology. **65:** 1199-1202

Minoia S, Petrozza A, D'Onofrio O, Piron F, Mosca G, Sozio G, Cellini F, Bendahmane A, Carriero F (2010) A new mutant genetic resource for tomato crop improvement by TILLING technology. BMC research notes **3**: 69

Mir N, Canoles M, Beaudry R, Baldwin E, Mehla CP (2004) Inhibiting tomato ripening with 1-methylcyclopropene. Journal of the American Society for Horticultural Science **129:** 112-120

Moon HS, Li Y, Stewart Jr CN (2010) Keeping the genie in the bottle: transgene biocontainment by excision in pollen. Trends in biotechnogy **28:** 3-8

Moore S, Vrebalov J, Payton P, Giovannoni J (2002) Use of genomics tools to isolate key ripening genes and analyse fruit maturation in tomato. Journal of experimental botany **53:** 2023-2030

Mostofi Y, Toivonen PM, Lessani H, Babalar M, Lu C (2003) Effects of 1-methylcyclopropene on ripening of greenhouse tomatoes at three storage temperatures. Postharvest Biology and Technology **27:** 285-292

Mounet F, Moing A, Kowalczyk M, Rohrmann J, Petit J, Garcia V, Maucourt M, Yano K, Deborde C, Aoki K (2012) Down-regulation of a single auxin efflux transport protein in tomato induces precocious fruit development. Journal of experimental botany **63:** 4901-4917

Moussatche P, Klee HJ (2004) Autophosphorylation activity of the Arabidopsis ethylene receptor multigene family. Journal of biological chemistry **279:** 48734-48741

Müller A (1927) An X-ray investigation of certain long-chain compounds. Proceedings of royal society of London **114:** 542-561

Murphy LJ, Robertson KN, Harroun SG, Brosseau CL, Werner-Zwanziger U, Moilanen J, Tuononen HM, Clyburne JA (2014) A simple complex on the verge of breakdown: isolation of the elusive cyanoformate ion. Science **344:** 75-78

Murr DP, and Yang SF (1975) Conversion of 5'-methylthioadenosine to methionine by apple tissue. Phytochemistry **14:** 1291-1292

Naito K, Kusaba M, Shikazono N, Takano T, Tanaka A, Tanisaka T, Nishimura M (2005) Transmissible and nontransmissible mutations induced by irradiating Arabidopsis thaliana pollen with γ-rays and carbon ions. Genetics **169:** 881-889

Nakatsuka A, Murachi S, Okunishi H, Shiomi S, Nakano R, Kubo Y, Inaba A (1998) Differential expression and internal feedback regulation of 1- aminocyclopropane-1-carboxylate synthase, 1-aminocyclopropane-1-carboxylate oxidase, and ethylene receptor genes in tomato fruit during development and ripening. Plant physiology **118:** 1295-1305

Negi S, Santisree P, Kharshiing EV, Sharma R (2010) Inhibition of the ubiquitin-proteasome pathway alters cellular levels of nitric oxide in tomato seedlings. Molecular plant **3:** 854-69

Negrao S, Almadanim C, Pires I, McNally K, Oliveira M (2011) Use of EcoTILLING to identify natural allelic variants of rice candidate genes involved in salinity tolerance. Plant genetics research **9:** 300-304

Neljubov D (1901) Ueber die horizontale Nutation der Stengel von Pisum sativumund einiger Anderer. Pflanzen Beih. Bot. Zentralbl. **10:** 128-139

Nevo E, Chen G (2010) Drought and salt tolerances in wild relatives for wheat and barley improvement. Plant cell and enviroment **33:** 670-685

Nieto C, Piron F, Dalmais M, Marco CF, Moriones E, Gómez-Guillamón ML, Truniger V, Gómez P, Garcia-Mas J, Aranda MA (2007) EcoTILLING for the identification of allelic variants of melon eIF4E, a factor that controls virus susceptibility. BMC plant biology **7:** 34

Nitsch JP (1952) Plant hormones in the development of fruits. The quarterly review of biology **27:** 33-57

Nitsch LM, Oplaat C, Feron R, Ma Q, Wolters-Arts M, Hedden P, Mariani C, Vriezen WH (2009) Abscisic acid levels in tomato ovaries are regulated by LeNCED1 and SlCYP707A1. Planta **229:** 1335-1346

Novikova GV, Moshkov IE, Smith AR, Hall MA (2000) The effect of ethylene on MAPKinase-like activity in Arabidopsis thaliana. FEBS letters **474:** 29-32

Nunes-Nesi A, Carrari F, Lytovchenko A, Smith AMO, Loureiro ME, Ratcliffe RG, Sweetlove LJ, Fernie AR (2005) Enhanced photosynthetic performance and growth as a consequence of decreasing mitochondrial malate dehydrogenase activity in transgenic tomato plants. Plant physiology **137:** 611-622

O'Malley RC, Rodriguez FI, Esch JJ, Binder BM, O'Donnell P, Klee HJ, Bleecker AB (2005) Ethylene-binding activity, gene expression levels, and receptor system output for ethylene receptor family members from Arabidopsis and tomato. The plant journal **41:** 651-659

Oeller PW, Lu M, Taylor LP, Pike DA, Theologis A (1991) Reversible inhibition of tomato fruit senescence by antisense RNA. Science **254:** 437-439

Ohme-Takagi M, Shinshi H (1995) Ethylene-inducible DNA binding proteins that interact with an ethylene-responsive element. The plant cell **7:** 173-182

Olmedo G, Guo HW, Gregory BD, Hourizadeh SD, Aguilar-Henonin L, Li H, Guzman P, Ecker JR (2006) ETHYLENE- INSENSITIVE5 encodes a 5'→3' exoribonuclease required for regulation of the EIN3-targeting F-box proteins EBF1/2. Proceedings of the National Academy of Sciences, USA **103:** 13286-13293

Omoni AO, Aluko RE (2005) The anti-carcinogenic and anti-atherogenic effects of lycopene: a review. Trends in food science and technology **16:** 344-350

Oms-Oliu G, Hertog M.L.A.T.M, Van de Poel B, Ampofo-Asiama J, Geeraerd A.H, Nicolai B.M (2011) Metabolic Characterization of tomato fruit during postharvest development, ripening, and postharvest shelf-life. Postharvest biology and technology **62:** 7-16

Opiyo AM, Ying TJ (2005) The effects of 1-methylcyclopropene treatment on the shelf life and quality of cherry tomato (Lycopersicon esculentum var. cerasiforme) fruit. International journal of food science & technology **40:** 665-673

Osorio S, Alba R, Damasceno CM, Lopez-Casado G, Lohse M, Zanor MI, Tohge T, Usadel B, Rose JK, Fei Z (2011) Systems biology of tomato fruit development: combined transcript, protein, and metabolite analysis of tomato transcription factor (nor, rin) and ethylene receptor (Nr) mutants reveals novel regulatory interactions. Plant physiology **157:** 405-425

Ouaked F, Rozhon W, Lecourieux D, Hirt H (2003) A MAPK pathway mediates ethylene signaling in plants. EMBO journal **22:** 1282-1288

Paiva SA, Russell RM (1999) β-Carotene and other carotenoids as antioxidants. Journal of the American college nutrition **18:** 426-433

Pascual L, Blanca JM, Canizares J, Nuez F (2009) Transcriptomic analysis of tomato carpel development reveals alterations in ethylene and gibberellin synthesis during *pat3/pat4* parthenocarpic fruit set. BMC plant biology **9:** 67

Peralta IE, Knapp S, Spooner DM (2006) Nomenclature for wild and cultivated tomatoes. Tomato genetics Cooperation reports **56:** 6-12

Peralta IE, Spooner DM (2001) Granule-bound starch synthase (*GBSSI*) gene phylogeny of wild tomatoes (Solanum L. section *Lycopersicon* [Mill.] Wettst. subsection *Lycopersicon*). American journal of botany **88:** 1888-1902

Peralta IE, Spooner DM, Knapp S (2008) Taxonomy of wild tomatoes and their relatives (Solanum sect. Lycopersicoides, sect. Juglandifolia, sect. Lycopersicon; Solanaceae).

Perry JA, Wang TL, Welham TJ, Gardner S, Pike JM, Yoshida S, Parniske M (2003) A TILLING reverse genetics tool and a web-accessible collection of mutants of the legume Lotus japonicus. Plant physiology **131:** 866-871

Pesquet E, Tuominen H (2011) Ethylene stimulates tracheary element differentiation in Zinnia elegans cell cultures. New phytologist **190:** 138-149

Pierik R, Tholen D, Poorter H, Visser EJW, Voesenek LACJ (2006) The Janus face of ethylene: growth inhibition and stimulation. Trends in plant science **11:** 176-183

Pirrello J, Jaimes-Miranda F, Sanchez-Ballesta MT, Tournier B, Khalil-Ahmad Q, Regad F, Latché A, Pech JC, Bouzayen M (2006) Sl-ERF2, a tomato ethylene response factor involved in ethylene response and seed germination. Plant cell and physiology **47:** 1195-1205

Pnueli L, Carmel-Goren L, Hareven D, Gutfinger T, Alvarez J, Ganal M, Zamir D, Lifschitz E (1998) The SELF-PRUNING gene of tomato regulates vegetative to reproductive switching of sympodial meristems and is the ortholog of CEN and TFL1. Development **125:** 1979-1989

Potuschak T, Lechner E, Parmentier Y, Yanagisawa S, Grava S, Koncz C, Genschik P (2003) EIN3-dependent regulation of plant ethylene hormone signaling by two Arabidopsis F box proteins: eBF1 and EBF2. Cell **115:** 679-689

Potuschak T, Vansiri A, Binder BM, Lechner E, Vierstra R, Genschik P (2006) The exonuclease XRN4 is a component of the ethylene response pathway in Arabidopsis. The plant cell **18:** 3047-3057

Powell AL, Nguyen CV, Hill T, Cheng KL, Figueroa-Balderas R, Aktas H, Ashrafi H, Pons C, Fernández-Muñoz R, Vicente A (2012) Uniform ripening encodes a Golden 2-like transcription factor regulating tomato fruit chloroplast development. Science **336:** 1711-1715

Prasad ME, Schofield A, Lyzenga W, Stone SL (2010) Arabidopsis RING E3 ligase XBAT32 regulates lateral root production through its role in ethylene biosynthesis. Plant physiology **153:** 1587-1596

Prasad ME, Stone SL (2010) Further analysis of XBAT32, an *Arabidopsis* RING E3 ligase, involved ethylene biosynthesis. Plant signaling and behaviour **5:** 1425-1429

Pratta G, Zorzoli R, Boggio SB (2004) Glutamine and glutamic acid levels and related metabolizing enzymes in tomato fruit with different shelf-life. Science and horticulture **100:** 341-347

Prischmann D, Dashiell K, Schneider D, Eubanks M (2009) Evaluating Tripsacum-introgressed maize germplasm after infestation with western corn rootworms (Coleoptera: Chrysomelidae). Journal of applied entomologist **133:** 10-20

Qiao H, Chang KN, Yazaki J, Ecker JR (2009) Interplay between ethylene, ETP1/ETP2 F-box proteins, and degradation of EIN2 triggers ethylene responses in *Arabidopsis*. Genes and development **23:** 512-521

Qiao H, Shen Z, S-sC Huang, Schmitz RJ, Urich MA, Briggs SP, Ecker JR (2012) Processing and subcellular trafficking of ER-tethered EIN2 control response to ethylene gas. Science **338:** 390-393

Qin G, Wang Y, Cao B, Wang W, Tian S (2012) Unraveling the regulatory network of the MADS box transcription factor RIN in fruit ripening. The plant journal **70:** 243-255

Qu X, Hall B, Gao Z, Schaller GE (2007) A strong constitutive ethylene-response phenotype conferred on Arabidopsis plants containing null mutations in the ethylene receptors *ETR1* and *ERS1*. BMC plant biology **7:** 3

Qu X, Schaller GE (2004) Requirement of the histidine kinase domain for signal transduction by the ethylene receptor ETR1. Plant physiology **136:** 2961-2970

Quail PH (2002) Photosensory perception and signalling in plant cells: new paradigms? Current opinion in plant biology **14:** 180-188

Quesada MA, Blanco-Portales R, Posé S, García-Gago JA, Jiménez-Bermúdez S, Muñoz-Serrano A, Caballero JL, Pliego-Alfaro F, Mercado JA, Muñoz-Blanco J (2009) Antisense down-regulation of the FaPG1 gene reveals an unexpected central role for polygalacturonase in strawberry fruit softening. Plant physiology **150:** 1022-1032

Rajala A, Peltonen-Sainio P (2001) Plant growth regulator effects on spring cereal root and shoot growth. Agronomy journal **93:** 936-943

Ramassamy S, Olmos E, Bouzayen M, Pech JC, and Latche A (1998) 1-aminocyclopropane-1-carboxylate oxidase of apple fruit is periplasmic. Journal of eexperimental botany **49:** 1909-1915

Rao AV, Agarwal S (2000) Role of antioxidant lycopene in cancer and heart disease. Journal of American college of nutrition **19:** 563-569

Ravanel S, Douce R, Rébeillé F (2011) Metabolism of folates in plants. Advances in botanical research **59:** 67-106

Redei GP, Koncz C (1992) Classical mutagenesis. In Arabidopsis. Koncz C, Schell J, Chua N-H (eds) Molecular Genetics. World Scientific Publisher, Singapore, 16-82

Redgwell RJ, Macrae E, Hallett I, Fischer M, Perry J, Harker R (1997a) In vivo and in vitro swelling of cell walls during fruit ripening. Planta **203:** 162-173

Reinhardt D, Kende H, and Boller T (1994) Subcellular-localization of 1-aminocyclopropane-1-carboxylate oxidase in tomato cells. Planta **195:** 142–146

Ren Z, Li Z, Miao Q, Yang Y, Deng W, Hao Y (2011) The auxin receptor homologue in *Solanum lycopersicum* stimulates tomato fruit set and leaf morphogenesis. Journal of eexperimental botany **62:** 2815-2826

Resnick JS, Rivarola M, Chang C (2008) Involvement of *RTE1* in conformational changes promoting ETR1 ethylene receptor signaling in Arabidopsis The plant journal **56:** 423-431

Resnick JS, Wen C-K, Shockey JA, Chang C (2006) *REVERSION-TO- ETHYLENE SENSITIVITY1*, a conserved gene that regulates ethylene receptor function in Arabidopsis. Proceedings of the National Academy of Sciences, USA **103:** 7917-7922

Richardson DL, Davies HV, Ross HA, Mackay GR (1990) Invertase activity and its relation to hexose accumulation in potato tubers. Journal of eexperimental botany **41:** 95-99

Rick C, Chetelat R (1995) Utilization of related wild species for tomato improvement. *In* I International symposium on Solanacea for fresh market **412:** 21-38

Rick CM, Uhlig JW, Jones AD (1994) High alpha-tomatine content in ripe fruit of Andean Lycopersicon esculentum var. cerasiforme: developmental and genetic aspects. Proceedings of the National Academy of Sciences, USA **91:** 12877-12881

Rigola D, van Oeveren J, Janssen A, Bonné A, Schneiders H, van der Poel HJ, van Orsouw NJ, Hogers RC, de Both MT, van Eijk MJ (2009) High-throughput detection of induced mutations and natural variation using KeyPoint™ technology. PLoS one **4:** e4761

Rivarola M, McClellan CA, Resnick JS, Chang C (2009) ETR1-specific mutations distinguish ETR1 from other Arabidopsis ethylene receptors as revealed by genetic interaction with RTE1. Plant physiology **150:** 547-551

Robert VJ, West MA, Inai S, Caines A, Arntzen L, Smith JK, Clair DAS (2001) Marker-assisted introgression of blackmold resistance QTL alleles from wild Lycopersicon

cheesmanii to cultivated tomato (*L. esculentum*) and evaluation of QTL phenotypic effects. Molecular breeding **8:** 217-233

Rocklin AM, Kato K, Liu HW, Que L, and Lipscomb JD (2004) Mechanistic studies of 1-aminocyclopropane-1-carboxylic acid oxidase: single turn over reaction. Journal of .biological. inorganic chemistry **9:** 171-182

Rodriguez FI, Esch JJ, Hall AE, Binder BM, Schaller GE, Bleecker AB (1999) A copper cofactor for the ethylene receptor ETR1 from *Arabidopsis*. Science **283:** 996-998

Roessner U, Wagner C, Kopka J, Trethewey RN, Willmitzer L (2000) Simultaneous analysis of metabolites in potato tuber by gas chromatography-mass spectrometry. The plant journal **23**: 131-142

Roessner-Tunali U, Hegemann B, Lytovchenko A, Carrari F, Bruedigam C, Granot D, Fernie AR (2003) Metabolic proofing of transgenic tomato plants overexpressing hexokinase reveals that the influence of hexose phosphorylation diminishes during fruit development. Plant physiology **133:** 84-99

Roman G, Lubarsky B, Kieber JJ, Rothenberg M, and Ecker JR (1995) Genetic analysis of ethylene signal transduction in Arabidopsis thaliana: five novel mutant loci integrated into a stress response pathway. Genetics **139:** 1393-1409

Rombaldi C, Lelievre JM, Latche A, Petitprez M, Bouzayen M, and Pech JC (1994) Immunocytolocalization of 1-aminocyclopropane-1-carboxylic acid oxidase in tomato and apple fruit. Planta **192:** 453-460

Ronen G, Carmel-Goren L, Zamir D, Hirschberg J (2000) An alternative pathway to beta -carotene formation in plant chromoplasts discovered by map-based cloning of beta and old-gold color mutations in tomato. Proceedings of the National Academy of Sciences, USA **97:** 11102-7

Ronen G, Cohen M, Zamir D, Hirschberg J (1999) Regulation of carotenoid biosynthesis during tomato fruit development: expression of the gene for lycopene epsilon-cyclase is down-regulated during ripening and is elevated in the mutant Delta. The plant journal **17:** 341-51

Rontein D, Dieuaide-Noubhani M, Dufourc EJ, Raymond P, Rolin D (2002) The metabolic architecture of plant cells: stability of central metabolism and flexibility of anabolic pathways during the growth cycle of tomato cells. Journal of biological chemistry **277:** 43948-43960

Rosati C, Aquilani R, Dharmapuri S, Pallara P, Marusic C, Tavazza R, Bouvier F, Camara B, Giuliano G (2000) Metabolic engineering of beta-carotene and lycopene content in tomato fruit. The plant journal **24:** 413-420

Ruan YL, Patrick JW, Bouzayen M, Osorio S, Fernie AR (2012) Molecular regulation of seed and fruit set. Trends in plant science **17:** 656-665

Saito T, Ariizumi T, Okabe Y, Asamizu E, Hiwasa-Tanase K, Fukuda N, Mizoguchi T, Yamazaki Y, Aoki K, Ezura H (2011) TOMATOMA: a novel tomato mutant database distributing Micro-Tom mutant collections. Plant cell and physiology **52:** 283-296

Sakai H, Hua J, Chen QHG, Chang C, Medrano LJ, Bleecker AB, Meyerowitz EM (1998) ETR2 is an ETR1-like gene involved in ethylene signaling in Arabidopsis. Proceedings of the National Academy of Sciences, USA **95:** 5812-5817

Saladié M, Matas AJ, Isaacson T, Jenks MA, Goodwin SM, Niklas KJ, Xiaolin R, Labavitch JM, Shackel KA, Fernie AR (2007) A revaluation of the key factors that influence tomato fruit softening and integrity. Plant physiology **144:** 1012-1028

Sarikamis G, Marquez J, Maccormack R, Bennett RN, Roberts J, Mithen R (2006) High glucosinolate broccoli: a delivery system for sulforaphane. Molecular breeding **18:** 219-228

Sauter M, Moffatt BM, Saechao MC, Hell R, and Wirtz M (2013) Methionine salvage and S-adenosylmethionine: essential links between sulfur, ethylene and polyamine biosynthesis. Biochemical journal. **451:** 145-154

Schaller GE, Bleecker AB (1995) Ethylene-binding sites generated in yeast expressing the Arabidopsis ETR1 gene. Science **270:** 1809-1811

Schaller GE, Ladd AN, Lanahan MB, Spanbauer JM, Bleecker AB (1995) The ethylene response mediator ETR1 from Arabidopsis forms a disulfide-linked dimer. Journal of biological chemistry **270:** 12526-12530

Schauer N, Zamir D, Fernie AR (2005) Metabolic profiling of leaves and fruit of wild species tomato: a survey of the *Solanum lycopersicum* complex. Journal of eexperimental botany **56:** 297-307

Schreck S (2002) The role of plastidial phosphoglucomutase in carbon partitioning. PhD thesis, university of East Anglia UK

Scott J, Rébeillé F, Fletcher J (2000) Folic acid and folates: the feasibility for nutritional enhancement in plant foods. Journal of the science of food and agriculture **80**: 795-824

Sebastia` CH, Hardin SC, Clouse SD, Kieber JJ, Huber SC (2004) Identification of a new motif for CDPK phosphorylation in vitro that suggests ACC synthase may be a CDPK substrate. Archies of biochemistry and biophysics **428:** 81-91

Serrani JC, Ruiz-Rivero O, Fos M, Garcia-Martinez JL (2008) Auxin-induced fruit-set in tomato is mediated in part by gibberellins. The plant journal **56:** 922-934

Seymour GB, Chapman NH, Chew BL, Rose JK (2013) Regulation of ripening and opportunities for control in tomato and other fruits. Plant biotechnology journal **11:** 269-278

Shakeel SN, Wang X, Binder BM, Schaller GE (2013) Mechanisms of signal transduction by ethylene: overlapping and non-overlapping signalling roles in a receptor family. AoB Plants. doi:10.1093/aobpla/plt1010

Shalata A, Tal M (1998) The effect of salt stress on lipid peroxidation and antioxidants in the leaf of the cultivated tomato and its wild salt-tolerant relative *Lycopersicon pennellii*. Physiologia plantarum **104:** 169-174

Shan Q, Wang Y, Chen K, Liang Z, Li J, Zhang Y, Zhang K, Liu J, Voytas DF, Zheng X, Zhang Y, Gao C (2013) Rapid and Efficient Gene Modification in Rice and Brachypodium Using TALENs. Molecular Plant **6:** 1365-1368

Sharma MK, Kumar R, Solanke AU, Sharma R, Tyagi AK, Sharma AK (2010) Identification, phylogeny, and transcript profiling of ERF family genes during development and abiotic stress treatments in tomato. Molecular genetics and genomics **284:** 455-475

Sharp RE (2002) Interaction with ethylene: changing views on the role of abscisic acid in root and shoot growth responses to water stress. Plant, cell and environment **25:** 211-222

Shibaoka H (1994) Plant hormone-induced changes in the orientation of cortical microtubules: alterations in the cross-linking between microtubules and the plasma membrane. Annual review of plant physiology and plant molecular biology **45:** 527-44

Shikazono N, Yokota Y, Kitamura S, Suzuki C, Watanabe H, Tano S, Tanaka A (2005) Mutation rate and novel *tt* mutants of *Arabidopsis thaliana* induced by carbon ions. Genetics **163:** 1449-1455

Shin K, Lee S, Song W-Y, Lee R-A, Lee I, Ha K, Koo J-C, Park S-K, Nam H-G, Lee Y (2015) Genetic identification of ACC-RESISTANT2 reveals involvement of LYSINE HISTIDINE TRANSPORTER1 in the uptake of 1-aminocyclopropane-1-carboxylic acid in Arabidopsis thaliana. Plant and Cell Physiology **56:** 572-582

Sim N-L, Kumar P, Hu J, Henikoff S, Schneider G, Ng PC (2012) SIFT web server: predicting effects of amino acid substitutions on proteins. Nucleic acid research **1**: 6

Singh R, Singh P, Pathak N, Singh VK, Dwivedi UN (2007) Modulation of mango ripening by chemicals: Physiological and biochemical aspects. Plant growth regulation **53:** 137-145

Sisler EC, Serek M (1997) Inhibitors of ethylene responses in plants at the receptor level: recent developments. Plant physiology **100:** 577-582

Skottke KR, Yoon GM, Kieber JJ, DeLong A (2011) Protein phosphatase 2A controls ethylene biosynthesis by differentially regulating the turnover of ACC synthase isoforms. PLoS genetics **7:** e1001370

Slade AJ, Knauf VC (2005) TILLING moves beyond functional genomics into crop improvement. Transgenic research **14:** 109-115

Smalle J, Haegman M, Kurepa J, Van Montagu M, van der Straeten D (1997) Ethylene can stimulate Arabidopsis hypocotyl elongation in the light. Proceedings of the National Academy of Sciences, USA **94**: 2756-2761

Smith CJ, Watson CF, Morris PC, Bird CR, Seymour GB, Gray JE, Arnold C, Tucker GA, Schuch W, Harding S (1990) Inheritance and effect on ripening of antisense polygalacturonase genes in transgenic tomatoes. Plant molecular biology **14:** 369-379

Smith DL, Abbott JA, Gross KC (2002) Down-regulation of tomato β-galactosidase 4 results in decreased fruit softening. Plant physiology **129:** 1755-1762

Smits BM, Mudde J, Plasterk RH, Cuppen E (2004) Target-selected mutagenesis of the rat. Genomics **83:** 332-3

Solano R, Stepanova A, Chao QM, Ecker JR (1998) Nuclear events in ethylene signaling: a transcriptional cascade mediated by ETHYLENE-INSENSITIVE3 and ETHYLENE-RESPONSE-FACTOR1. Genes and development **12:** 3703-3714

Somerville C, Koorneef M (2002) A fortunate choice: the history of Arabidopsis as a model plant. Nature review on genetics **3:** 883-889

Spooner DM, Nderson GJA, Ansen RKJ (1993) Chloroplast DNA evidence for the interrelationships of tomatoes, potatoes, and pepinos (Solanaceae). American journal of botany **80:** 676-688

Sreelakshmi Y, Gupta S, Bodanapu R, Chauhan VS, Hanjabam M, Thomas S, Mohan V, Sharma S, Srinivasan R, Sharma R (2009) NEATTILL: A simplified procedure for nucleic acid extraction from arrayed tissue for TILLING and other high-throughput reverse genetic applications. Plant method **6:** 3

Srivastava A, Handa AK (2005) Hormonal regulation of tomato fruit development: a molecular perspective. Journal of plant growth regulation **24:** 67-82

Stadler L, Sprague G (1936) Genetic Effects of Ultra-Violet Radiation in Maize: I. Unfiltered Radiation. Proceedings of the National Academy of Sciences, USA **22:** 572

Stadler LJ (1928) Genetic effects of X-rays in maize. Proceedings of the National Academy of Sciences, USA **14:** 69

Stadler LJ (1929) Chromosome number and the mutation rate in Avena and Triticum. Proceedings of the National Academy of Sciences, USA **15**: 876

Stahl W, Heinrich U, Aust O, Tronnier H, Sies H (2006) Lycopene-rich products and dietary photoprotection. Photochemical photobiology and science **5:** 238-242

Stearns JC, Glick BR (2003) Transgenic plants with altered ethylene biosynthesis or perception. Biotechnology advances **21:** 193-210

Su L, Diretto G, Purgatto E, Danoun S, Zouine M, Li Z, Roustan J-P, Bouzayen M, Giuliano G, Chervin C (2015) Carotenoid accumulation during tomato fruit ripening is modulated by the auxin-ethylene balance. BMC plant biology **15:** 114

Subcellular localization and In vivo interaction of the *Arabidopsis thaliana* ethylene receptor family members. Molecular plant **1:** 308-320

Sudha RR, Amutha S, Muthulaksmi W, Baby R, Indira K, Mareeswari P (2007) Influence of pre and post-harvest chemical treatments on physical characteristics of sapota (Achras sapota L.) var. PKM 1. Journal of agricultural and biological science **3:** 450-452

Sun L, Sun Y, Zhang M et al. (2012a) Suppression of 9-cis-epoxycarotenoid dioxygenase, which encodes a key enzyme in abscisic acid biosynthesis, alters fruit texture in transgenic tomato. Plant physiology **158:** 283-298

Takahashi H, Kobayashi T, Sato-Nara K, Tomita K-o, Ezura H (2002) Detection of ethylene receptor protein Cm-ERS1 during fruit development in melon (Cucumis melo L.). Journal of eexperimental botany **53:** 415-422

Tamura T, Picciano MF (2006) "Folate and human reproduction," American journal of Clinical nutrition **83:** 993-1016

Tan S-T, Xue H-W (2014) Caseine kinase 1 regulates ethylene synthesis by phosphorylating and promoting turnover of ACS5. Cell reports **9:**1692-1702

Tang D, Christiansen KM, Innes RW (2005) Regulation of plant disease resistance, stress responses, cell death, and ethylene signaling in Arabidopsis by the EDR1 protein kinase. Plant physiology **138:** 1018-1026

Tarun AS, Lee JS, Theologis A (1998) Random mutagenesis of 1-aminocyclopropane-1-carboxylate synthase: a key enzyme in ethylene biosynthesis. Proceedings of the National Academy of Sciences, USA **95:** 9796–9801

Tatsuki M, and Mori H (2001) Phosphorylation of tomato 1 -aminocyclopropane-1-carboxylic acid synthase, LE-ACS2, at the C-terminal region. Journal of biological chemistry **276:** 28051-28057

Taylor IB (1986) Biosystematics of tomato. In: The tomato crop. A scientific basis for improvement, Atherton, J and Rudich, G (eds.), Chapman, pp1-34

Taylor N, Greene EA (2003) PARSESNP: A tool for the analysis of nucleotide polymorphisms. Nucleic acid research **31:** 3808-3811

Theologis A, Oeller PW, Wong LM, Rottmann WH, Gantz DM (1993) Use of a tomato mutant constructed with reverse genetics to study fruit ripening, a complex developmental process. Developmental genetics **14:** 282-95

Thomas RL, Jen JJ (1975) Phytochrome-mediated carotenoids biosynthesis in ripening tomatoes. Plant physiology **56:** 452-453

Thomas TR, Shackel KA, Matthews MA (2008) Mesocarp cell turgor in *Vitis vinifera* L. berries throughout development and its relation to firmness, growth, and the onset of ripening. Planta **228:** 1067-1076

Tieman DM, Ciardi JA, Taylor MG, Klee HJ (2001) Members of the tomato LeEIL (EIN3-like) gene family are functionally redundant and regulate ethylene responses throughout plant development. The plant journal **26:** 47-58

Tieman DM, Klee HJ (1999) Differential expression of two novel members of the tomato ethylene-receptor family. Plant physiology **120:** 165-172

Tigchelaar EC, Mcglasson WB, Franklin MJ (1978) Natural and ethephon-stimulate dripening of F1 hybrids of the ripening inhibitor (*rin*) and non-ripening (*nor*) mutants of tomato (*Lycopersicon esculentum* Mill.). Australian Journal of plant physiology **5:** 449-456

Till BJ, Cooper J, Tai TH, Colowit P, Greene EA, Henikoff S, Comai L (2007) Discovery of chemically induced mutations in rice by TILLING. BMC plant biology **7:** 19

Till BJ, Jankowicz-Cieslak J, Sági L, Huynh OA, Utsushi H, Swennen R, Terauchi R, Mba C (2010) Discovery of nucleotide polymorphisms in the Musa gene pool by Ecotilling. Theoretical and applied genetics **121:** 1381-1389

Till BJ, Reynolds SH, Greene EA, Codomo CA, Enns LC, Johnson JE, Burtner C, Odden AR, Young K, Taylor NE (2003) Large-scale discovery of induced point mutations with high-throughput TILLING. Genome research **13:** 524-530

Till BJ, Reynolds SH, Weil C, Springer N, Burtner C, Young K, Bowers E, Codomo CA, Enns LC, Odden AR (2004) Discovery of induced point mutations in maize genes by TILLING. BMC plant biology **4:** 12

Till BJ, Zerr T, Bowers E, Grene EA, Comai L, Henikoff S (2006) Highthroughput discovery of rare human nucleotide polymorphisms by ECOTILLING. Nucleic acids research **34:** 99

Till BJ, Zerr T, Comai L, Henikoff S (2006) A protocol for TILLING and Ecotilling in plants and animals. Nature protocol **1:** 2465-2477

Toivonen PM, Brummell DA (2008) Biochemical bases of appearance and texture changes in fresh-cut fruit and vegetables. Postharvest biology and technology **48:** 1-14

Tomato Genome Consortium (2012) The tomato genome sequence provides insights into fleshy fruit evolution. Nature **485:** 635-641

Tournier B, Sanchez-Ballesta MT, Jones B, Pesquet E, Regad F, Latché A, Pech JC, Bouzayen M (2003) New members of the tomato ERF family show specific expression pattern and diverse DNA-binding capacity to the GCC box element. FEBS letters **550:** 149-154

Trainotti L, Tadiello A, Casadoro G (2007) The involvement of auxin in the ripening of climacteric fruits comes of age: the hormone plays a role of its own and has an intense interplay with ethylene in ripening peaches. Journal of eexperimental botany **58:** 3299-3308

Triques K, Sturbois B, Gallais S, Dalmais M, Chauvin S, Clepet C, Aubourg S, Rameau C, Caboche M, Bendahmane A (2007) Characterization of Arabidopsis thaliana mismatch specific endonucleases: application to mutation discovery by TILLING in pea. The plant journal **51:** 1116-1125

Tsai H, Missirian V, Ngo KJ, Tran RK, Chan SR, Sundaresan V, Comai L (2013) Production of a high-efficiency TILLING population through polyploidization. Plant physiology **161:** 1604-1614

Tsang DL, Edmond C, Harrington JL, and Nühse TS (2011) Cell wall integrity controls root elongation via a general 1-aminocyclopropane-1-carboxylic acid-dependent, ethylene-independent pathway. Plant physiology **156:** 596-604

Tsuchisaka A, Theologis A (2004) Unique and overlapping expression patterns among the Arabidopsis 1-amino-cyclopropane-1-carboxylate synthase gene family members. Plant physiology **136**: 2982-3000

Tsuchisaka A, Yu G, Jin H, Alonso JM, Ecker JR, Zhang X, Gao S, Theologis A (2009) A combinatorial interplay among the 1-aminocyclopropane-1-carboxylate isoforms regulates ethylene biosynthesis in Arabidopsis thaliana. Genetics **183:** 979-1003

Tucker GA (1993) Introduction: respiration and energy. In: Seymour, G.B., Taylor,J.E., Tucker, G.A. (Eds.), Biochemistry of Fruit Ripening. Chapman & Hall, London, pp. 3-9

Valle EM, Boggio SB, Heldt HW (1998) Free amino acids composition of phloem sap and growing fruit of Lycopersicon esculentum. Plant cell and physiology **39:** 458–461

Van de Poel B, Bulens I, Markoula A, Hertog ML, Dreesen R, Wirtz M, Vandoninck S, Oppermann Y, Keulemans J, Hell R (2012) Targeted systems biology profiling of tomato fruit reveals coordination of the yang cycle and a distinct regulation of ethylene biosynthesis during postclimacteric ripening. Plant physiology **160:** 1498-1514

Van de Poel B, Van Der Straeten D (2014) 1-aminocyclopropane-1-carboxylic acid (ACC) in plants: more than just the precursor of ethylene! Front in plant science, **5:** p 640

Van de Poel B, Vandenzavel N, Smet C, Nicolay T, Bulens I, Mellidou I, Vandoninck S, Hertog ML, Derua R, Spaepen S, Vanderleyden J, Waelkens E, De Proft MP, Nicolai BM, Geeraerd AH (2014) Tissue specific analysis reveals a differential organization and regulation of both ethylene biosynthesis and E8 during climacteric ripening of tomato. BMC plant biology **14:** 11

Van Harten AM (1998) Mutation breeding, Theory and Practical Applications. Cambridge University Press, Cambridge, United Kingdom pp 127-140

Vandenbussche F, Vriezen WH, Smalle J, Laarhoven LJ, Harren FJ, Van Der Straeten D (2003) Ethylene and auxin control the *Arabidopsis* response to decreased light intensity. Plant physiology **133:** 517-527

Vankadavath RN, Hussain AJ, Bodanapu R, Kharshiing E, Basha PO, Gupta S, Sreelakshmi Y, Sharma R (2009) Computer aided data acquisition tool for high-throughput phenotyping of plant populations. Plant methods **5:** 1

Ververidis P, John P (1991) Complete recovery in vitro of ethylene-forming enzyme-activity. Phytochemistry **30:** 725-727

Vivian-Smith A, Koltunow AM (1999) Genetic analysis of growth-regulator-induced parthenocarpy in *Arabidopsis*. Plant physiology **121:** 437-451

Vogel JP, Woeste KE, Theologis A, Kieber JJ (1998) Recessive and dominant mutations in the ethylene biosynthetic gene *ACS5* of Arabidopsis confer cytokinin insensitivity and ethylene overproduction, respectively. Proceedings of the National Academy of Sciences, USA **95:** 4766-4771

Vriezen WH, Feron R, Maretto F, Keijman J, Mariani C (2008) Changes in tomato ovary transcriptome demonstrate complex hormonal regulation of fruit set. New phytologist **177:** 60-76

Vysotskaya L, Wilkinson S, Davies WJ, Arkhipova T, Kudoyarova G (2011) The effect of competition from neighbours on stomatal conductance in lettuce and tomato plants. Plant, cell and environment **34:** 729-737

Wada H, Matthews MA, Shackel KA (2009) Seasonal pattern of apoplastic solute accumulation and loss of cell turgor during ripening of *Vitis vinifera* fruit under field conditions. Journal of eexperimental botany **60:** 1773-1781

Wagner C (1995) "Biochemical role of folate in cellular metabolism," in Folate in Health and Disease, L.B.Bailey, Ed., pp. 23–42, Marcel Dekker, New York, NY, USA,

Wang F, Sanz A, Brenner ML, Smith A (1993) Sucrose synthase, starch accumulation, and tomato fruit sink strength. Plant physiology **101:** 321-327

Wang H, Schauer N, Usadel B, Frasse P, Zouine M, Hernould M, Latche A, Pech JC, Fernie AR, Bouzayen M (2009) Regulatory features underlying pollination-dependent and independent tomato fruit set revealed by transcript and primary metabolite profiling. The plant cell **21:** 1428-1452

Wang J, Chen G, Hu Z, Chen X (2007) Cloning and characterization of the EIN2-homology gene LeEIN2 from tomato. DNA sequence **18:** 33-38

Wang KLC, Yoshida H, Lurin C, and Ecker JR (2004) Regulation of ethylene gas biosynthesis by the Arabidopsis ETO1 protein. Nature **428:** 945-950

Wang W, Hall AE, O'Malley R, Bleecker AB (2003) Canonical histidine kinase activity of the transmitter domain of the ETR1 ethylene receptor from *Arabidopsis* is not required for signal transmission. Proceedings of the National Academy of Sciences, USA **100:** 352-357

Wang Y, Wyllie SG, Leach DN (1996) Chemical changes during the development and ripening of the fruit of *Cucumis melo* (cv. Makdimon). Journal of agricultural and food chemistry **44:** 210-216

Waters MT, Langdale JA (2009) The making of a chloroplast. EMBO J **28:** 2861-2873

Wen X, Zhang C, Ji Y, Zhao Q, He W, An F, Jiang L, Guo H (2012) Activation of ethylene signaling is mediated by nuclear translocation of the cleaved EIN2 carboxyl terminus. Cell research **22:** 1613-1616

Wendt T, Holm P, Starker C, Christian M, Voytas D, Brinch-Pedersen H, Holme I (2013) TAL effector nucleases induce mutations at a pre-selected location in the genome of primary barley transformants. Plant molecular biology **83:** 279-285

White MF, Vasques J, Yang SF, Kirsch JF (1994) Expression of apple 1-aminocyclopropane-1-carboxylate synthase in Escherichia coli: kinetic characterization of wild-type and ative site mutant forms. Proceedings of the National Academy of Sciences, USA **91:** 12428–12432

Wienholds E, van Eeden F, Kosters M, Mudde J, Plasterk RH, Cuppen E (2003) Efficient target-selected mutagenesis in zebrafish. Genome research **13:** 2700-2707

Wilkinson J, Lanahan M, Yen H, Giovannoni JJ, Klee HJ (1995) An ethylene-inducible component of signal transduction encoded by *Never-ripe*. Science **270:** 1807-1809

Wilkinson S, Davies WJ (2010) Drought, ozone, ABA and ethylene: new insights from cell to plant to community. Plant, cell and environment **33:** 510-525

Willats WG, McCartney L, Mackie W, Knox JP (2001) Pectin: cell biology and prospects for functional analysis. Plant molecular biology **47:** 9-27

Wills R, Ku V (2002) Use of 1-MCP to extend the time to ripen of green tomatoes and postharvest life of ripe tomatoes. Postharvest Biology and Technology **26:** 85-90

Wilson RL, Kim H, Bakshi A, Binder BM (2014) The ethylene receptors ETHYLENE RESPONSE1 and ETHYLENERESPONSE2 have contrasting roles in seed germination of Arabidopsis during salt stress. Plant physiology **165:** 1353-1366

Winkler S, Schwabedissen A, Backasch D, Bökel C, Seidel C, Bönisch S, Fürthauer M, Kuhrs A, Cobreros L, Brand M (2005) Target-selected mutant screen by TILLING in Drosophila. Genome research **15:** 718-723

Woeste KE, Kieber JJ (2000) A strong loss-of-function mutation in *RAN1* results in constitutive activation of the ethylene response pathway as well as a rosette-lethal phenotype. The plant cell **12:** 443-455

Woeste KE, Ye C, Kieber JJ (1999) Two Arabidopsis mutants that overproduce ethylene are affected in the posttranscriptional regulation of 1-aminocyclopropane-1-carboxylic acid synthase. Plant physiology **119:** 521-529

Woof J, Burton D (2004) "Human antibody-Fc receptor interactions illuminated by crystal structures". Nature review of immunology **4:** 89-99

Wrzodak A, Gajewski M (2015) Effect of 1-MCP Treatment on Storage Potential of Tomato Fruit. Journal of Horticultural Research **23:** 121-126

Wu JL, Wu C, Lei C, Baraoidan M, Bordeos A, Madamba MR, Ramos-Pamplona M, Mauleon R, Portugal A, Ulat VJ, Bruskiewich R, Wang G, Leach J, Khush G, Leung H (2005) Chemical and irradiation-induced mutants of indica rice IR64 for forward and reverse genetics. Plant molecular biology **59:** 85-97

Wyllie SG, Fellman JK (2000) Formation of volatile branched chain esters in banana (Musa sapientum L.). Journal of agricultural and food chemistry **48:** 3493-3496

Xia J, Mandal R, Sinelnikov IV, Broadhurst D, Wishart DS (2012) MetaboAnalyst 2.0-a comprehensive server for metabolomic data analysis. Nucleic acid research **1**:7

Xie F, Liu Q, Wen C-K (2006) Receptor signal output mediated by the ETR1 N-terminus is primarily subfamily I receptor dependent. Plant physiology **142:** 492-508

Xin Z, Wang ML, Barkley NA, Burow G, Franks C, Pederson G, Burke J (2008) Applying genotyping (TILLING) and phenotyping analyses to elucidate gene function in a chemically induced sorghum mutant population. BMC plant biology **8:** 103

Xiong AS, Yao QH, Li X, Fan HQ, Peng RH (2003) Double antisense ACC oxidase and ACC synthase fusion gene introduced into tomato by agrobacterium-mediated transformation and analysis the ethylene production of transgenic plants. Acta Biol Exp Sin **36:** 35-41

Xiong AS, Yao QH, Peng RH, Li X, Han PL, Fan HQ (2005) Different effects on ACC oxidase gene silencing triggered by RNA interference in transgenic tomato. Plant cell and reports **23:** 639-46

Xu SL, Rahman A, Baskin TI, and Kieber JJ (2008) Two leucine-rich repeat receptor kinases mediate signaling, linking cell wall biosynthesis and ACC synthase in Arabidopsis. The plant cell **20:** 3065-3079

Yamagami T, Tsuchisaka A, Yamada K, Haddon WF, Harden LA, Theologis A (2003) Biochemical diversity among the 1-amino-cyclopropane-1-carboxylate synthase isozymes encoded by the Arabidopsis gene family. Journal of biological chemistry **278:** 49102-49112

Yang J, Peng S, Visperas RM, Sanico AL, Zhu Q, Gu S (2000) Grain-filling pattern and cytokinin content in the grains and roots of rice plants. Plant growth regulation **30:** 261-270

Yang SF (1985) Biosynthesis and action of ethylene. Hortscience **20:** 41-5

Yang SF, Hoffman NE (1984) Ethylene biosynthesis and its regulation in higher plants. Annual review on plant physiology **35:** 155-189

Ye ZB, Li HX, Zheng YL, Liu HL (1996) Inhibition of introducing antisense ACC oxidase gene into tomato genome on expression of its endogeous gene. Journal of Huazhong agriculture university **15:** 305-9

Yip W-K, Yang SF (1988) Cyanide Metabolism in Relation to Ethylene Production in Plant Tissues. Plant physiology **88:** 473-476

Yokotani N, Tamura S, Nakano R, Inaba A, Kubo Y (2003) Characterization of a novel tomato EIN3-like gene (*LeEIL4*). Journal of eexperimental botany. **54:** 2775-2776

Yoo S-D, Cho Y-H, Tena G, Xiong Y, Sheen J (2008) Dual control of nuclear EIN3 by bifurcate MAPK cascades in C_2H_4 signalling. Nature **451:** 789-795

Yoon GM, Kieber JJ (2013) 1-Aminocyclopropane-1-carboxylic acid as a signalling molecule in plants. AoB Plants **5:** plt017

Yoon GM, Kieber JJ (2013a) 14-3-3 regulates 1-aminocyclopropane-1-carboxylate synthase protein turnover in Arabidopsis. The plant cell **25:** 1016-1028

Yoon GM, Kieber JJ (2013b) ACC synthase and its cognate E3 ligase are inversely regulated by light. Plant signaling and behaviour **8**

Yoshida H, Nagata M, Saito K, Wang KLC, and Ecker JR (2005) Arabidopsis ETO1 specifically interacts with and negatively regulates type 2 1-aminocyclopropane-1-carboxylate synthases. BMC plant biology **5:** 14

Yoshida H, Wang KL, Chang CM, Mori K, Uchida E, and Ecker JR (2006) The ACC synthase TOE sequence is required for interaction with ETO1 family proteins and destabilization of target proteins. Plant molecular.biology **62:** 427-437

Young TE, Meeley RB, Gallie DR (2004) ACC synthase expression regulates leaf performance and drought tolerance in maize. The plant journal **40:** 813-825

Zanor MI, Osorio S, Nunes-Nesi A, et al (2009) RNA interference of LIN5 in tomato confirms its role in controlling Brix content, uncovers the influence of sugars on the levels of fruit hormones, and demonstrates the importance of sucrose cleavage for normal fruit development and fertility. Plant physiology **150:** 1204-1218

Zhang F, Maeder ML, Unger-Wallace E, Hoshaw JP, Reyon D, Christian M, Li X, Pierick CJ, Dobbs D, Peterson T (2010) High frequency targeted mutagenesis in *Arabidopsis thaliana* using zinc finger nucleases. Proceedings of the National Academy of Sciences of the USA **107:** 12028-12033

Zhang H, Tan G, Wang Z, Yang J, Zhang J (2009) Ethylene and ACC levels in developing grains are related to the poor appearance and milling quality of rice. Plant growth regulation **58:** 85-96

Zhang Y, Zhang F, Li X, Baller JA, Qi Y, Starker CG, Bogdanove AJ, Voytas DF (2013) Transcription activator-like effector nucleases enable efficient plant genome engineering. Plant physiology **161:** 20-27

Zhang ZH, Ren JS, Clifton IJ, and Schofield CJ (2004) Crystal structure and mechanistic implications of 1-aminocyclopropane-1-carboxylic acid oxidase-The ethylene-forming enzyme. Chemical biology **11:** 1383-1394

Zhao B, Liu K, Zhang H, Zhu Q, Yang J (2007) Causes of poor grain plumpness of two line hybrids and their relationships to the contents of hormones in rice grain. Agricultural sciences in China **6:** 930-940

Zhao TY, Thackera R, Corum III JW, Snyder JC, Meeley RB, Obendorf RB, Downie B (2004) Expression of the maize galactinol synthase gene family. I. Expression of two different genes during seed development and germination. Plant physiology **121:** 634-646

Zhou D (1996) Molecular cloning of a tomato cDNA (accession no. U4279) encoding an ethylene receptor. Plant physiology **110:** 1435

Zhou HQ, Wang HW, Zhu K, Sui SF, Xu PL, Yang SF, Li N (1999) The multiple roles of conserved arginine 286 of 1-aminocyclopropane-1-carboxylate synthase. Coenzyme binding, substrate binding, and beyond. Plant physiology **121:** 913–919

Zhou L, Vandersteen J, Wang L, Fuller T, Taylor M, Palais B, Wittwer C (2004) High-resolution DNA melting curve analysis to establish HLA genotypic identity. Tissue antigens **64:** 156-164

Zhou X, Liu Q, Xie F, Wen C-K (2007) RTE1 is a Golgi-Associated and ETR1-dependent negative regulator of ethylene responses. Plant physiology **145:** 75-86

Zhu D, Maier A, Lee J-H, Laubinger S, Saijo Y, Wang H, Qu L-J, Hoecker U, Deng XW (2008) Biochemical characterization of Arabidopsis complexes containing CONSTITUTIVELY PHOTOMORPHOGENIC1 and SUPPRESSOR OF PHYA proteins in light control of plant development. The plant cell **20:** 2307-2323

APPENDIX

Supplementary Table 1. List of tomato accessions used in the study

S.No.	Accession No.	Source
1.	2-141	TGRC
2.	A. Arka	IIVR
3.	Agata-30	IIVR
4.	ALT9797	IIVR
5.	Arka Vikas (Reference cultivar)	IIVR
6.	Azad No.1	IIVR
7.	BL-1208	IIVR
8.	BT-111-3-2-3	IIVR
9.	Castle Rock	IIVR
10.	Cerasiformae	IIVR
11.	Cherry Red	IIVR
12.	Chiku Grande	IIVR
13.	CLN-2998	IIVR
14.	DT-10	IIVR
15.	DVKT-1	IIVR
16.	EC1129	NBPGR
17.	EC14073	NBPGR
18.	EC1753	NBPGR
19.	EC2630	NBPGR
20.	EC 315478	NBPGR
21.	EC 320571	NBPGR
22.	EC32211	NBPGR
23.	EC 520053	NBPGR
24	EC007345	IIVR
25.	EC007785	NBPGR
26.	EC009046	IIVR
27.	EC16788	NBPGR
28.	EC012689	NBPGR
29.	EC10662	NBPGR
30.	EC1087	NBPGR
31.	EC11309	NBPGR
32.	EC114375	NBPGR
33.	EC1177297	NBPGR
34.	EC1191	NBPGR
35.	EC12689	NBPGR
36.	EC12692	NBPGR
37.	EC129604	NBPGR
38.	EC13736	NBPGR
39.	EC13904	NBPGR
40.	EC14073	NBPGR

41.	EC14078	NBPGR
42.	EC144336	NBPGR
43.	EC15127	NBPGR
44.	EC155	NBPGR
45.	EC161645	NBPGR
46.	EC163598	NBPGR
47.	EC163605	NBPGR
48.	EC16368	NBPGR
49.	EC164465	NBPGR
50.	EC164660	NBPGR
51.	EC164665	NBPGR
52.	EC16780	NBPGR
53.	EC16786	NBPGR
54.	EC16788	NBPGR
55.	EC16790	NBPGR
56.	EC168283	NBPGR
57.	EC168290	NBPGR
58.	EC170047	NBPGR
59.	EC177371	NBPGR
60.	EC1914	NBPGR
61.	EC193538	IIVR
62.	EC20636	NBPGR
63.	EC20639	NBPGR
64.	EC237288	NBPGR
65.	EC241446	NBPGR
66.	EC251581	NBPGR
67.	EC251649	NBPGR
68.	EC252	NBPGR
69.	EC25265	NBPGR
70.	EC25563	NBPGR
71.	EC25772	NBPGR
72.	EC26150	NBPGR
73.	EC26684	NBPGR
74.	EC2673	NBPGR
75.	EC27251	NBPGR
76.	EC273966	IIVR
77.	EC27885	NBPGR
78.	EC2790	NBPGR
79.	EC279088	NBPGR
80.	EC2791	NBPGR
81.	EC27910	NBPGR
82.	EC27960	NBPGR
83.	EC27960	NBPGR

84.	EC2798	NBPGR
85.	EC27995	NBPGR
86.	EC2802	NBPGR
87.	EC28356	NBPGR
88.	EC2977	NBPGR
89	EC2990	NBPGR
90.	EC29914	NBPGR
91.	EC29933	NBPGR
92.	EC29969	NBPGR
93.	EC2997	IIVR
94.	EC30303	NBPGR
95.	EC3176	NBPGR
96.	EC31767	NBPGR
97	EC320571	NBPGR
98.	EC320583	NBPGR
99.	EC321425	NBPGR
100.	EC3216	NBPGR
101.	EC32287	NBPGR
102.	EC32481	NBPGR
103.	EC32557	NBPGR
104.	EC3261	NBPGR
105.	EC326139	NBPGR
106.	EC338717	NBPGR
107.	EC338725	NBPGR
108	EC33878	NBPGR
109.	EC339058	IIVR
110.	EC339066	NBPGR
111.	EC3414425	IIVR
112.	EC34477	NBPGR
113.	EC34480	NBPGR
114.	EC35236	NBPGR
115.	EC35240	NBPGR
116.	EC-35240	NBPGR
117.	EC35242	NBPGR
118.	EC35244	NBPGR
119.	EC35272	NBPGR
120.	EC35293	NBPGR
121.	EC35322	NBPGR
122.	EC35360	NBPGR
123.	EC357828	NBPGR
124.	EC362933	NBPGR
125.	EC362941	NBPGR
126.	EC362948	NBPGR

127.	EC362949	NBPGR
128.	EC362958	NBPGR
129.	EC363863	NBPGR
130.	EC363942	NBPGR
131.	EC3668	NBPGR
132.	EC368832	NBPGR
133.	EC368883	NBPGR
134.	EC368943	NBPGR
135.	EC369020	NBPGR
136.	EC370867	IIVR
137.	EC372	NBPGR
138.	EC373378	NBPGR
139.	EC381554	NBPGR
140.	EC383117	NBPGR
141.	EC398405	IIVR
142.	EC398600	NBPGR
143.	EC398614	NBPGR
144.	EC398684	NBPGR
145.	EC398685	NBPGR
146.	EC398687	NBPGR
147.	EC398688	NBPGR
148.	EC398695	NBPGR
149.	EC398697	NBPGR
150.	EC398699	NBPGR
151.	EC398701	NBPGR
152.	EC398704	NBPGR
153.	EC398707	NBPGR
154.	EC398710	NBPGR
155.	EC398711	NBPGR
156.	EC398712	NBPGR
157.	EC398714	NBPGR
158.	EC398715	NBPGR
159.	EC398716	NBPGR
160.	EC398717	NBPGR
161.	EC429	NBPGR
162.	EC433607	NBPGR
163.	EC439542	NBPGR
164.	EC443369	NBPGR
165.	EC4506	NBPGR
166.	EC458213	NBPGR
167.	EC470413	NBPGR
168.	EC487	NPGRB
169.	EC490128	NBPGR

170.	EC490130	NBPGR
171.	EC492	NBPGR
172.	EC494372	IIVR
173.	EC498372	NBPGR
174.	EC5050	IIVR
175.	EC501577	NBPGR
176.	EC520046	NBPGR
177.	EC 52055	NBPGR
178.	EC520052	NBPGR
179.	EC520059	NBPGR
180.	EC520065	IIVR
181.	EC520075	NBPGR
182.	EC520076	IIVR
183.	EC520077	IIVR
184.	EC520078	IIVR
185.	EC520079	IIVR
186.	EC521039	NBPGR
187.	EC521048	NBPGR
188.	EC521049	NBPGR
189.	EC521061	NBPGR
190.	EC521067	NBPGR
191.	EC521068	NBPGR
192.	EC521070	NBPGR
193.	EC521077	NBPGR
194.	EC521078	IIVR
195.	EC521079	NBPGR
196.	EC521080	IIVR
197.	EC521082	NBPGR
199.	EC521083	NBPGR
200.	EC521086	NBPGR
201.	EC526146	NBPGR
202.	EC528362	NBPGR
203.	EC528365	IIVR
204.	EC528366	NBPGR
205.	EC528367	IIVR
206.	EC528372	NBPGR
207.	EC528373	NBPGR
208.	EC528374	NBPGR
209.	EC528388	NBPGR
210.	EC529081	NBPGR
211.	EC529083	NBPGR
212.	EC529085	NBPGR
213.	EC529086	NBPGR

214.	EC531800	NBPGR
215.	EC531801	NBPGR
216.	EC531802	NBPGR
217.	EC531805	NBPGR
218.	EC5358139	IIVR
219.	EC538139	NBPGR
220.	EC538141	NBPGR
221.	EC538146	NBPGR
222.	EC538148	NBPGR
223.	EC538149	NBPGR
224.	EC538153	NBPGR
225.	EC538455	NBPGR
226.	EC546727	NBPGR
227.	EC562073	NBPGR
228.	EC5627	IIVR
229.	EC565216	NBPGR
230.	EC57442	NBPGR
231.	EC5863	NBPGR
232.	EC5888	NBPGR
233.	EC6053	NBPGR
234.	EC6192	NBPGR
235.	EC6486	NBPGR
236.	EC6488	NBPGR
237.	EC6845	NBPGR
238.	EC7317	NBPGR
239.	EC742	NBPGR
240.	EC7785	NBPGR
241.	EC7912	NBPGR
242.	EC8372	IIVR
243.	EC8591	NBPGR
244.	EC8630	NBPGR
245.	EC8822	NBPGR
246.	EC8936	NBPGR
247.	EC9046	NBPGR
248.	F6030	IIVR
249.	F6102	IIVR
250.	Feb.2	IIVR
251.	Feb.4	IIVR
252.	FLA7171	IIVR
253.	Gujrat Tomato	IIVR
254.	H-24	IIVR
255.	H-86	IIVR
256.	H-88-78-2	IIVR

257.	H-88-78-5	IIVR
258.	H-88-87	IIVR
259.	IC 469697	NBPGR
260.	IC447706	NBPGR
261.	IC447708	NBPGR
262.	IC469597	NBPGR
263.	IC469628	NBPGR
264.	IC469648	NBPGR
265.	IC469653	NBPGR
266.	IC469682	NBPGR
267.	IC469714	NBPGR
268.	IIHR2201	IIVR
269.	IIVR 121	IIVR
270.	IIVR2200	IIVR
271.	KT15	IIVR
272.	LA0012	TGRC
273.	LA0180	TGRC
274.	LA0215	TGRC
275.	LA0266	TGRC
276.	LA0274	TGRC
277.	LA0276	TGRC
278.	LA0292	TGRC
279.	LA0505	TGRC
280.	LA0516	TGRC
281.	LA0517	TGRC
282	LA0533	TGRC
283.	LA0744	TGRC
284.	LA0806	TGRC
285	LA0842	TGRC
286.	LA0854	TGRC
287.	LA1016	TGRC
288.	LA1021	TGRC
289.	LA1088	TGRC
290.	LA1089	TGRC
291.	LA1090	TGRC
292.	LA1091	TGRC
293.	LA1504	TGRC
294.	LA1506	TGRC
295.	LA1795	TGRC
296.	LA1996	TGRC
297.	LA2133	TGRC
298.	LA2374	TGRC
299.	LA2400	TGRC

300.	LA2529	TGRC
301.	LA2713	TGRC
302.	LA2714	TGRC
303.	LA2715	TGRC
304.	LA2818	TGRC
305.	LA2921	TGRC
306.	LA2968	TGRC
307.	LA2999	TGRC
308.	LA3012	TGRC
309.	LA3024	TGRC
310.	LA3121	TGRC
311.	LA3144	TGRC
312.	LA3202	TGRC
313.	LA3203	TGRC
314.	LA3229	TGRC
315.	LA3231	TGRC
316.	LA3233	TGRC
317.	LA3234	TGRC
318.	LA3237	TGRC
319.	LA3243	TGRC
320.	LA3246	TGRC
321.	LA3247	TGRC
322.	LA3317	TGRC
323.	LA3430	TGRC
324.	LA3465	TGRC
325.	LA3530	TGRC
326.	LA3532	TGRC
327.	LA3534	TGRC
328.	LA3537	TGRC
329.	LA3538	TGRC
330.	LA3539	TGRC
331.	LA3551	TGRC
332.	LA3554	TGRC
333.	LA3579	TGRC
334.	LA3630	TGRC
335.	LA3754	TGRC
336.	LA3770	TGRC
337.	LA3903	TGRC
339.	LA4024	TGRC
340.	LA4104	TGRC
341.	M.local	IIVR
342.	M-88-78-3	IIVR
343.	Mount favest	IIVR

344.	Mutant	IIVR
345.	N2298	BJJ
346.	N2369	BJJ
347.	N2389	BJJ
348.	N2403	BJJ
349.	N2411	BJJ
350.	N2448	BJJ
351.	N2465	BJJ
352.	N2501	BJJ
353.	N2664	BJJ
354.	N2675	BJJ
355.	N2764	BJJ
356.	N2812	BJJ
357.	N2829	BJJ
358.	N2832	BJJ
359.	N4210	BJJ
360.	N4218	BJJ
361.	N4241	BJJ
362.	Nandi	IIVR
363.	P.Gaurav	IIVR
364.	P.Pink	IIVR
365.	P.Rohit	IIVR
366.	PBC(Punjab Chuhara)	IIVR
367.	PDT-3-1	IIVR
368.	PKM-1	IIVR
369.	Pusa Rohini	IIVR
370.	Pusa-Gaurav	IIVR
371.	Rashmi	IIVR
372.	S.local	IIVR
373.	S-2-95-1-3-1	IIVR
374.	Sankranti	IIVR
375.	Sel-14	IIVR
376.	Siberia	IIVR
377.	Superbug	IIVR
378.	T.Local	IIVR
379.	T-HL	IIVR
380.	TLBR-12	IIVR
381.	TLBR-2	IIVR
382.	TLBR-3	IIVR
383.	TLBR-4	IIVR
384.	Type-1	IIVR
385.	Vaibhav	IIVR
386.	VLT-34	IIVR

387.	WIR13717	IIVR
388.	WIR3768	IIVR
389.	WIR3928	IIVR
390.	WIR3957	IIVR
391.	WIR4361	IIVR

TGRC: Tomato Genetics Resource Center at University of California, Davis (tgrc.ucdavis.edu/).

IIVR: Indian Institute of Vegetable Research, Varanasi, U. P., India (www.iivr.org.in/).

NBPGR: National Bureau of Plant Genetic Resources, New Delhi, India (www.**nbpgr**.ernet.in/).
(http://www.nbpgr.ernet.in:8080/PGRPortal/(S(o3cy12bkoz5s5e55w0dacf2a))/AdvancePassportSearch.aspx).

BSS: Bejo Sheetal Seeds Pvt. Ltd. Jalna, India (http://www.bejosheetalseeds. com/).

IIHR: Indian Institute of Horticulture Research, India (http://www.iihr.res.in/)

Supplementary Table 2. Reporting metabolite data in this study

Reporting metabolite data was presented according to the recommendation by Fernie et al., (2011)

Level	Aspect	Information	Fill in
General aspect	Type of metabolome analysis	Targeted metabolite analysis	TRUE
		Non-targeted metabolite class scale profiling	FALSE
		Non-targeted metabolome scale profiling	FALSE
		Non-targeted finger printing of mass features	FALSE
	Type of quantification	Absolute or quantification	Relative quantification
	Type of reference samples	Chemically defined	standard reference compounds aquired in chemical companies
		Biologically defined	-
	Type of replication	Analytical (same analytical sample preparation)	1
		Technological (same biological preparation)	2 (in different amount of plant material)
		Biological (same experimental condition)	5
		Full experiment	145
	Type of technology	Reference publication	Lisec et al., (2006)
	Sample preparation		chemical derivatized as described in protocol
		Method of chromatography/separation	Lisec et al., (2006)
		Method of ionization	- 70 MeVolt hard ionization
		Method of detection	electron impact ionization
Metabolite/mass feature	Metabolite	Metabolite name	see below
		Metabolite sum formula	see below
		Metabolite structure and public source of metabolite identifier	Metabolites were identified in comparison to database entries of authentic standards (Kopka *et al.*, 2005; Schauer *et al.*, 2005).
	Identification	Identification process	manually supervized with Xculibar and Metalign
		By authentic mass isotopomer added to one or all	FALSE

	biological sample(s)	
	By authentic reference compound within a co-processed reference mixture	FALSE
	By authentic reference compound previously mapped to the analytical system	TRUE
	Reference library	Metabolites were identified in comparison to database entries of authentic standards in NIST and Golm database (Kopka et al., 2005; Schauer et al., 2005)
	type of mass spectrum	
	By match of molecular mass (single mass fragment)	
	By match of fragments	YES
	By match of fragmentation pattern	YES
	type of retention index	
	By match of retention time (index) to reference library	fatty acid methylesters (FAMEs)
Quantification	Type of quantification	relative quantification by internal standard and sample fresh weight
Validity testing	Recovery testing (chemical analog)	not performed
	Recovery testing (internally added mass isotopomer)	not performed
	Recovery testing (mixture of most divergent samples from the experiment)	not performed
	Test for linear range	not performed
	Limit of quantification (LOQ)	not performed
	Limit of detection (LOD)	not performed

Experiment title: Metabolite profiles of tomato tissues for the organ or tissues mentioned below.
Plant species: *Solanum lycopersicum*
Organ/tissue: For leaf sample- leaf collected from 7th nodes of 45 days old green house grown plants were used (M82 and mutants*)*; for fruits- MG, TUR and RR stages of green house grown *acs2-1, acs2-2* and WT (M82) plants were used.
Analytical tool: GC/TOF-MS.